

Some pages of this thesis may have been removed for copyright restrictions.

If you have discovered material in AURA which is unlawful e.g. breaches copyright, (either yours or that of a third party) or any other law, including but not limited to those relating to patent, trademark, confidentiality, data protection, obscenity, defamation, libel, then please read our [Takedown Policy](#) and [contact the service](#) immediately

The Effect of Certain Hydrophilic Polymers
on Suspension Stability

by

Sai-Lung Law

A thesis presented for the degree of

Doctor of Philosophy

of the

University of Aston in Birmingham

October 1981

The University of Aston in Birmingham

The Effect of Certain Hydrophilic Polymers
on Suspension Stability

by

Sai-Lung Law

Submitted for the degree of Doctor of Philosophy, 1981.

The adsorption of nonionic surface active agents of polyoxyethylene glycol monoethers of n hexadecanols on polystyrene latex and nonionic cellulose polymers of hydroxyethyl cellulose, hydroxypropyl cellulose and hydroxypropyl methylcellulose on polystyrene latex and ibuprofen drug particles have been studied. The adsorbed layer thicknesses were determined by means of microelectrophoretic and viscometric methods. The conformation of the adsorbed molecules at the solid-liquid interface was deduced from the molecular areas and the adsorbed layer thicknesses. Comparison of the adsorption results obtained from polystyrene latex and ibuprofen particles was made to explain the conformation difference between these two adsorbates.

Sedimentation volumes and redispersibility values were the main criteria used to evaluate suspension stability. At low concentrations of surface active agents, hard caked suspensions were found, probably due to the attraction between the uncoated areas or, the mutual adsorption of the adsorbed molecules on the bare surface of the particles in the sediment. At high concentrations of hydroxypropyl cellulose and hydroxypropyl methylcellulose, heavily caked sediments were attributed to network structure formation by the adsorbed molecules.

An attempt was made to relate the characteristics of the suspensions to the potential energy of interaction curves. Generally, the agreement between theory and experiment was good, but for hydroxyethyl cellulose-ibuprofen systems discrepancies were found. Experimental studies showed that hydroxyethyl cellulose flocculated polystyrene latex over a rather wide range of concentrations; similarly, hydroxyethyl cellulose-ibuprofen suspensions were also flocculated. Therefore, it is suggested that a term to account for flocculation energy of the polymer should be added to the total energy of interaction. A rheometric method was employed to study the flocculation energy of the polymer.

Key Words: Hydrophilic polymers
Suspension stability

Contents

Page

Summary

Memorandum

Acknowledgements

List of tables

List of figures

Section 1	Introduction	1
1:1	Suspensions	1
1:2	Stability of pharmaceutical suspensions	3
1:3	Outline of present work	16
Section 2	Theory	18
2:1	Polymers in solution	18
2:2	Adsorption	20
2:3	Steric stabilization	27
2:3:1	Classical thermodynamic approach	28
2:3:1:1	Entropic stabilization	30
2:3:1:2	Enthalpic stabilization	31
2:3:1:3	Combined entropic-enthalpic stabilization	32
2:3:2	Statistical thermodynamic theories	32
2:3:2:1	Entropy theories	32
2:3:2:2	Enthalpy theories	35
2:3:2:3	Entropy plus enthalpy theories	38
2:3:2:4	Elastic theories	44
2:4	Electrostatic stabilization	45
2:4:1	The charge in the electric double layer	45
2:4:2	The diffuse double layer	46
2:4:3	The inner part of the double layer	48
2:4:4	Overlapping double layers and interparticulate repulsion	49
2:5	Attraction	51
2:5:1	The microscopic approach	52
2:5:2	The macroscopic approach	55
2:5:3	The effect of an adsorbed layer on attraction	57
Section 3	Materials	
3:1	Nonionic surface active agents	60
3:2	Nonionic water soluble cellulose polymers	60
3:3	Polystyrene latex	64
3:4	Drug	67
3:5	Characterization of materials	68
3:5:1	Nonionic surface active agents	68
3:5:1:1	Critical micelle concentration	68

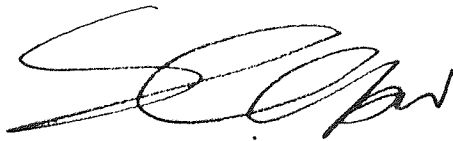
3:5:1:2	Partial specific volume	68
3:5:2	Nonionic water soluble celluloses	69
3:5:2:1	Molecular weight	70
3:5:2:2	Partial specific volume of electrolyte	80
3:5:3	Polystyrene latex	80
3:5:4	Drug	86
Section 4 Adsorption		108
4:1	Methods	108
4:1:1	Rate of adsorption measurements	108
4:1:2	Determination of adsorption isotherms	109
4:1:2:1	Nonionic surface active agents on polystyrene latex	110
4:1:2:2	Nonionic water soluble cellulose polymers on polystyrene latex and ibuprofen	110
4:1:3	Determination of adsorbed layer thickness	110
4:1:3:1	Microelectrophoretic technique	111
4:1:3:2	Viscometry	
4:1:4	Surface tension measurements	114
4:1:5	Contact angle measurements	115
4:2	Results and discussion	116
4:2:1	Rate of adsorption	116
4:2:2	Adsorption of Texofors on polystyrene latex	120
4:2:3	Adsorption of Celluloses	123
4:2:3:1	Polystyrene latex	123
4:2:3:2	Ibuprofen	132
4:2:3:3	Binding forces	135
Section 5 Stability		155
5:1	Methods	155
5:1:1	Preparation of suspensions	155
5:1:2	Microelectrophoresis	156
5:1:3	Sedimentation volume	164
5:1:4	Redispersibility	164
5:1:5	Flocculation studies	164
5:1:6	Determination of Hamaker constants	165
5:1:7	Determination of polymer-solvent interaction parameters	167
5:2	Results and discussion	168
5:2:1	Electrophoretic characterization	168
5:2:1:1	Polystyrene latex	168
5:2:1:2	Ibuprofen	171
5:2:2	Effect of nonionic surface active agents on the stability of polystyrene latex	172
5:2:2:1	Polystyrene latex in the presence of nonionic surface active agents	172
5:2:2:2	Polystyrene latex in the presence of nonionic surface active agents with electrolyte	180
5:2:3	Effect of nonionic celluloses on the stability of polystyrene latex	186
5:2:4	Effect of nonionic celluloses on the stability of ibuprofen	195
5:2:5	Hamaker constants	201
5:2:6	Polymer-solvent interaction parameters	203
5:2:7	Potential energy of interaction between particles	205

5:2:7:1	Polystyrene latex and nonionic surface active agent systems	205
5:2:7:2	Polystyrene latex and nonionic surface active agents in the presence of electrolyte	208
5:2:7:3	Polystyrene latex and nonionic cellulose systems	210
5:2:7:4	Ibuprofen and nonionic cellulose systems	211
Section 6 Rheometric studies		248
6:1	Methods	248
6:1:1	Instrument	248
6:1:2	Settling studies	249
6:1:3	Rheometric studies of particle aggregation	252
6:2	Results and discussion	254
6:2:1	The effect of viscosity on the settling of particles and the sediment conditions after settling	254
6:2:2	Particle-particle interactions of aggregated suspension in the presence of Hydroxyethyl Cellulose polymers	255
Section 7 Conclusions		267
References		273

MEMORANDUM

This dissertation, which is being submitted for the degree of Doctor of Philosophy in the University of Aston in Birmingham, is an account of the work carried out under the supervision of Dr. J.B. Kayes in the Department of Pharmacy the University of Aston in Birmingham from October 1978 to October 1981.

Except where acknowledged by references in the text, the work described herein is claimed to be original and has not been submitted for any other award.

A handwritten signature in black ink, appearing to read 'Sai-Lung Law', with a stylized flourish at the end.

Sai-Lung Law

October 1981.

ACKNOWLEDGEMENTS

I wish to express my appreciation to Dr. J.B. Kayes for his advice and encouragement given to me during the course of this work.

I am indebted to Professor M.R.W. Brown for making available to me the facilities of the Department of Pharmacy.

Thanks are also due to Dr. I. Conda and Dr. D.A. Rawlins for their useful discussions.

List of Tables

Table	Title	Page
1	Different types of steric stabilization	30
2	Critical micelle concentrations of Texofors in water	68
3	Values of partial specific volume of Texofors	69
4	Physical characteristics of HEC, HPC and HPMC	73
5	Refractive index increment data	76
6	Molecular weights and second virial coefficients of HEC, HPC and HPMC	79
7	Partial specific volumes of HEC, HPC and HPMC	80
8	Rate constants of HEC adsorption	118
9	Equilibrium adsorption values for Texofors on polystyrene latex and griseofulvin	120
10	Adsorbed layer thicknesses of Texofors on polystyrene latex	121
11	Adsorbed layer thicknesses of Celluloses on polystyrene latex	125
12	Molecular dimensions of Celluloses from viscometric measurement and from Catalin models	127
13	Data of adsorption of Celluloses on polystyrene latex	129
14	Data of adsorption of Celluloses on ibuprofen	133
15	Adsorbed layer thicknesses of Celluloses on ibuprofen	134
16	Characteristics of suspensions of polystyrene latex in the presence of Texofors	176
17	Characteristics of suspensions of polystyrene latex in the presence of Texofors with aluminium ions	184
18	Characteristics of suspensions of polystyrene latex in the presence of Celluloses	
19	Concentrations of Celluloses in the adsorbed layer for polystyrene latex	193
20	Characteristics of suspensions of ibuprofen in the presence of Celluloses	199
21	Concentrations of Celluloses in the adsorbed layer for ibuprofen	200

Table	Title	Page
22	The Hamaker constants of materials	202
23	Polymer-solvent interaction parameters for Celluloses in water	204
24	Effect of the Hamaker constant of the adsorbed Texofor A45 on V_A .	207
25	The relation of the depth of minimum and the redispersibility	209
26	The depths of the steric minima and the characteristics of suspensions	212
27	Yield values of the suspensions and suspension medium of ibuprofen-HEC systems.	256

List of Figures

Figure	Title	Page
1	Potential energy of interaction for electrostatic repulsion and van der Waals attraction	106
2	The influence of electrolyte concentration on the total potential energy of interaction	6
3	Schematic potential energy diagram for steric stabilization	11
4	Structure of adsorbed polymer molecules	20
5	Schematic representation of particles in sterically stabilized dispersion	29
6	Schematic representation of enthalpic stabilization	31
7	Overlap of adsorbed layers on the approach of two spherical particles	37
8	Structure of cellulose molecule	61
9	Structure of Natrosol 250	62
10	Structure of Klucel	63
11	Structure of Hydroxypropyl methylcellulose	64
12	dm/dw determination of the Texofors	89
13	Huggins plots for HEC, HPC and HPMC	90
14	Refractive index increment of HEC	91
15	Refractive index increment of HPC	92
16	Refractive index increment of HPMC	93
17	Diagram of the Photo Gonio Diffusometer	94
18	Light scattering measurement of HEC	95
19	Light scattering measurement of HPC	96
20	Light scattering measurement of HPMC	97
21	dm/dw determination of HEC	98
22	dm/dw determination of HPC	99
23	dm/dw determination of HPMC	100
24	Particle size distributions of polystyrene latex 3 and 4	101
25	Particle size distributions of polystyrene latex 4A and 4B	102

Figure	Title	Page
26	Particle size distribution of polystyrene latex 3B	103
27	Conductometric titration of latex 3B	104
28	Conductometric titration of latex 4A.	105
29	Particle size distributions of ibuprofens	106
30	Diagram of the Photoextinction sedimentometer	107
31	Diagram of the Coulter Counter	107
32	Huggins plots of Celluloses in the presence of NaCl solution	138
33	Rate of adsorption of HPMC	139
34	Rate of adsorption of HPC	140
35	Rate of adsorption of HEC	141
36	Isotherms for Texofors adsorbed on polystyrene latex	142
37	Isotherms for HEC adsorbed on polystyrene latex	143
38	Isotherms for HPC adsorbed on polystyrene latex	144
39	Isotherms for HPMC adsorbed on polystyrene latex	145
40	η_r against ϕ plots of HPC on polystyrene latex 4A	146
41	η_r against ϕ plots of HPMC on polstyrene latex 4A	147
42	Isotherms for HEC adsorbed on ibuprofen	148
43	Isotherms for HPC adsorbed on ibuprofen	149
44	Isotherms for HPMC adsorbed on ibuprofen	150
45	Internal conformation difference of the adsorbed polymer	135
46	Contact angle measurements of HEC on ibuprofen and polystyrene surfaces	151
47	Contact angle measurements of HPC on ibuprofen and polystyrene surfaces	152
48	Contact angle measurements of HPMC on ibuprofen and polystyrene surfaces	153
49	Surface tension measurements of the Celluloses	154
50	Mobility - pH plots for polystyrene latex 3B and 4A	214
51	Mobility - pH plots for ibuprofens	215

Figure	Title	Page
52	Mobility - concentration plots for polystyrene latex in the presence of Texofors	216
53	Schematic representation of the situation at a charged interface in the presence and absence of adsorbed polymers	173
54	Schematic representation of the mutual adsorption of adsorbed molecules on close contact particles	178
55	Mobility - concentration plots for polystyrene latex in the presence of Texofors with aluminium ions	217
56	Adsorption isotherm of Texofor A10 and mobility curve in the presence of Texofor A10 with aluminium ions	218
57	Adsorption isotherm of Texofor A18 and mobility curve in the presence of Texofor A18 with aluminium ions	219
58	Adsorption isotherm of Texofor A30 and mobility curve in the presence of Texofor A30 with aluminium ions	220
59	Adsorption isotherm of Texofor A45 and mobility curve in the presence of Texofor A45 with aluminium ions	221
60	Adsorption isotherm of Texofor A60 and mobility curve in the presence of Texofor A60 with aluminium ions	222
61	Photomicrographs of polystyrene latex in the presence of Texofor A18 with aluminium ions	224
62	Mobility - concentration plots for polystyrene latex in the presence of HEC	225
63	Mobility - concentration plots for polystyrene latex in the presence of HPC	226
64	Mobility - concentration plots for polystyrene latex in the presence of HPMC	227
65	Characteristics of polystyrene latex-HPMC 603 suspensions	228
66	Absorbance - concentration plots of polystyrene latex in the presence of HEC	229
67	Absorbance - concentration plots of polystyrene latex in the presence of HPC	230
68	Absorbance - concentration plots of polystyrene latex in the presence of HPMC	231
69	Mobility - concentration plots for ibuprofen in the presence of HEC	232
70	Mobility - concentration plots for ibuprofen in the presence of HPC	233

Figure	Title	Page
71	Mobility - concentration plots for ibuprofen in the presence of HPMC	234
72	Total potential energy curves for polystyrene latex in the presence of Texofor A10	235
73	Total potential energy curves for polystyrene latex in the presence of Texofor A18	236
74	Total potential energy curves for polystyrene latex in the presence of Texofor A30	237
75	Total potential energy curves for polystyrene latex in the presence of Texofor A45	238
76	Total potential energy curves for polystyrene latex in the presence of Texofor A60	239
77	Total potential energy curves for polystyrene latex in the presence of Texofors with electrolyte	240
78	Total potential energy curves for polystyrene latex in the presence of HEC	242
79	Total potential energy curves for polystyrene latex in the presence of HPC	243
80	Total potential energy curves for polystyrene latex in the presence of HPMC	244
81	Total potential energy curves for ibuprofen in the presence of HEC	245
82	Total potential energy curves for ibuprofen in the presence of HPC	246
83	Total potential energy curves for ibuprofen in the presence of HPMC	247
84	Diagram of the Weissenberg Rheogoniometer	259
85	Settling curves for ibuprofen in the presence of HPMC 603	260
86	Settling curves for ibuprofen in the presence of HPMC 606	261
87	Settling curves for ibuprofen in the presence of HPMC 615	262
88	Shear stress - shear rate curves for ibuprofen-HEC L suspensions	263
89	Shear stress - shear rate curves for ibuprofen-HEC J suspensions	265

1:1 Suspensions

A suspension is a two phase system in which the dispersed phase of insoluble solid particles is distributed somewhat uniformly throughout the dispersion medium or continuous phase.

In general, the size of the particles in pharmaceutical suspensions usually exceeds colloidal dimensions which are roughly between one nanometer and one micron. Pharmaceutical suspensions can be distinguished from colloidal dispersions in the sense that the particles of pharmaceutical suspensions will settle down on standing as a result of the gravitational force whereas with colloidal dispersions the particles can be dispersed throughout the medium by ambient thermal agitation and Brownian motion.

Suspensions are an important class of pharmaceutical dosage form and they have a number of advantages over other presentations: (a) the high surface area of medicament in suspension exposed provides high availability for absorption or adsorption; (b) they are convenient for administration, when the patient has difficulty in swallowing an oral unit dosage form of insoluble medicament; (c) insoluble drugs often have an unpleasant taste, therefore, by addition of suitable flavours to the dispersion medium, the unpleasant taste is easily masked; (d) irritations and unwanted local side effects may be prevented, for example, it has been shown (1) that an aspirin suspension does not cause mucosal ulceration while an aspirin tablet does; (e) administration of a suspension by injection may result in a depot effect.

Three general classes of suspensions are used in pharmacy (2): oral, parenteral and externally applied suspensions. Oral suspensions such as oral antibiotic syrups, pediatric drops, antacids, toxin adsorbents and radioopaque suspensions are commonly used. The solids content of an oral suspension may vary considerably. For example, the amount of solid in the oral antibiotic syrups is normally between 250 to 500 mg per 5 ml dose. The suspended material in pediatric drops is generally greater. Bulky insoluble dispersed solids are used in antacids, adsorbents and radioopaque suspensions. Most of the oral suspensions in the pharmaceutical field are water based. In cases where some of the drugs have an unstable shelf-life, the dosage form may be presented as a dry drug granulation or powder mixture which is made into a suspension at the time of dispensing by the addition of an appropriate vehicle. Parenteral suspensions contain from 0.5 to 30 per cent of solid particles. The physical factors of suspension injections e.g. particle size, shape and viscosity should be such as to facilitate injection and to give a depot effect of the medicament. The vehicles used for parenteral suspensions include aqueous and nonaqueous for example sterile water for injection and some parenterally acceptable oily substances. Externally used suspensions are prepared for dermatological, cosmetic and protective purposes. These preparations usually require the use of high concentrations of active ingredients. The dispersion media used are of great variety such as aqueous, nonaqueous and semisolid which make the product easier to apply.

Suspensions are also used in veterinary practice for example the internally used anthelmintics and the externally used pesticides. Further important areas where suspensions are used are in the mining engineering, paint and printing industry and plant protection.

technology (insecticides and herbicides).

The physical properties of a good pharmaceutical suspension are: (a) the medicament in suspension should not form a hard mass on storage but should readily disperse on shaking to enable accurate dose measurement to be made; (b) the suspension should have a suitable viscosity so that it may be easily removed from the container or it is able to pass through a syringe needle; (c) an acceptable appearance.

Polymers or surface active agents are useful in formulation of suspensions. The functions of these substances are to aid wetting of the insoluble powder, break the aggregation of particles, increase the suspending effect of the vehicle by increasing viscosity or by forming a structure. Furthermore, these agents may form a bridge between particles by adsorption to bring about particle aggregation (13,101) and they may coat on the particle surface to form a protective layer which ensures the stability of the suspension.

1:2 Stability of pharmaceutical suspensions

A physical stable pharmaceutical suspension, like a true colloidal dispersion, is such that the particles do not settle down and form sediment on the bottom of the container on standing but are distributed homogeneously throughout the medium. However, this situation is seldom realised because of the effect of the gravitational field on the suspended particles; in the event that sedimentation occurs, the sediment must not form a hard cake which prevents redispersion by shaking. When the drug particles form a hard cake, resuspension may

not occur even after vigorous shaking, and since the cake may contain the active ingredients, a uniform dosage distribution can not be assured. Therefore, in the formulation of ^a pharmaceutical suspension, a sediment of loose structure which can be redispersed easily by mild shaking is designed. This is likely to be a flocculated suspension. In colloid science, stable refers to particles that do not flocculate or coagulate. This apparently anomalous situation with the two systems can lead to confusion. Thus, some of the major differences between suspensions of flocculated and deflocculated particles are listed as follows:

Flocculated suspensions

- (a) Particles form loose aggregations.
- (b) Rate of sedimentation is high; a sediment is formed rapidly.
- (c) Particles settle as a floc with a large volume of sediment.
- (d) The sediment is loosely structured and a hard cake does not form.
- (e) The sediment is easy to redisperse.
- (f) The suspension is somewhat unsightly and the supernatant is always obvious and clear.

Deflocculated suspensions

- (a) Particles remain in suspension as separate entities.
- (b) Rate of sedimentation is low; a sediment is formed slowly.
- (c) Each particle settles separately; the volume of sediment is small.
- (d) The sediment is closely packed and a hard cake is formed.
- (e) The sediment is difficult, if not impossible, to redisperse.
- (f) The suspension has a pleasing appearance, since the suspended material remains suspended for a relatively long time. The supernatant also remains cloudy even when settling is apparent.

The above term of flocculation is used for all aggregations which include electrolyte coagulation, polymer flocculation etc. irrespective

of mechanism. Where flocculation is induced by additives this is usually called 'controlled flocculation'. In most published works no distinction is made between the phenomena of these aggregations (2,7,8). The mechanisms of coagulation, flocculation and deflocculation will be detailed in the following paragraphs.

In order to understand the mechanisms of particle interactions and the factors controlling the stability of suspensions it is necessary to consider the DLVO theory, which involves forces of van der Waals attraction and electrostatic repulsion, and steric stabilization, which is due to the repulsive effect of the interacted adsorbed polymer or surface active agent layers on the surfaces of particles.

The DLVO theory was developed independently by Derjaguin and Landau in the USSR (3) and by Verwey and Overbeek in the Netherlands (4) in the 1940s. This theory states that the stability of lyophobic colloids or colloidal particles are subject to energy of long range van der Waals attraction, V_A , and energy of repulsion, V_R , due to the interaction of electrical double layers surrounding the particles. These two energies may be summated to produce the total energy of interaction of particles, V_T , i.e.

$$V_T = V_A + V_R \quad (1)$$

The general features of the curve of potential energy of interaction plotted as a function of the distance between two similar particles, d , are given in Fig. 1.

V_R has the feature of decreasing exponentially with distance whereas V_A decreases as an inverse power of the distance. V_T shows

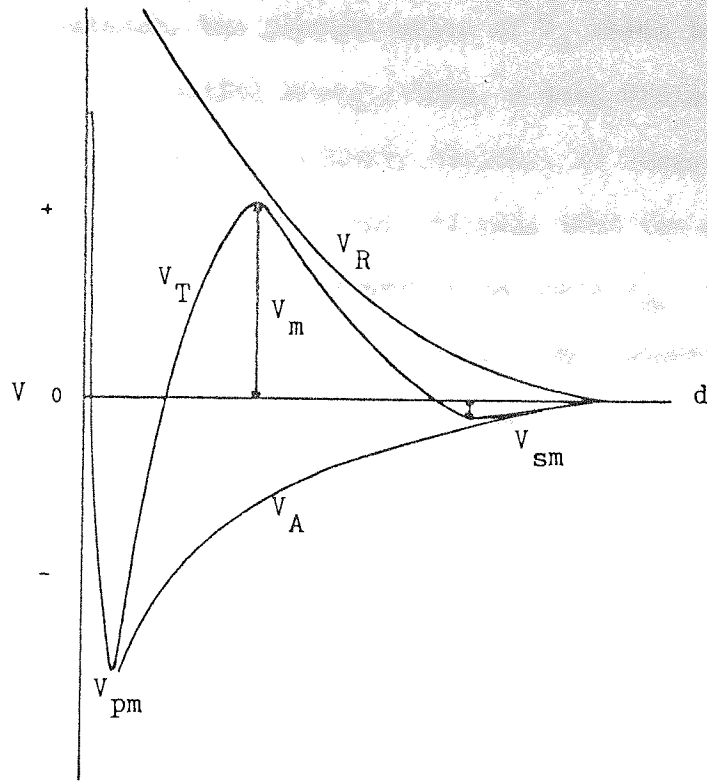


Fig. 1

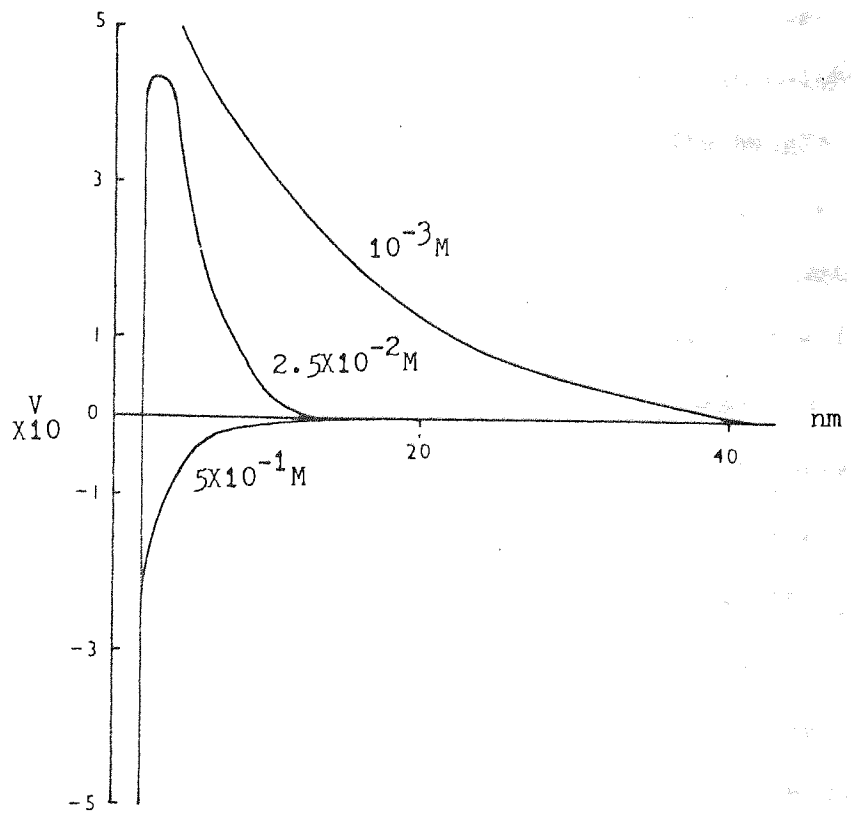


Fig. 2 (274)

that at very small distance, the predomination of V_A leads to very large negative value of potential energy; thus, a deep minimum, V_{pm} , is formed. This is termed the primary minimum. At large distance, as the electrostatic repulsion decays more rapidly than van der Waals attraction a second smaller minimum appears with depth V_{sm} . At intermediate distance the electrostatic repulsion may predominate showing a maximum in the total potential energy curve, V_m . Some important characteristic features of these potential energy curves are given and these are related to particle aggregation phenomena as follows: (a) The potential energy maximum, V_m , must be surmounted before particles can make lasting contact in the primary minimum. If the barrier is large compared with the thermal energy KT ($K =$ Boltzmann constant, $T =$ temperature) of the particles no such contact will occur and the system is stable in the colloid sense; the system is a deflocculated system. Otherwise, the system is aggregated. The height of the energy barrier depends upon the added electrolyte (5) i.e. the ionic strength of the bulk solution as shown in Fig. 2 where displacement of V_m to larger distances and increase in height of V_m with decreasing electrolyte concentration occur. The height of V_m is also affected by the potential from the particle surface to the bulk solution i.e. the surface potential, ψ_0 (5); V_m increases with increasing values of ψ_0 as would be expected in view of the increase of repulsion. Furthermore, the Hamaker constant, the interaction in terms of atom polarizabilities between like particles in a medium (see Section 2:5 for details), of the system are also one of the factors affecting the V_m of the total energy curve (5) in which V_m decreases as values of the Hamaker constant increase. (b) If the depth of secondary minimum is greater than KT then the particles should aggregate with a film of liquid between them. Since both the

attractive and repulsive forces are proportional to the particle radius, the secondary minimum should become increasingly significant with increasing particle size. The effect will also increase with increasing electrolyte concentration which reduces the distance over which the repulsive force operates, but this also reduces the energy barrier and promotes aggregation. Systems which have aggregated in the secondary minimum tend to be reversible i.e. they can be readily redispersed by shaking. In some cases, particles might on standing pass from the secondary to the primary minimum. (c) If the attractive force completely overwhelms the repulsive force, the particles will trap into the primary minimum. Those in the primary minimum need considerably more energy to redisperse and it may be considered as irreversible coagulation in the colloid sense. However, if the particles in such a system form a voluminous sediment with open structure, clustered particles in the open structure will be easily redistributed by shaking. Such is useful in pharmaceutical suspensions.

La Mer (12) distinguished coagulation as aggregation of particles due to reduction of electrical double layer potential by adding simple salts and flocculation as aggregation because of polymers, metal ions and polyelectrolytes forming bridging and crosslinking binding between particles. These definitions were emphasized by Ecanow et al (11). Bondi et al (14) suggested that flocculation mechanism can be classified as (a) adsorption bridging (b) crosslinking or chemical bridging (c) DLVO aggregation in secondary minimum; coagulation can be defined by (a) film-film bonding (b) DLVO aggregation in the primary minimum. Ottewill (6) proposed that the term coagulation should be used when it is clear that the particle association processes are occurring under primary minimum conditions i.e. as in the

particle aggregation processes which occur with lyophobic sols on the addition of simple electrolytes. The term flocculation will be used to describe secondary minimum association and the joining together of particles by bridging with polymer molecules. Thus, flocculation is a particle association process in which in the associated state the average distance between the particles is considerably greater than the order of atomic dimensions and hence the aggregate formed in this way has an open structure. Coagulation, however, leads to the formation of a compact aggregate structure in which the average distance of separation between the particles can be of the order of atomic dimensions. Ecanow et al (11) have shown that coagulation produces aggregates with relatively nonporous structures which lead to the formation of caked suspension. Bondi et al (14) have found that the sediment is dense and the supernatant is cloudy for a coagulated system and as the concentration of added electrolyte increases the sedimentation volume of the coagulated suspension increases. Hiestand (13) has stated that the flocs produced by adding electrolytes coagulated in the primary minimum would be expected to produce coarse and compact masses with a curdled appearance. Matthews and Rhodes (16) have claimed that both coagulation and flocculation give the same value of sedimentation volume but that the aggregates in the coagulated suspension are less granular and the supernatant more opalescent and the coagulated suspension is more easily dispersed than the flocculated suspension. The above reports give different values for the volume of sediment, the appearance and the redispersibility of coagulated suspensions. As the formulations of the suspensions were different, for example in Ecanow's case (11) the suspension contained an equal volume of glycerin, and surface active agent was present in the suspension

in Bondi's experiment (14), it would give different results of sedimentation volume, appearance of suspension and redispersibility. It has been pointed out by Hiestand (13) that the aggregation of coagulated suspensions is determined by the kinetics of the process. Schenkel and Kitchner (18) demonstrated that a rapid aggregation rate results in a higher sedimentation volume. Thus, when some of the factors of the suspensions, for example viscosity, particle size and amount of added electrolyte, are different, it will affect the kinetics of the coagulation process. Hence, it is difficult to use sedimentation volume, appearance and redispersibility in defining coagulation and also flocculation and to use these phenomena in the comparison of coagulation and flocculation; these would produce ambiguity. Therefore, in this work, the term coagulation is defined as particles aggregating in the primary minimum and flocculation is defined as particles associating in the secondary minimum.

Another mechanism for dispersion stabilization is steric stabilization which is the stabilizing action of repulsive energy generated from the overlapped region of adsorbed nonionic polymer or surface active agent layers of particles. This repulsive energy, V_S , is essentially a short range term. V_S can be included in the electrostatic repulsive and van der Waals attractive energy of interaction of Eq.(1); therefore, the total energy of interaction becomes (6, 19)

$$V_T = V_A + V_R + V_S \quad (2)$$

The energy curves are illustrated qualitatively in Fig. 3. The curve of V_S shows a steep increase in repulsion on close approach and possesses a sharp cut-off at the distance of twice the adsorbed layer thickness.

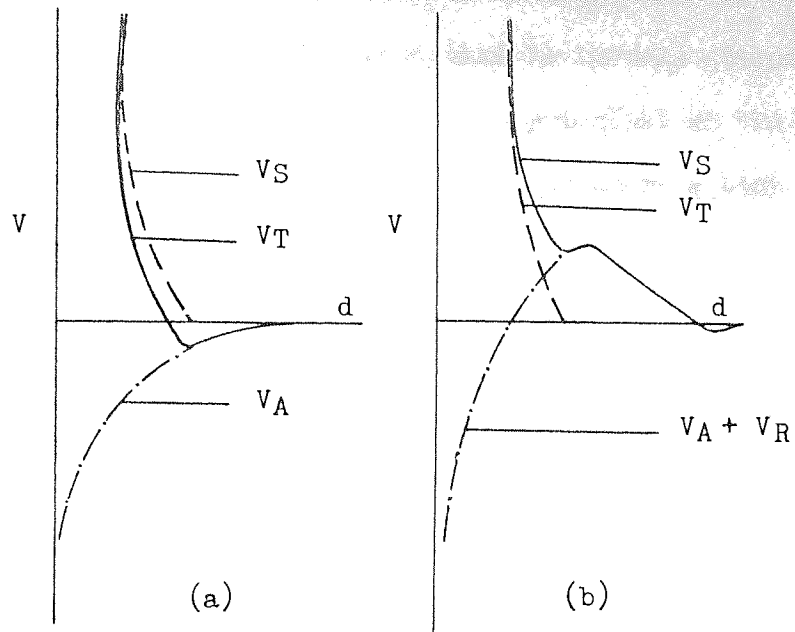


Fig. 3 Schematic potential energy diagram for steric stabilization

The effect of V_S in the presence (Fig. 3b) and absence (Fig. 3a) of electrostatic interaction give a clear picture that the entry of particles into a deep primary minimum is made virtually impossible by the presence of a steric barrier. Particles are therefore restricted in the shallow primary minimum created by the adsorbed layer or simply stabilized as a deflocculated system. Hence, from the total energy curves (Figs 1 and 3), it is clear that a physically stable pharmaceutical suspension may be :

- (a) a flocculated system
- (b) a coagulated system with open structure
- (c) a steric coagulated system.

The technique used to produce a non-caked suspension - the so called controlled flocculation approach - was first introduced by Haines and Martin (21,20). They found that the charge surrounding

suspended particles can be modified by addition of electrolytes. In their experimental studies, the addition of aluminium chloride to sulphamerazine suspensions, it showed that in certain concentration range of electrolyte, the zeta potential (the potential at the plane of shear around the particle) reduced to zero and produced a high sedimentation volume and a non-caked suspension.

In the controlled flocculation approach to suspension formulation, the suspended particles can be aggregated by using not only electrolytes but also polymers, surface active agents and liquids etc (13). As suggested by Kayes (22), the term of controlled flocculation should cover all aggregations of particles which are :

- (a) primary minimum coagulation
- (b) secondary minimum flocculation
- (c) bridging flocculation by polymers or by metal ion-polyelectrolytes etc.

Recently, Schott (23) has demonstrated that a colloiddally dispersed solid (bentonite) can also be employed as a flocculating agent in controlled flocculation of bismuth subnitrate suspensions.

Ecanow and co-workers (24,25,26), however, criticized the works of Haines and Martin and repeated their experiments. They found that a precipitation reaction occurred with the added aluminium chloride solution and the wetting agent, dioctyl sodium sulphosuccinate. They attributed the flocculation in the sulphamerazine suspension to a chemical reaction which took place between the dioctyl sodium sulphosuccinate anion and the aluminium ion. They questioned the use of zeta potential in these works to assess flocculation;

since flocculation was reported to have occurred immediately on mixing, the true zeta potential could not have been measured. Furthermore, they doubted that the particles were in macro-particulate suspension rather than in colloidal dispersion; even if van der Waals forces are presumably present, it has not been shown to be of significance in the type of system where particles are above the colloidal size range ($2\mu\text{m}$). However, the existence of secondary minimum flocculation with large particles has been shown with $10\mu\text{m}$ polystyrene latex particles (18) and direct measurement of van der Waals forces between macroscopic bodies, molecularly smooth sheets of muscovite mica, has been proved by Tabor and Winterton (28,29,30). As shown in Section 2:5, the van der Waals attractive energy is proportional to the radius of the interacting particles. It is expected that large particles will respond more actively than small particles.

Matthews and Rhodes carried out a series of investigations on the controlled flocculation. For example, they have compared the mechanism of flocculation due to chemical bridging and coagulation resulting from reduction of zeta potential (16); they have studied the effect of a number of variables such as pH values (31), particle size dependence (31,35), various electrolytes of tri, di and mono valence (32), different surface active agents in the dispersion medium with electrolytes or without electrolytes (33) and different types of drug suspensions (32) upon flocculation and coagulation. They also employed the DLVO theory in the interpretation of drug particles coagulation. It was suggested that coagulation occurs in a primary minimum whose depth is restricted due to the steric effect of the adsorbed surface active agent layers (32). Generally speaking, the results were semiquantitative although a number of assumptions were

involved in their calculations. They strongly support the concept of controlled flocculation used in the formulation of pharmaceutical suspensions. However, it should be emphasized that the use of aluminium chloride in controlled flocculation suffers from complex ion formation due to the hydrolysis of aluminium ion if the pH value is not controlled properly at $\text{pH} < 4$. Such hydrolysed complex ions of aluminium may play a significant role in reducing settling of particles by some mechanism other than by the compression of double layer effect. Further support by Short and Rhodes showed that controlled flocculation technique can be successfully applied to the formulation of hydrocortisone and norgestrel suspensions (34).

Kayes (22) has investigated the effect of anionic, cationic and nonionic surface active agents on the stability of drug suspensions of betamethasone, griseofulvin, nalidixic acid and thiabendazole; confirmation has been made that the DLVO theory and steric terms of adsorbed layers can be applied to coarse suspension systems.

Other works on stability of pharmaceutical suspensions include such as DeKay and co-workers (36) who studied sulphamerazine suspensions with methyl celluloses and alginates by means of microelectrophoresis to measure zeta potential of the drug particles and they (57, 58) also studied the rheological effect of various kinds of polymers and polymer compound systems on the stability of drug suspensions; Nash and Haeger (37) who examined silica dispersions with electrolytes and surface active agents; James and Goddard (38, 39) who studied barium sulphate preparations with hydrophilic colloidal materials; Otsuka et al (40,41,42) who investigated

flocculation - deflocculation behaviour of various types of drug suspensions such as sulphathiazole, naphthalene, chloroamphenicol, α -alumina and graphite with different surface active agents of nonionic, cationic and anionic and PVP-ionic surface active agent complexes; Felmeister et al (43) who studied polymer induced flocculation suspensions; Caramella et al (44) who compared the adaptability for suspensions of sulphamethoxypyridazine and its N'-acetyl derivative with different wetting agents; Takamura et al (45,46,47) who, in studying sulpha drug suspensions, investigated the effect of adsorption of cationic surface active agent and a number of variables such as pH, electrolytes etc. on the dispersibility; Farley and Lund (48) who defined the ideal characteristics of a suspending agent to be used in extemporaneous dispensing suspensions.

More recently, Liao and Zatz (49) have studied the flocculation of local anesthetic suspensions of benzocaine and butamben containing polyoxyethylene nonylphenols. Zatz (50) has demonstrated the effect of formulation additives on flocculation of dispersions stabilized by nonionic surface active agents. Zatz and co-workers (51) investigated the flocculation action of a cationic polymer on sulphamerazine particles. The effect of particle shape on coarse suspensions became a matter of concern to Heyd and Dhabhar (52). They have studied two forms of calcium carbonate particles i.e. one with an asymmetric and needle like and the other with symmetric and barrel like particle shape; they found that the latter showed no sign of caking on storage.

There is little published work on steric stabilization in the area of pharmaceutical suspensions. Recently, Kayes and Rawlins

(53,56) have measured the adsorbed layer thickness of two groups of nonionic surface active agents i.e. nonylphenyl ethoxylates (NPE) and polyoxyethylene-polyoxypropylene block co-polymers (Pluronic) and polyvinyl alcohols (PVA) on the surface of dispersed particles. They have investigated the effect of adsorbed NPE and PVA on the redispersibility of diloxanide furoate suspensions (54). In a subsequent paper (55), they have found that the aggregation of drug particles in the energy minimum of the steric effect was, for NPE, dependent upon the concentration of polymer in the adsorbed phase whereas for Pluronic, due to a combination of two mechanisms: (a) high interparticulate attraction due to high interfacial surface active agent concentration, (b) insufficient steric stabilization to prevent aggregation due to low adsorbed layer ethylene oxide concentrations.

1:3 Outline of present work

The formulation of non-caked suspensions remains a challenging problem to the formulator. Especially for those particles having a large size, since the density of the particles is usually greater than that of the vehicle. As a result of storage settling will occur and caking may follow. It is clear from the above references that controlled flocculation is the method to approach this problem by means of electrolytes, surface active agents and polymers etc.

Nonionic water soluble cellulose polymers are widely used in the formulation of suspensions because of their surface active, suspending, thickening and protective colloid effect and their

pH compatibility (undergo little viscosity change over pH range of from 2 to 12) and electrolyte compatibility (181). However, since most of the processes are patented (59), there is little published work on the mechanism of action of these substances.

In this work, a series of nonionic surface active agents and three groups of nonionic water soluble cellulose polymers are used. The adsorption of polymers and surface active agents are investigated. The types of sediment, redispersibility and the potential energy of attraction, electrostatic repulsion and steric effect are taken into account in considering the stabilization of particulate systems. The flocculation behaviour of the suspensions due to the presence of the polymers are also investigated. An attempt is made to compare the results of drug suspension systems with those of a model systems of a well characterized polystyrene latex dispersions.

2:1 Polymers in solution

In the understanding of the polymer adsorption, the structure of the polymer at an interface and the interaction between particles coated with adsorbed polymer layers, the solvent quality of the medium is very important. According to Flory (2), the dimensions of long chain molecules in solution are dependent on the interaction between chain elements; such interactions are conveniently divided into two classes. One, the short-range interactions between atoms or groups separated by only a small number of valence bonds and secondly, the long-range interactions between non-bonded groups separated in the basic chain structure by many valence bonds. Such interactions are therefore identical with van der Waals forces between the parts of two different molecules. The case where the chain is without long-range interactions and short-range interactions predominate is called the 'unperturbed' chain and here the root mean square end to end distance is given by $\langle r^2 \rangle_0$. Where long-range interactions occur, as a result of the superposition of both types of interactions, the root mean square end to end distance of a linear polymer in dilute solution is given by

$$\langle r^2 \rangle = a^2 \langle r^2 \rangle_0 \quad (3)$$

a^2 is the expansion factor due to osmotic swelling of the randomly coiled chain caused by solvent-polymer interaction which is known as the excluded volume effect.

Flory (56) and Huggins (61) made use of the lattice model to develop a theory for solutions which deviate from ideal behaviour

known as the Flory-Huggins theory. They calculated the entropy of mixing for polymer solutions.

$$\Delta S_m = -K(N_1 \ln v_1 + N_2 \ln v_2) \quad (4)$$

where subscript 1 denotes the solvent and 2 the polymer, N denotes number of moles and v is volume fraction.

The heat of mixing is given by

$$\Delta H_m = x_1 K T N_1 v_2 \quad (5)$$

where x_1 is defined by Flory as the interaction energy per solvent molecule. Combining the entropy and heat of mixing gives the Flory-Huggins expression for the free energy of mixing of a polymer solution:

$$\Delta G_m = K T (N_1 \ln v_1 + N_2 \ln v_2 + x_1 N_1 v_2) \quad (6)$$

For dilute polymer solutions, the model used in the Flory-Huggins treatment is not suitable because it does not take account for the inherent nonuniformity of the polymer segment. Flory and krigbaum (60) described another model, which consists of the dispersion of polymer clouds or dilute clusters of polymer segments separated on the average by regions of free solvent which have a Gaussian distribution. They derived

$$\Delta H_1 = K T k_1 v_2^2 \quad (7)$$

$$\Delta S_1 = K \psi_1 v_2^2 \quad (8)$$

$$\Delta G_1 = K T (k_1 - \psi_1) v_2^2 \quad (9)$$

where ΔH_1 , ΔS_1 and ΔG_1 are the respective partial molar quantities.

k_1 and ψ_1 are parameters which correct for the deviations from ideal solution. The correction to the Flory temperature Θ ($= k_1 T / \psi_1$) is

$$\psi_1 - k_1 = \psi_1 \left(1 - \frac{\Theta}{T} \right) \quad (10)$$

and to x_1 is

$$\psi_1 - k_1 = 1/2 - x_1 \quad (11)$$

At the temperature $T = \Theta$ the partial molar energy due to polymer-solvent interactions is zero and deviations from ideal solution behaviour vanish. The excluded volume effect also vanishes i.e. there are no net interactions. At temperatures above and below Θ the excluded volume is positive and negative respectively. At the Θ condition, $\alpha = 1$ and the polymer chain dimensions are unperturbed by intramolecular interactions. Since α depends on the entropy parameter ψ_1 , it is large in a good solvent.

2:2 Adsorption

Consideration of the structure of adsorbed polymers at the solid-liquid interface was first described by Jenkel and Rumbach (62). They considered that the polymers are partially adsorbed on the nonporous surface. Each molecule is anchored at one point or a few points are adsorbed onto active sites with the remainder extended out into the liquid phase. In other words, the adsorbed polymer molecules are in the form of 'tails', 'loops' and 'trains' for single point attachment, partial attachment and total attachment respectively, as shown in Fig. 4.

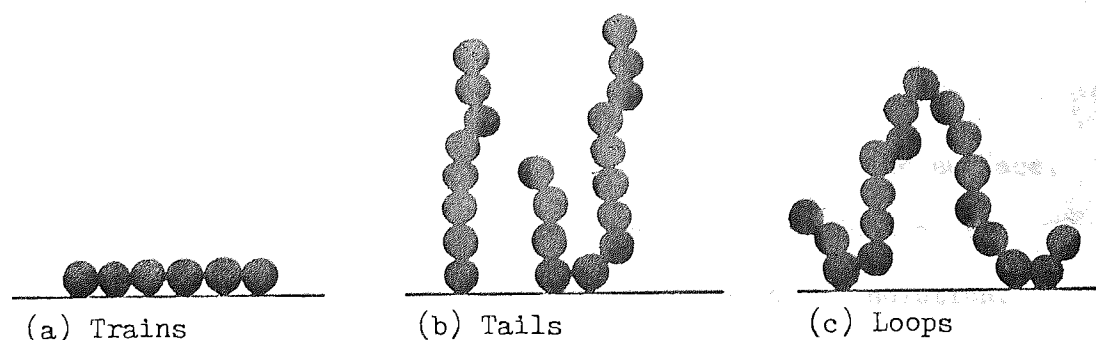


Fig. 4

The structure and conformation of the adsorbed polymer molecules was studied by the dependence of polymer adsorption on the molecular weight of the polymers (63,64). Models (Fig. 4) were set up to calculate the dependence of the maximum adsorption, A_m , on the molecular weight, M , through the equation

$$A_m = K M^a \quad (12)$$

where K and a are constants. Equation (12) was found to apply to trains (Fig. 4) with a equal to zero (63). In the second and third cases of Fig. 4, the polymer molecules are attached to the surface by a single segment leading to a bristle like form of adsorbed film in which the adsorption is directly proportional to molecular weight i.e. $a = 1$. For the adsorbed polymers forming a layer of contiguous rigid spheres with a radius equal or proportional to the radius of gyration in solution, the value of a will also be zero. For the case, where the adsorbed polymer conformations are in a random coil state, then $0 < a < 1$. For example, for the completely entangled and interwound adsorbed polymer where the segment density as a function of distance from the surface is similar to that of a free randomly coiled polymer in solution, a is equal to 0.5. Under these circumstances the solvent is in theta condition. Silberberg (65) also developed a quantitative approach for estimating the structure of the adsorbed layer. He suggested that a decreases with the molecular weight of the adsorbed polymer.

Dealing with the amount of polymer adsorbed onto the surface, Koral et al (66) assumed that the adsorbed polymers adopt a Gaussian distribution of coils from the surface to the solution. These adsorbed polymers are bound at the surface on the adsorption sites in the form mentioned by Jenkel and Rumbach (62) forming a single adsorbed layer. The maximum amount adsorbed can be estimated by

the equation

$$A_m = \frac{S M}{\pi R^2 N_A} \quad (13)$$

where S is the specific surface area for the adsorbed polymer, M is the molecular weight, R is the radius of gyration of the polymer coil and N_A is the Avogadro number. However, experiment for adsorption of polyvinyl acetate on metal powders in various solvents (66) showed values which were several times greater than the theoretical results. This can be explained by the adsorbed polymer molecules changing from low surface coverage to high surface coverage due to compression or mutual entanglement of the polymers. As a result, the configurational entropy of the adsorbed molecules decreases to compensate for the increase in enthalpy which occurs during adsorption. This leads to an increase in adsorption.

Langmuir (68) developed an equation based on the assumption that molecules are adsorbed on the active sites of the surface forming a monolayer and this process is thermodynamically reversible. This is known as the Langmuir isotherm which is

$$Y = \frac{Y_m b c}{1 + b c} \quad (14)$$

where Y is the amount of polymer adsorbed at concentration c , Y_m is the amount of polymer adsorbed at saturation and b is a constant. Published work (66,69,70,71,72) has shown that the agreement between the experimental isotherms and the calculated models is fairly good at low polymer concentrations and with low molecular weight polymers. However, at high polymer concentrations and with high molecular weight polymers, the agreement is poor (64). This is because the experimentally accessible region ordinarily consists of a slowly changing plateau region and as concentration increases the isotherm becomes much less steep.

Simha, Frisch and Eirich (73) provided a model for polymer adsorption which fits the experimental values very well. They assumed that in infinitely dilute solution the more or less flexible random coiled polymers characterized by a Gaussian distribution of end to end distance localize on the adsorption sites of the surface. Each of the polymer segments interacts with one adsorption site only forming a monolayer on the surface. A simpler form of that equation is

$$[Y \exp(2 K_1 Y)] / (1 - Y)^{\langle V \rangle} = K c \quad (15)$$

where Y is the fraction of the surface coverage of the polymer segments at the concentration c , $\langle V \rangle$ is the average number of segments adsorbed on the surface per chain of polymers, K and K_1 are constants which deal with the mutual interaction of polymer molecules and the effect of solvent on adsorption. The competitive adsorption of solvent and polymers is ignored. Comparison with the Langmuir isotherm (72) showed that this isotherm rises steeply at low concentration and after that the surface coverage depends only slightly upon concentration. If the polymer is attached with one segment on a single site of surface, K_1 tends to zero and $\langle V \rangle$ equals one. Thus, Equation (15) is transformed into the Langmuir equation for monolayer coverage. The value of $\langle V \rangle$ should also increase with increasing flexibility of the polymer chain. The increase of flexibility which results from increase in temperature could overcome other factors and explain observed cases of increased adsorption with increase in temperature. However, due to the complexity of the adsorption process, it is difficult to enter various interaction factors into a suitable equation with the expectation of finding a satisfactory quantitative description of the system within the

limitation of the model. For example, the SFE theory was derived initially for low surface coverages and does not work with high surface coverages (70).

Silberberg (74) criticized the SFE assumption of a Gaussian distribution of adsorbed polymer in contact with a reflecting wall. He (74,75) found that the SFE theory predicts loops of polymers that are too long, the adsorbed layers are too large and can not explain the large values of the fraction of attached polymer segments and the molecular weight dependence of the adsorption. He also pointed out that the shape of the polymer molecules was not determined correctly and did not appear as a variable in the full thermodynamic treatment. Silberberg developed a theory based on the concept of a partition function for adsorbed polymer molecules between the surface and the bulk solution. The adsorbed polymer molecules exist in two energy states at an interface. That is to say, trains of adsorbed polymer segments form on the surface whereas loops extend into the bulk solution. Silberberg considered the behaviour of an isolated polymer molecule on the surface. The loop size was uniform for a given adsorbed polymer and its shape was independent of the length of the molecule. A partition function was set up for the system in order to calculate the required thermodynamic parameters. By equating the chemical potential of the polymer in the adsorbed state and in the bulk solution, it was then possible to determine the adsorption isotherm. Although Silberberg's treatment can not be considered as universal, it is very useful for an understanding of the adsorption processes of polymers and it is a base for the further development of theories of adsorption (77 - 90).

Hoeve et al (77,78,90) used a statistical treatment for a polymer molecule adsorbed on a surface. A low surface coverage was considered and mutual interactions of the adsorbed molecules were neglected. The partition function was derived for a polymer molecule with sequences of repeating units adsorbed at an interface and other sequences looped at the surface only at their ends. Their treatment predicts large loops and few units adsorbed for small free energies of adsorption and small loops and more units adsorbed for large free energies of adsorption when the chains are flexible. This is in contrast to Silberberg's theory and also in partial disagreement with the SFE theory. In later work, the theory was made more accurate by allowing for the excluded volume effect (88) and heat of mixing (89). The total free energy of interaction and adsorption of polymer chain is given by

$$\Delta G = \Delta G_1 + \Delta G_2 + \Delta G_3 \quad (16)$$

where ΔG_1 arises from the adsorption of the polymer chain, ΔG_2 is the change in free energy of polymer segment interaction and ΔG_3 is due to the contribution of excluded volume effect.

Hoffmann and Forsman (91,92) have also calculated the thermodynamic properties of the adsorbed polymers. The free energy of an adsorbed polymer was derived

$$\Delta G = \Delta G_m + E_1 - T \Delta S_c \quad (17)$$

where ΔG_m , which is derived from the Flory-Huggins theory, is the free energy of mixing of solvent molecules and segments of adsorbed molecules, E_1 is the surface interaction energy, ΔS_c is the configurational entropy and T is the temperature. The isotherm was then calculated by equating the partial molar free energy of polymers at the surface to that of polymers in bulk solution for each specified amount of

surface coverage. Predictions of adsorption were in good agreement with the reported experimental values (91). They showed that for the sparsely covered adsorption surface, where intermolecular interaction of the adsorbed molecules is negligible, the equilibrium solution concentrations are below the range that can be determined experimentally and the amount adsorbed should increase with molecular weight. They also pointed out the limited applicability of theories which assume the absence of intermolecular interaction of the adsorbed polymer.

Hesselink (93,94) has studied the segment density distribution of a polymer adsorbed on the surface. He calculated the segment density distribution function $\rho(i,x)$ for single loops and tails composed of i segments at distance x from the surface. The probability $\rho(i,k,x)$ was expressed as the product of the probability of finding the terminal segment of a chain of k segment at x . For homopolymers and random co-polymers, Hesselink derived the density distribution $\rho(i,x)$ according to Hovee's loop size distribution function. The exponential decrease of $\rho(i,x)$ with distance from the surface agrees with other theories (79,80,81,82,90). However, for the cases of the short polymer chain and high surface coverage adsorption, errors will be introduced due to the large end effect (80) of the adsorbed molecules and the complexity arising from the dependence on the amount adsorbed, the average size of the adsorbed chain and the solvent quality. Nevertheless, this approach offers a useful method for studying polymer adsorption and also in the calculation of steric repulsion.

Generally speaking, in the above theories the interaction energy between the solvent and the polymer segment and the polymer segment and the adsorbent surface determine the adsorption of the polymer.

Either of these effects may predominate or they may counteract. There is a critical value of net interaction energy beyond which adsorption takes place. Then, the number of adsorbed segments and the amount adsorbed increase rapidly with increasing interaction energy and level off at equilibrium. However, if the adsorbed molecules train on the surface, the net energy will reach a maximum with a high number of adsorbed segments but a smaller amount of adsorbed polymer.

For adsorption of surface active agents on the solid surface, the above theories of chain segment distribution are not suitable due to the short chain structure and the low molecular weight of the surface active agents. However, the adsorption pattern always shows a Langmuir type of monolayer formation (95,96,97,40) but multilayer adsorption has also been found (97). The driving force of adsorption depends on the change in the free energy of the system made up of the changes in enthalpies and entropies of the interaction of surface-solvent-adsorbate.

2:3 Steric stabilization

The mechanism for the adsorbed polymer stabilization of colloidal particles was first investigated by Zsigmondy (98) in 1901. He reported that gold sols were protected against aggregation with electrolytes by adding gelatin. This indicates that addition of large amounts of a hydrophilic colloid stabilizes the system as an adsorbed layer is formed on the particle surface protecting the particle. This phenomenon is termed protection (2).

Heller and Pugh (99) reported on the non-electrostatic method of stabilizing colloidal particles using nonionic polymer stabilizers which they termed 'steric stabilization'. They suggested that steric stabilization is due to the nonionic flexible polymer molecules adsorbed on particles and most likely extended with major segments in the interior of the surrounding medium. Only slight interpenetration of the polymer chains which extend outward from neighbouring particles would be expected. These protruding chains keep the particles at distances too large to give a van der Waals attractive energy sufficient to bridge the particles together.

In earlier work, van der Waarden (100) investigated the degree to which hydrocarbons prevented the aggregation of finely divided carbon-black particles in a hydrocarbon medium. He found that aromatic hydrocarbons with aliphatic side chains of sufficient length stabilized the dispersion and that stabilizing efficacy increased with both the number and length of the chains. In recent years, some understanding of the mechanisms by which the adsorbed polymers can impart dispersion stability has emerged. Quantitative theories of steric stabilization seem applicable.

2:3:1 Classical thermodynamic approach

Napper (101) suggested that the easiest mechanistic approach to steric stabilization is through energy consideration using the Gibbs-Helmholtz equation

$$\Delta G = \Delta H - T \Delta S \quad (18)$$

According to the second law of thermodynamics, a spontaneous process involving a system and its surroundings proceeds in the direction

of increased disorderliness. The greater the disorderliness the greater the positive entropy change ΔS . The free energy change ΔG , which is invariably negative for a natural process, is obviously in the right direction for a spontaneous reaction. The converse also holds. A system tends to oppose those changes which lead to the imposition of orderliness. Such entropic opposition does not necessarily prevail because a favourable enthalpy change may override an unfavourable entropy. However, when the enthalpy change is negligible work must be expended to increase the order in a system. This work required can be referred to a potential energy barrier to the occurrence of the process.

Napper (102,103,104) developed a model to examine the steric effect (Fig. 5).

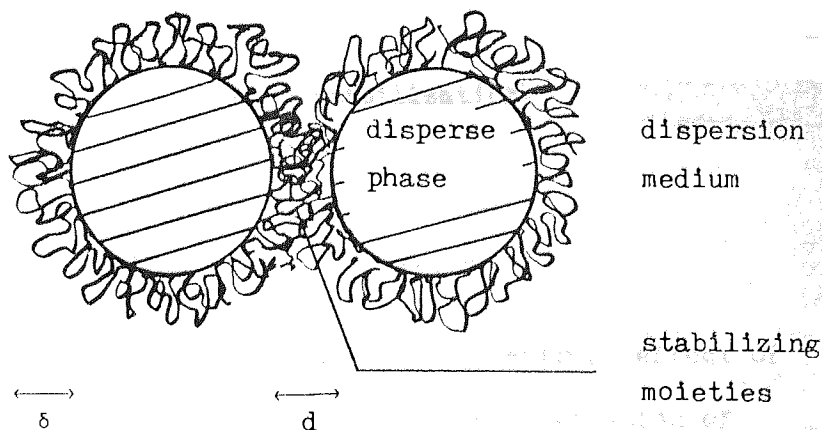


Fig. 5

For two particles with the distance of surface separation d greater than twice the maximum extension 2δ of the adsorbed polymer chain there should be no direct interaction between the adsorbed layers. The only effect is that of the van der Waals forces. On closer approach where the interparticle distance is less than 2δ , the volumes occupied by the adsorbed molecules overlap and result in an interpenetration and compression interaction of the polymer molecules in the adsorbed layers leading to a change of ΔG . From Eq. (18),

ΔG must be positive for steric stabilization to take place. If ΔG is negative, particles are aggregated by the adsorbed polymer chains. If ΔG is zero, deviation from ideality vanishes; this is due to the exact equality of ΔH and $T\Delta S$. At this point polymer molecules can telescope one another without net segment-segment interaction. This condition is termed the theta (θ) condition whereas the temperature and the solvent property are called θ -temperature and θ -solvent respectively. There are three different ways to obtain a positive ΔG as shown in Table 1.

ΔG	ΔH	ΔS	$ \Delta H / T \Delta S $	Stability Type
+	+	+	> 1	Enthalpic
+	-	-	< 1	Entropic
+	+	-	$\cong 1$	Combined enthalpic and entropic

Table 1 Different types of steric stabilization.

2:3:1:1 Entropic stabilization

Napper (101) used a model to illustrate the entropy effect of stabilization. Because of compression and/or interpenetration of the polymer chains a decrease in entropy results. According to the second law of thermodynamics, this decrease in entropy generates a repulsive energy. If it overrides the energy from the enthalpy of interpenetration and/or compression, stabilization is obtained. In principle, entropically stabilized dispersions are characterized by flocculation on cooling (105) and are predominant in nonaqueous dispersions (106).

2:3:1:2 Enthalpic stabilization

Enthalpic stabilization arises when both ΔH and ΔS are positive and $\Delta H > T \Delta S$. This means that the enthalpy change ΔH in the interaction prevents flocculation and a positive value of ΔG results.

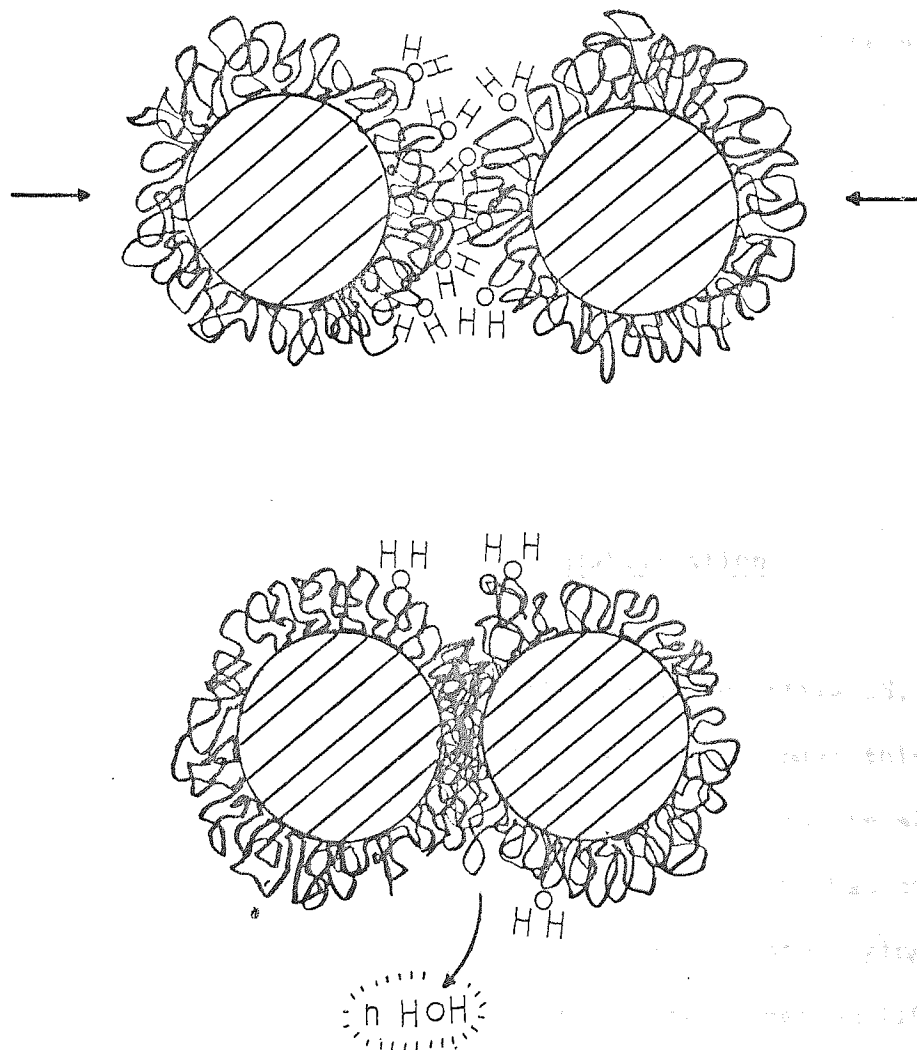


Fig. 6 Schematic representation of enthalpic stabilization.

As shown in Fig. 6, when two particles with stabilizing polymers approach together, interpenetration and/or compression of polymer chains occurs. The polymer chains of the adsorbed layers contact in the interaction zone prior to the water-polymer molecules interaction.

Thus, the structuring of the polymer molecules and water molecules is destroyed causing some of the hydrated water molecules to be excluded from the interaction zone. The excluded water molecules have greater degrees of freedom than those in the hydrated state. This randomness of motion results in an increase in entropy which outweighs the reduction in entropy due to the interacting polymer segments. According to the principle of equipartition of energy, the greater degrees of freedom of water molecules must be supplied with energy. As a result, heat is adsorbed i.e. a positive free energy change resulted from $|\Delta H| > T |\Delta S|$. This generates a repulsive force between the particles and the system is stabilized. In general, enthalpic stabilization is characterized by flocculation on heating because $T \Delta S$ increases more rapidly than ΔH (105). This mechanism is more important in aqueous systems (106,103).

2:3:1:3 Combined entropic-enthalpic stabilization

For the situation with a positive ΔH and negative ΔS , ΔG would always be positive to stabilize the system. Under this condition, flocculation would not occur at an accessible temperature since the Θ -temperature would be negative. It seems likely that combined entropic-enthalpic stabilization is a 'buffer state' lying between enthalpic stabilization and entropic stabilization (104).

2:3:2 Statistical thermodynamic theories

2:3:2:1 Entropy theories

The quantitative calculation of the energy due to the steric

effect was first considered by Mackor (107). He postulated a model of rigid or flexible rod like molecules adsorbed onto a flat interface with small surface coverage and it was assumed that all orientations of the rods at the interface had equal probability of occurrence. When the flat plates are separated infinitely the free energy due to the adsorbed rod is ΔG_{∞} but as the plates come together with a distance smaller than the length of the adsorbed rod the change in the free energy will be ΔG_d . This can be calculated from

$$\Delta G_r = \Delta G_{\infty} - \Delta G_d \quad (19)$$

ΔG_r results primarily from the loss of configurational entropy of the adsorbed rod. However, due to the small surface coverage permitted in this model the calculated repulsive energy ΔG_r is too small. Mackor and van der Waals (108) used a more sophisticated approach for the treatment of higher surface coverage interactions. They used a lattice model with adsorbed molecules which were assumed to be dumb-bell shaped occupying two adjacent lattice sites on two parallel adsorbing planes. When the planes are brought together, and interaction of the adsorbed layers results in a loss of configurational entropy of the adsorbed molecules. The free energy of the system increases. This free energy change varies with the number of layers of molecular sites considered in the lattice model. The free energy decreases with increasing the number of layers. Undoubtedly, this thermodynamic expression is correct and should occur with very simple adsorbed molecules. However, its applicability is limited for polymer molecules, since stabilizing polymer molecules rarely conform to the demanding geometric and volumetric requirements.

Bagchi and Vold (109) and Ash and Findenegg (110) have extended Mackor's theory so as to calculate the interaction energy between

two spherical particles and parallel planes respectively. However, it is clear that the basic approach is unable to handle flexible multi-segment polymer chains and high molecular weight polymer molecules.

Clayfield and Lumb (111) carried out statistical computations to obtain the configurational entropy loss of the flexible polymer chains on compression. They assumed that the random polymer chains were terminally adsorbed on the surface. A lattice model with a bond angle of 90° was used. They studied polymer chains up to 300 links. These authors derived equations for sphere-sphere and sphere-plate interactions. They found that in a constant thickness of adsorbed layer, increasing the flexibility and the number of links of the adsorbed polymers increases the repulsive free energy. Adsorbed random co-polymers having the same adsorbed layer thickness as that of a terminally adsorbed polymer gave strong steric repulsion. However, in these calculations, no allowance was made for the nature of the solvent into which the polymer chains were immersed and thus their applicability is restricted to athermal dispersion media only (102,104).

Later, Bagchi and Vold (112,113) developed a somewhat different model and suggested that when colloidal particles coated with polymeric adsorbed layers come into interaction, the polymer chains in the adsorbed layers undergo denting rather than interpenetration and compression. This corresponds to compression of the chains attached to one surface on contact with chains attached to the other. For the entropy energy calculation, the normalized distribution function of polymer chains from Weidman et al (114) was used. Because solvent quality is not involved in the calculation its application

is restricted to the condition where the repulsive free energy is set equal to $-T \Delta S$ (115). As examined by Napper et al (116) the repulsive potential obtained from this model is too large.

In conclusion, the above theories only deal with the contribution to the interaction energy from the loss of configurational entropy of the adsorbed polymer molecules. It is clear that they are incomplete because solvent properties are ignored. As pointed out by Fischer (117) and Napper (102), the solvent power of the dispersion medium can be critical in determining the stability of sterically stabilized dispersions.

2:3:2:2 Enthalpy theories

Fischer (117) was the first to investigate the quality of solvent power when two adsorbed polymer layers interpenetrate. Due to the decrease of the chemical potential of solvent molecules in the interpenetration zone, a potential gradient is created between the solvent molecules in the interpenetration zone and those in the external dispersion medium. As a result, the external solvent molecules diffuse into the interaction zone generating an excess osmotic pressure. This excess osmotic pressure forces the polymer chains and therefore the particles apart from each other. In Fischer's model (Fig. 7), the solution is ideal when particles are far apart but when particles are brought together ideality vanishes. An excess osmotic pressure π_e is created in the overlapped volume. Thus,

$$\pi_e V_1 = \Delta u_d - \Delta u_\infty \quad (20)$$

where V_1 is the partial molar volume of the solvent and Δu is the change of potential energy. π_e is related to the second virial

coefficient B of the polymer in free solution using the Flory-Huggins theory:

$$\Delta G_{\text{osmotic}} = 2B R T c^2 \delta V \quad (21)$$

or

$$\Delta G_{\text{osmotic}} = B N_A c^2 K T \frac{4\pi}{3} (\delta - d/2)^2 (3a + 2\delta + d/2) \quad (22)$$

where c is the mean segment concentration in the adsorbed layer and δV is the overlapped volume.

According to Eq. (22), in a good solvent B is positive and thus a repulsive force is generated to stabilize the system. Whereas, in a bad solvent B is negative and particles tend to aggregate together. If $B = 0$, the free energy is also equal to zero i.e. a theta condition.

Ottewill and Walker (19) followed Fischer's theory and developed an equation for the repulsive free energy

$$\Delta G_s = \frac{4\pi K T c^2}{3 V_1 \rho^2} (\psi_1 - \chi_1) (\delta - d/2)^2 (3a + 2\delta + d/2) \quad (23)$$

where ρ is the density of the adsorbed layer, χ_1 is the Flory interaction parameter which characterizes the interaction energy of the polymer chains per solvent molecule, V_1 is the molecular volume of the solvent molecules and ψ_1 is the entropy parameter for interaction of solvent and adsorbed polymer molecules. They assumed that ψ_1 is given the ideal value of 0.5. Then, provided that $\chi < 0.5$, the free energy of interaction will be positive and consequently repulsion will occur.

Although Matthews and Rhodes (32) made use of Eq. (23) to

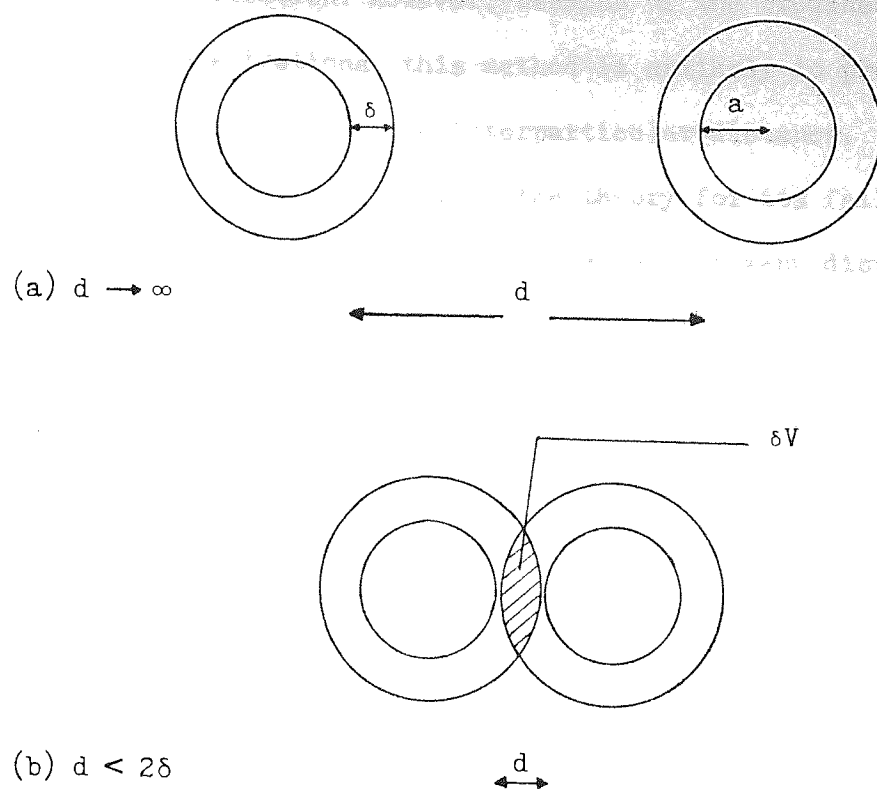


Fig. 7 Overlap of adsorbed layers on the approach of two spherical particles with adsorbed layer thickness δ and overlapped volume δV at distance d .

describe the steric effect in pharmaceutical suspensions, there are several shortcomings to these theories. As criticized by Napper et al (118), these theories only consider the interpenetration effect of the polymer chains but do not take into account the compression effect. Secondly, all virial coefficients higher than the second are ignored. Thirdly, these theories assume that the segment concentration and segment density in the adsorbed layer are constant but in fact they vary with the distance normal to the particle surface.

Bagchi (113) used the model in the previous work for entropy calculations (112) (Section 2:3:2:1). He considered the enthalpy of the polymer segment-solvent interaction using experimentally accessible

parameters in his calculation. However, because of the crudeness of the mean polymer concentrations, this method is unlikely to predict the correct dependence of ΔH on the interparticular distance.

Napper et al (116) have also criticized the theory for its failure to indicate the strong correlation which is observed for many dispersions between the critical flocculation and the theta points.

2:3:2:3 Entropy plus enthalpy theories

A very important sign post to the complete development of the theory of steric stabilization was proposed by Meier (119). He suggested that the mutual repulsive free energy of the adsorbed polymer chains on the surface is due to the volume restriction effect and the osmotic pressure effect. He studied a model system in which the polymer chains are adsorbed at one of their end segments onto the surface and the adsorbed polymer molecules are sufficiently long and flexible that the chains obey random-flight statistics.

For the volume restriction effect, the positive free energy arises from the loss of configurational entropy as the approaching surfaces reduce the volume available to the polymer chains. Based on the diffusion ~~diffusion~~ equation, the volume restriction term, $\Delta G_{VR}(d)$, was derived

$$\Delta G_{VR}(d) = - 2nKT \ln P_N(d) \quad (24)$$

where n is the number of chains per unit area on the two surfaces and $P_N(d)$ is the volume restriction function which gives the probability that all chain segments and the free ends of the chains are within a distance d of the surface on which the chain is adsorbed.

The osmotic pressure effect is due to the mixing of the polymer

molecules and solvent molecules in the interaction zone. As surface with adsorbed polymer segments are brought together the density of polymer segments increases. The consequent change in free energy, ΔG_m , can be derived using the Flory-Krigbaum theory (60). Indeed,

$$\Delta G_m(\delta) = 6(2\pi)^{\frac{1}{2}} (a^2 - 1) K T n B(\delta) \quad (25)$$

where a is the chain expansion factor, $B(\delta)$ is the segment density functions.

Meier's theory showed that at high surface coverage, the energy of mixing is important in stabilization; whereas, at low surface coverage, the volume restriction effect is predominant. The problem which arose in this theory was due to the use of an incorrect segment density distribution function which apparently allowed penetration of the impenetrable particle surface and thus the osmotic free energy was underestimated.

Hesselink (93,94) has corrected Meier's error and recalculated the configurational statistics of adsorbed polymers on the approach of a second surface. Hesselink, Vrij and Overbeek (120) extended Meier's theory to systems in which the polymer molecules were adsorbed onto a flat surface with many segments attached in equal tails, in equal loops, in a loop size distribution derived by Hovee et al (90) for homopolymers where all the segments have ^{an} a priori ~~an~~ equal chance to become adsorbed, and in loop size distribution for a co-polymer attached to the surface with anchor segments randomly distributed along the chain. They calculated the, ΔG_{VR} , free energy per unit area for the volume restriction effect at a distance d between two plates.

$$\Delta G_{VR} = - 2 K T \sum_i n_i \ln R(i, d) \quad (26)$$

where n_1 is equal to the number of tails or loops containing 1 segments, as given by the appropriate size distribution (93,94) in the case of homopolymers or random co-polymers and $R(i,d)$ is the relative loss of configuration of tails and loops (94). In the case of equal loops, the equation derived was (94)

$$\Delta G_{VR} = 2vKT V(i,d) \quad (27)$$

where v is the number of molecules per unit surface area and $V(i,d)$ is the volume restriction function. The osmotic free energy contribution ΔG_m was given by for example, for equal loops,

$$\Delta G_m = 2(2\pi/9)^{\frac{1}{2}} v^2 KT (a^2 - 1) \langle r^2 \rangle M(i,d) \quad (28)$$

where $\langle r^2 \rangle^{\frac{1}{2}}$ is the r.m.s. end to end distance of the polymer chain and $M(i,d)$ is the osmotic pressure mixing function. Combining the free energies from the volume restriction and mixing effects gives the total repulsive energy of the steric effect

$$\Delta G_s = \Delta G_{VR} + \Delta G_m \quad (29)$$

comparing experimental results with theoretical calculations of steric stabilization (117,119,120), Evans and Napper (118,121) found that Fischer's theory fitted qualitatively but was not quantitatively correct (see Section 2:3:2:2). The theories of Meier and Hesselink, Vrij and Overbeek failed to describe the results even qualitatively since the simple combination of the volume restriction term and the mixing term led to an insidious error. The separate calculation of the loss of configurational entropy of the polymer chains implies that pure solvent is mixed with compressed polymer whereas mixing of solvent should be with random, not compressed, polymer. Evans and Napper suggested that two separate regions of close approach must be distinguished: the interpenetration domain which is characterized by an interparticulate separation of between one and two contour lengths

of the stabilizer chains and the interpenetration plus compression domain which is entered on closer approach. Based on the Flory-Krigbaum theory, they considered equations of steric repulsive energy for tails between two flat plates, equal spheres and unequal spheres (118). The approach predicts that the repulsive potential energy ΔG_s per unit area, for example, for two flat plates is given by:

$$\Delta G_s^{fp} = 2W^2 N_A (v_2^2/v_1) (0.5 - X_1) KTR \quad (30)$$

where

$$R = \int_0^d \rho_d^2 dx - \int_0^\infty \rho_\infty^2 dx + \int_0^d \rho_d \rho_d' dx \quad (31)$$

In Eq. (30), W is the weight of the stabilizing polymer per unit area of the particle surface, N_A is Avogadro's number, v_2 is the partial specific volume of the polymer, v_1 is the volume of the solvent molecule and X_1 is the Flory interaction parameter; note that in this equation the volume exclusion term is omitted. In Eq. (31), ρ_d is the normalized segment density distribution function for a separation d in the direction x normal to the surface and ρ_d' is the mirror image of ρ_d obtained by reflection and translation of the coordinate axis in the second plane. These segment density distribution functions are taken from the work of Hesselink (93,94,120). The first two integral terms in Eq. (31) are derived from the compression of the stabilizing chains in the domain where the minimum separation of the two surfaces is smaller than the contour length, L , of the polymer chains in the adsorbed layer i.e. $0 < d < L$ whereas the third integral term arises from intermolecular interpenetration in the domain of $L < d < 2L$.

Note that this theoretical prediction shows good qualitative agreement with the experimental results (121).

Using the Derjaguin method (122), it is possible to calculate the repulsive potential energy for two identical spheres, ΔG_s^S , provided that the thickness of the adsorbed layer is much less than the particle radius a . Thus,

$$\Delta G_s^S = 2\pi a w^2 N_A (v_2^2/v_1) (0.5 - \chi_1) KTS \quad (32)$$

where

$$S = \int_{d_0}^{\infty} R dd$$

is taken from d_0 , the minimum separation, to ∞ of $R dd$.

To make their theory quantitative, Smitham, Evans and Napper (116) compared the results from their earlier theory (118) with the experimental data given by Doroszkowski and Lambourne (123). They found that the theoretical repulsive energy was too small at large distances and too large at small distances. The reason for this is that the parameters R , for flat plates, and S , for spheres, in the previous theory (118) use isolated chain segment density distribution function; this results in insufficient extension of the chains normal to the interface. Using different segment density functions, they proposed a more sophisticated theory in which several models for monodispersed adsorption of polymer chains were given. For example, at exponential segment density distribution for polymer loops (125), if $L \leq d_0 < 2L$ (only interpenetration can occur), for two flat plates,

$$R_i = b^2 (2L - d_0) e^{-bd_0} / (1 - F')^2 \quad (33)$$

where $F' = e^{-bL}$ is the fraction of segment with b as the scaling constant in the exponential distribution function; Smitham and Napper (125) found that $F' = 0.01$ is appropriate for an exponential, whereas

for two spheres,

$$S_1 = [e^{-2bL} + e^{-bd_0} (2bL - bd_0 - 1)] / (1 - F')^2 \quad (34)$$

if $0 < d_0 < L$ (interpenetration plus compression can occur),

for two flat plates,

$$R_{1+c} = [B(1 - e^{-2Bd_0}) + 2B^2d_0e^{-Bd_0} - b(1 - e^{-2bL})] / 2(1 - F'')^2 \quad (35)$$

where $F'' = e^{-Bd_0}$ and $B = bL/d_0$; the magnitude of the scaling factor B depends upon the plate separation,

and again for two spheres,

$$S_{1+c} = bL [e^{-2bL} + 2e^{-bL} - 1 + 2e^{-bL}(e^{-bL} - 1)/bL + (e^{-2bL} + 2e^{-bL} - 1) \ln L_0 + (1 - e^{-2bL})_{L_0}] / 2(1 - F') \quad (36)$$

where $L_0 = d_0/L$ and F' is set equal to F'' for consistency.

To calculate the repulsive energy between two flat plates or two spheres the relevant values of R or S are substituted into Eq. (30) or Eq. (32) respectively for each of the appropriate domains.

They also developed theories for interpenetration and interpenetration plus compression at constant (116) and Gaussian (116, 124) segment density distribution for polymer tails between two flat plates and between two spheres.

Hesslink (126) considered the arguments of Napper et al (118, 121, 127). He showed that Napper's comparison of experimental observations with theoretical curves with the omission of the volume restriction term from the interaction equation was invalid for low

surface coverage but for high and medium surface coverage the osmotic repulsion was usually much larger than the volume restriction term and the latter neglect was justified. Hesselink also compared the increase in free energy per tail with the HVO theory and with Dolan and Edward's statistical calculation of the volume restriction effect (128) in which allowance was made not only for restriction of configurational freedom caused by the second particle but also for the excluded volume due to the polymer segment.

2:3:2:4 Elastic theories

Elastic energy generated by the polymers in the adsorbed layer stabilizing the particles was first suggested by Jäckel (129) and later emphasized by Ottewill (97). However, their work was handicapped by lack of information about the elastic moduli of the adsorbed layers. Napper et al (130, 124) used the Flory net-work theory (27) to develop equations for elastic energy contributions. They considered that elastic energy contribution occurs only when particles are compressed i.e. in the $0 < d_0 < L$ domain.

At exponential segment density distribution function of polymer loops, for two flat plates (125)

$$\Delta G_{fp}^E = 2KTv[D - 1 - \ln D]/(1 - F'') \quad (37)$$

where $D = d_0/L$ and $v =$ number of attached chains per unit area,

$$\Delta G_S^E = 2\pi KTVaL [(1 - D^2)/2 + D \ln D]/(1 - F'') \quad (38)$$

comparison of theory and experiment of the total free energy (124) showed that agreement was not good at small distances of separation due to the significant contribution of elastic energy to the total free energy.

Although the foregoing theories of steric stabilization are not quantitatively reliable they provide a consistent qualitative interpretation of steric stabilization. In summary, some of the important governing factors can be drawn out:

- (a) the conformation of the polymer at the interface
- (b) the segment density distribution in the adsorbed layer
- (c) the concentration of polymer in the adsorbed layer
- (d) the molecular weight of the adsorbed polymer
- (e) the solvent quality of the medium.

2:4 Electrostatic stabilization

2:4:1 The charge in the electric double layer

When ions are present there will be a variation in their density near the interface. Suppose that it were possible to divide the bulk phase into two, each of the separated phases would carry an equal and opposite charge. This is the formation of the electric double layer. Most solids, when in contact with an aqueous medium, acquire a surface charge forming an electric double layer. Charging mechanisms are as follows:

- (a) Ionization: the dissociation of any ionogenic groups present on the particle leave a charged surface. For example, the functional groups $-\text{COOH}$ and $-\text{SO}_4$ of polystyrene latex ionize at high pH giving a negative charge. Proteins carry positive or negative charges depending on pH.
- (b) Ion adsorption: the unequal adsorption of positively and negatively charged ions provides a surface charge on the particle. Usually, ions with high charge number and also surface active agents

with a hydrophobic and charged part will determine the surface charge after adsorption. Haydon (131) has suggested that the occurrence of a negative zeta potential can not in general be due to hydroxyl ion adsorption but is because the cations are unable to approach the interface as closely as the anions. This situation generally holds in various degrees for a number of simple 1:1 and 2:1 inorganic electrolytes.

(c) Ion dissolution: ionic substances can acquire a surface charge by virtue of dissolution of the ions of which they are composed. For example, an excess of I^- ions remains on AgI particles when they are suspended in aqueous medium.

The surface charge influences the distribution of nearby ions in the medium. Ions of opposite charge (counter ions) are attracted to the surface in the inner phase of the double layer and ions of like charge (co-ions) are repelled away from the surface in the outer phase of the double layer; this together with thermal mixing of the ions leads to a diffuse distribution of ions.

2:4:2 The diffuse double layer

A theory of the diffuse part of an infinite plane double layer was proposed by Gouy (132) and Chapman⁽¹³³⁾. The model they used is based on the assumptions that the concentration of ions within the dispersion medium must be low in order that interactions between ions may be neglected. The charge is assumed to be uniformly distributed on the flat surface. Ions in the dispersion medium are treated as point charges of negligible volume. The dispersion medium is regarded as having the same value of permittivity ϵ throughout the diffuse layer. The ions in

the solution are assumed to obey a Boltzmann distribution where the potential decay is approximately exponential.

$$n_i = n_0 \exp(-Ze\psi / KT) \quad (39)$$

where n_i is the number of ions of type i per unit volume at a distance from the interface where the potential is ψ , n_0 is number of ions in the bulk solution, Z is either a positive or negative ion valency and e is the electronic charge. The electric potential ψ and the density of the space charge ρ in the solution are related by Poisson equation

$$\frac{d^2\psi}{dx^2} = -\rho/\epsilon \quad (40)$$

The charge density can be related to the ion concentration which is given by the summation of the ionic charge

$$\rho = \sum Z e n_i \quad (41)$$

Combining Eqs (40), (41) and (39), the Poisson-Boltzmann equation is obtained

$$\frac{d^2\psi}{dx^2} = -1/\epsilon \sum Z e n_0 \exp(-Ze\psi/KT) \quad (42)$$

The solution of this expression (5), with the boundary conditions taken into account, can be written in the form

$$\psi = \frac{2KT}{Ze} \ln\left(\frac{1 + r \exp(-kx)}{1 - r \exp(-kx)} \right) \quad (43)$$

where

$$r = \frac{\exp(Ze\psi_0/2KT) - 1}{\exp(Ze\psi_0/2KT) + 1} \quad (44)$$

and

$$k = \left(\frac{2e^2 n_0 Z^2}{\epsilon KT} \right)^{\frac{1}{2}} \quad (45)$$

If $Ze\psi_0/2KT \ll 1$, the Debye-Huckel approximation can be applied (134)

i.e.

$$\exp(Ze\psi_0/2KT) = 1 + Ze\psi_0/2KT$$

Therefore, the Eqs (43) and (44) become

$$\psi = \psi_0 \exp(-kx) \quad (46)$$

or

$$kx = \ln \psi_0 / \psi \quad (47)$$

showing that at low potentials the potential decreases exponentially with distance from the charged surface. Close to the charged surface, where the potential is relatively high and the Debye-Huckel approximation invalid, the potential decreases at a greater than exponential rate. Eq. (46) also shows that $1/k$ has the dimensions of length. It is customary to refer to it as the thickness of the diffuse double layer which is dependent on the concentration of the added electrolyte. Increase of electrolyte concentration results in a reduction of the double layer thickness.

2:4:3 The inner part of the double layer

The Gouy-Chapman model of the electric double layer outlined above contains some unrealistic factors. For example, the ions are treated as point charges; any specific effects related to ion size are neglected. Stern (135) proposed a model in which the double layer is divided into two parts separated by a plane (Stern plane) located at about a distance of s from the surface; s is called the thickness of the Stern layer. In the first part, the inner region, the ions are adsorbed specifically to the surface by electrostatic or van der

Waals forces which are strong enough to overcome thermal agitation. The centres of any adsorbed ions are located in the Stern layer i.e. between the surface and the Stern plane. The electric potential in this region drops linearly with distance from a value ψ_0 at the surface to a value ψ_s which is called the Stern potential. The ions remaining in the second part, beyond the Stern plane from the diffuse part of the double layer, are treated according to the Gouy-Chapman theory.

A more sophisticated model than that of Stern's was proposed by Grahame (136) who subdivided the Stern layer into two further regions i.e. the inner Helmholtz region, immediately adjacent to the interface, contains a layer of specifically adsorbed ions; these ions are no longer hydrated. The outer Helmholtz region contains the hydrated counterions and the outermost surface of this region lies at the distance of closest approach to the surface of the hydrated ion corresponding to the outer limit of the Stern region.

The Gouy-Chapman, the Stern and the Grahame models assume that charges are distributed uniformly on the surface. However, the surface charges are not smeared out but are as an assembly of discrete charges surrounded by space depleted of other counterions. This effect was introduced by Esin and Markov (137). Levine et al (138) incorporated this effect into the Stern-Langmuir isotherm and found that this theory predicts that under certain conditions, ψ_s goes through a maximum as ψ_0 is increased. This explains the experimental observations that zeta potentials for silver iodide sols go through a maximum as the surface potential is increased.

2:4:4 Overlapping double layers and interparticulate repulsion

The interaction of overlapping double layers will cause an electrostatic repulsive force between the particles. Derjaguin and Landau (3) and Verwey and Overbeek (4) made use of the Gouy-Chapman theory for the diffuse part of the double layer to take account of this interaction. For flat plates the free energy of repulsion V_R is given by the expression

$$V_R = \frac{64nKT}{k} \left(\frac{\exp(Ze\psi_0/2KT) - 1}{\exp(Ze\psi_0/2KT) + 1} \right)^2 \exp(-kd) \quad (48)$$

where n is the number of ions per unit volume of solution. For spherical particles, which are probably more relevant to the case of suspensions, Derjaguin (122) developed a method for calculating the repulsive potential when the range of interaction is small compared with the radius of the spheres (i.e. $ka \gg 1$). Hence,

$$V_R = \frac{\epsilon a \psi_0^2}{2} \ln(1 + \exp(-kd)) \quad (49)$$

Eqs (48) and (49) are only valid for the case of small interactions (i.e. $d \gg 1/k$), and low potentials ($\psi_0 < 50\text{mV}$). However, it is generally considered that the equations can be used as an approximation for most suspensions. The repulsive energy in the above derivations takes no account of the Stern layer effect, as the direct influence of the interaction of the Stern layers occurs only when the interaction distance is very small and the surface potential is very high. Verwey and Overbeek (5) pointed out that for weak interactions, the Stern potential will be practically unaffected and the surface potential can be replaced by the Stern potential. In practical terms, the zeta potential is usually a valid approximation to the Stern potential. In the case of spheres having high potentials and separated by short distances, Loeb et al (139) developed a complex numerical solution for the repulsive potential. Hogg et al (140) derived a

general expression for two unequal spheres with different surface potentials but this is only applicable when surface potentials are as small as 25 mV. Other situations such as constant potential and constant charge with small and large separations between parallel plates and between spheres have been examined by Honig and Mul (141). For complex geometry of rod like particles, interactions have been calculated by Brenner and McQuarrie (142).

2:5 Attraction

The attraction between two neutral atoms was first introduced by van der Waals to explain the properties of nonideal gas molecules (143). Later, this theory was developed by Keesom (144), Debye (145) and London (146) for interactions of Dipole-dipole, dipole-induced dipole and induced dipole - induced dipole molecules respectively. The London interaction is the most important attraction since the energy contributions are much larger than those of the other two types.

The London-van der Waals force also called the London dispersion force is due to the charge fluctuations associated with the motions of electrons in the atoms. The frequency of electronic motions is 10^{15} or 10^{16} per second. The fluctuations in one atom polarize the adjacent atom leading to an attractive force between them.

These three types of van der Waals forces show an attractive energy depending on the inverse sixth power of the distance between the two atoms. For the case of aggregation of atoms, the total energy of interaction according to Keesom and Debye forces is not equal to the sum of the individual interaction energies but is usually much smaller. The London energy between two atoms, however, is to the first

approximation independent of the interactions with other atoms, this makes the total London interaction energy between atoms a simple summation of the separate energies. The energy of attraction, for hydrogen like atoms, is given by

$$V_L = - 3hva^2/4r^6 \quad (50)$$

where r is the distance of separation, a is the polarizability between two atoms, h is Planck's constant and v is the characteristic oscillatory frequency of an electron.

2:5:1 The microscopic approach

Following the concept of the attractive force between gas molecules developed by London, Kallmann and Willstatter (154) suggested that the approximate additivity of the van der Waals forces could lead to much stronger and much longer range attractions when apply to colloidal systems. From this idea, Hamaker (147) derived expressions for the attraction of two spheres of radius a in a vacuum with a distance r between their centres.

$$V_A = - \frac{A}{6} \left(\frac{2a^2}{r^2 - 4a^2} + \frac{2a^2}{r^2} + \ln \frac{r^2 - 4a^2}{r^2} \right) \quad (51)$$

For small separations between the spheres i.e. $d \ll a$, Eq. (51)

becomes

$$V_A = - Aa/12d \quad (52)$$

where A is the Hamaker constant;

$$A = (3/4)\pi^2 hva^2 q^2 \quad (53)$$

in which q is the number of atoms per volume of material.

In practice, the colloidal plates or particles are surrounded

by a dispersion medium, and not a vacuum, the Hamaker constant must take account of the effect of the medium. Therefore,

$$A = A_{11} + A_{22} - 2A_{12} \quad (54)$$

where A_{11} and A_{22} are Hamaker constants for the material of the particle and the medium respectively and A_{12} is the associated constant for particle-medium interaction. For A_{12} , it is generally assumed that

$$A_{12} = (A_{11}A_{22})^{\frac{1}{2}} \quad (55)$$

then

$$A = (A_{11}^{\frac{1}{2}} - A_{22}^{\frac{1}{2}})^2 \quad (56)$$

Verwey and Overbeek (4) showed that the attractive energy for two infinite colloidal plates of thickness D and a distance d from each other in a vacuum is given by

$$V_A = - \frac{A}{48\pi} \left[\frac{1}{(d/2)^2} + \frac{1}{(d/2 + D)^2} + \frac{1}{(d/2 + D/2)^2} \right] \quad (57)$$

If the distance between two plates is small compared with their thickness, Eq. (57) simplifies to

$$V_A = - A/12 d^2 \quad (58)$$

Thus, from the above equations, the attractive energy decays comparatively slowly with increasing distance indicating the long range character of the London-van der Waals forces. For very small distances the attractive energy tends to assume an infinitely large negative value and the approximation used is not valid. In addition, Born repulsion between the electron clouds will come into action at very short distance.

The expressions derived above for V_A are not suitable when the attractive force operates over a distance comparable with or larger than 10 nm. For greater distances retardation effect occur due to the finite time electromagnetic waves take to travel

from one atom to another. This retards the process of dipolar attractive energy between atoms of two interacting particles. This effect was first considered by Casimir and Polder (148) who suggested that the London energy decreases as $1/r^7$ instead of as $1/r^6$ for large distance between the atoms. Thus, the corrected equation is given by

$$V_L = - 3h\nu a^2/4r^6 \cdot f(p) \quad (59)$$

in which

$$p = 2\pi r/\lambda;$$

$$\text{for } 0 < p < 3, \quad f(p) = 1.01 - 0.14p$$

$$\text{and for } 3 < p < \infty, \quad f(p) = 2.45/p - 2.04/p^2$$

For practical purposes Schenkel and Kitchner (18) suggested that for distances of particle separations of about 10 to 200 nm, the attractive energy is more accurately expressed by

$$V_A (\text{partially retarded}) = - \frac{Aa}{\pi} \left(\frac{2.45\lambda}{120d^2} - \frac{\lambda^2}{1045d^3} + \frac{\lambda^3}{5.62 \times 10^4 d^4} \right) \quad (60)$$

where λ is the wavelength of intrinsic oscillations of atoms, $\lambda = 10^{-7}$ m. Whereas for distances greater than 200 nm, the attraction is given by

$$V_A (\text{fully retarded}) = - \frac{2.45 Aa\lambda}{120\pi d^2} \quad (61)$$

For retardation occurring between two parallel flat plates and thin films, equations were proposed by Hunter (149) and Sheludko et al (150) respectively. Hunter (149) also tabulated the relation between D and d for correction of the attractive energy. Clayfield et al (151,152) have derived expression for interactions of two spheres and of a sphere and plate according to the Casimir-Polder equation.

Vincent (153) (Section 2:5:3) has recently developed equations for more accurate calculation of the retardation effect. He also criticized both the sets of equations of Schenkel and Kitchener and Clayfield et al in that the former equations break down at a certain distance and for the latter, deviation occurs at large separations and especially for small particles.

2:5:2 The macroscopic theory

The macroscopic treatment of dispersion forces is due to Lifshitz (158). He considered the interacting phases as being continuous and the interaction as occurring through a continuous medium characterized by their permittivity as a function of a characteristic frequency. Within all media the electrons are in continuous motion; this motion gives rise to a long-wave fluctuating electromagnetic field which exists even at absolute zero due to zero point motion; at finite temperatures there are further contributions due to thermal effects. Lifshitz calculated the interaction energy between two flat plates in a vacuum. Later, Lifshitz et al (159) applied this method to two flat plates separated by a third medium.

Following from Lifshitz's theory, Parsegian and Ninham have extended the calculations of interactions across a single thin film (161,162) and a triple films in air (163) and water (160). They derived a general equation (160) for the free energy of non-retarded attraction between two semiinfinite flat plates separated by a medium.

$$V_A = - A(d,T)/12\pi d^2 \quad (62)$$

where

$$A(d,T) = 1.5KT \sum_{n=0}^{\infty} I(\epsilon_n, d).$$

Here, d is the distance between two flat plates, T is the temperature of interaction and ϵ_n is related to the permittivity of the plates and the medium. $A(d,T)$ in Eq. (62) is very similar in form to the result derived by Verwey and Overbeek (Eq. (58)) for a similar configuration from pairwise summation procedures in which A takes on the form of Hamaker constant. However, $A(d,T)$ is now a function of the distance of surface separation and interacting temperature and also involves the permittivity of the materials. Thus, it can not be described in terms of a constant; this should be defined as a 'Hamaker function'.

From the studies of Parsegian and Ninham, several conclusions can be drawn:

- (a) the pairwise summation procedure in the Hamaker approach is in principle incorrect; the van der Waals force between liquid layers is more complex than the simple sum of individual interactions between unit segments of the constituent materials;
- (b) for aqueous systems, because of the highly polar nature of liquid water much of the van der Waals force in this medium comes from polarization at infrared and microwave rather than ultraviolet frequencies;
- (c) by virtue of the low frequency conditions, the van der Waals forces are temperature dependent;
- (d) permittivities are well enough known through the range of frequencies to draw these conclusions and to make quantitative numerical estimates with little ambiguity.

Considerable extensions of Lifshitz's theory have been made to include to the study of temperature dependence (164), the effect of dielectric permittivities of materials (165- 169), and the evaluation of Hamaker functions (168-170). Langbein (171), using a quite different approach, has derived equations for the dispersion forces between spherical particles having a homogeneous layers adsorbed on the surfaces in terms of macroscopic fluctuation fields and the permittivity of the system. Ninham and co-workers have investigated the interaction between two spheres (172) and in some detail the attractive force between thin parallel dielectric cylinders with retarded (173) and unretarded (174) interactions and with the effect of particle anisotropy (175) and with particle conductivity (176). The attractions between ellipsoidal particles and between an ellipsoid and a plane have also been calculated (177). Parsegian (178) and Mitchell and Ninham (179) have discussed the interaction between thin rods at all angles. In addition, complete expressions allowing for the retardation effect have been derived for flat plates with isotropic layers adsorbed on the surfaces (180).

2:5:3 The effect of an adsorbed layer on attraction

The effect of a homogeneous adsorbed layer on the van der Waals attraction between two spheres was considered by Vold (155). She found that the attractive energy due to the presence of the adsorbed layer is always decreased but that the effect is only appreciable in the case of very small particles (<50 nm), or quite thick layers (>2 nm). She also concluded that to obtain maximum protection for a given layer thickness of adsorbed material the Hamaker constants for medium (A_m), particle (A_p) and material (A_s) must be in the order

of $A_m < A_p < A_s$ or $A_m > A_p > A_s$. However, Vold's work has been criticised by Osmond, Vincent and Waite (156). They reevaluated the Hamaker constants influence on the 'Vold effect' and found that the maximum protection effect is in the order of $A_s > A_m > A_p$ and $A_s < A_m < A_p$. They also analyzed the conditions under which the presence of adsorbed layers leads to a net increase or decrease in attraction.

Vincent (153) has extended the above models (155,156) to a consideration of the interaction between particles of various geometries and also of the effects of retardation.

For the general case of two spheres of radii a_1, a_2 , and Hamaker constants A_{p1}, A_{p2} , having adsorbed layers of thickness δ_1, δ_2 , and Hamaker constants A_{s1}, A_{s2} , in a medium of Hamaker constant A_m , the van der Waals attractive energy is given by

$$\begin{aligned}
 -12 V_A = & H_{s1s2} \left(A_{s1}^{\frac{1}{2}} - A_m^{\frac{1}{2}} \right) \left(A_{s2}^{\frac{1}{2}} - A_m^{\frac{1}{2}} \right) + \\
 & H_{p1p2} \left(A_{p1}^{\frac{1}{2}} - A_{s1}^{\frac{1}{2}} \right) \left(A_{p2}^{\frac{1}{2}} - A_{s2}^{\frac{1}{2}} \right) + \\
 & H_{p1s2} \left(A_{p1}^{\frac{1}{2}} - A_{s1}^{\frac{1}{2}} \right) \left(A_{s2}^{\frac{1}{2}} - A_m^{\frac{1}{2}} \right) + \\
 & H_{p2s2} \left(A_{p2}^{\frac{1}{2}} - A_{s2}^{\frac{1}{2}} \right) \left(A_{s1}^{\frac{1}{2}} - A_m^{\frac{1}{2}} \right) \quad (63)
 \end{aligned}$$

where H is the geometric function,

$$H(x,y) = \frac{x}{x^2 + xy + x} + \frac{y}{x^2 + xy + x + y} + 2 \ln \left(\frac{x^2 + xy + x}{x^2 + xy + x + y} \right) \quad (64)$$

and $x = \Delta/2r_1, y = r_2/r_1$, where for

$$\begin{aligned}
 H_{s1s2} & : \Delta = d, \quad r_1 = a_1 + \delta_1, \quad r_2 = a_2 + \delta_2; \\
 H_{p1p2} & : \Delta = d + \delta_1 + \delta_2, \quad r_1 = a_1, \quad r_2 = a_2; \\
 H_{p1s2} & : \Delta = d + \delta_1, \quad r_1 = a_1, \quad r_2 = a_2 + \delta_2; \\
 H_{p2s1} & : \Delta = d + \delta_2, \quad r_1 = a_1 + \delta_1, \quad r_2 = a_2.
 \end{aligned}$$

The attractive energy for two identical spheres as derived by Vold is readily obtained from the above equation. The retardation effect on the H functions for short range H_S and long range H_L interaction between two spheres are expressed as

$$H_S = a \left[\frac{y}{u} + \frac{y}{y+u} + 2 \ln \left(\frac{u}{u+y} \right) \right] + \frac{8br_1^2}{c} \left[2y + (2u+y) \ln \left(\frac{u}{u+y} \right) \right] \quad (65)$$

$$H_L = \frac{a'}{10c} \left[\frac{y(1+y)^2}{u^2} + \frac{y(1-y)^2}{(u+y)^2} - \frac{2(y^2+y+1)}{u} + \frac{2(y^2-y+1)}{u+y} + 4 \ln \left(\frac{u+y}{u} \right) \right] + \frac{b'}{60r_1^2} \left[\frac{2}{u+y} - \frac{2}{u} + \frac{y^2+y+1}{u^2} - \frac{y^2-y+1}{(u+y)^2} - \frac{y(1+y)^2}{u^3} - \frac{y(1-y)^2}{(u+y)^3} \right] \quad (66)$$

where $u = x^2 + xy + x$, $c = r_1 + r_2 + \Delta$,

$$a = 1.01, \quad b = 0.14(2\pi/\lambda), \quad a' = 245(\lambda/2\pi), \quad b' = 2.04(\lambda/2\pi)^2.$$

H_S is valid at a distance not greater than the critical separation of two particles i.e. $\Delta < \Delta_c$, where for $\Delta > \Delta_c$, H_L should be used. The critical separation can be determined by

$$\Delta_c = 109 - 107 \log a + 3.75(\log a)^2 - 4.5(\log a)^3 \quad (67)$$

As expected, retardation decreases the van der Waals attractive force more as the particle separation increases and its effect is greater with larger particles.

The distilled water used in all experiments was doubly distilled from a Fisons Fi-stream all glass still. General chemicals used were of Analytical Reagent grade.

3:1 Nonionic surface active agents

The nonionic surface active agents used were the commercial Texofor range of polyoxyethylene glycol monoethers n hexadecanols (Glovers Chemicals Ltd). These have the general formula $C_{16}H_{33}(CH_2CH_2O)_nOH$ with n taken as 10, 18, 30, 45 and 60 for Texofor A10, A18, A30, A45 and A60 respectively. Molecular weight based on the molecular formula are as follows:

A10 ($C_{16}E_{10}$) : 683

A18 ($C_{16}E_{18}$) : 1035

A30 ($C_{16}E_{30}$) : 1564

A45 ($C_{16}E_{45}$) : 2225

A60 ($C_{16}E_{60}$) : 2886

In this study, purification was not attempted as they would be used in this state in pharmaceutical practice.

3:2 Nonionic water soluble cellulose polymers

Cellulose is a naturally occurring polymer. The chemical structure of the cellulose molecule, as shown in Fig. 8, consists of anhydroglucose units condensed through the 1-4' positions forming a chain molecule. The number of anhydroglucose units in a chain may be of the order of several thousands. Each anhydroglucose unit in the chain contains a primary hydroxyl group in the 6- position and

secondary hydroxyl groups in the 2- and 3- position. Cellulose is essentially polymolecular, the individual molecules differing widely in the number of the anhydroglucose units they contain, the extent of the polymolecularity of a sample having a great influence on its physical properties. Within a cellulose fibre the chain molecules are bound laterally one to another by hydrogen bonds in such a way as to form crystallites separated by amorphous regions. The reactivity of the cellulose in the amorphous regions is greater than in the crystallites. Although the cellulose molecule has been widely investigated no definite conclusion can be drawn as to its size (181).

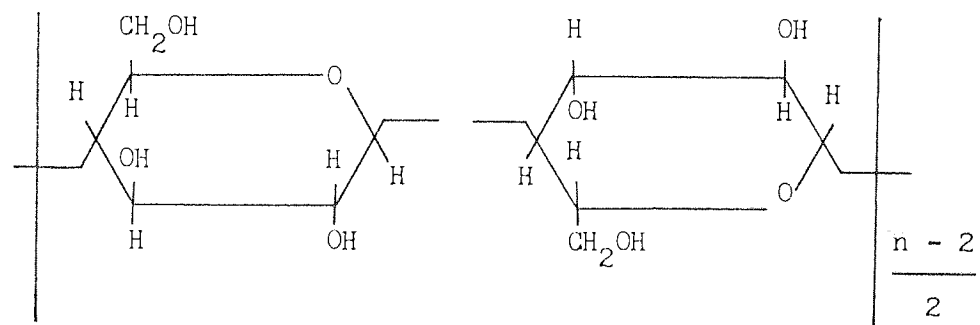


Fig. 8 Structure of cellulose

The three reactive hydroxyl groups in the ring structure of the cellulose can be regarded as similar to the hydroxyl functional group of an alcohol. Reactions occurring with these groups form products whose properties can be characterized according to the reactions and substituents, for example ethers of cellulose which include hydroxyethyl cellulose, hydroxypropyl cellulose and hydroxypropyl methyl cellulose etc. The number of hydroxyl groups in the anhydroglucose unit which is substituted in any reaction is known as the degree of substitution or DS. All three hydroxyl

groups can be substituted. The product from such a reaction will have a DS of three. The substituent can polymerize to form a side chain reacting at the previously substituted hydroxyls. The total substitution will thus be expressed in the average number of moles of substituent attached to each anhydroglucose unit which is known as MS.

In this study, three groups of ether-celluloses were used. (a) Hydroxyethyl cellulose (HEC) (182): hydroxyethyl cellulose, the hydroxyethyl ether of cellulose, is a nonionic water soluble polymer. It was obtained from Hercules Incorporated (Delaware, U.S.A.) known as Natrosol 250R which has MS of 2.5. The R signifies that the hydroxyethyl cellulose has been treated with a small amount of glyoxal to provide fast dispersion and easier dissolving in water. Such treatment does not alter solution viscosity or other solution characteristics and the cellulose chemical structure (182). The structure of Natrosol 250 is shown in Fig. 9.

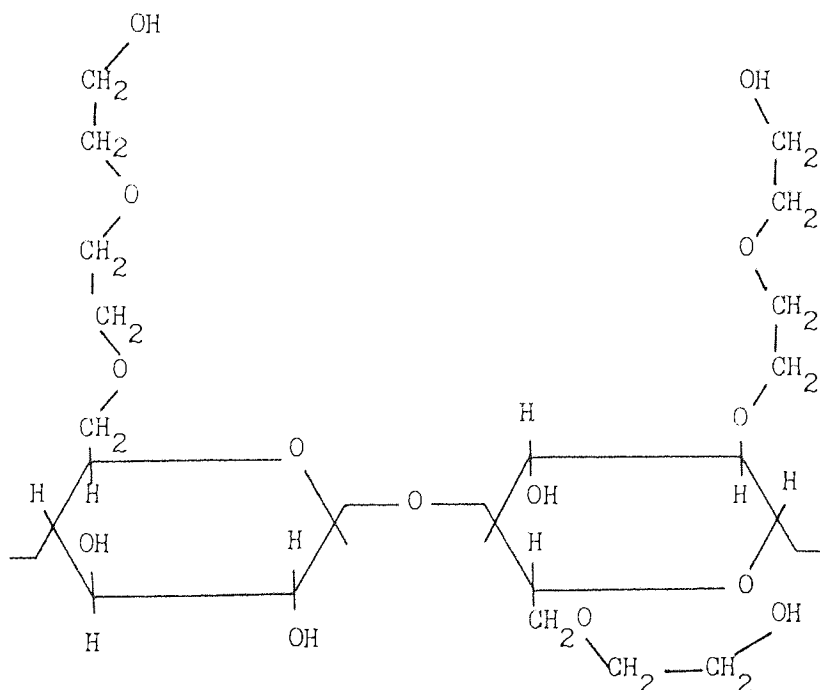


Fig. 9 Structure of Natrosol 250

Two low viscosity grades, Natrosol 250R J and Natrosol 250R L, were used here.

(b) Hydroxypropyl cellulose (HPC) (183): the hydroxypropyl cellulose used was Klucel (Hercules Incorporated, Delaware, U.S.A.) having a MS of 3.0. The structure is given in Fig. 10.

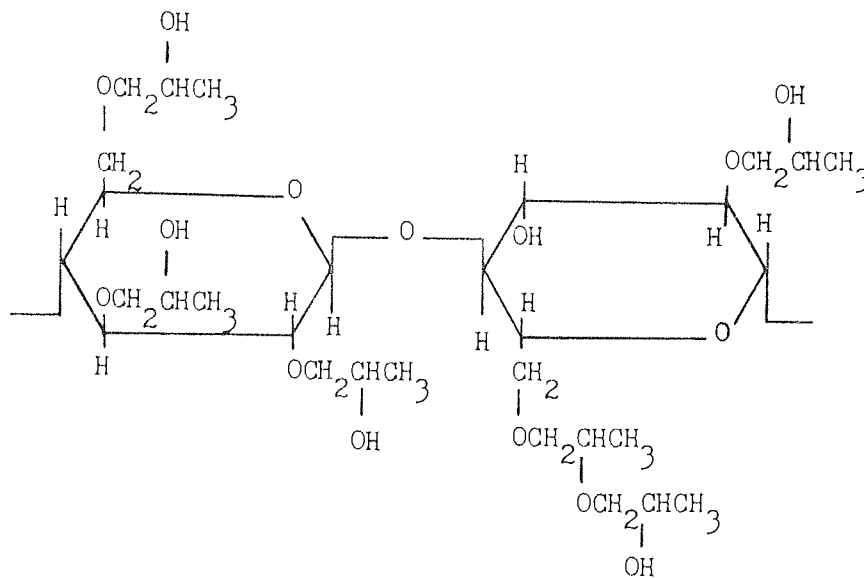


Fig. 10 Structure of Klucel

Klucel is manufactured by treating alkali cellulose with propylene oxide at elevated temperatures and pressures. The propylene oxide is substituted on the anhydroglucose unit through an ether linkage at the three reactive hydroxyl groups. The hydroxypropyl substituents in the cellulose chain contain almost entirely secondary hydroxyl groups which are available for further reaction with the oxides and charring out may take place. This results in formation of side chains containing more than one mole of combined propylene oxide

Hydroxypropyl cellulose is a water soluble polymer with nonionic properties. In this study, low viscosity grade hydroxypropyl celluloses were used. They were Klucel L and Klucel E.

(c) Hydroxypropyl methylcellulose (HPMC) (184): the hydroxypropyl methylcellulose is prepared by reacting methylcellulose through hydroxypropylation (181) thus it is also called the propylene glycol ether of methylcellulose. The structure is shown in Fig. 11.

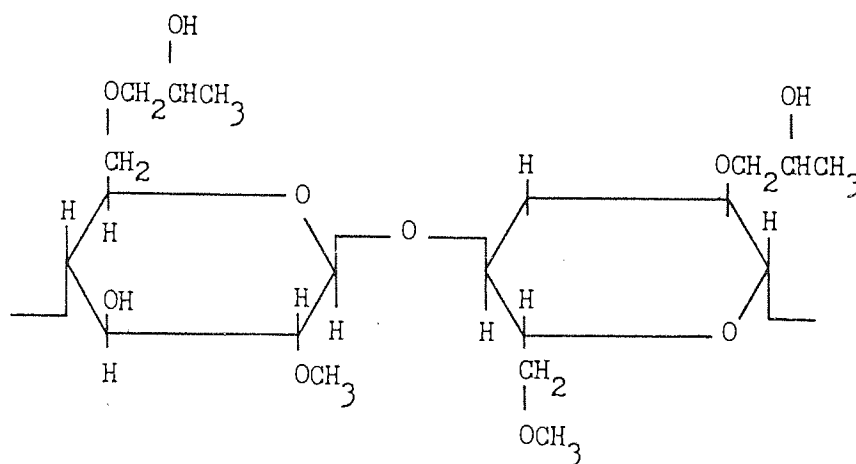


Fig. 11 Structure of hydroxypropyl methylcellulose

It is a nonionic water soluble cellulose. Three commercially available samples of hydroxypropyl methylcellulose were used. They were Pharmacoat 603, Pharmacoat 606 and Pharmacoat 615 with viscosity (2% solution) of about 3, 6 and 15 cps respectively.

3:3 Polystyrene latex

The polystyrene latices used were prepared according to the

method of Chung li and others (185). Potassium persulphate (Fisons A.R. grade) was used as the initiator and was recrystallized twice from distilled water at room temperature. The crystals were then dried in a desiccator with silica gel. They were recrystallized again if the storage time exceeded two weeks. Styrene (B.D.H. Reagent grade) was purified by distillation at 40 - 50⁰C in an atmosphere of nitrogen (B.O.C. white spot) at a pressure of ca. 5 mm Hg. The purified styrene was stored under nitrogen at 5⁰C.

All polymerizations were carried out in a 1 litre three-necked round bottom flask. A PTFE T-paddle stirrer (type Q-ST 7/2) was inserted into the central neck of the flask. The stirrer speed was maintained at 350 rpm and checked frequently with a stroboflash. The remaining two outlets of the flask were used for a water condenser and a nitrogen inlet. Nitrogen was bubbled continuously throughout the reaction, at a low flow rate to minimize evaporation, in order to remove oxygen from the system. The reaction was carried out at a constant temperature in a thermostatted water bath for 24 hrs.

Initially the major part of the water was added to the flask. The required quantity of sodium chloride dissolved in 30 cm³ of water was then added and washed in with a further 20 cm³ of water. After a period of 10 min equilibration in the thermostatted bath, with nitrogen passing, the styrene was added. A further 15 min was allowed for the contents of the flask to attain the bath temperature before the required quantity of potassium persulphate in 30 cm³ of water was added; this was washed in with a further 20 cm³ of water. At the end of the reaction time, the flask was removed from the water bath and allowed to stand for a few minutes until the monomer formed a separate phase on the surface. The latices

were then dialysed against distilled water by using well boiled Visking dialysis tubing. The water for dialysis was changed every 24 hrs. The ratio of water to latex used for dialysis was about 20 to 1. The time required for dialysis was about four weeks. Dialysis considered to be complete when the conductivity of the dialysate become close to that of distilled water (ca. $1.5 \times 10^{-6} \text{ ohm}^{-1} \text{ cm}^{-1}$ at 25°C). In order to avoid contamination of latices with silicates leached from the glass, Pyrex containers were used for dialysis. The purified latices were stored in Pyrex containers in a cool place.

The latices were prepared either by the method indicated or by a two stage method, involving seeded growth:

(a) Latex 3 and 4 - These were prepared by a single stage reaction at a temperature of 65°C . The quantities of materials used were as follows:

Water	708 cm^3
Styrene	921 cm^3
Potassium persulphate	0.1913 g
Sodium chloride	1.1170 g

After dialysis the W/V percentage content was obtained by evaporation of a known volume of latex in an oven at 70°C under pressure. The weight of dried latex was determined. The W/V percentage for latex 3 and 4 was 5.58 and 4.93 respectively.

(b) Latex 3B and 4A - These preparations were carried out by a seeded growth method at 60°C . The seeds used were latex 3 and 4 for latex 3B and 4A respectively. For this type of reaction the seed latex was added first and washed in with the distilled water. The quantities used were:

Styrene	80 cm^3
---------	------------------

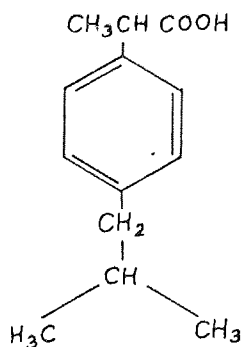
Sodium chloride	1.0260 g
Potassium persulphate	0.3470 g
Seed latex 3 (latex 4)	271 cm ³ (326 cm ³)
Water to	800 cm ³

Thus, the initial number concentration of seed in the flask was 2.2×10^{10} per cm³. After dialysis the W/V percentage contents of solid for each dispersion were 4.70 for 3B and 6.49 for 4A.

(c) Latex 4B - This was prepared by the seeded growth reaction. 237 cm³ latex 4A was used in the polymerization which gave a particle concentration of 3.7×10^9 per cm³ in an initial total volume of 800 cm³. The quantities of styrene, sodium chloride and potassium persulphate used and the reaction procedures were the same as those described in (b). The W/V percentage content after dialysis was 6.27.

3:4 Drug

Ibuprofen B.P. (Boots Co. Ltd, Nottingham) whose chemical name is 2-(4-isobutyl phenyl) propionic acid



with molecular weight of 206.3. It is a white crystalline nonhygroscopic powder and insoluble in water. Two batches were obtained (batch No. CMG 09839T and 9692) and used without purification as supplied.



3:5 Characterization of materials

3:5:1 Nonionic surface active agents

3:5:1:1 Critical micelle concentration (cmc)

The iodine method of Ross and Oliver (186) was adopted. Results are given in Table 2 together with literature values.

Texofor	cmc M $\times 10^{-5}$	Literature value M $\times 10^{-5}$	Reference
A10	5.75	6.00	187
A18	3.47	3.85	187
A30	2.00	2.20	187
A45	1.91	1.75	187
A60	1.23	1.10	157

Table 2 Critical micelle concentrations of Texofors in water at 25⁰C.

3:5:1:2 Partial specific volume

The Texofors were also characterized in terms of their partial specific volume. The partial specific volumes of polymer are important in the theories of polymer solution and elsewhere such as in calculating the solvent interaction parameter, χ_1 .

Measurements of the partial specific volume of the Texofors were made at 25⁰ \pm 0.1⁰C in the concentration range 0.1 - 3 per cent W/V. The pycnometer used was a cylindrical glass vessel with a capillary

cap holding about 25 cm³. Filling was accomplished by means of a syringe and particular care was taken to exclude air bubbles. Buoyancy corrections were applied to each weighing. The partial specific volume, v_2 , was calculated from the formula of Kraemer (188).

$$v_2 = v_s \left[1 - \left(\frac{1-w}{m} \right) \frac{dm}{dw} \right] \quad (68)$$

where v_s is the specific volume of the solution, m is the weight of the pycnometer contents and w is the weight fraction of the solute. $\frac{dm}{dw}$ was determined as the slope of a linear m against w plot given in Fig. 12. As v_2 is essentially a constant at ordinary temperature and pressure for a given solute-solvent system (192), the values for the Texofors were calculated as shown in Table 3.

Texofor	$\frac{dm}{dw}$	v_2
A10	0.5113	0.9504
A18	0.7837	0.9225
A30	0.9591	0.9056
A45	1.1876	0.8828
A60	1.2604	0.8756

Table 3 Values of partial specific volume of Texofors.

3:5:2 Nonionic water soluble celluloses

HEC is readily soluble in either hot or cold water. In the preparation of solutions, room temperature distilled water was used. HPMC and HPC are insoluble in water above 60°C and 45°C

respectively. Thus, in the preparation of HPMC and HPC solutions hot water with a temperature higher than the polymer insoluble temperature was used to disperse the polymer granules to prevent gelatinous masses, then cold water was added. A magnetic stirrer was used for 24 hrs to ensure complete solution. Because of some very small foreign particles and crystal like particles which were not dissolved even after stirring for 48 hrs filtration was made through a 5 μm membrane filter (Oxiod Ltd). In order to prevent reduction in the concentration of the solution after filtration the filters and the filtration assembly were soaked in the Cellulose solutions for 24 hrs then rinsed with distilled water several times and dried before use. The first 10 cm^3 of the Cellulose filtrate which washed through the filter was discarded and the rest of filtrate was used in this study. The filtered Cellulose solutions were stored at 5⁰C and used within 7 days.

3:5:2:1 Molecular weight

The molecular weight of the Celluloses used were determined by viscometric and light scattering measurements.

(a) Viscometry: The viscometer used was a U-tube Ostwald-type (Techinco Ltd). It was selected to give a flow time in excess of 100 sec for the measuring liquid. Thus, a kinetic energy correction was not necessary (215). Before each measurement the viscometer was cleaned with chromic acid and rinsed thoroughly with distilled water, then preconditioned with the test solution for 24 hrs; the solution discarded and the viscometer rinsed thoroughly with distilled water again. Drying was accomplished in an oven at 105⁰C under

reduced pressure. The measurements were made in a viscometer bath at $25^0 \pm 0.1^0\text{C}$ (Series III Viscometer bath, Townson and Mercer Ltd). Five flow times were taken for each sample with the difference not greater than 0.2% from the mean. Timing was made by an electrical timer calibrated to 0.02 sec. Relative viscosities η_r of the solutions were calculated by means of the equation

$$\eta_r = \frac{t_s \rho_s}{t_0 \rho_0} \quad (69)$$

where t is the flow time and ρ is the density and the subscripts s and 0 refer to the solution and solvent respectively.

The intrinsic viscosity $[\eta]$ is an important parameter in characterization of polymers and is of particular value in the estimation of average molecular weight. It is determined from a plot of η_{sp}/c vs c as c approaches zero in which c is the concentration and η_{sp} is the specific viscosity obtained from the relation

$$\eta_{sp} = \eta_r - 1 \quad (70)$$

The most popular equation which correlates η_{sp} and c was given by Huggins (189) when for low concentrations

$$\eta_{sp} = [\eta] + K'[\eta]^2 c \quad (71)$$

The second term on the right of Eq. (71) takes account of solute-solvent interaction and K' is a constant termed the Huggins constant. It is independent of molecular weight at a given temperature. For solid uncharged spheres K' is approximately 2.0 as found both by theory (190) and by experiment (191). For flexible polymer molecules in good solvents K' is often near 0.35 (189). Higher values of K' occur in poor solvents than in good solvents. For

hydroxyethyl cellulose (MS 1.67) K' was found to increase linearly with increasing intrinsic viscosity at a given temperature (192). Results for HEC, HPC and HPMC for the Huggins equation are shown in Fig. 13 and Table 4.

Mark (193) and Houwink (194) first proposed to calculate the molecular weight of a polymer by the following equation

$$[\eta] = KM^a \quad (72)$$

where K and a are constants. Once K and a have been established for a given polymer in a given solvent at a specified temperature the molecular weight can be obtained from the intrinsic viscosity. The exponent a under the theta condition for an unperturbed random polymer coil is 0.5. For a rod like molecule a is equal to 2 (195). According to the Flory-Krigbaum theory for a flexible linear polymer a varies from 0.5 to 0.8 (27).

The molecular weights of the Celluloses used were determined by the following equations:

for HEC (199) in water at 25⁰C,

$$[\eta] = 9.49 \times 10^{-5} M_w^{0.87} \quad (73)$$

for HPC (198) in ethanol at 25⁰C,

$$[\eta] = 2.6 \times 10^{-5} M_w^{0.915} \quad (74)$$

for HPMC (197) in water at 20⁰C,

$$[\eta] = 3.39 \times 10^{-4} M_n^{0.88} \quad (75)$$

Results are shown in Table 4. For HPC in water at 25⁰C, the Mark-Houwink equation was established as

$$[\eta] = 6.25 \times 10^{-5} M_w^{0.84}$$

Cellulose	$[\eta]$	K'	a	M
HEC L (water)	1.400	0.486	0.87	62,000
HEC J	2.041	0.921		95,000
HPC E (ethanol)	1.139	0.439	0.915	120,000
HPC L	1.379	0.662		146,000
HPC E (water)	1.105	0.489	0.84	120,000
HPC L	1.317	0.619		146,000
HPMC 603(water)	0.483	1.104	0.88	4,000
HPMC 606	1.089	0.500		10,000
HPMC 615	1.554	0.575		15,000

Table 4 Physical characteristics of HEC, HPC and HPMC

(b) Light scattering: When a beam of light is incident upon a molecule, a certain fraction of the light will undergo scattering and some may be absorbed while the remainder will be transmitted. Rayleigh (200) showed that scattering of light by small, non-absorbing, spherical particles is caused by optical inhomogeneities. Particles act as a secondary source for the emission of scattered radiation of the same wavelength as the incident light. For an unpolarized incident beam, the intensity of light scattered exhibits an angular dependence. In solutions, part of the light scattering arises from fluctuations in concentration. Debye (201) showed that in the case of molecules whose dimensions are less than about $1/20$ of the wavelength, λ , of the incident light, the turbidity, τ , due to concentration fluctuations is related to the molecular weight, M , of the solute by

$$Hc/\tau = 1/M + 2Bc \quad (76)$$

where c is the concentration of polymer in solution, B is the second virial coefficient and H is a constant given by

$$H = 32\pi^3 n_0^2 (dn/dc)^2 / 3N_A \lambda_0^4 \quad (77)$$

where n_0 is the refractive index of the solvent, n that of the solution and λ_0 is the wavelength in vacuo of the light used. τ is calculated from the intensity of the light scattered at a known angle for example $\theta = 90^\circ$ hence

$$\tau = (16\pi/3) R_{90} \quad (78)$$

where R_{90} is the Rayleigh ratio at 90° which refers to primary scattering from unit volume of solution. Therefore, Eq. (76)

can be expressed in the alternate form

$$Kc/R_{90} = 1/M + 2Bc \quad (79)$$

where

$$K = 2\pi^2 n_0^2 (dn/dc)^2 / N_A \lambda_0^4 \quad (80)$$

Molecular weight can be obtained by extrapolation of a plot of Kc/R_{90} against c to infinite dilution.

There are, however, many polymers having dimensions comparable to the wavelength of the incident light. If the particle size exceeds $\lambda/20$, scattered light waves, coming from different parts of the same particle, will interfere with one another, which will cause a reduction of the intensity of the scattered light to a fraction $P(\theta)$ given by

$$P(\theta) = 1 - 16\pi^2 n^2 / 3\lambda_0^2 \cdot \sin^2 \theta / 2 \cdot R^2 + \dots \quad (81)$$

where R is the radius of gyration of the polymer molecule. Zimm (202) showed that a correction for the excess light scattered Eq. (79) can be rewritten as

$$Kc/R_g = 1/M P(\theta) + 2Bc + \dots \quad (82)$$

As $P(\theta) \rightarrow 1$ for $\theta \rightarrow 0$, Zimm suggested a plot of Kc/R_g against $\sin^2\theta/2 + kc$, where k is an arbitrary constant chosen to spread out the data. Thus, a grid like graph is obtained. Allowing extrapolation to $c = 0$ and $\theta = 0$ the extrapolated points are joined into two lines meeting at the same intercept of Kc/R_g . The reciprocal of the intercept is equal to the molecular weight and the two slopes provide values to calculate B and R^2 .

(a) Preparation of dust free solutions: Because of the strong dependence of the intensity of scattering on the volume of particles, great care was taken to prevent contamination with dust and impurities. All glassware and measuring cells used were filled with chromic acid, soaked overnight and then rinsed several times with dust free distilled water. They were then placed under a laminar flow cabinet for drying. Stock solutions were prepared as described in Section 3:5:2. Solutions for measurements were prepared by dilution of the stock solutions. The dedusting technique of the solutions was operated under the laminar flow cabinet using filtration under pressure through $0.22 \mu\text{m}$ membrane filters which were previously preconditioned with the polymer solution under test. Each solution was filtered at least four times. The concentrations of the filtered polymer solution were checked by the phenol and sulphuric acid method (see Section 4:1). It was found that variations in concentration before and after filtration were not significant.

(b) Refractive index increment: Values of the refractive index increment, dn/dc , were obtained by means of a differential refractometer (Brice-Phoenix, Model BP-2000-V). The limiting sensitivity is about 3 unit in the sixth decimal place of the refractive index difference while the range is 0.01 units. A differential cell of Phoenix Cat. R-100-4 was used. It extended the range of the instrument to 0.07 units and reduced the sensitivity by a factor of one seventh to approximately 2 units in the fifth decimal place. The instrument was calibrated with solution of potassium chloride and sodium chloride at 25⁰C. For calibration purposes the values of the refractive index differences of potassium chloride solution and distilled water and sodium chloride and distilled water were used according to the manufacturer's instructions (203). Values of dn/dc for the HEC and HPMC in water and HPC in ethanol were measured at 25⁰C in the concentration range 0.05 to 0.2 g/dl at 546 nm. The results are presented in Table 5 and Figs 14,15 and 16.

Cellulose	dn/dc cm ³ /g
HEC	0.144
HPC	0.140
HPMC	0.137

Table 5 Refractive index increment data

(c) Light scattering measurements: Light scattering measurements were made with a Photo Gonio Diffusometer (Model 42000, FICA). A diagram of the instrument is given in Fig. 17. This instrument is characterized by a fine optical system. The light source is a high

intensity vapour mercury lamp (SP-500 type, Philips). Residual fluctuations in light intensity are compensated for by a standard phototube which samples a portion of the incident light beam. The sample cell and optical parts of the instrument are immersed in a benzene bath whose temperature is controlled by a Churchill circulating water pump. Since the glass cell has a refractive index close to that of benzene, corrections due to reflections at air-glass interface are eliminated.

The instrument was set according to the operation manual. Calibration was made by using a glass scattering standard supplied by the manufacturer and it was checked by perfectly dust free A.R. grade benzene. The dissymmetry values, for example (i_{30}/i_{150}) , (i_{45}/i_{135}) for benzene were 1.006 and 1.000 respectively, which were the same as the results quoted for dust free benzene in the instrument manual (204). The turbidity for perfectly dust free water determined was $1.69 \times 10^{-5} \text{ cm}^{-1}$ which is in good agreement with the literature values of $1.69 \times 10^{-5} \text{ cm}^{-1}$ (205), $1.7 \times 10^{-5} \text{ cm}^{-1}$ (206) and $1.8 \times 10^{-5} \text{ cm}^{-1}$ (207) at the wavelength of 546 nm and 25°C.

All polymer solutions and solvents for light scattering measurement were carried out at a constant temperature of 25°C and at the wavelength of 546 nm. The concentrations studied were in the range 0.05 - 0.2 g/dl. Measurements were also made at 436 nm which gave the same value of Kc/R as at 546 nm, indicating the absence of fluorescence. The dissymmetry ratio, (i_{45}/i_{135}) , of the solvent, dust free water, was 1.10. The dissymmetry ratio of the solution was calculated from the equation

$$Z_{45,135} = (i_{45} - i_{s,45}) / (i_{135} - i_{s,135}) \quad (83)$$

in which i_s was the intensity of the incident light of the solvent. In most cases, the $Z_{45,135}$ of the Cellulose solutions showed a high value of ca 2. With the aid of an observation window, which was used to check fluctuations due to impurities and dusts contained in the measuring cell of the instrument; it was found that the solutions were in perfect condition. These high dissymmetries were possibly due to the wide molecular weight distribution (198) of the cellulose polymers used.

If the scattered light is incompletely polarized, the vertically polarized incident light will give both vertically and horizontally polarized scattered light or vice versa. There may be a small contribution to the measured intensity arising from fluctuations in orientation of the solute. The application of this correction requires a knowledge of the depolarization factor, Q , which is given by

$$Q = (i_{h,90} - i_{oh,90}) / (i_{v,90} - i_{ov,90}) \quad (84)$$

where i_h and i_{oh} are the intensities of the horizontally polarized light of the solution and the solvent respectively. i_v and i_{ov} are the intensities diffused in vertically polarized light by the solution and solvent respectively. The subscript 90 means that the measurement is at the observation angle of 90° position. The Q for the Celluloses studied were found to vary from ∞ to 0.007 as predicted for polymer solutions in the literature (196,204). Thus, the molecular weights should be multiplied by a correction factor, the Cabannes factor, $(6 - 7Q)/(6 + 6Q)$. In this case, the Cabannes factors were close to unity and the depolarization corrections could be neglected. Unfortunately, because of the high dissymmetry of the measured scattered intensity, it was not possible to obtain a

Zimm plot. Thus, the root mean square radius of gyration could not be calculated. However, it is sufficient to plot the curve according to Eq. (79) to obtain the molecular weights and second virial coefficients. The results of the measurements are shown in Figs 18, 19 and 20 and the molecular weights of the Celluloses used together with their second virial coefficients are shown in Table 6.

Cellulose	Molecular weight		Second virial coefficient mole cm ³ /g ²
	Light scattering	Viscometry	
HEC L	100,000	62,000	9.11X10 ⁻⁴
HEC J	150,000	95,000	8.28X10 ⁻⁴
HPC E	144,000	120,000	4.34X10 ⁻⁵
HPC L	170,000	146,000	9.54X10 ⁻⁴
HPMC 603	25,000	4,000	1.94X10 ⁻³
HPMC 606	36,000	10,000	6.65X10 ⁻⁴
HPMC 615	48,000	15,000	6.83X10 ⁻⁴

Table 6 Molecular weights and second virial coefficients of HEC, HPC and HPMC.

As shown in Table 5, the molecular weights found by light scattering vary considerably from those found by viscometry. The higher values may be due to the polydispersibility of the unfractionated cellulose molecules in solution. For HPMC the molecular weights obtained from viscometry are number average molecular weights, M_n , and from light scattering are weight average molecular weights, M_w . The M_w/M_n ratios vary from 3.2 to 6.3, which compare with the M_w/M_n literature values of 11.6 for unfractionated HPC (198) and 3.2 for fractionated HEC (192).

3:5:2:2 Partial specific volume

The method used has been described in Section 3:5:1:2. The concentration range studied was from 0.05 to 0.2 g/dl and the temperature was at 25⁰C. The m against w plots are shown in Figs 21, 22 and 23 for HEC, HPC and HPMC solutions respectively. The results of partial specific volume are given in Table 7.

Cellulose	dm/dw	v ₂	Average v ₂
HEC L	2.5321	0.7475	0.7475
HEC J	2.5321	0.7475	
HPC E	1.2242	0.8789	0.8789
HPC L	1.2242	0.8788	
HPMC 603	1.9634	0.8045	0.8046
HPMC 606	1.9634	0.8046	
HPMC 615	1.9634	0.8046	

Table 7 Partial specific volumes of HEC, HPC and HPMC.

3:5:3 Polystyrene latex

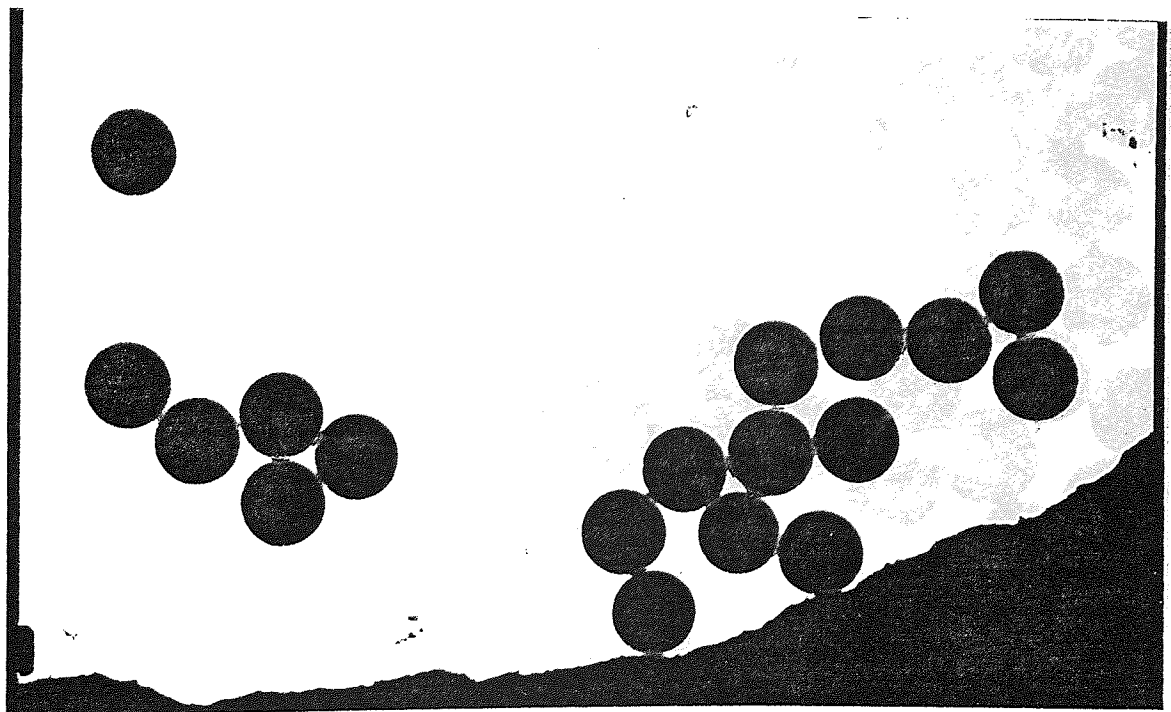
(a) Particle size analysis: Samples were examined under the transmission electron microscope (Jeol Jem 100 B) which was well calibrated at the Department of Metallurgy, Aston University. The particle size determinations were made manually. For each sample at least 300 particles were measured. Photographs of the samples which were monodisperse are given on the following plates. Histograms of the



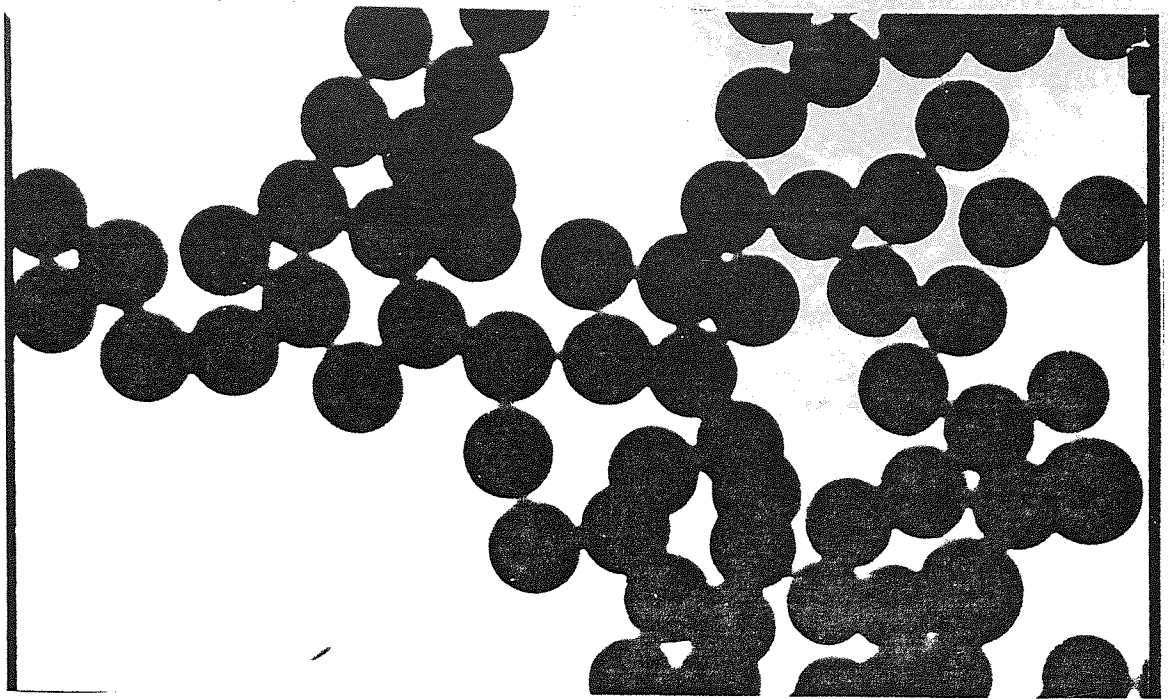
LATEX 3



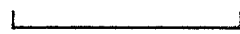
5 micron



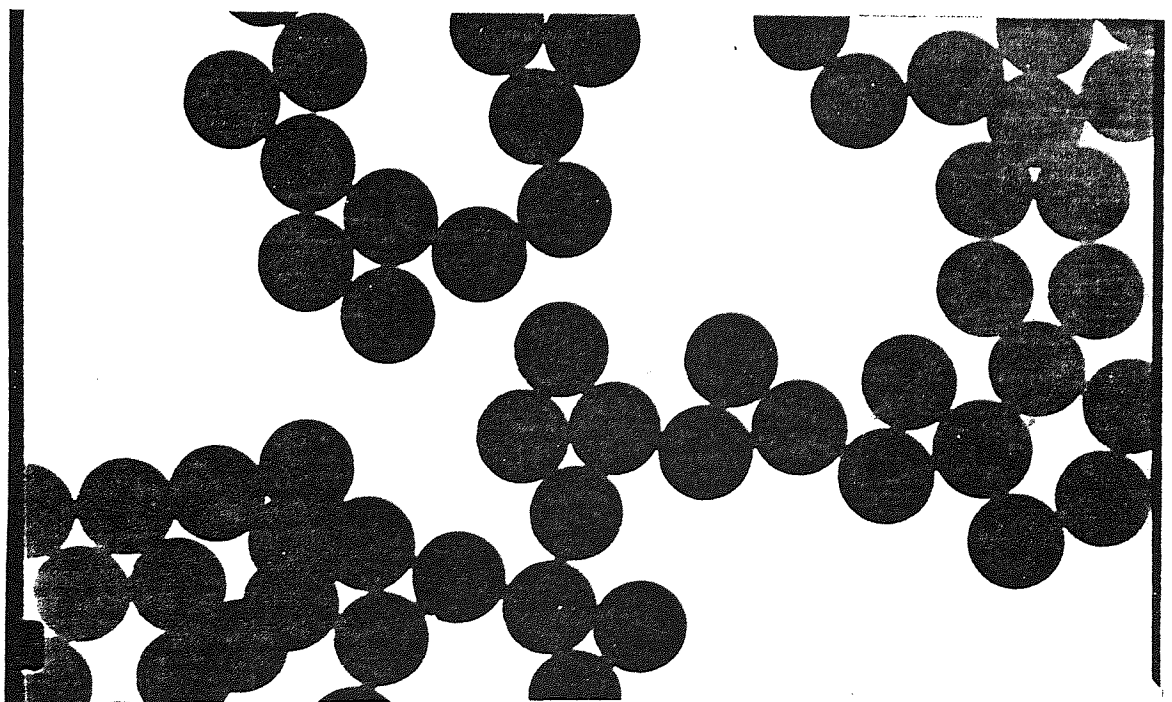
LATEX 4



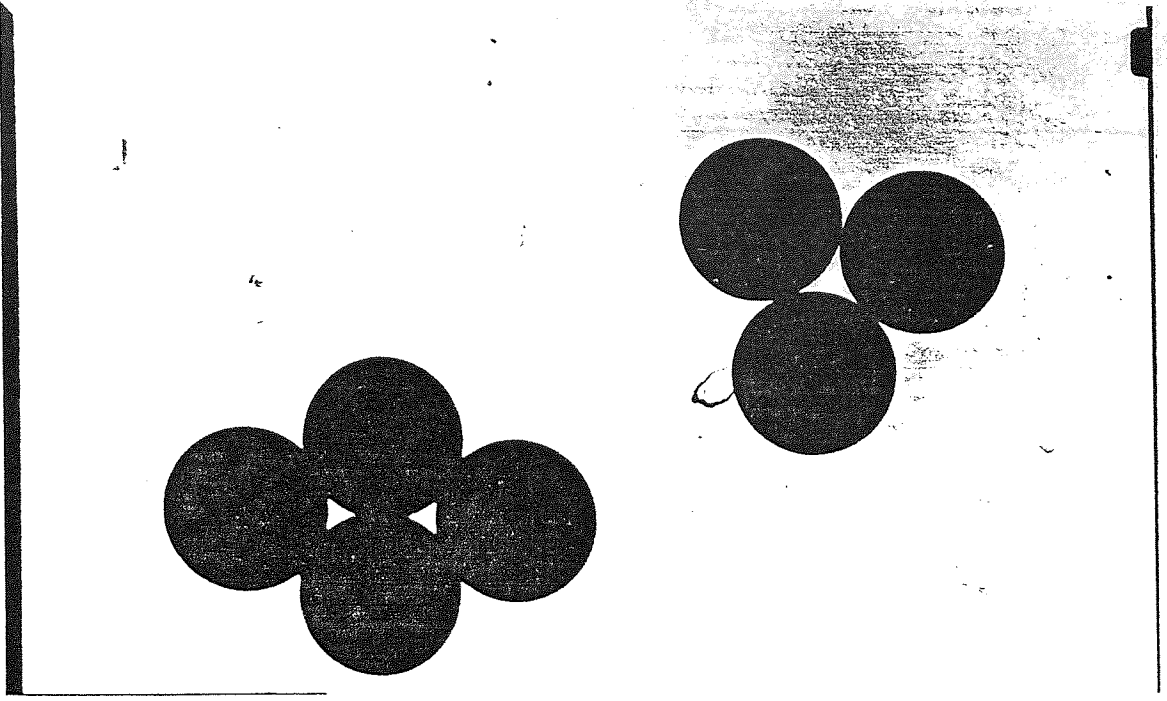
LATEX 3B



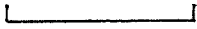
5 micron



LATEX 4A



LATEX 4B



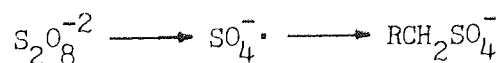
5 micron

particle size distribution are given in Figs 24, 25 and 26. The data obtained are as follows:

Batch of latex	Mean diameter μm	Mold diameter μm	Variation on the mean %
3	1.160	1.17	2.1
4	1.184	1.17	3.3
3B	2.083	2.06	5.8
4A	2.111	2.08	2.9
4B	4.341	4.40	7.4

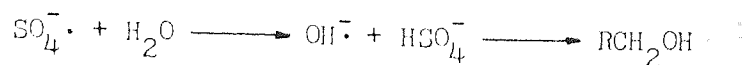
(b) Surface groupings analysis: The formation of surface charge groupings on the latex particle depends on the method of preparation (208). In the method of preparation used here, potassium persulphate was used as an initiator. The persulphate decomposes to form free radicals during polymerization which originate groupings on the latex surface. There are two types of acidic groupings, one of which is much stronger than the other i.e. sulphate and carboxyl groups. Whereas, hydroxyl group may also be present.

The sulphate groupings formed on the latex surface are clearly a consequence of the interaction between monomer molecules in the aqueous phase ~~and the~~ and the generated free radicals of the persulphate ion (209) i.e.

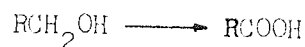


Kolthoff and Miller (210) have shown that the sulphate ion radicals

react with water to form hydroxyl radicals which may combine with the monomer molecules by establishing hydroxyl groupings on the latex surface.



Due to oxidation during the polymerization hydroxyl groupings can also be oxidized to carboxyl groupings



Therefore, because of the presence of the sulphate and carboxyl groupings on the latex surface, the latex particles are negatively charged as shown by Ottewill and Shaw (211).

It is possible to determine the types and the numbers of ionizable end groups on the surface of the latex by conductometric titration (209) with carbonate free sodium hydroxide solution. The titrations were carried out with a 5 cm³ sample of dialysed latex dispersion in a thermostatted glass container at 25⁰C. The latex dispersion was stirred by means of a magnetic stirrer and a continuous stream of nitrogen was passed over the dispersion to exclude carbon dioxide. Conductivity determinations were made with a Wayne Kerr B642 conductivity bridge having platinum electrodes. 0.001 N sodium hydroxide solution was added by using an Agla micrometer syringe. Results obtained for latex 3B and 4A are shown in Figs 27 and 28 respectively; these indicate that the surface of the latex contained both sulphate and carboxyl groupings which show two distinct regions in the curves.

The number of charged groups per unit area of the latex surface can be estimated by knowing the specific surface area and the equivalents of NaOH used. The results are summarized as:

	Latex 3B	Latex 4A
No. of $-SO_4/m^2$	9.53×10^{16}	4.90×10^{17}
No. of $-COOH/m^2$	1.32×10^{17}	7.74×10^{17}
$m^2/-SO_4$	1.05×10^{-17}	2.04×10^{-18}
$m^2/-COOH$	7.59×10^{-18}	1.29×10^{-18}

When the surface grouping is completely ionized there is one electron of charge of $1.60 \times 10^{-19}C$ for that area.

3:5:4 Drug-Ibuprofen B.P.

(a) Melting point: The melting point was determined by a Melting Point Apparatus (Gallenkamp) and found to be $78.0 - 80.0^{\circ}C$ for batch 9692 and batch CMG 09839T. The literature value (213) is $74 - 76^{\circ}C$.

(b) Density: The density of ibuprofen powder was obtained by using a pycnometer of 25 cm^3 and nonionic surface active agent (0.1% w/v Pluronic F68 with density of 0.998 in water at $25^{\circ}C$) as dispersing agent at $25^{\circ}C$. The densities of both batches were found to be 1.20 g/cm^3 .

(c) Particle size analysis: For batch 9692, the particle size distribution was obtained using a photoextinction sedimentometer (Evans Electroselenium Ltd) (Fig. 30). The basic principle of the

photosedimentation technique is the combination of the gravitational settling of the particle (Stokes' equation) and the photoelectric measurement (Lambert-Beer equation) (214). In this method, saturated ibuprofen solution was used as the suspension fluid and the dispersing agent used was 0.1% W/V Pluronic F68. The experimental temperature was at 25⁰C. The result of the particle size distribution is shown in Fig. 29 on log probability scales. The weight mean 50% size is 21.0 μm .

For batch CMG 09839T, the Coulter Counter method (model TA) was used to determine the particle size distribution at Boots Co Ltd, Nottingham. A diagram of the instrument is shown in Fig. 31. As a particle suspended in the conducting liquid passes through a small orifice, with electrodes on either side, a change in electrical resistance occurs. This change of resistance generates a voltage pulse whose amplitude is proportional to the volume of the particle. This pulse is amplified, sized and counted. From the derived data the size distribution of the suspended particles may be determined. In this experiment, the conducting electrolyte used was ibuprofen saturated saline. The result of the size distribution is given in Fig. 29. The mean value 50% size diameter is 24.6 μm .

(d) Specific surface area: Specific surface areas of both batches of ibuprofen were obtained using a Quantosorb at Boots Co Ltd. The results are:

Batch 9692 - 0.61 m^2/g

Batch CMG 09839T - 0.55 m^2/g

Specific surface area, S_w , may also be calculated using (2)

$$S_w = \frac{6}{Dd_{vs}} \quad (85)$$

where D is density of the particle and d_{vs} is the mean volume-surface diameter of the particle which can be obtained according to the Hatch-Choate equation (2).

$$\log d_{vs} = \log d_g - 1.151 \log^2 \sigma_g \quad (86)$$

in which d_g is the geometric mean diameter which is the 50% log-probability plot of particle size distribution (Fig. 29) and σ_g is the geometric standard deviation

$$\sigma_g = \frac{84\% \text{ size}}{50\% \text{ size}} = \frac{50\% \text{ size}}{16\% \text{ size}} \quad (87)$$

The calculated specific surface areas of each batch are:

Batch 9692 - 0.3 m²/g

Batch CMG 09839T - 0.24 m²/g

Compared with those obtained from the Quantosorb, the agreement for the above results is not good. This^{is} probably because the assumption in Eq. (85) that the particles are spherical.

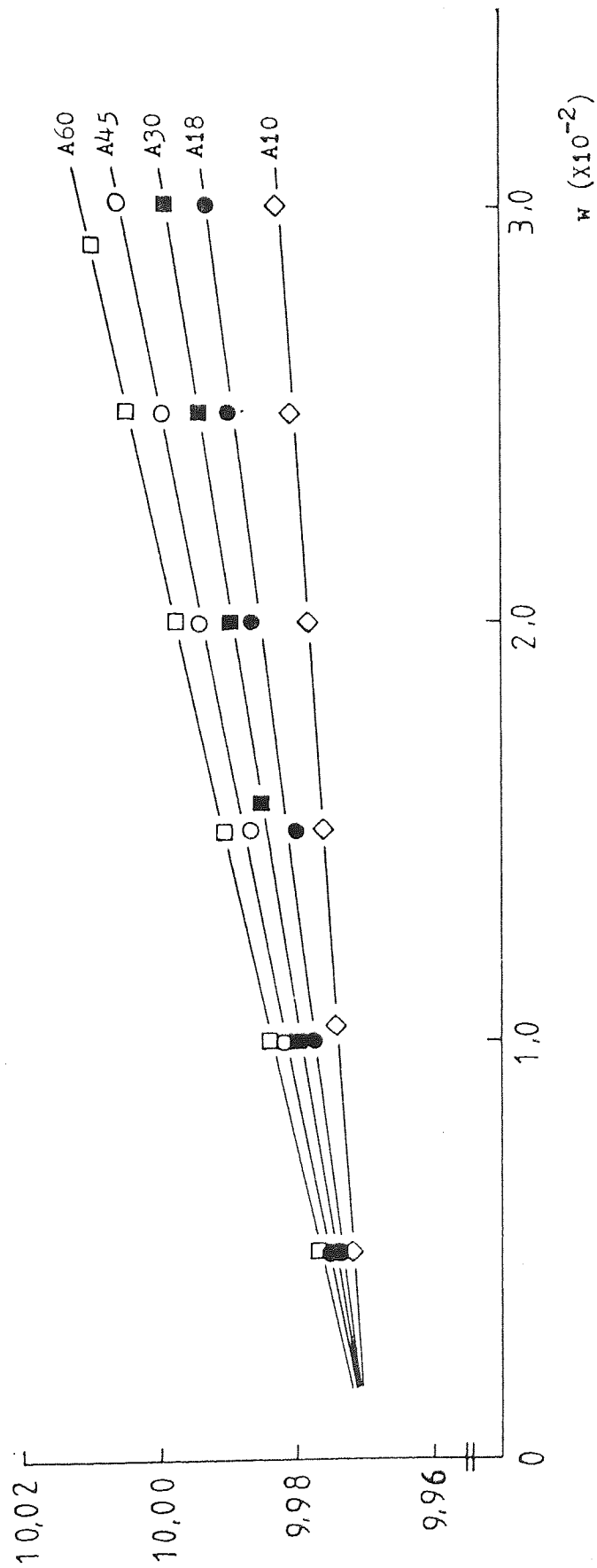


Fig. 12 dm/dw determination of the Texofors.

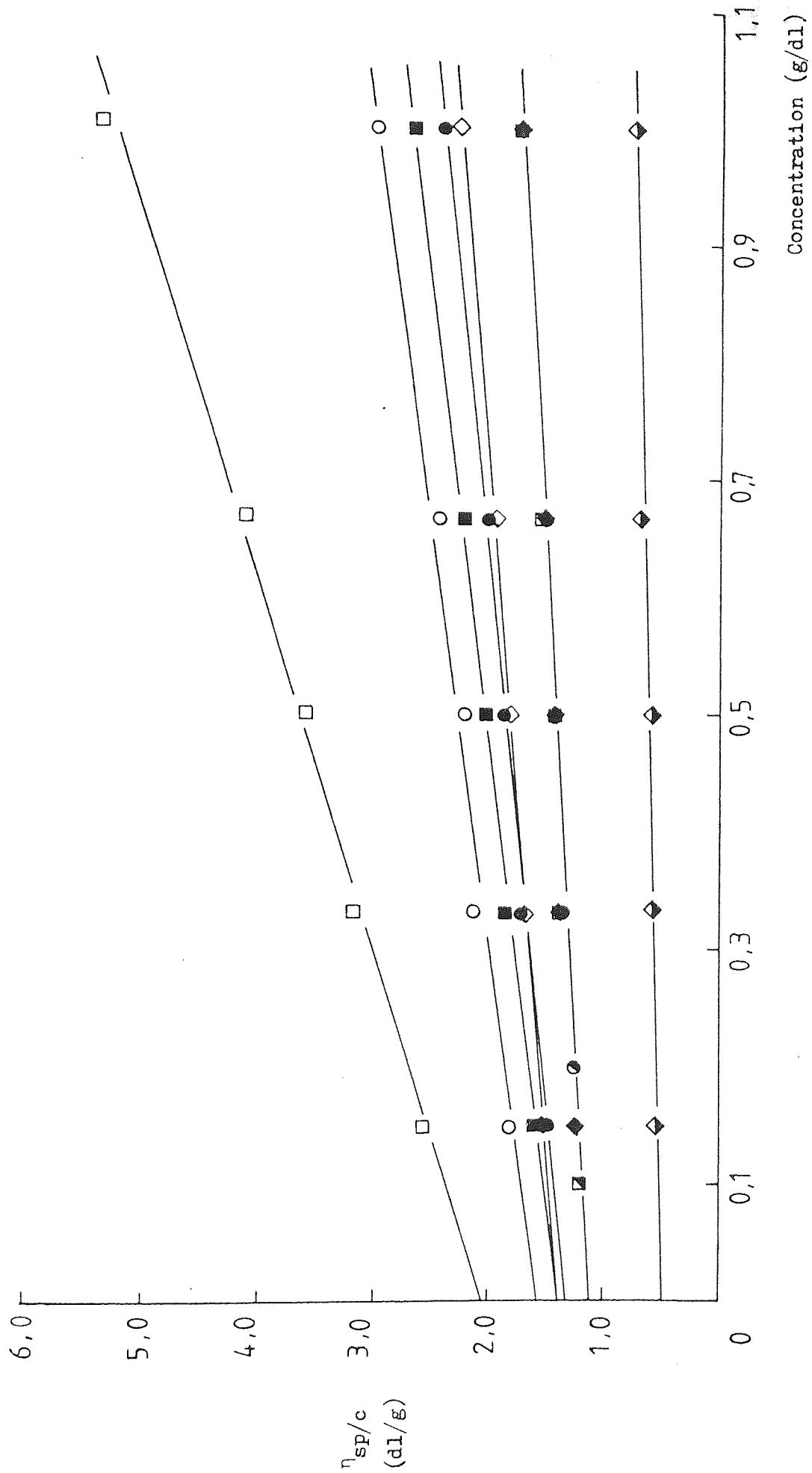


Fig. 13 Huggins plots for HEC, HPC and HPMC. ◆ HPMC 603, ◆ HPMC 606, O HPMC 615 in water at 20°C;

● HPC E, ■ HPC L in ethanol at 25°C; ▲ HPC E, ● HPC L in water at 25°C; ◇ HEC L, □ HEC J in water at 25°C

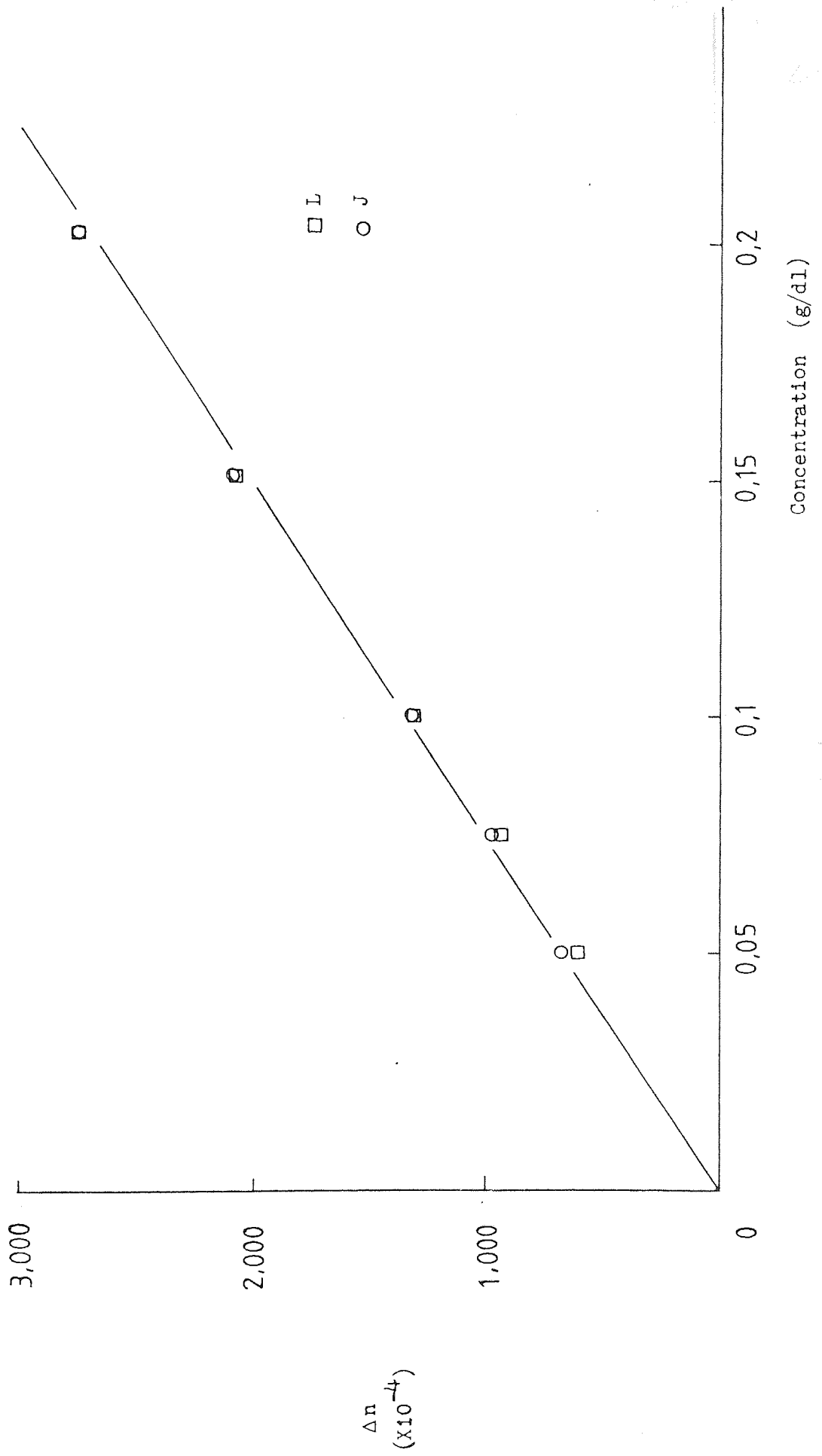


Fig. 14 Refractive index increment of HEC.

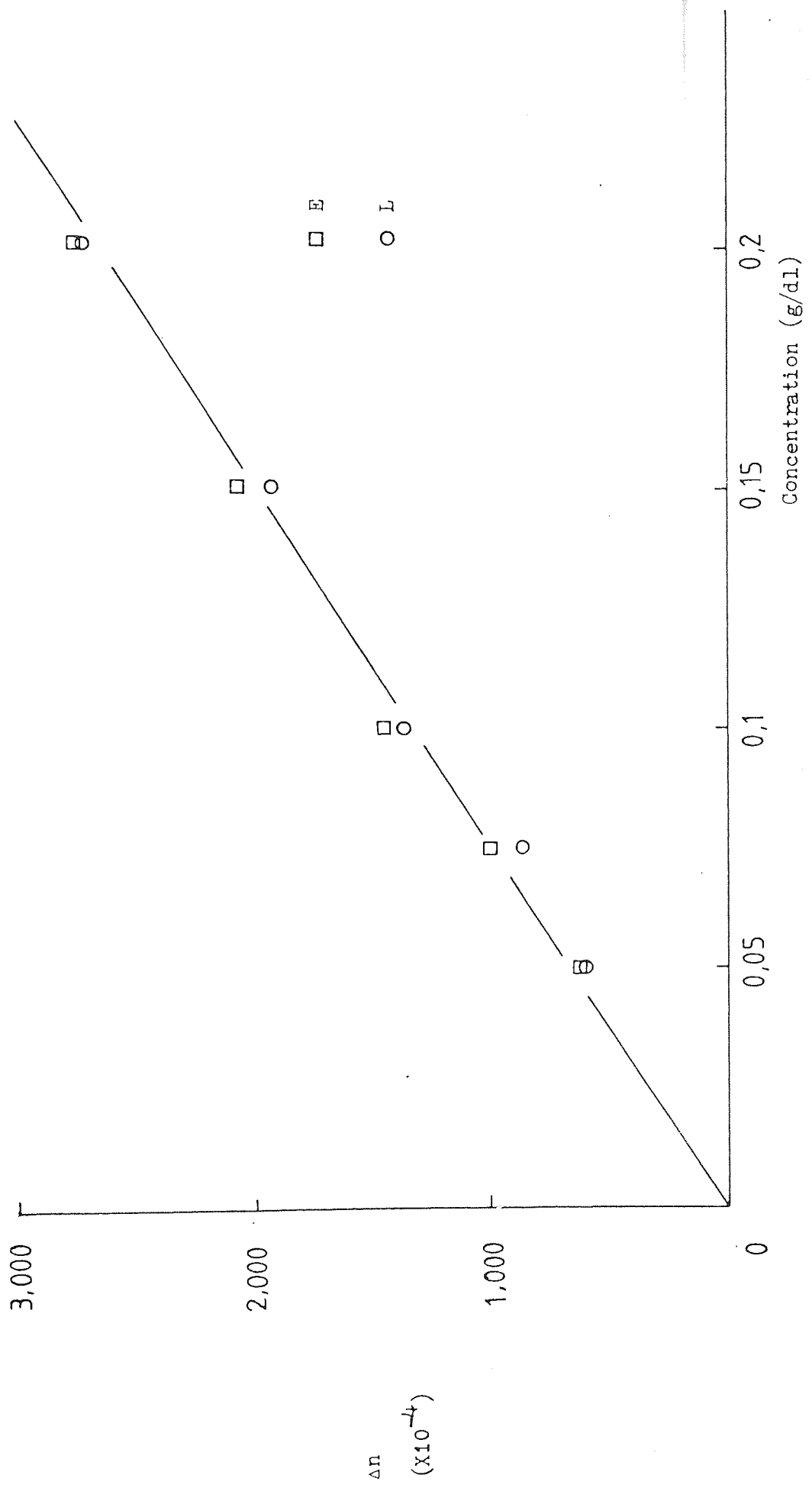


Fig. 15 Refractive index increment of HPC.

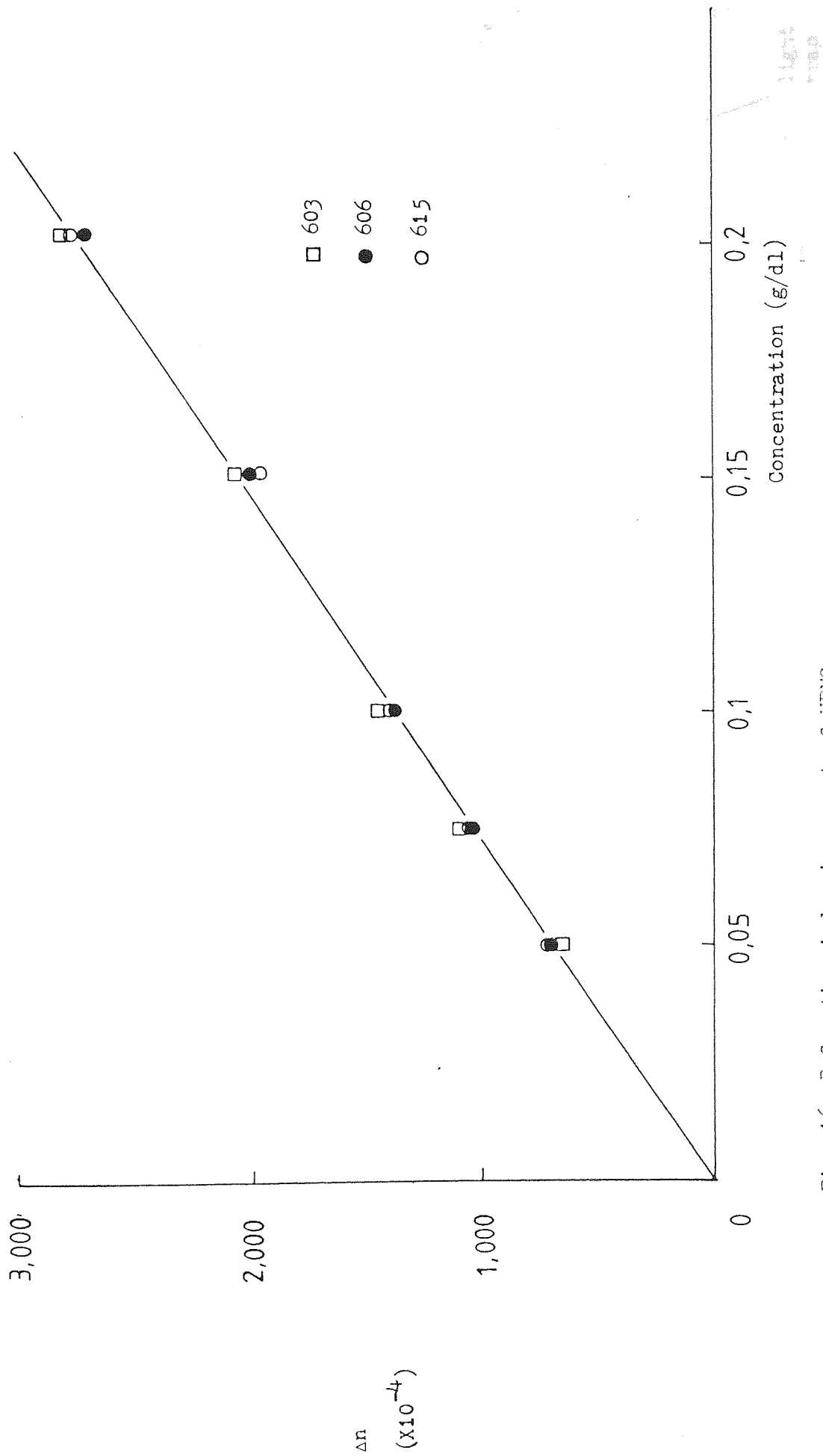


Fig. 16 Refractive index increment of HPMC.

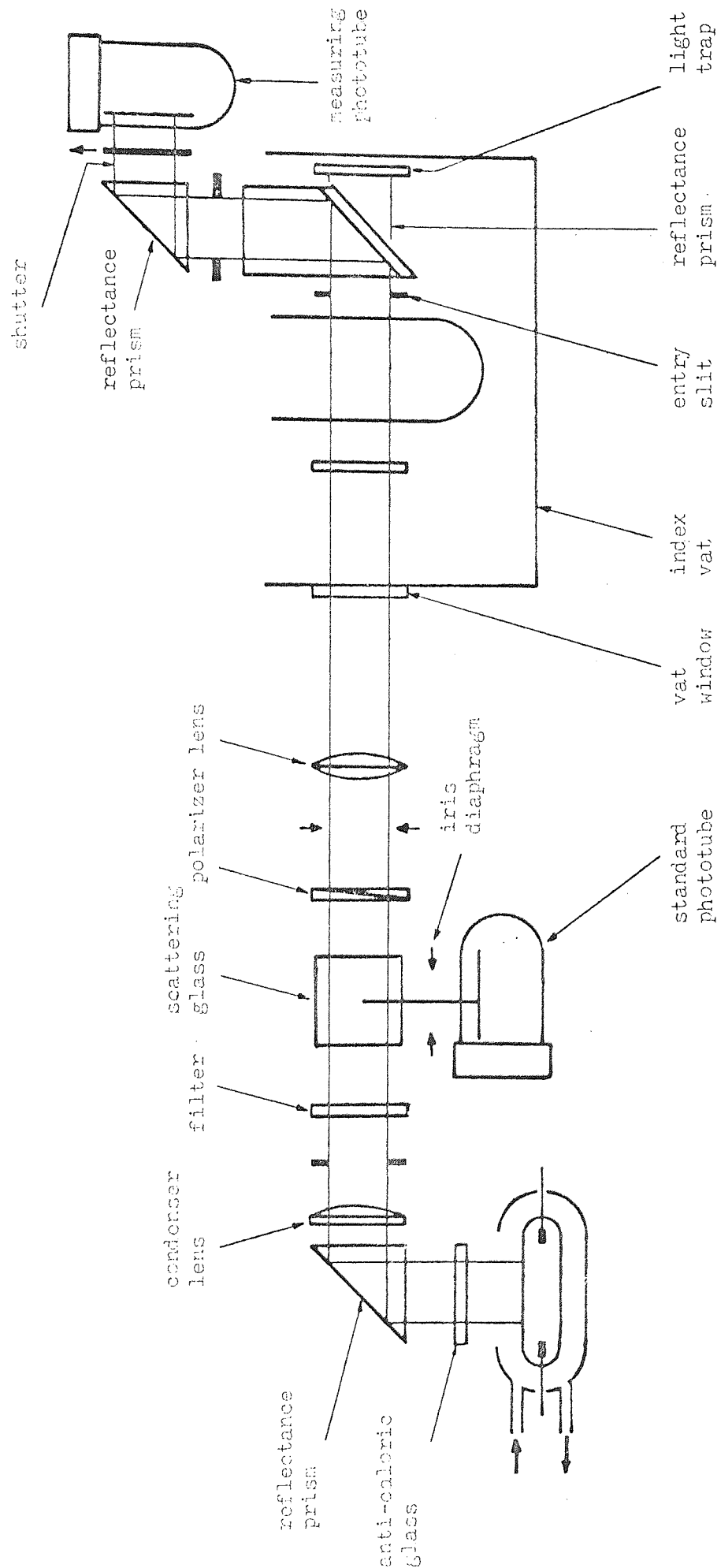


Fig. 17 Diagram of the Photo Gonio Diffusometer.

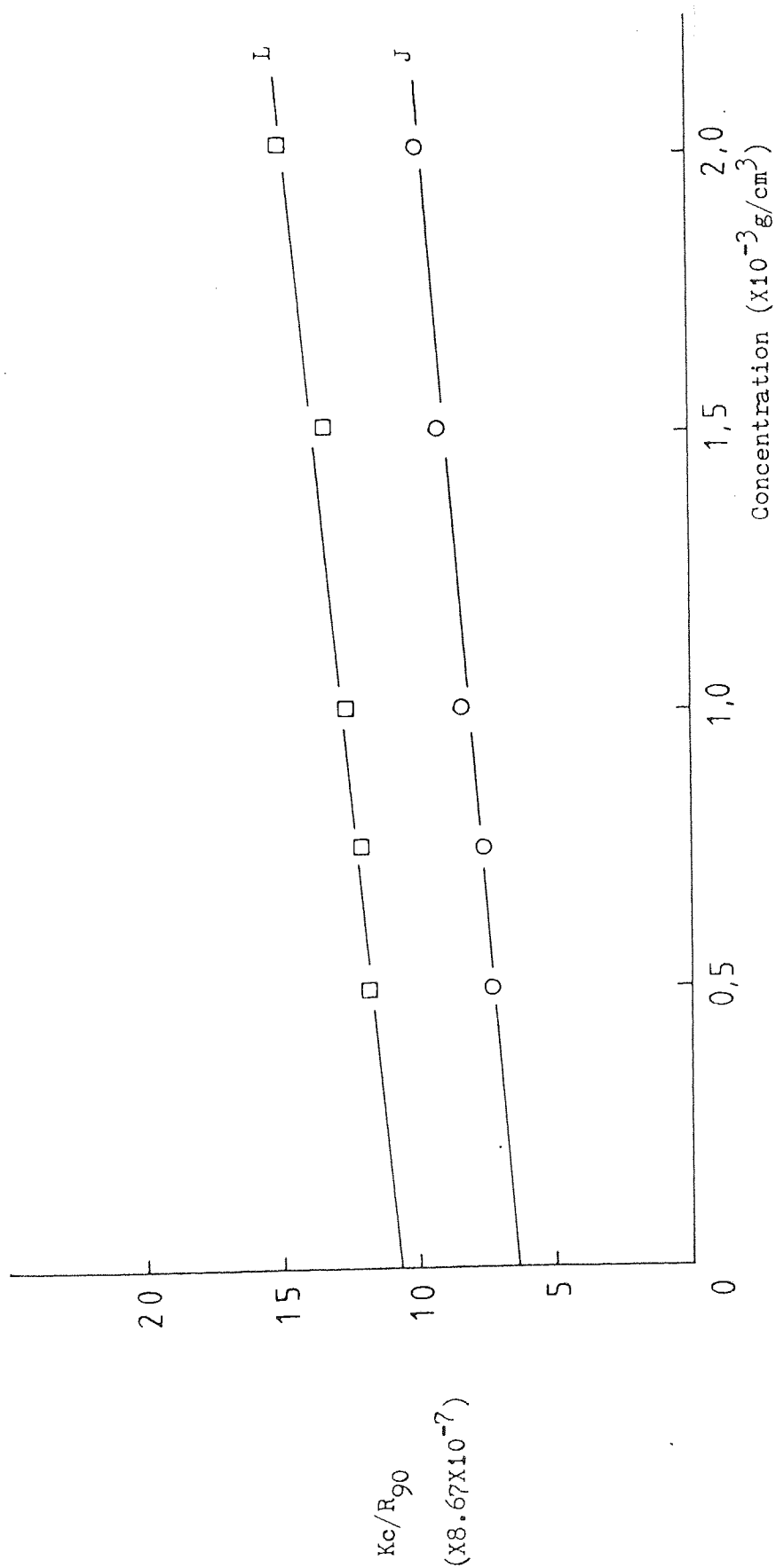


Fig. 18 Light scattering measurement of HEC.

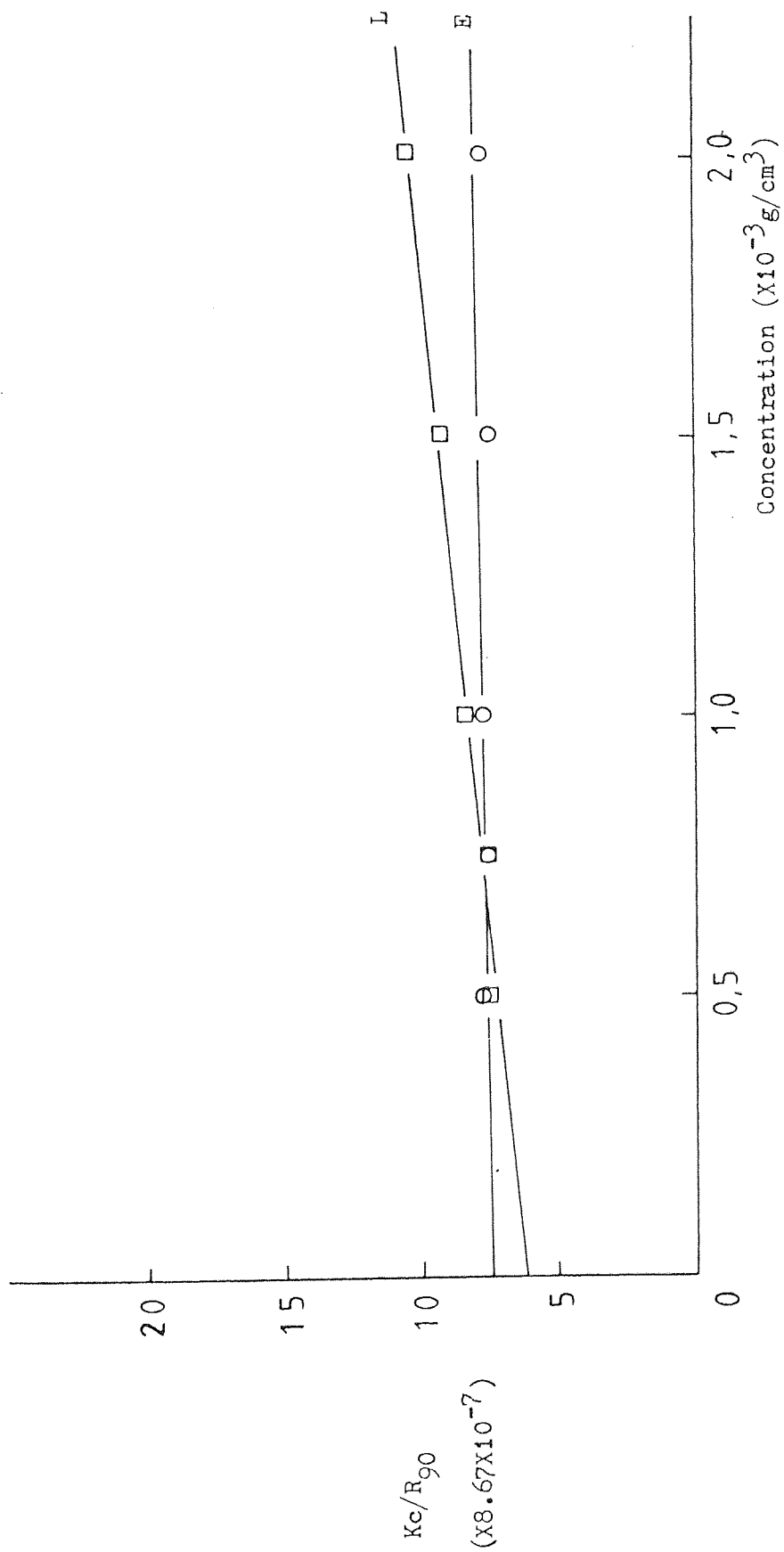


Fig. 19 Light scattering measurement of HFC.

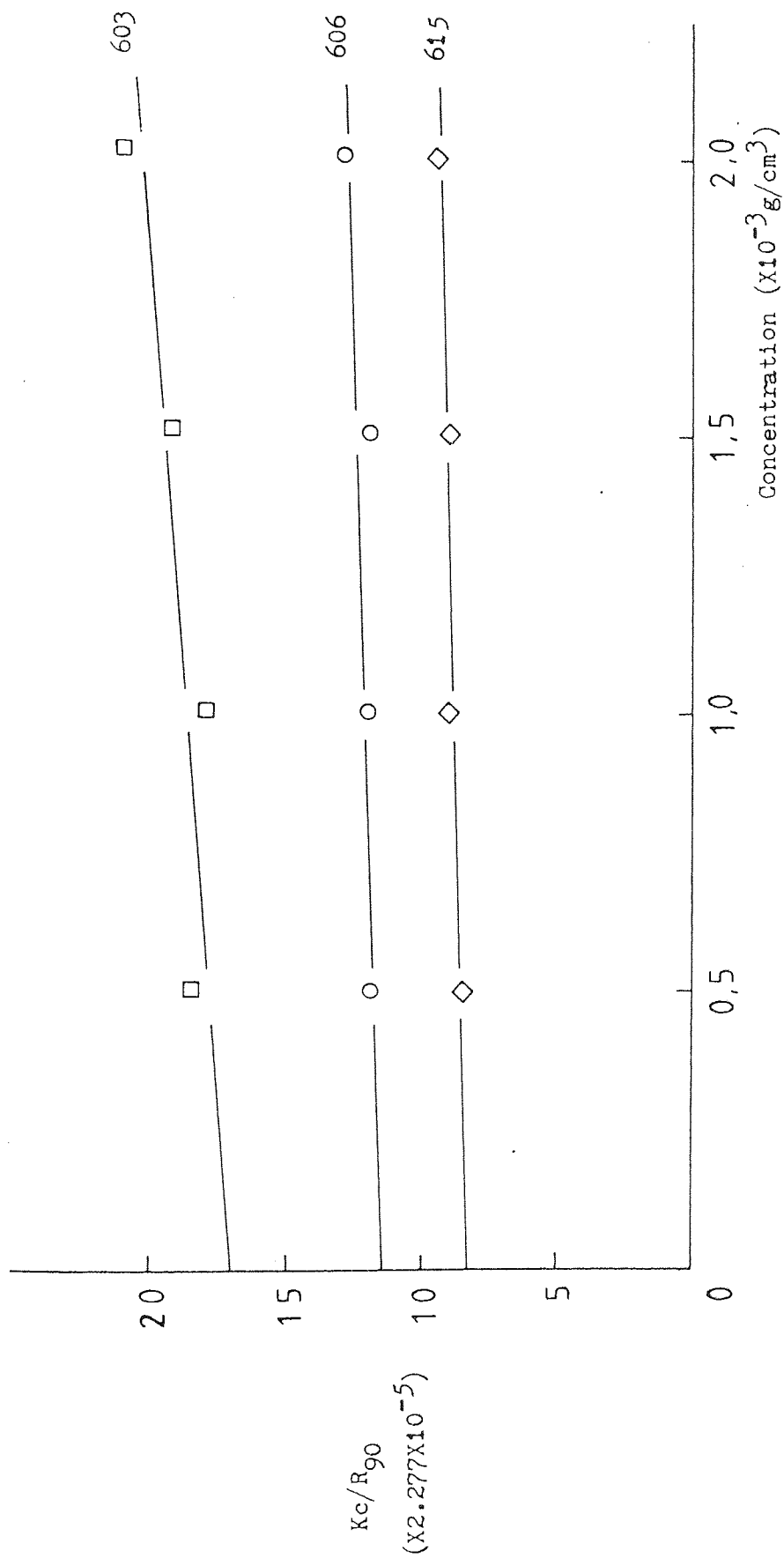


Fig. 20 Light scattering measurement of HPMC.

□ L
○ J

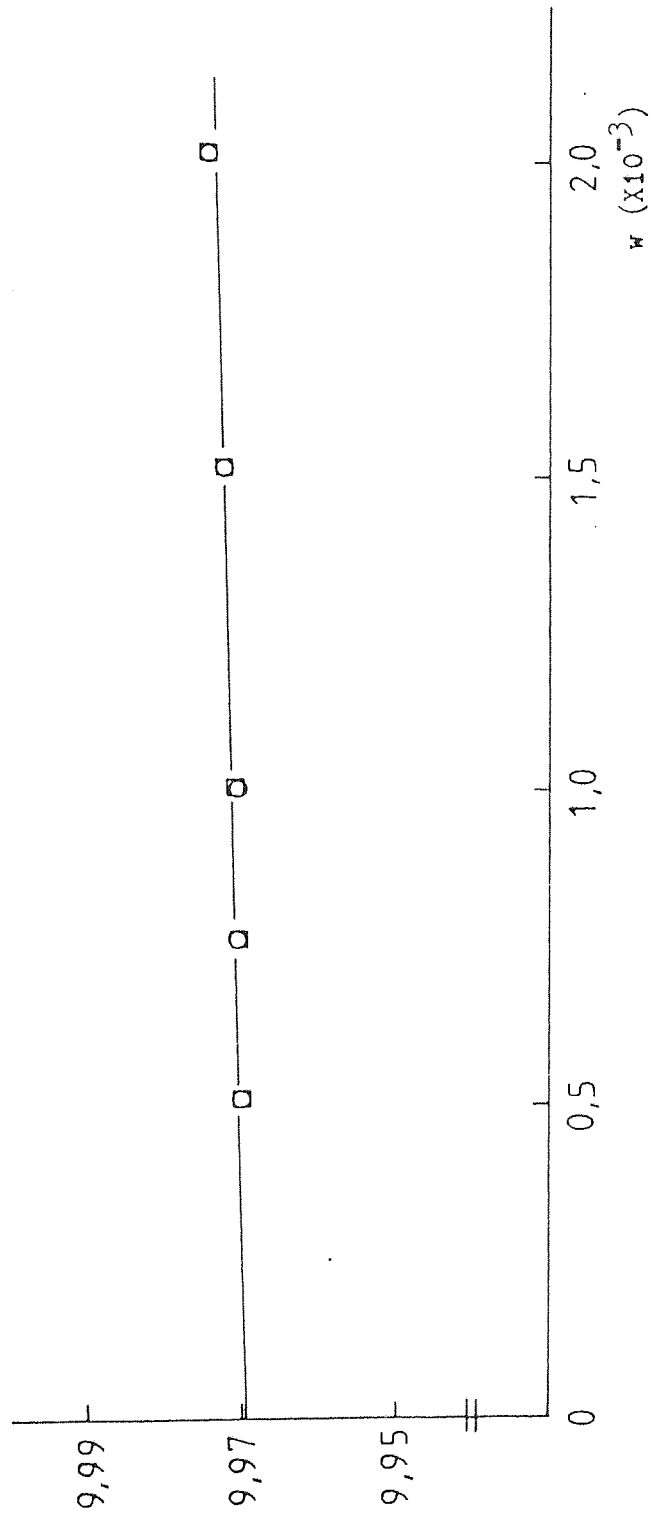


Fig. 21 dm/dw determination of HEC.

□ E

○ L

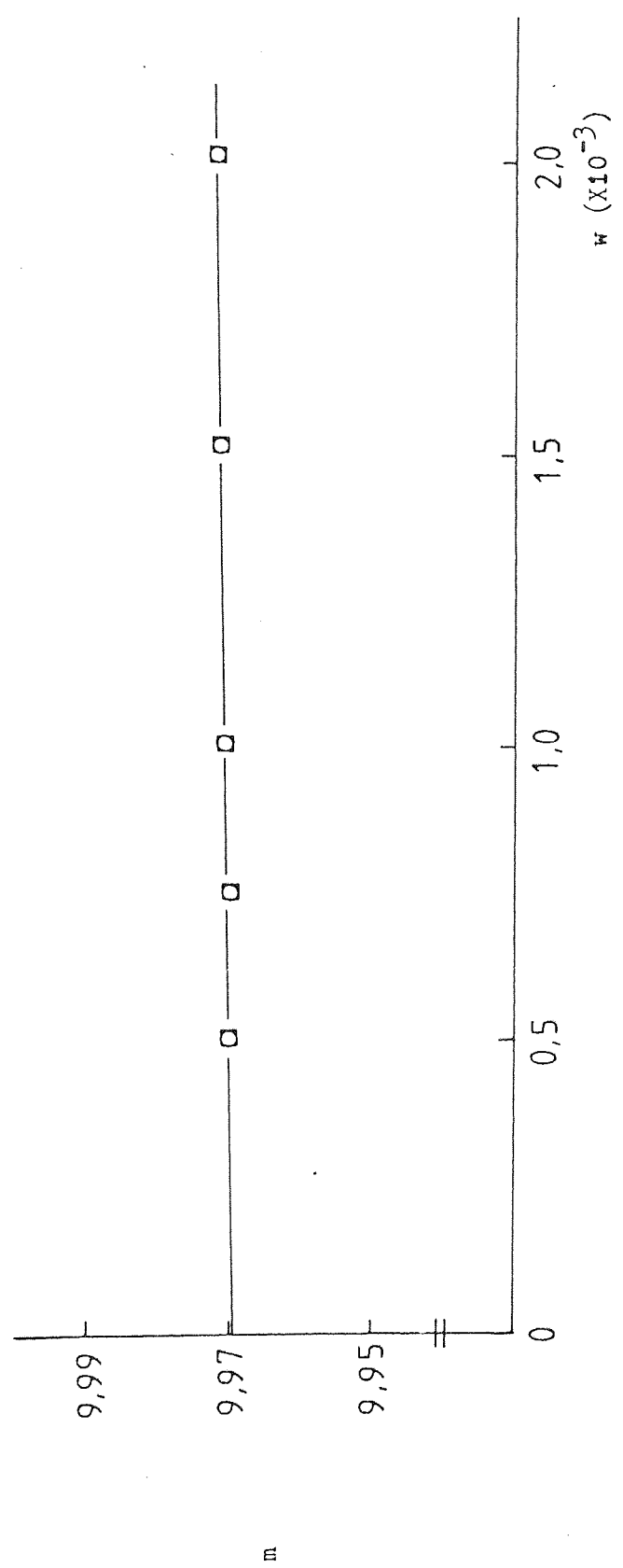


Fig. 22 dm/dw determination of HPC.

- 603
- 606
- ◇ 615

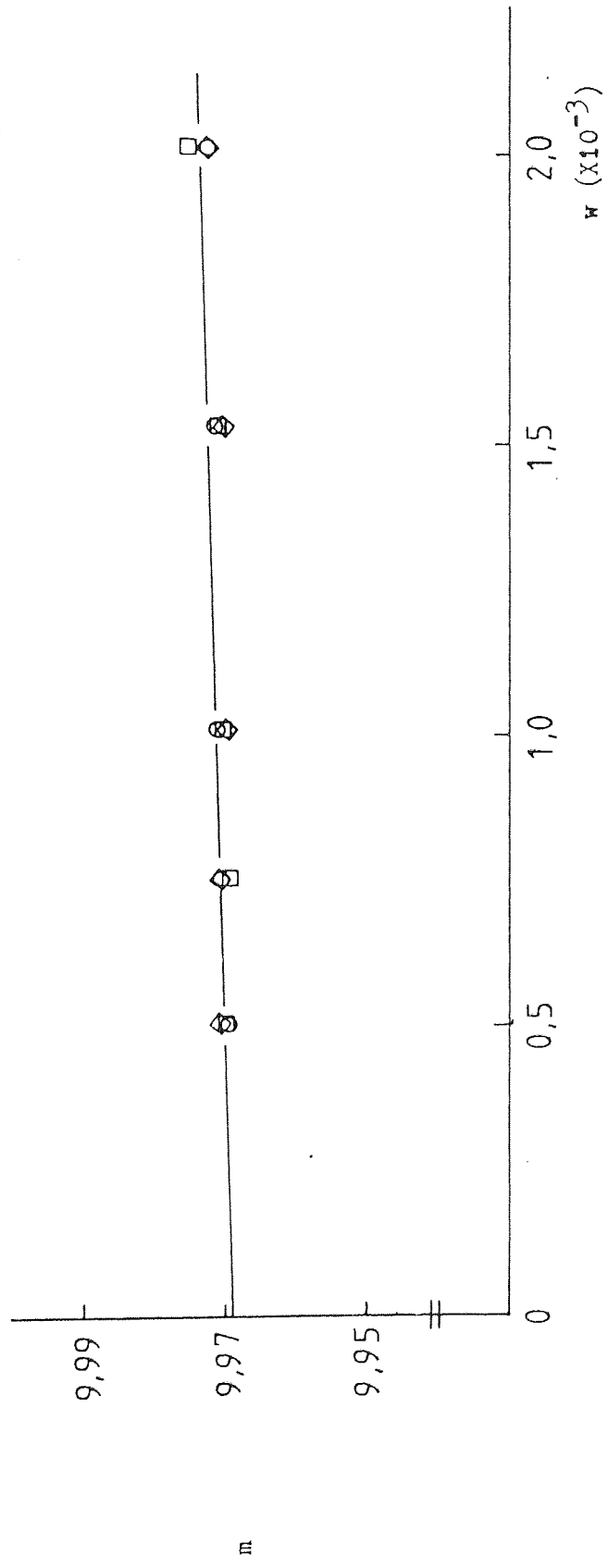


Fig. 23 dm/dw determination of HPMC.

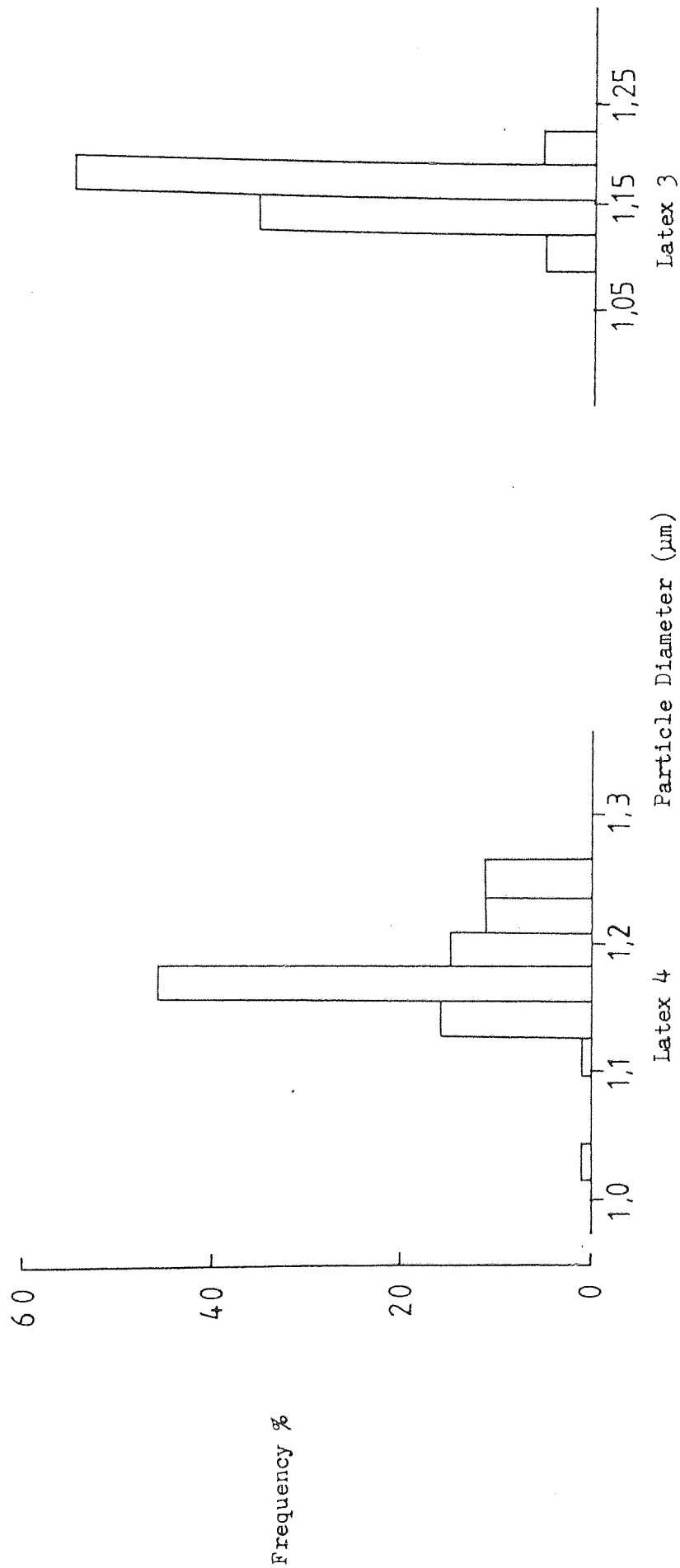


Fig. 24 Particle size distributions of polystyrene latex 3 and 4 .

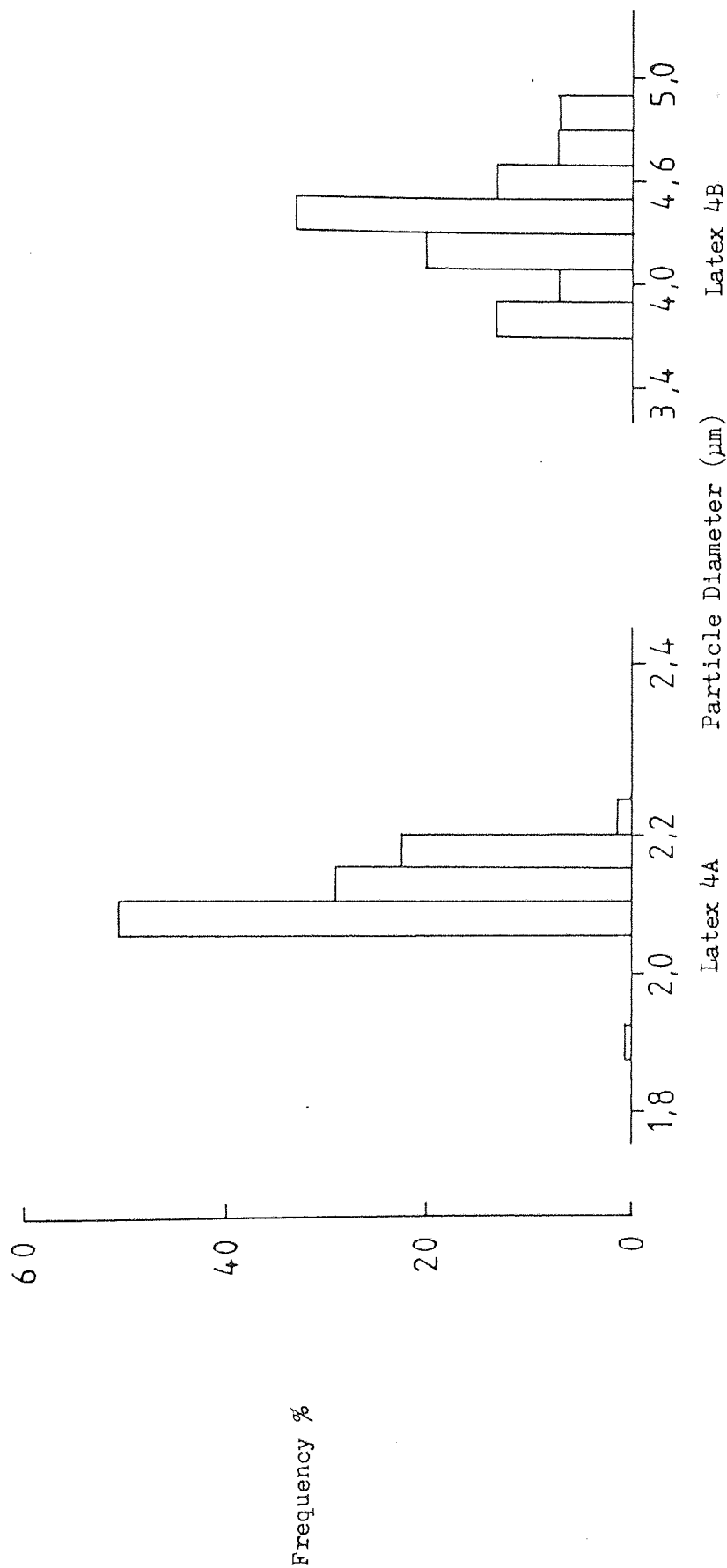


Fig. 25 Particle size distributions of polystyrene latex 4A and 4B.

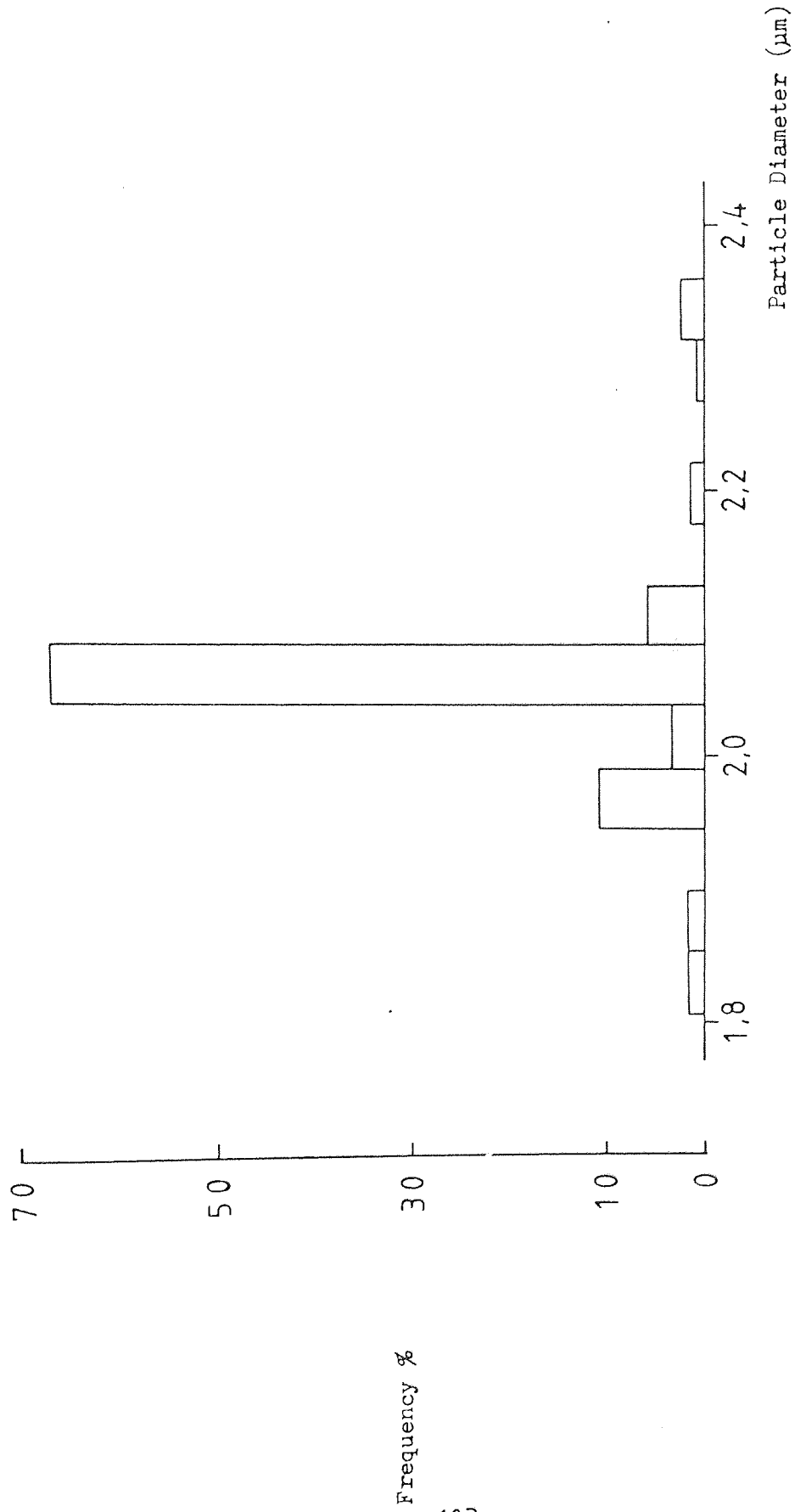


Fig. 26 Particle size distribution of polystyrene latex 3B.

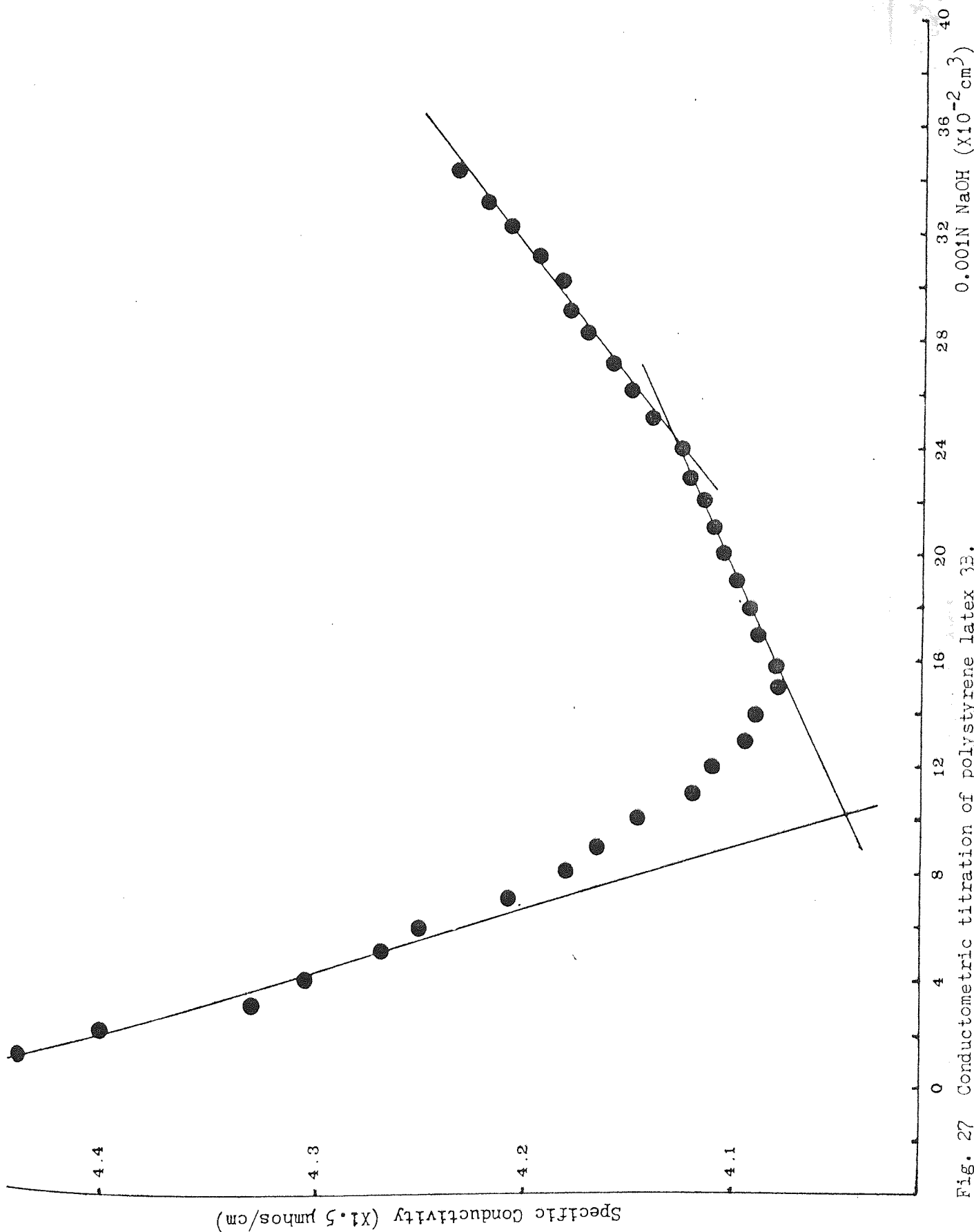


Fig. 27 Conductometric titration of polystyrene latex 3B.

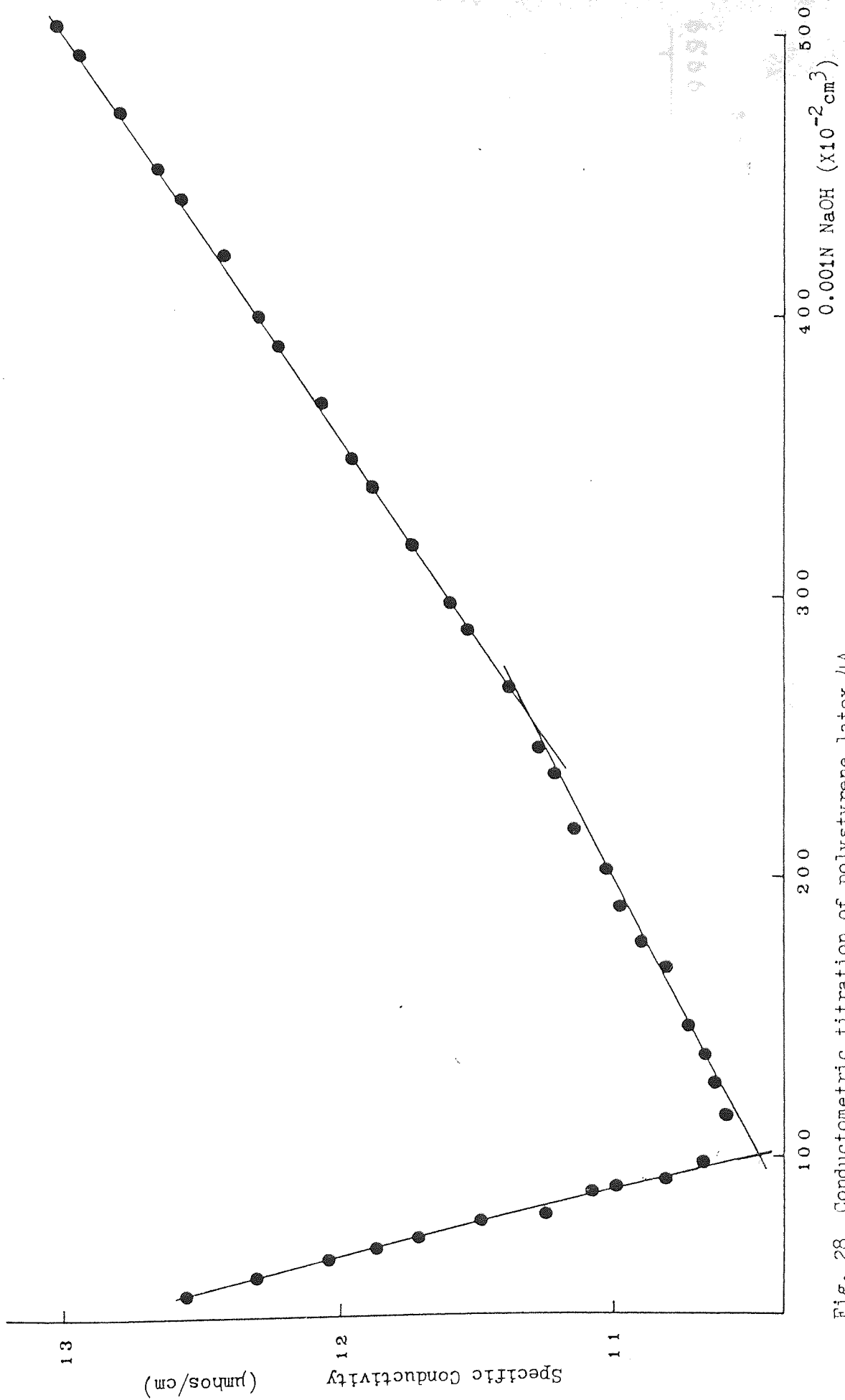


Fig. 28 Conductometric titration of polystyrene latex 4A.

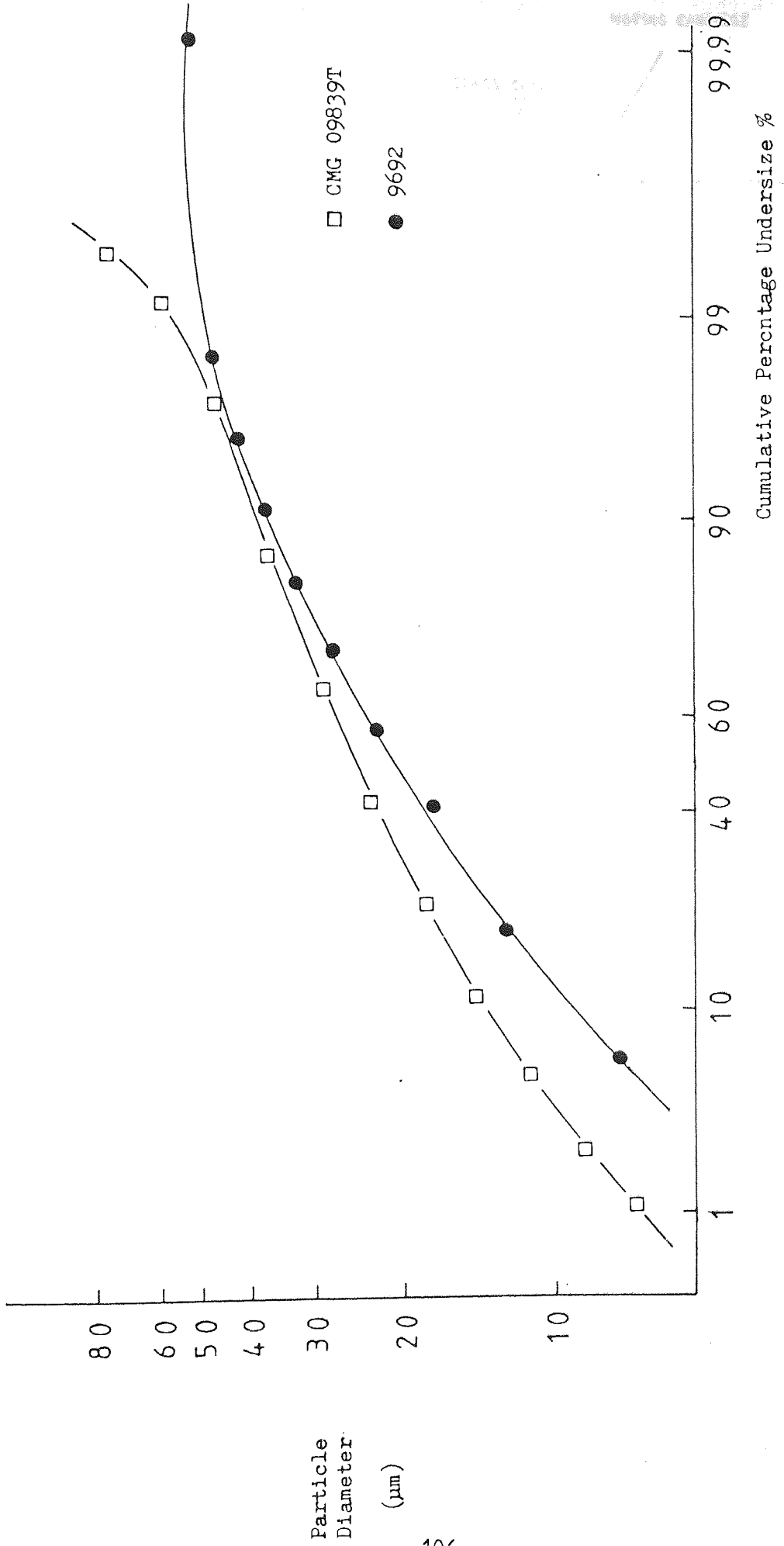


Fig. 29 Particle size distributions of ibuprofens.

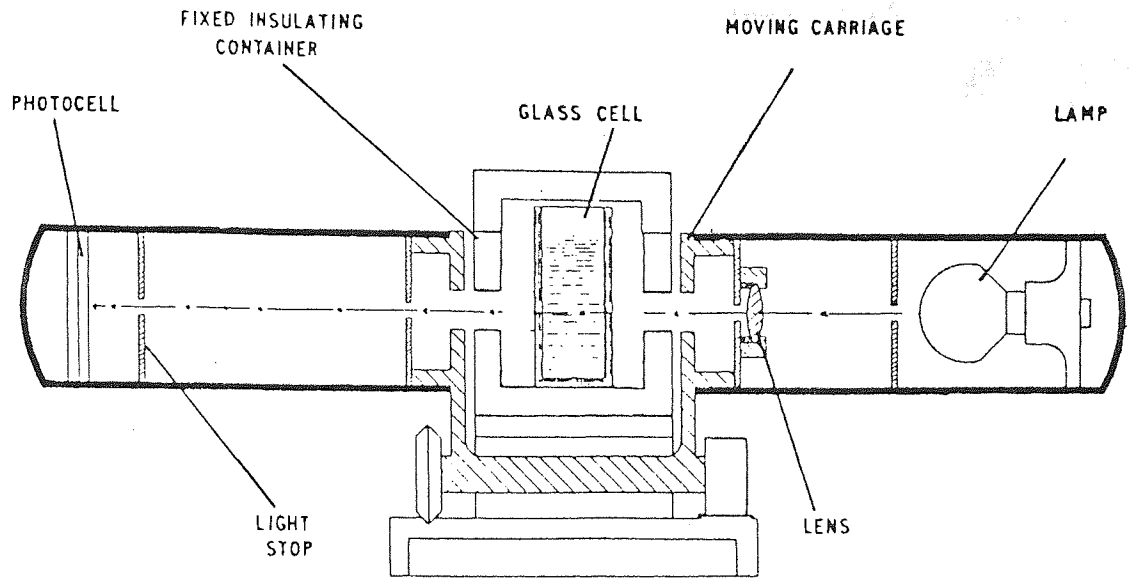


Fig. 30 Diagram of the Photoextinction Sedimentometer.

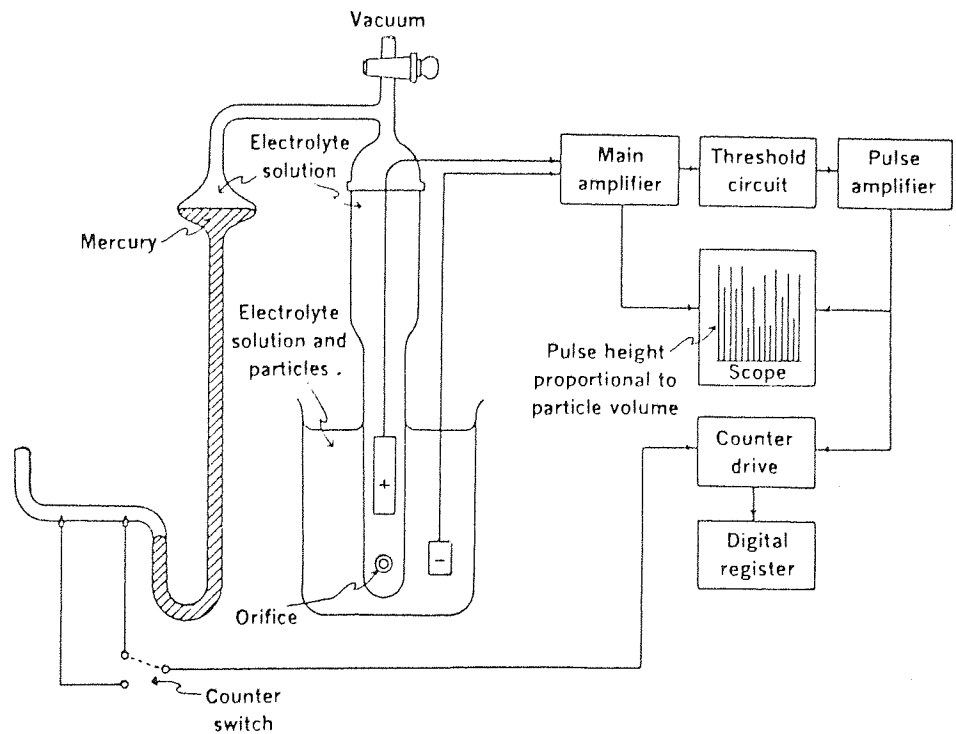


Fig. 31 Diagram of the Coulter Counter.

SECTION 4 ADSORPTION

4:1 Methods

4:1:1 Rate of adsorption measurements

The amount of polymer adsorbed on the solid surface was determined from the change in concentration of the polymer in the dispersion. Since the amount adsorbed is dependent on the time allowed for the establishment of equilibrium i.e. the rate of adsorption, this requires careful consideration if one is to obtain satisfactory isotherms and establish a procedure which can be applied to subsequent experiments on the stability of dispersions.

The rate of adsorption of Texofors on polystyrene latex was used according to the data obtained by Elworthy and Guthrie (95).

For the rate measurements for HEC, HPC and HPMC adsorptions, 1 g ibuprofen in 20cm³ of 0.1g/dl test solution was placed in a 40 cm³ preconditioned glass tube with a polyethylene stopper and the tube was sealed with parafilm. The pH of the suspension was adjusted to 4.0. The tube was shaken by a Whirlimixer (Fisons Ltd) until the powder dispersed and then sonicated in an ultrasonic bath (Kerry Ltd) for 20 minutes. Care was taken to prevent heating during the treatment by continuous replacement by the cooling water. The suspension was allowed to equilibrate in a shaking water bath at the rate of 120 throws per minute and at a temperature of $25^0 \pm 0.1^0$ C. Measurements were made every 24 hrs for 7 days.

The rate of adsorption on polystyrene latex was carried out

using HEC J only. 5 cm^3 of polystyrene latex 4B was added and mixed with HEC J stock solution to a volume of 10 cm^3 in a pretreated 20 cm^3 glass tube. The final concentration of the HEC J in the suspension was 0.1 g/dl . The mixing and equilibration procedures adopted were as described above.

To determine the amount adsorbed the supernatant of the suspension after equilibrium was analysed. The supernatant was obtained by filtration through a $1 \mu\text{m}$ membrane filter. The filter and the syringe used were preconditioned with the polymer solution studied (see Section 3:5:2). The first portion of the filtrate was discarded as adsorption would occur on the filtration assembly. The analytical method used was according to Milwidsky (233). 0.2 cm^3 of phenol solution (5 g in 95 cm^3 water) was mixed with 5 cm^3 of the test supernatant and then 10 cm^3 of concentrated sulphuric acid (98%) was added gradually and swirled to mix the ingredients. A brown colour developed almost immediately and reached a maximum in less than two minutes. The extinction was measured in 10 mm cells at 490 nm using a Unicam SP600 Series 2 spectrophotometer. High concentrations of the supernatant were diluted as necessary. Calibration curves were linear in the concentration region of interest. The error in the analysis was of the order of $\pm 2\%$. Blank test showed no interference by the latex in the measurements.

Adsorption of polymer onto the apparatus was neglected as all the apparatus used was preconditioned with polymer solution. It could be assumed that there was no adsorption loss.

4:1:2 Determination of adsorption isotherms

4:1:2:1 Nonionic surface active agents on polystyrene latex

Texofor A10, A18, A30, A45 and A60 were used. The concentration range studied was above and below cmc. Polystyrene latex (3B) 2 cm³, stock solution of Texofor and water to 10 cm³ were placed in a 20 cm³ surface active agent treated screw-capped centrifuge glass tube. The pH of the suspension was 6.0 adjusted by using NaOH and HCl. The tube was sealed with water proof parafilm and the suspension mixed with a Whirlimixer and allowed to equilibrate in a constant shaking (120 throws/min) water bath at 25⁰ ± 0.1⁰C for 24 hrs. The supernatant of the suspension was obtained by centrifuging (MSE HS 18) at 10,000 rpm for 1 hr. 5 cm³ of the supernatant was used for analysis by the iodine method mentioned in Section 3:5:1:1. The calibration curves obtained were linear. The latex did not interfere ^{with} the assay as found by checking with a blank sample.

4:1:2:2 Nonionic water soluble cellulose polymers on polystyrene latex and ibuprofen

Adsorption determinations were carried out on polystyrene latex 4B and on ibuprofen with HEC, HPC and HPMC at 25⁰ ± 0.1⁰C. The concentration range studied was 0.005 - 0.2 g/dl Celluloses. The pH for polystyrene latex adsorption was 6.0 and for ibuprofen adsorption was 4.0. The method used was as described in Section 4:1:1. The time allowed for equilibrium adsorption was 4 days. Adsorption on polystyrene latex in the presence of 10⁻³M NaCl and at different pH values also studied.

4:1:3 Determination of adsorbed layer thickness

The adsorption of nonionic polymer molecules on the particle surface would cause the electrokinetic plane of shear to move further into the solution and lead to a decrease in zeta potential. Consequently, this decreases the mobility of the particle which can be found by using the microelectrophoretic technique. If the adsorbed polymer molecule is assumed to have no influence on the charge distribution in the diffuse double layer, the surface charge density of the particle and the specific adsorbed ions in the Stern plane, the electrokinetic thickness of the adsorbed layer can be obtained from the equation given by Overbeek (5).

$$k(x-\Delta) = \ln \left[\frac{(\exp(Ze\zeta/2KT) + 1) (\exp(Ze\zeta_0/2KT) - 1)}{(\exp(Ze\zeta/2KT) - 1) (\exp(Ze\zeta_0/2KT) + 1)} \right] \quad (88)$$

where k is the Debye-Huckel reciprocal thickness of the diffuse double layer, ζ is the zeta potential of the particle with adsorbed polymers, ζ_0 is the zeta potential of the bare particle and Δ is the thickness of the Stern layer which was assumed to have a value of 0.4 nm (234). This equation is similar to Eq. (43) for flat plates in which the potential decays from the surface to the diffuse part of the double layer. However, when the zeta potential is used instead of the surface potential the thickness of Stern layer should be included as polymer adsorption starts at the surface.

This method of determining the thickness of the adsorbed layer was used for Texofors adsorbed on polystyrene latex and for Celluloses on polystyrene latex and on ibuprofen. Calculations were based on the plateau region of the electrophoretic mobility curves as well as the

adsorption isotherms where a monolayer of adsorbed polymers was complete.

The experimental procedures are detailed in Section 5:1.

4:1:3:2 Viscometry

The viscometric method for determining the thickness of the adsorbed layer is based on the Einstein equation (235) of viscosity which predicts that when rigid, electrically neutral spheres are suspended in the continuous phase, the viscosity of the continuous phase η_0 is increased according to the relationship:

$$\eta = \eta_0 (1 + 2.5\phi) \quad (89)$$

or

$$\eta_r = 1 + 2.5\phi \quad (90)$$

where η is the viscosity of the dispersion, ϕ is the volume fraction of the particles and η_r is the relative viscosity. The Einstein equation is only applicable to a dilute dispersion in which the disperse phase volume does not exceed 2% (i.e. volume fraction of 0.02). For concentrated dispersions a great variety of modified Einstein equations have been developed (224). A general form of the equation is

$$\eta_r = 1 + E_0\phi + E_1\phi^2 + \dots \quad (91)$$

where E_0 is the Einstein coefficient which depends on the shape of the uncharged particles e.g. 2.5 for sphere, 2.8 for a prolate spheroid of axial ratio 2/1 (236), E_1 is the interaction coefficient which can be found by fitting experimental data. Vand (237) and Mooney (238) derived the following general equation

$$\eta_r = \exp[(E_0\phi)/(1 - k\phi)] \quad (92)$$

where E_0 and K are the constants which refer to the shape factor of the particle and the hydrodynamic interaction effect respectively. Mooney (238) suggested that E_0 is 2.5 which is equivalent to Einstein's constant and K is about 1.35 for monodisperse suspended spheres.

If the adsorbed polymers form a rigid layer and do not deform under shear stress, the apparent increase in volume ϕ of the particle may be estimated by Eqs (90), (91) or (92) in which

$$\phi = fv \quad (93)$$

where

$$f = \left(\frac{\text{radius of particle} + \text{adsorbed layer thickness}}{\text{radius of particle}} \right)^3$$

which is a factor that corrects for the adsorbed layer thickness and v is the actual volume of the particle. Thus, the adsorbed layer thickness may be determined using Eq. (93).

The polystyrene latex samples used in this experiment were latex 4A and a latex prepared by Rawlins (15) with a diameter of 0.1725 μm and a percentage content of 0.0052 g/cm^3 (reevaluated value). Celluloses used were HEC, HPC and HPMC. Dispersions of known latex volume fraction were prepared by adding the Cellulose solution to the requisite amount of latex so as to give a concentration that equilibrium plateau adsorption took place. 10^{-1} M sodium chloride solution was added to suppress the electroviscous effect. As shown in Fig. 32, the presence of 10^{-1} M NaCl has little influence on the intrinsic viscosity i.e. it does not alter the conformation of the polymers in solution. The pH of the dispersion was 6.0. The mixing and adsorption procedures given in Section 4:1:1 were followed. 4 days were allowed for adsorption to occur. The viscosities of the dispersions were measured

by U-tube viscometers at 25⁰C as described in Section 3:5:2:1. The samples were centrifuged at 10,000 rpm for one hr. and two hrs for large and small latex respectively. The viscosity of the supernatant liquid was measured as described above. For polystyrene latex in HEC flocculation of the particles occurred but in HPC and HPMC particles showed no flocculation. Thus, in the HEC systems latex particles flocculated to form a clustered sediment with a clear supernatant and with large latex particles in HEC, aggregates were clearly visible under the microscope. Therefore, in the formulation of HEC-latex dispersions, Pluronic F68 was used as a dispersing agent to prevent flocculation of the particles. The amount of Pluronic F68 used was at such a concentration (0.1% W/V) as to give maximum adsorption (15). First, the latex dispersions were equilibrated with the Pluronic F68 at 25⁰C for 24 hrs to allow adsorption to take place. Then, the Celluloses were added and the mixing, adsorption and measurement procedures were followed in the manner given above. Dispersions were examined by the microscope. No flocculation of the particles was found.

4:1:4 Surface tension measurements

The surface tensions of the Cellulose solutions were measured by the Wilhelmy plate technique in conjunction with a micro-force balance (CI Electronics Ltd, MK 2B) (216). The plate used was a polished platinum plate having dimensions of 10 mm X 5 mm X 0.025 mm. Before each measurement the platinum plate was cleaned by heating to red heat and then used immediately after cooling. The instrument was calibrated by using a liquid of known surface tension (212). All measurements were made after thermal equilibrium was reached. The calibration curve of the readings from the electrical balance against

known surface tensions was a good straight line.

Measurements on Cellulose solutions were carried out at 25⁰C in the concentration range of 0.05 - 0.2 g/dl. The results taken were means of at least ten readings.

4:1:5 Contact angle measurements

Contact angles were measured with a Goniometer (The Precision Tool and Instrument Co Ltd). The Goniometer was mounted on a travelling microscope which was placed on a levelling bench fitted with an illumination system. Sample liquids of known volume (0.005 cm³) were carefully dropped onto the surface of the measuring solid using an Agla syringe fitted with a fine needle. Saturated solutions of the solid material were used as the medium in order to prevent dissolution. The droplet was covered with a glass box saturated with vapour of the testing solution. The Goniometer was aligned and focused on the solid-liquid interface. The contact angles were taken from both sides of the droplet. At least four individual droplets of each sample were examined and the results tabulated were the average of eight readings. Measurements were carried out at a constant temperature of 20⁰C.

The preparation of the polystyrene surfaces for contact angle measurements was accomplished by dissolving the dried latex in dioxan and spreading the solution onto microscope slide and then evaporating the solvent in a vacuum desiccator. Ibuprofen surfaces were prepared by ^amelting method. A thin layer of ibuprofen powder was spread over a microscope slide after which the slide was placed on a hot plate

whose temperature was controlled at the melting point of ibuprofen (78⁰C). After the ibuprofen powder had just melted, the slide was removed from the hot plate. Another clean glass slide was used to cover the melted ibuprofen immediately and was fixed by a clamp on a horizontal plate. After the ibuprofen solidified the cover glass slide was separated leaving a smooth drug surface. The melting point of the ibuprofen was checked before and after melting; it remained unchanged. Another method used for preparing the solid surfaces involved a tablet punch technique (Wilkinson STD 1 reciprocating tablet machine with 1/2 inch diameter dies). With this method it was not easy to obtain a smooth surface due to the sticking of drug powder to the punch and die, but this method is commonly used in contact angle studies on pharmaceutical powders (230). The contact angle measurements with the contact surfaces obtained using a punch involved only water as the contact liquid. Results were compared with those of the surfaces obtained by the melting method. The contact angle between water and the ibuprofen surface made by the melting method was 85⁰ ± 2⁰ and by the punch method was 83⁰ ± 2⁰. This indicates that these two methods are comparable. Scanning electron microscope examination of the ibuprofen compact surfaces and polystyrene films showed them to be quite smooth within the limits of resolution.

4:2 Results and discussion

4:2:1 Rate of adsorption

The time required for polyoxyethylene glycol monoalkyl ether molecules to reach equilibrium on griseofulvin drug surface was within 16 hrs (95). Other workers using the same series of nonionic surface active agents used equilibrium times of 24 hrs on polystyrene

latex (19) and 18 hrs on silver iodide (232), although an equilibration was approached in much shorter times. It has been shown (217,76) that low molecular weight polymers equilibrate more rapidly than high molecular weight polymers, since diffusion of the low molecular weight polymers to the adsorbent surface takes less time. Howard and McConnel (217) showed that the adsorption of low molecular weight ($M_n = 390$) polyethylene oxide on activated carbon, Aerosil silica and nylon attained equilibrium in about 2 hrs whereas high molecular weight ($M_n = 190,000$) samples needed up to 24 hrs. In the experiments here, measurements were taken after 24 hrs which was a reasonable time for the establishment of equilibrium adsorption.

The results of the rate of adsorption of Celluloses on ibuprofen are given in Figs 33,34 and 35. The adsorption of HEC J on latex is shown in Fig. 35.

Establishment of equilibrium for HEC on ibuprofen needed about 4 days for high molecular weight polymer and about 3 days for low molecular weight polymer. For HPC on ibuprofen the time taken for equilibrium to be reached was less than 2 days and for HPMC less than 3 days. The formulation and the experimental procedures in these systems was the same and therefore the factors which affected the adsorption are due to the molecular weight and the chemical nature of the polymer. From Figs 33, 34 and 35, the kinetic curves show a steep initial slope for low molecular weight polymers while for high molecular weight polymers the curves rise slowly. The dependence of molecular weight on rate of adsorption is affected by the diffusion process of the polymer molecules. In general, the higher the molecular weight of the polymer the slower the diffusion rate. Diffusion equations

have been used by some workers to describe the kinetics of polymer adsorption (76,217,218,219). However, these kinetic equations do not always fit experimental results (76,217) because the dependence of adsorption on the duration of the process is influenced by a number of factors, such as the molecular weight and the molecular weight distribution of the polymer, the type of adsorbent, the concentration of the solution and the surface coverage etc, which are so complex that the applicability of the kinetic equation has been limited. Kipling (219) in his monograph gave an equation

$$kt = \ln \frac{A_m}{A_m - A} \quad (94)$$

where A is the amount adsorbed in time t, A_m is the amount adsorbed at saturation and k is a rate constant.

The curves of the rate of adsorption (Figs 33, 34 and 35) agree approximately with this equation. For example, with HEC the rate constants were derived by drawing the best rate curve through the experimental points. The A values were obtained from these curves and $\ln[A_m/(A_m - A)]$ was plotted against t. The rate constants found are shown in Table 8.

Cellulose	Adsorbent	k (per day)
HEC L	Ibuprofen	1.99
HEC J	Ibuprofen	0.73
HEC J	Polystyrene Latex	2.39

Table 8 Rate constants of HEC adsorption.

It is found that for HEC adsorbed on ibuprofen, HEC J, the high molecular weight fraction, has the small k of slower adsorption rate than HEC L, the low molecular weight fraction, the large k of faster adsorption rate. For HEC J adsorbed on ibuprofen and polystyrene latex, the k values (Table 8) are very different 0.73/day and 2.39/day respectively. The equilibrium time for adsorption on porous materials may be much longer than for nonporous adsorbents, since polymer molecules need to penetrate the pores and displace the trapped solvent or gas. Furthermore, the rate of adsorption on porous surfaces is dependent on the pore size. Ibuprofen exists in the form of a crystalline powder which can be regarded as a nonporous adsorbent. Polystyrene latex is synthesized by styrene polymerization to form a rigid particle which should have a smooth surface. This was shown to be true in the high magnification electron micrograph. Therefore, there should be little effect of porosity on the establishment of equilibrium adsorption. Looking at the effect of regularity of surface on adsorption, Koral et al (66) found that the time for the equilibrium adsorption of polyvinyl acetate on the irregular surface of an activated alumina was much longer than that for the adsorption on a smooth surface of iron and tin powder. Here, the regularity effect may be applied to the rate of adsorption of HEC J on ibuprofen and polystyrene latex. As ibuprofen has a more irregular surface than polystyrene latex, the rate of adsorption will be slower on ibuprofen than on polystyrene latex. Another possible factor affecting the rate of HEC J adsorption on ibuprofen and polystyrene latex is the flocculation effect of the adsorbent particles. Ibuprofen particles when suspended in water formed aggregates because of their hydrophobic properties and some of them floated on the top of the fluid and some of them aggregated at the bottom. As a result, void spaces were created among the aggregates.

However, for the polystyrene latex system, due to the method of synthesis was in the aqueous base, it was dispersed homogeneously. Therefore, one expects that the polymers in the aggregated ibuprofen system will give a slower adsorption rate.

4:2:2 Adsorption of Texofors on polystyrene latex

The adsorption isotherms of Texofors adsorbed onto polystyrene latex are shown in Fig. 36. Langmuir type isotherms were obtained over the concentration range studied. The maximum amount adsorbed occurred in most of the cases above the cmc. The plateau values and the published values on griseofulvin (95) are given in Table 9.

Texofor	Equilibrium adsorption		Literature value
	mol/m ² X10 ⁻⁶	nm ² /molecule	
A10	3.30	0.50	3.12
A18	2.33	0.71	-
A30	1.50	1.11	-
A45	1.20	1.38	0.65
A60	0.70	2.37	0.44

Table 9 Equilibrium adsorption values for Texofors on polystyrene latex and on griseofulvin (literature value).

The adsorbed layer thicknesses calculated from electrophoretic data using Eq. (88) are shown in Table 10.

Texofor	Zeta potential -mV	Thickness of adsorbed layer nm
A10	57.3	1.9 ± 0.4
A18	54.3	2.3 ± 0.6
A30	47.0	3.5 ± 0.5
A45	43.0	4.3 ± 0.7
A60	39.7	5.0 ± 0.5

Table 10 Adsorbed layer thicknesses of Texofors on polystyrene latex

The maximum adsorptions of Texofors on polystyrene latex were greater than the published values for adsorption on griseofulvin (Table 9). This is probably due to the differences in hydrophobicity of the adsorbent surfaces. Similar effects have been found with other systems (15). Differences may also be due to the use of the Hatch-Choate relation in the calculation of the specific surface area of griseofulvin. The Hatch-Choate equation gives only approximate value of specific surface area; this is shown in Section 3:5:4 and in the literature (2,7). However, the adsorption patterns on polystyrene latex and on griseofulvin are similar.

Table 9 shows that as the molecular chain length of the Texofor increases the maximum amount adsorbed decreases and the area occupied per molecules increases. Table 9 also shows that the amount adsorbed is dependent on the polyoxyethylene chain length. On the other hand, Table 10 shows that the adsorbed ^{layer} thickness increases with increasing the molecular chain length. If adsorption occurs via the polyoxyethylene chain only, a constant adsorbed layer thickness could result, due to

the protruding of the C₁₆ chain of the molecules, and an increase in adsorption area per molecule would occur. If adsorption occurs with only the hydrocarbon chain of the molecule attached on the surface, there would be a constant molecular adsorption area and an increase in adsorbed layer thickness with increasing molecular chain length. However, neither of these cases fit the observations found in Tables 9 and 10. Therefore, it is likely from the increase in molecular adsorption area and in adsorbed layer thickness that the Texofor molecules were adsorbed on the surface in a loop form with both the polyoxyethylene and the hydrocarbon chain attached to the surface. These results found here confirm the observations of Elworthy and Guthrie (95) who studied these surface active agents on griseofulvin and of Kayes (221) who studied polystyrene latex (0.761 μm diameter).

The adsorption functions of these looped molecules may be due to the hydrophobic effect of the hydrocarbon chain and to the hydrogen bonding of the polyoxyethylene chain to the surface. The surface of the polystyrene latex as described in Section 3:5 contains three kinds of possible groupings i.e. the carboxyl, sulphate and hydroxyl groups which occupy about 1/15 of the surface area. The majority of the surface of the polystyrene latex which was composed of the constituents of styrene can be regarded as hydrophobic in nature. Adsorption of the hydrocarbon chain will occur on these hydrophobic sites by means of hydrophobic bonding which would result from restructuring of the hydrogen bonding between the water molecules leading to an increase of entropy which favours adsorption (222). The hydrophilic polyoxyethylene chain adsorption may occur through the ether oxygen of the chain and the hydrogen atom of the surface groupings by means of hydrogen bonding. The surface groupings available for

hydrogen bonding are the hydroxyl groups and some of the unionized acidic groups. At pH 6.0, most of the acidic groups are ionized. hydrogen bonding may also occur between the solvation sheath of the bound water molecules surrounding the acidic groups and the ether oxygens. Furthermore, the hydrated water molecules associated with the hydrophilic ethylene oxides can also play a role in the adsorption by hydrogen bonding between the solvated surface groupings. Finally, adsorption may occur on the hydrophilic sites by ion-dipole association with the ionized acidic groups (229).

4:2:3 Adsorption of Celluloses

4:2:3:1 Polystyrene latex

The nonionic water soluble celluloses used were HEC L, HEC J, HPC E, HPC L, HPMC 603, HPMC 606 and HPMC 615. Results are shown in Figs 37, 38 and 39. For HEC adsorption (Fig. 37), the curves show that initially adsorption increases rapidly with increasing concentration. Then, for HEC J, the adsorption levels off at about 0.07 g/dl and increases again after the plateau region. However, for HEC L, the adsorption levels off at about 0.1 g/dl but true equilibrium adsorption is not attained and a slight increase of adsorption is found. The adsorption isotherms HPC and HPMC (Figs 38 and 39 respectively) show similar profiles i.e. a steep initial slope, a plateau region which may represent monolayer adsorption and then a substantial increase in adsorption which is possibly due to multilayer adsorption.

It appears that pH and the presence of 10^{-3} M NaCl do not alter the adsorption patterns within the limits of the experimental error.

Adsorbed layer thicknesses of Celluloses on polystyrene latex obtained from both small (diameter $0.1725 \mu\text{m}$) and large (latex 4A, diameter $2.111 \mu\text{m}$) particles by viscometry are given in Table 11. As the highest volume fraction of the polystyrene latex used in the measurements was $0.009 (<0.02)$, the Einstein equation (Eq.(90)) was used to obtain more accurate results. The graphs plotted of η_r against ϕ are shown in Figs 40 and 41 for HPC and HPMC on latex 4A ($2.111 \mu\text{m}$) respectively. Good straight lines (correlation coefficient not less than 0.97) were obtained indicating that the experimental data fit the equation very well. The adsorbed layer thicknesses on small latex ($0.1725 \mu\text{m}$) were measured using the single concentration method of Droszkowski and Lambourne (224). The volume fraction used was 0.0013.

An attempt was made to use Eqs (91) and (92). However, the results obtained from the plots for example $(\eta_r - 1/\phi)$ vs ϕ or $(\ln \eta_r/\phi)$ vs $\ln \eta_r$ did not correlate either with those obtained from the Einstein equation or the results obtained by calculation of molecular length. The reliability of these results is doubtful. This is probably due to the dilute volume fractions used in this experiment which are applicable to the Einstein equation only whereas Eqs (91) and (92) are for concentrated dispersions.

The adsorbed layer thicknesses of Celluloses on polystyrene latex calculated from electrophoretic data by using Eq. (88) are also shown in Table 11.

Table 11 shows that within experimental error the thickness of the adsorbed layer of the Celluloses is not dependent on the particle

Cellulose	Adsorbed layer thickness nm			Zeta potential -mV
	Viscometry		Microelectro- phoretic method with latex 4A	
	Diameter 2.111 μm (latex 4A)	Diameter 0.1725 μm		
HEC L	-	53.6	21.0 \pm 1.2	6.9 \pm 0.8
HEC J	-	52.8	19.9 \pm 1.0	7.5 \pm 0.7
HPC E	51.2	42.8	15.0 \pm 0.7	13.1 \pm 0.9
HPC L	29.8	32.1	13.6 \pm 0.6	14.4 \pm 0.9
HPMC 603	22.9	17.0	12.5 \pm 1.2	16.3 \pm 2.0
HPMC 606	24.8	27.9	14.8 \pm 0.6	12.7 \pm 0.8
HPMC 615	41.3	36.4	22.5 \pm 2.0	5.7 \pm 1.2

Table 11 Adsorbed layer thicknesses of Celluloses on polystyrene latex.

size of the polystyrene latex. The agreement of the adsorbed layer thickness obtained from viscometry and from the microelectrophoretic method is not good. Garvey et al (228) have studied four methods for determining the adsorbed layer thickness of polyvinyl alcohol on polystyrene latex particles. They found that results obtained from microelectrophoretic method were not accurate when compared with results obtained from ultracentrifugation, IFS and slow speed centrifugation methods. Here, when comparing the microelectrophoretic adsorbed layer thickness values with those results obtained from viscometry one found that the former have considerably lower values. This suggests that the results obtained by the microelectrophoretic method are not

reliable since several assumptions were made in these calculations.

The conformation of polymers in the unadsorbed states can be used as a guide for the investigation of the conformation of adsorbed polymers. In solution, the conformation of the polymer is determined by the intramolecular and intermolecular interactions and the solvent conditions as mentioned in Section 2:1. In an attempt to obtain the molecular dimensions of the Celluloses used, examination of solutions was made using light scattering as described in Section 3:5:2. This was not successful probably because of the wide size distribution of the molecular substances. Another method used is due to Simha (225) and Kraema (226). They developed equations of a semiempirical nature relating the intrinsic viscosity to the axial ratio of the molecule. The basic assumption is that the polymer in solution is considered as an ellipsoid of revolution which hydrodynamically produces the same effect as the real molecule. The equation given by Simha is

$$[\eta] = 0.207f^{1.732} \quad (95)$$

where f is the axial ratio which is equal to l/d in which l is the length and d is the diameter of the molecule. Kraema gave an expression

$$l = \left(\frac{6f^2 M v_2}{N_A} \right)^{\frac{1}{3}} \quad (96)$$

where M is the molecular weight and v_2 is the partial specific volume and N_A is the Avogadro number. This treatment of the molecular dimensions of polymers was used by Badgley and Mark (227). They compared the dimensions of cellulose acetate molecules in acetone and in methyl cellosolve obtained both by this method and by an X-ray method and found reasonable agreement for low molecular weight fractions but divergence between the results occurred for high molecular weight fractions.

Eqs (95) and (96) have been used to calculate the molecular dimensions of the Celluloses here. The results are shown in Table 12 together with the results obtained from Catalin models.

Cellulose	Viscometry		
	Length nm	Diameter nm	Molecular area nm ²
HEC L	76.2	1.8	137.2
HEC J	100.7	1.9	191.3
HPC E	83.7	2.2	184.1
HPC L	95.7	2.2	210.5
HPMC 603	30.3	1.3	39.39
HPMC 606	50.4	1.4	70.56
HPMC 615	63.6	1.4	89.04
Catalin model			
HEC L	195.1	2.0	390.2
HEC J	292.6	2.0	585.2
HPC E	220.7	1.6	353.1
HPC L	260.6	1.6	417.0
HPMC 603	44.3	1.4	62.02
HPMC 606	79.3	1.4	111.0
HPMC 615	106.1	1.4	148.5

Table 12 Molecular dimensions of Celluloses from viscometry and Catalin models.

For HPMC, the magnitudes of the molecular length obtained from viscometry and from Catalin models are comparable but for HEC and HPC, they diverge markedly. This indicates that the HPMC molecule is rather rigidly extended. The HEC and HPC molecules are also rigid but as their molecular length increases the rigidity decreases. This is also shown in Table 4 in which the a values of Eq. (72) are 0.87, 0.84 and 0.88 for HEC, HPC and HPMC respectively, indicating that the molecules are somewhat nonflexible. The flexibility of the Cellulose molecules is restricted by their six membered ring and ether linkage and by intramolecular hydrogen bonding.

Considering the conformation of the adsorbed molecules, there are three possible arrangements of the Cellulose molecules on the surface: (a) adsorption via backbone with substituted branches extended into the solution, (b) adsorption via substituted branches, (c) adsorption via both backbone and substituted branches the molecule being partially attached to the surface.

If one assumes backbone adsorption, then from the Catalin model, a repeating unit (RU), of two monomers of β 1 - 4 anhydroglucose units occupies an area of 0.25 nm^2 when the molecules adsorb flat on the surface. From Celluloses adsorption results (Table 13), adsorption areas from 0.13 to 0.77 nm^2 per RU on polystyrene latex surfaces are shown. It seems therefore that Cellulose chains might adsorb as a flat layer on the surface. However, the adsorbed layer thicknesses obtained from this model lie within the range $0.4 - 0.9 \text{ nm}$ which is far less than the values obtained from experiment (Table 11) in which the adsorbed layer thicknesses varied from 17 to 53.6 nm from viscometry and 11 to 23 nm from microelectrophoretic

measurement. It therefore appears unlikely that backbone adsorption is taking place. Moreover, as given by Eq. (12), the amount adsorbed at the point of saturation is independent of the molecular weight of the polymer when it lies flat on the surface. However, experiment shows that the amount adsorbed varies with molecular weight. It would appear therefore that molecules of the Celluloses do not follow the backbone adsorption assumption.

Cellulose	Plateau adsorption mg/g	Area occupied per molecule nm ² /molecule		Area occupied per RU nm ² /RU
		Light scattering data	Viscometric data	
HEC L	9.10	23.99	14.82	0.13
HEC J	5.10	64.60	41.00	0.23
HPC E	5.30	59.30	49.41	0.27
HPC L	3.70	97.66	86.47	0.40
HPMC 603	1.25	34.95	6.98	0.77
HPMC 606	3.20	24.60	6.83	0.33
HPMC 615	4.55	23.10	7.20	0.23

Table 13 Data of adsorption of Celluloses on polystyrene latex (plateau values for HEC taken at 0.1 g/dl equilibrium concentration).

For the HEC and HPC samples studied here, the average number of moles of substituted branch for ethylene oxide chain and hydroxypropyl chain attached to one repeating anhydroglucose unit are 2.5 and 3.0 respectively. The projected areas calculated from the Catalin models of the substituted branches are 0.44 nm² for HEC

and 0.72 nm^2 for HPC. The Catalin areas of substituted branches of HPMC i.e. the hydroxyl, hydroxypropyl and methyl are about 0.45 nm^2 . From Table 13, the experimental results at the plateau adsorption fall in the range of areas derived from the Catalin models. This means that adsorption could have been accomplished via these side chains either with all attached or with one side attached on the polystyrene latex surface. Again, however, comparing the adsorbed layer thicknesses obtained from these models, which vary from 1.5 to 2 nm depending on the orientations and structures of the extended branches with the experimental results (Table 11), this possibility can be ruled out.

The forces governing adsorption will be hydrogen bonding, van der Waals forces and hydrophobic effects (see Section 4:2:3:3). In the absence of specific adsorption for backbone or substituted branches of the Celluloses, the adsorption functioning groups of both the anhydroglucose and substituted units will be involved in the energy contributions. That is to say, the Cellulose molecules adsorb on the surface via both backbone and substituted branches. As suggested by Jenkel and Rumbach (62), the polymer molecules adsorbed on the surface generally form 'wrinkles' or loops extending from the surface into the solution. These wrinkles or loops form a characteristic 'bristle' on the surface. Only the segments of the chains which are at the end of the wrinkles or loops take part in the adsorption site, while the other segments do not directly interact with the adsorbent and are bound to it only via other segments. In this case, the total adsorption areas at the plateau region per RU from the model are 1.10, 1.40 and 1.20 nm^2 for HEC, HPC and HPMC respectively. Compared with the experimental occupied area per RU (Table 13), one suggests that partial adsorption of the molecules may have taken place. From the

significant difference between the experimental values of the occupied areas per molecule (Table 13) and the values calculated from a flat adsorbed molecule (Table 12) and from the difference between the adsorbed layer thicknesses (Table 11) and the length of the molecules (Table 12), it is indeed possible that the Cellulose molecules adsorbed with backbone and substituted branches partially anchored on the surface forming wrinkles and loops with part of the segments extended into the solution.

The dependence of molecular weight on adsorption for HEC, HFC and HPMC is shown in Figs 37, 38 and 39 respectively. For HEC and HFC the amount adsorbed decreases with increasing molecular weight but for HPMC the amount adsorbed increases with increasing molecular weight. The area per molecule (Table 13) for HEC and HFC shows an increase as molecular weight increases while HPMC gives no significant change with increasing molecular weight within experimental error. This indicates that for HEC and HFC, the higher molecular weight molecules adopt a flatter adsorption conformation on the particle surface. This confirmed from the results of the adsorbed layer thicknesses (Table 11). Therefore, the adsorption decreases as molecular weight increases due to the decrease of the area available for adsorption. For HPMC, the different molecular weight molecules attach to the surface with the same values of occupied area and the adsorbed layer thickness increases with increasing molecular weight. That is to say, for higher molecular weight molecules more segments of the adsorbed polymers extend into the solution and this results in an increase in adsorption as molecular weight increases.

If the system becomes aggregated, the dependence of molecular

weight on adsorption would decrease as the amount adsorbed increases. This is because the aggregated particles form a porous structure i.e. a porous adsorbent. The probability that the low molecular weight polymers enter into the pores is greater than that of the high molecular weight polymers. As a result, the amount of low molecular weight polymers adsorbed is higher than the amount of high molecular weight polymers. In this study of HPMC, HPC and HEC, only HEC systems show aggregation (Section 5:2) and thus this explanation could be applied to HEC adsorption and the effect of molecular weight.

At high equilibrium concentrations, a sudden increase of the amount adsorbed is shown in the adsorption isotherms indicating the formation of the multilayers. As mentioned in Section 2:2, the driving force for adsorption is the change in free energy of the system i.e. the summation of the enthalpies and entropies of the surface-solvent-adsorbate to give a negative value which favours adsorption. If the adsorbate molecules on the surface attract one another this provides extra negative free energy. As a result, the adsorption process will lead by a phase transition to a dense surface layer then to a formation of multilayers. Multilayer formation can be due to the formation of surface crystallization or aggregation since it has been shown that cellulose molecules can develop a crystalline form (192). Silberberg (85) has proposed a multilayer adsorption model and considered that multilayer formation can be regarded as the polymer phase separation in the adsorption process.

4:2:3:2 Ibuprofen

The adsorption isotherms are shown in Figs 42, 43 and 44 for HEC, HPC and HPMC respectively. Similar adsorption patterns to those

on polystyrene latex are found with ibuprofen but for HEC and HPC multilayer adsorptions on ibuprofen occur at concentrations lower than on polystyrene latex. The plateau adsorptions of the monolayer and the molecular areas are given in Table 14.

Cellulose	Plateau adsorption mg/g	Area occupied per molecule nm ² /molecule	
		Light scattering data	Viscometric data
HEC L	3.20	30.08	18.66
HEC J	2.10	68.89	43.46
HPC E	1.60	86.47	72.19
HPC L	0.55	297.0	255.0
HPMC 603	0.40	48.13	9.60
HPMC 606	0.80	43.92	12.21
HPMC 615	1.20	38.52	12.03

Table 14 Data of adsorption of Celluloses on ibuprofen.

The values of the adsorbed layer thickness of Celluloses on ibuprofen obtained by the microelectrophoretic method are shown in Table 15.

Generally, the plateau adsorptions found on ibuprofen (Table 14) are lower than those on polystyrene latex and higher molecular areas are found on ibuprofen than on polystyrene latex. However, The same general trends were found with ibuprofen as with polystyrene latex i.e. the dependence of the amount adsorbed on molecular weight,

Cellulose	Zeta potential -mV	Thickness of adsorbed layer nm
HEC L	7.7 ± 2.3	12.7 ± 3.6
HEC J	8.7 ± 2.3	11.5 ± 3.4
HPC E	4.2 ± 1.5	18.6 ± 4.1
HPC L	6.4 ± 1.7	14.5 ± 3.4
HPMC 603	8.0 ± 2.2	12.3 ± 3.4
HPMC 606	3.5 ± 0.7	20.0 ± 2.9
HPMC 615	2.6 ± 0.6	23.1 ± 3.2

Table 15 Adsorbed layer thicknesses of Celluloses on ibuprofen.

the relation between the molecular adsorbed area and the molecular occupied area in the unadsorbed state, the relation of the adsorbed layer thickness to the molecular weight and the molecular adsorbed area. This indicates that the adsorption mechanism on ibuprofen and the basic conformations of the adsorbed polymers were similar to those on polystyrene latex.

Comparing the values of the adsorbed layer thickness on ibuprofen (Table 15) with those obtained on polystyrene latex (Table 11) by the same technique shows that although the errors of the results with ibuprofen are high, the mean values of the thickness of the adsorbed layers for HPC and HPMC on both ibuprofen and polystyrene latex are of the same magnitude; however, for HEC, the mean values of the adsorbed layer thickness are lower with ibuprofen. This may

be due to the internal conformations of the adsorbed HPC and HPMC molecules being different on polystyrene latex and ibuprofen. As shown in Fig. 45, the number of anchor sites on ibuprofen for polymer adsorption is reduced and therefore the molecules occupy larger areas when adsorb on the surface.

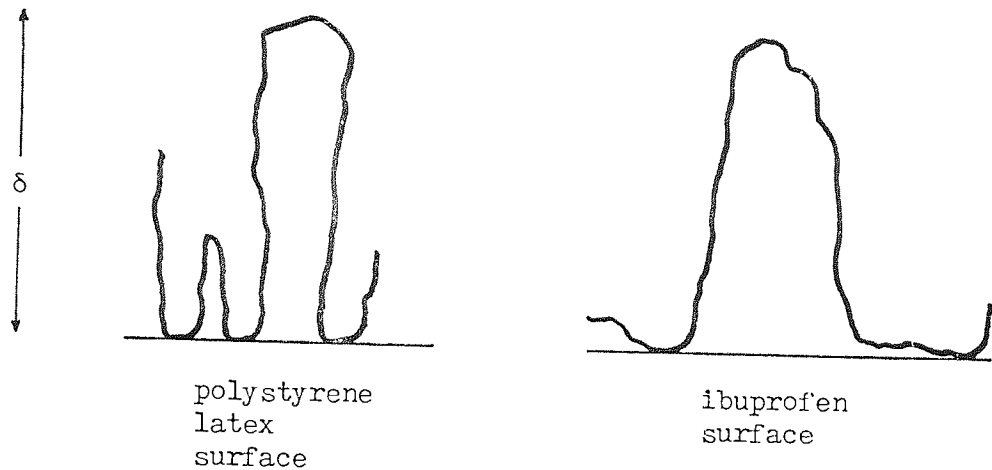


Fig. 45 Internal conformation difference of the adsorbed polymer.

For HEC adsorbed on ibuprofen, one would envisage that the adsorbed molecules would adopt a flatter conformation which occupy large areas on the surface.

4:2:3:3 Binding forces

The binding forces for nonionic polymers adsorbed onto a solid surface are due to hydrogen bonding and van der Waals forces; a third force is the indirect hydrophobic bonding which arises from the restructuring of the water molecules which generates a negative free energy for adsorption.

The hydrophobicity of the surface can be estimated from the

knowledge of the value of the contact angle between the surface and liquid. The Young equation for the contact angle θ of a liquid L on a solid surface S is

$$\gamma_L \cos\theta = \gamma_S - \gamma_{LS} - \pi \quad (97)$$

where γ is the interfacial or surface tension and π is the equilibrium spreading pressure of the saturated vapour on the solid surface. In many approaches to the theory of contact angles, it is assumed that π is approximately zero (215).

The contact angles between the polystyrene and ibuprofen surfaces and the Cellulose solutions of HEC, HPC and HPMC are shown in Figs 46, 47 and 48 respectively. In these figures, all curves show that the contact angle decreases with increasing concentration of the Celluloses and then up to a certain concentration it remains steady. In the concentration range studied, the contact angles show no significant variation with the molecular weight of the Celluloses within experimental error.

The surface tension measurements of Cellulose solutions (Fig. 49) show that within the concentration range studied, the surface tensions are in a steady state and are independent of both change in concentration and in molecular weight. This has also been observed by Chang and Gray (231) with HPC polymers in the concentration range $1 - 10^4$ ppm. They suggested that this phenomenon was analogous to the behaviour of solutions of conventional surface active agents above their cmc where the plateau surface concentration corresponds to the complete surface coverage and the surface tension corresponds to that of the pure polymer. Therefore, the contact angles in these concentration regions

will have little dependence on either concentration or molecular weight.

The contact angles on polystyrene and ibuprofen surfaces show that the polystyrene surface was more hydrophobic. When polystyrene is prepared as latex particles, the surface contains carboxyl, hydroxyl and sulphate groupings. The area of one carboxyl or sulphate group is about 0.2 nm^2 but the area occupied by one carboxyl group is 1.29 nm^2 and sulphate group is 2.04 nm^2 on polystyrene latex 4A in this study. Although hydroxyl groups may be present there is quite a large hydrophobic area which favours hydrophobic bonding. The larger amount adsorbed of Celluloses on polystyrene latex than those on ibuprofen indicates that hydrophobic bondings are probably participating in the adsorption.

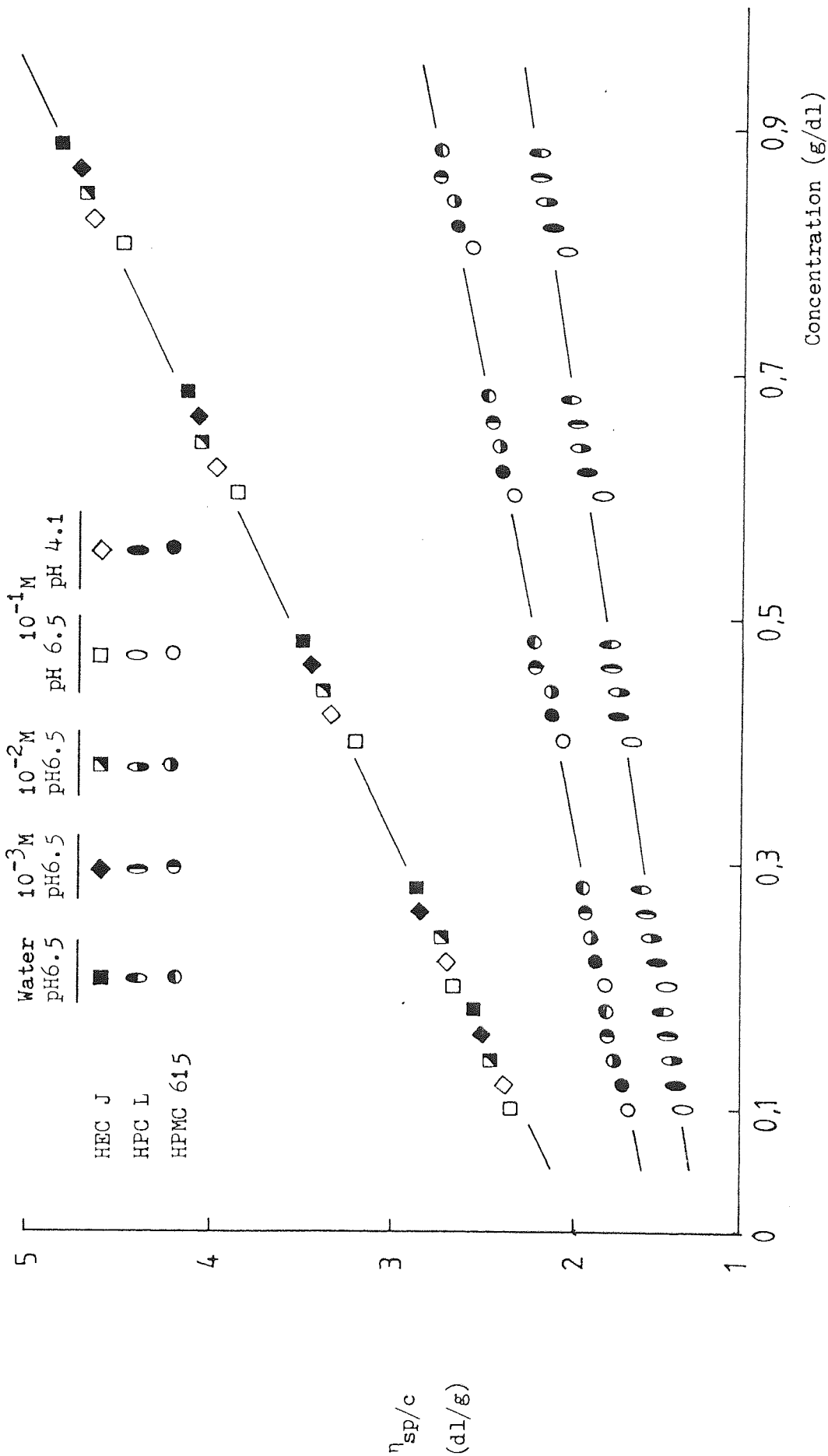


Fig. 32 Huggins plots of Celluloses in the presence of NaCl solution.

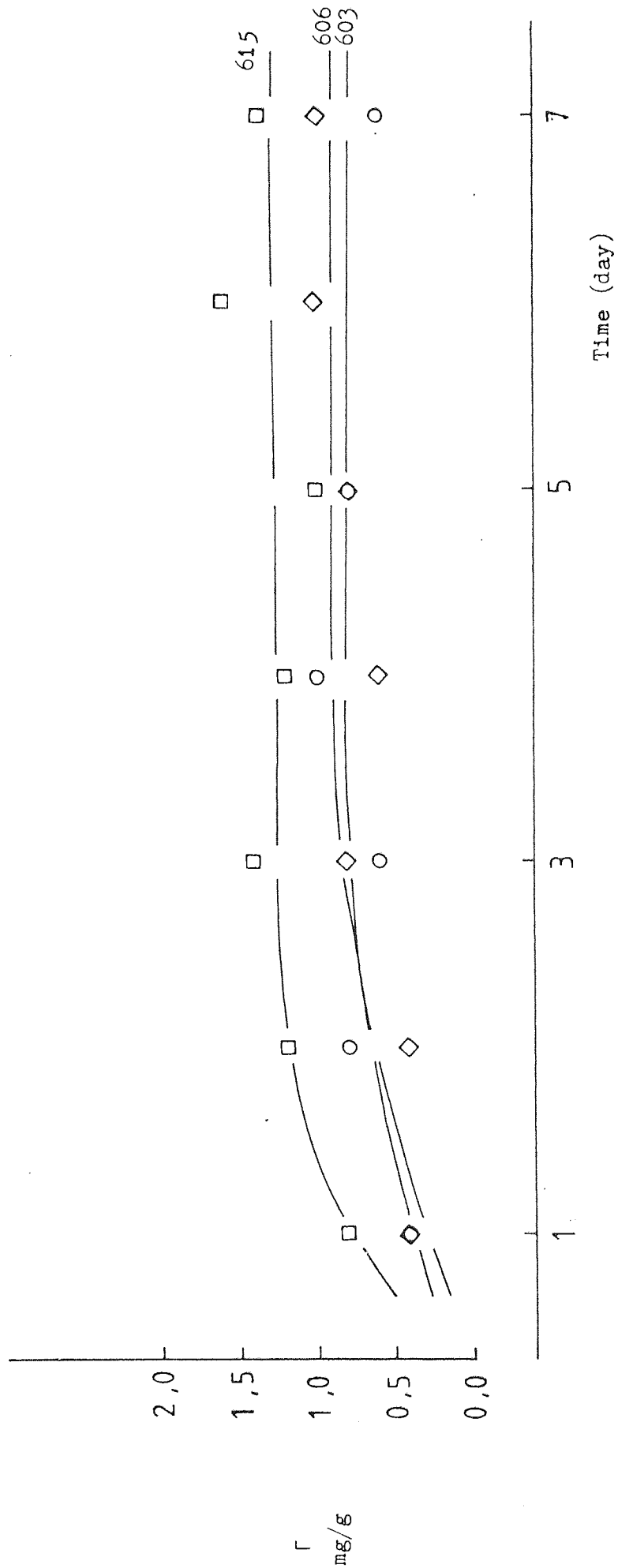


Fig. 33 Rate of adsorption of HPMC.

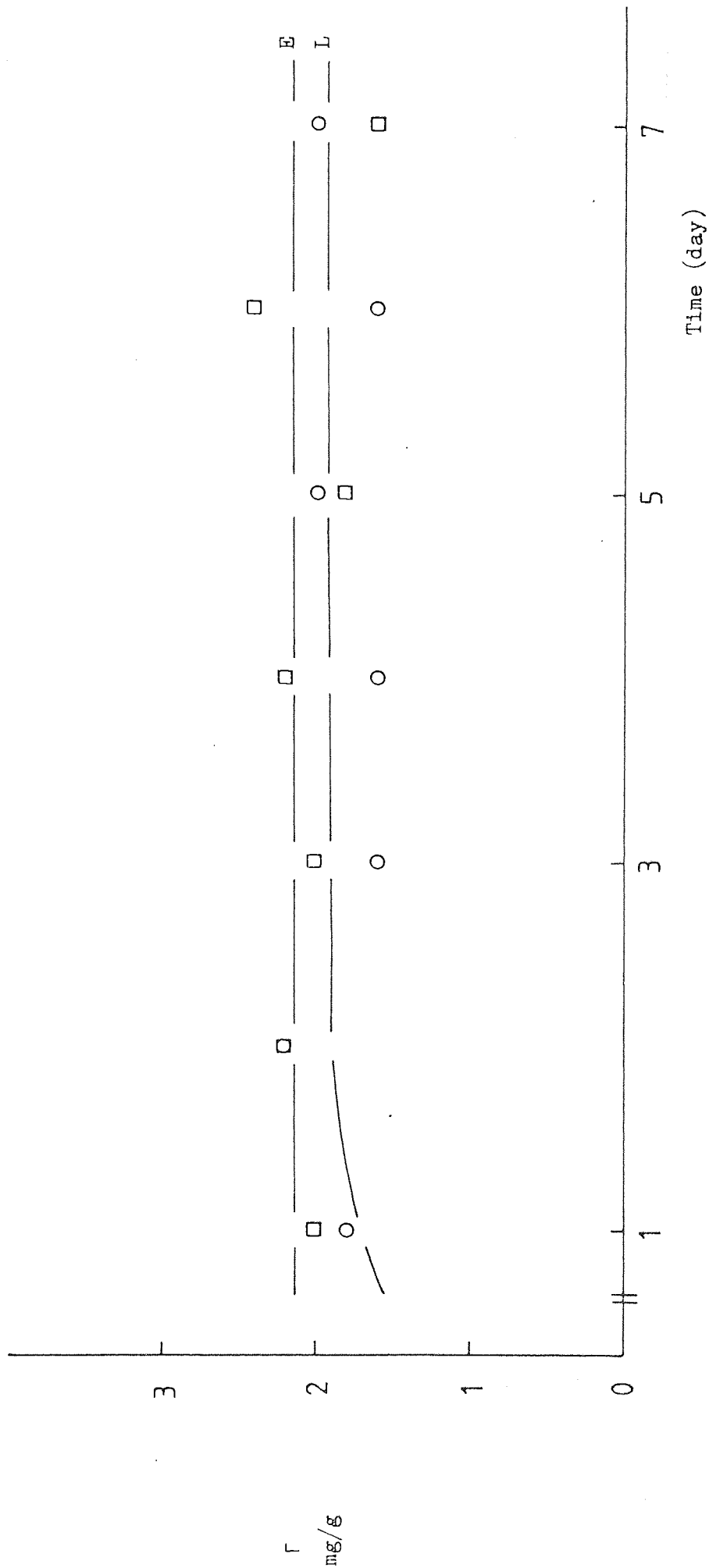


Fig. 34 Rate of adsorption of HPC.

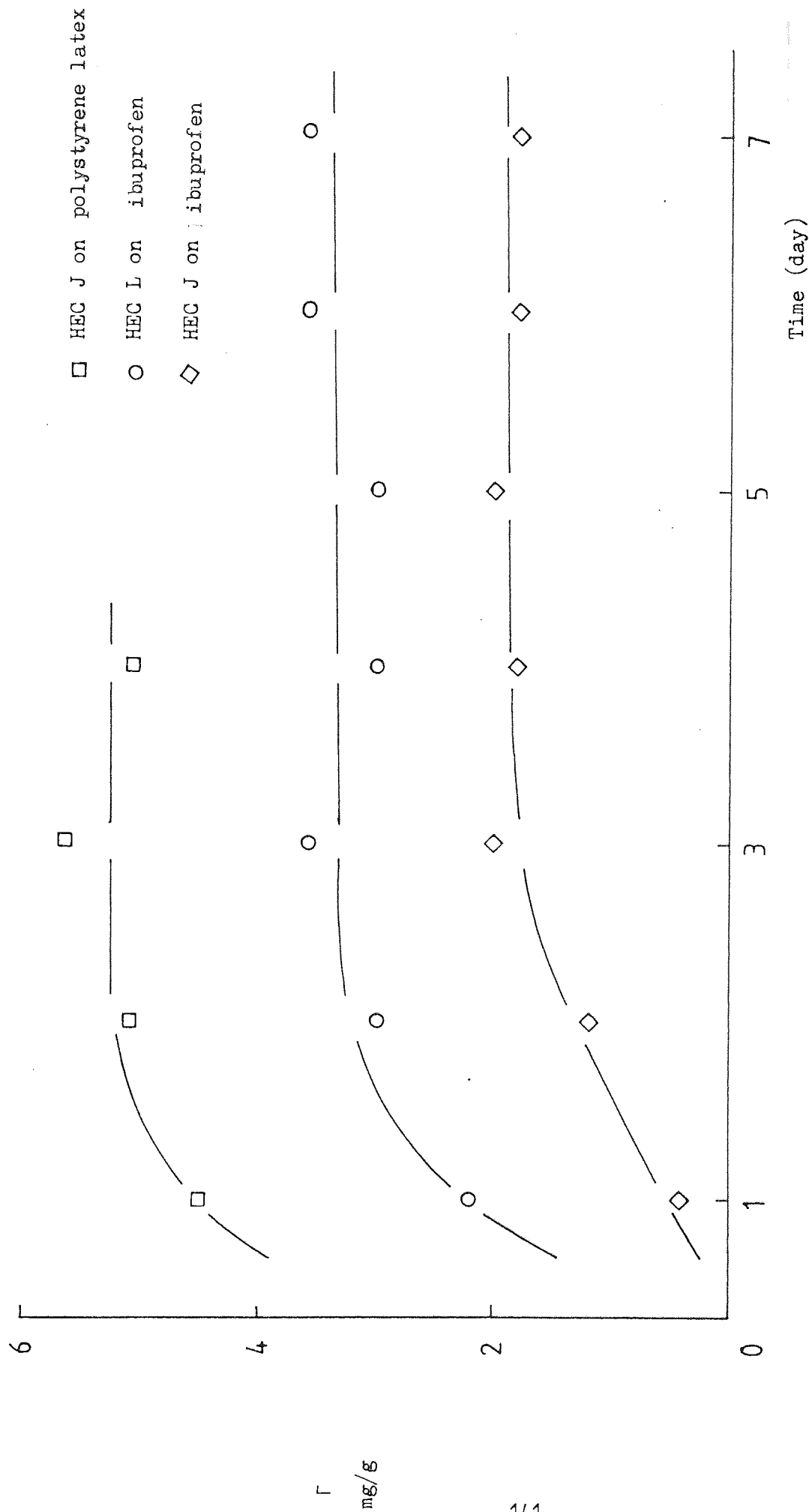


Fig. 35 Rate of adsorption of HEC.

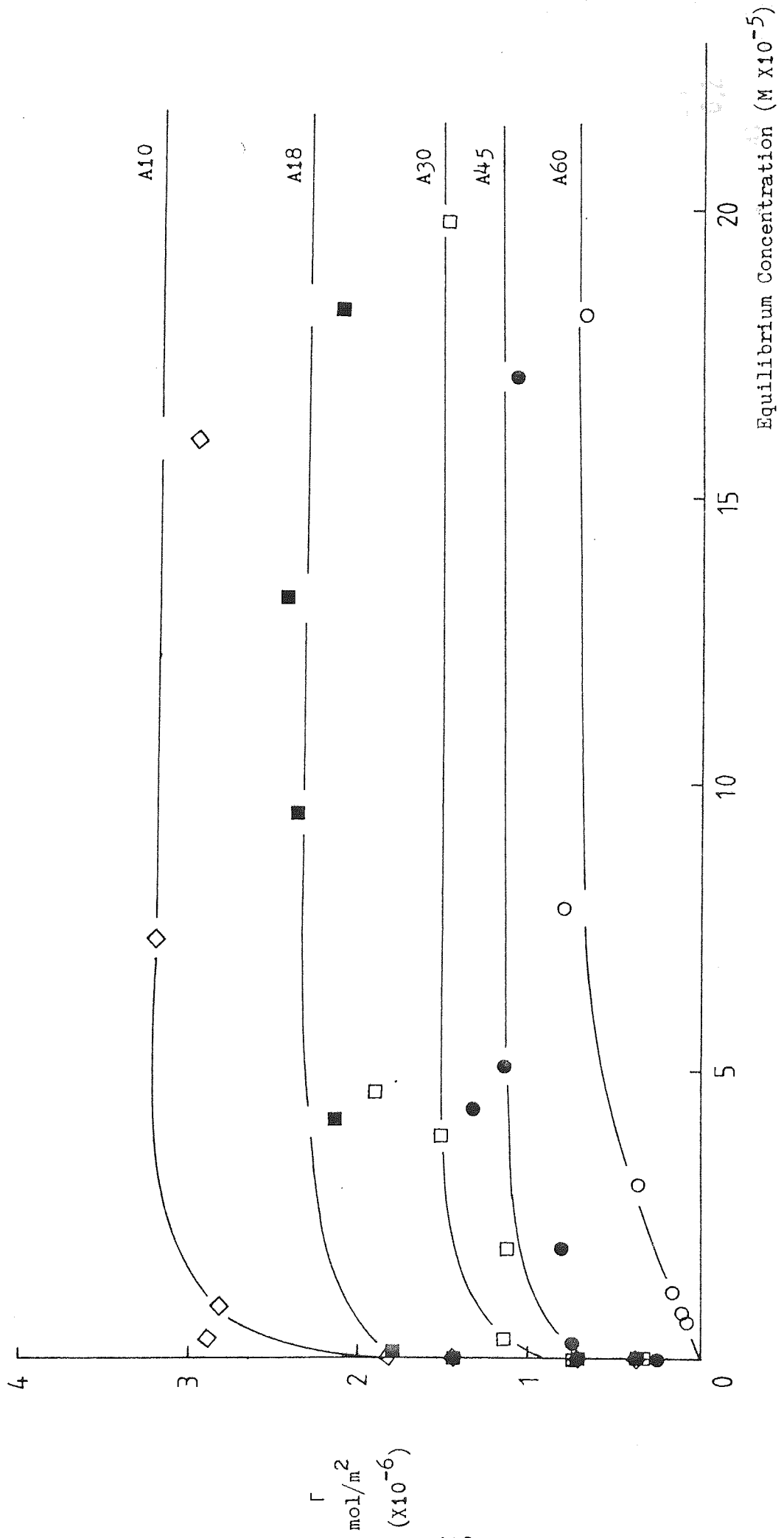


Fig. 36 Isotherms for Texofors adsorbed on polystyrene latex.

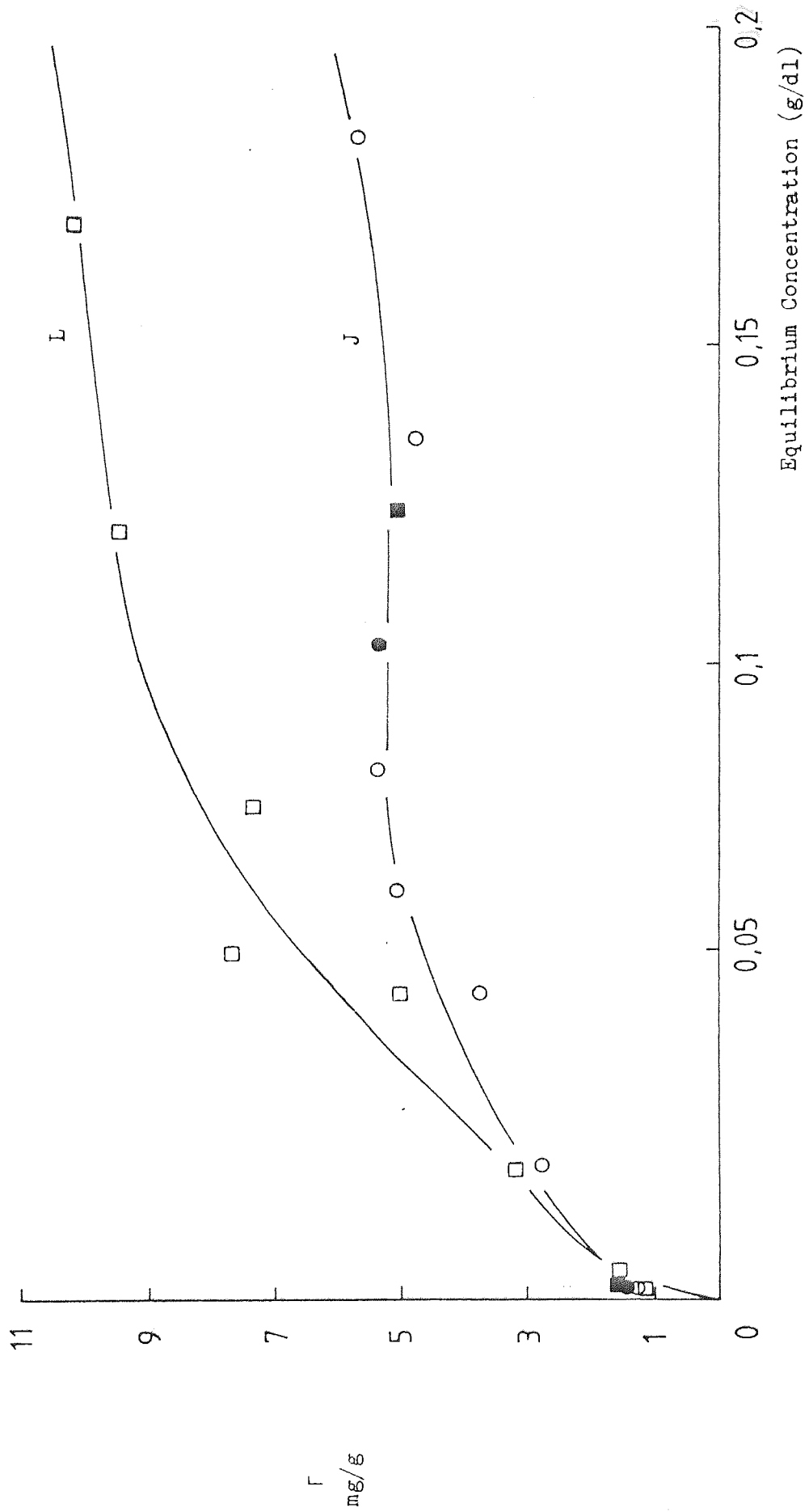


Fig. 37 Isotherms for HEC adsorbed on polystyrene latex.

● at pH 3.0 ■ in 10^{-3} M NaCl

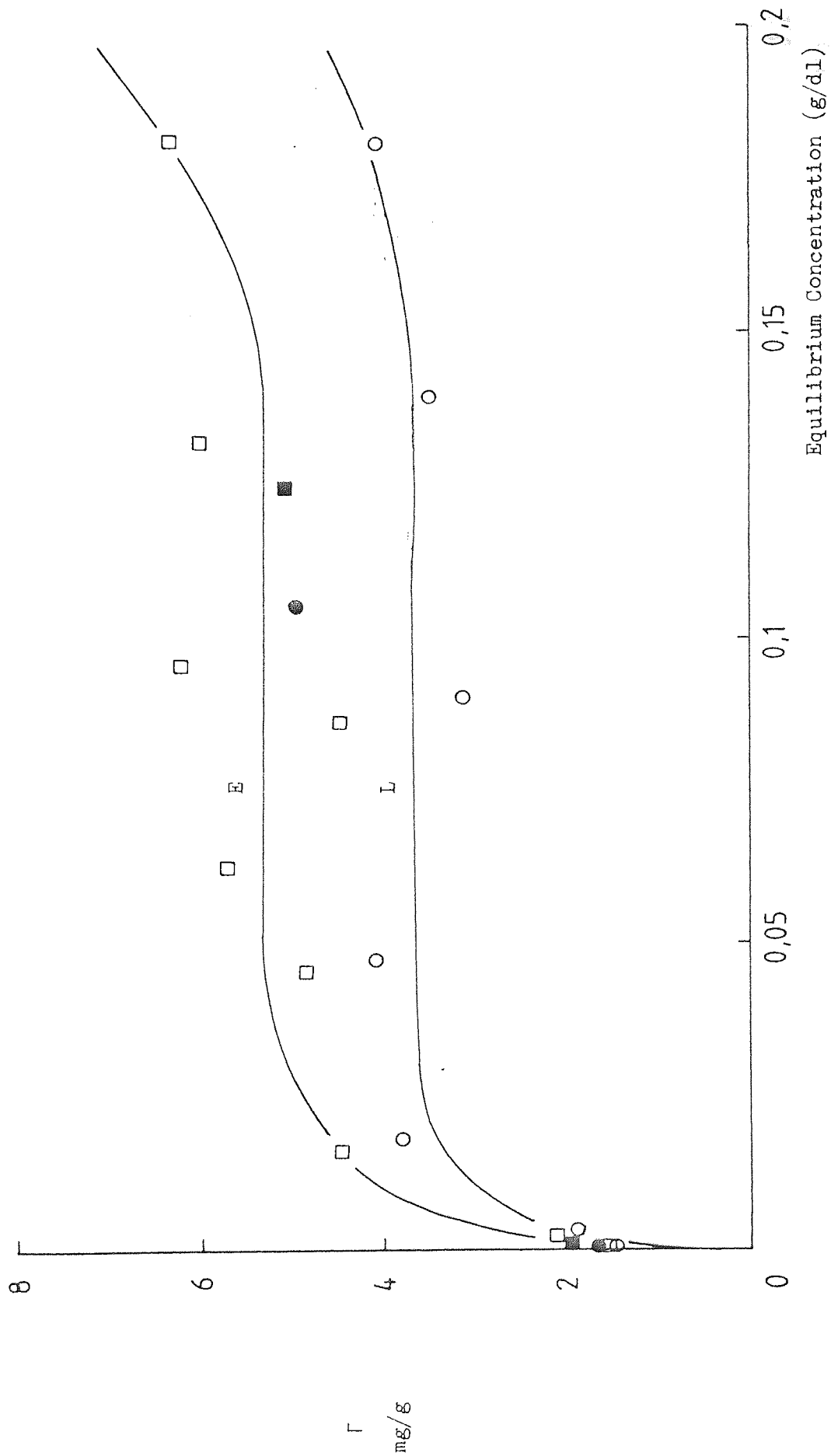


Fig. 38 Isotherms for HFC adsorbed on polystyrene latex.

● at pH 3.0 ■ in 10^{-3} M NaCl

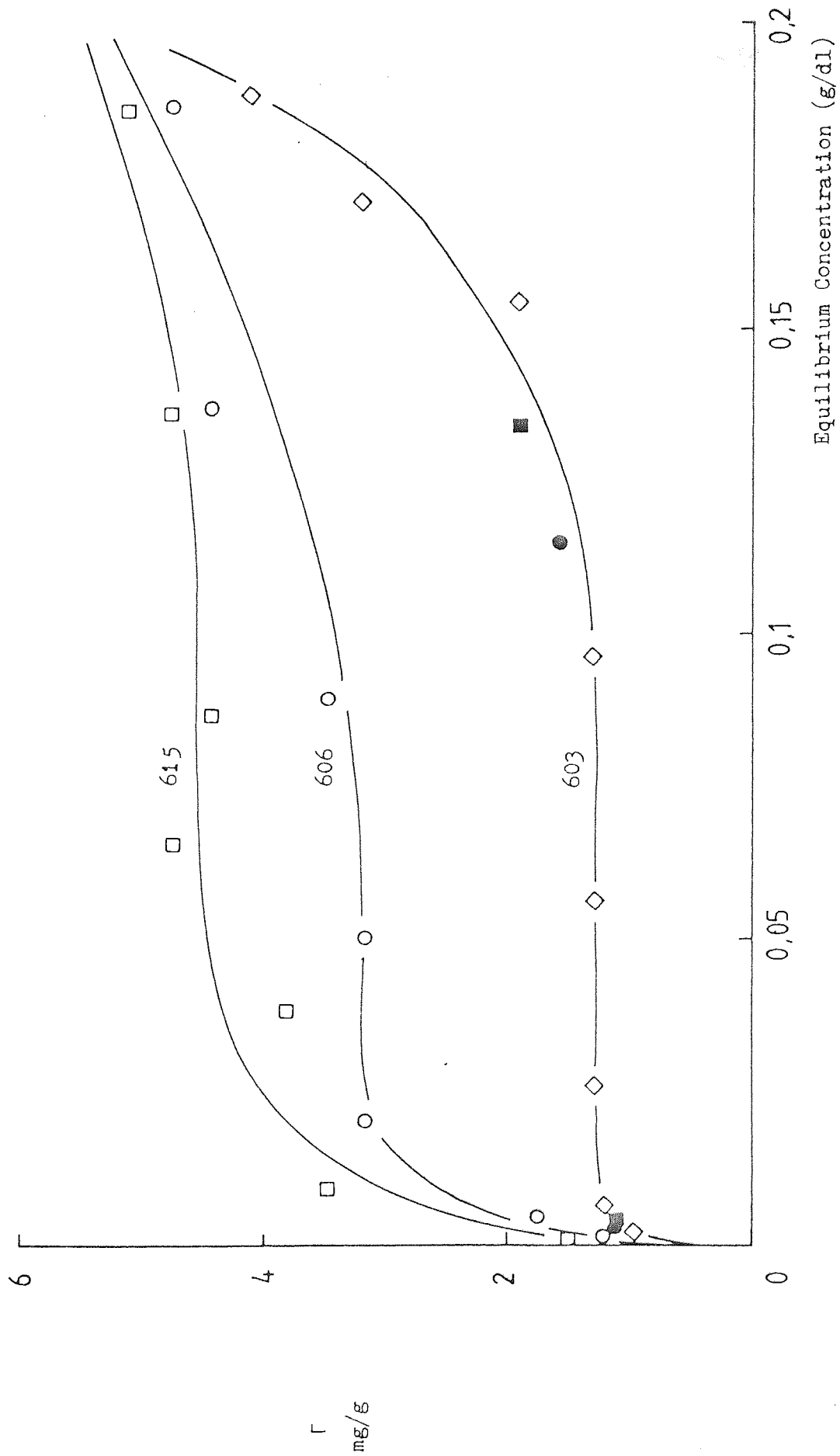


Fig. 39 Isotherms for HPMC adsorbed on polystyrene latex.

● at pH 3.0 ■ in 10^{-3} M NaCl

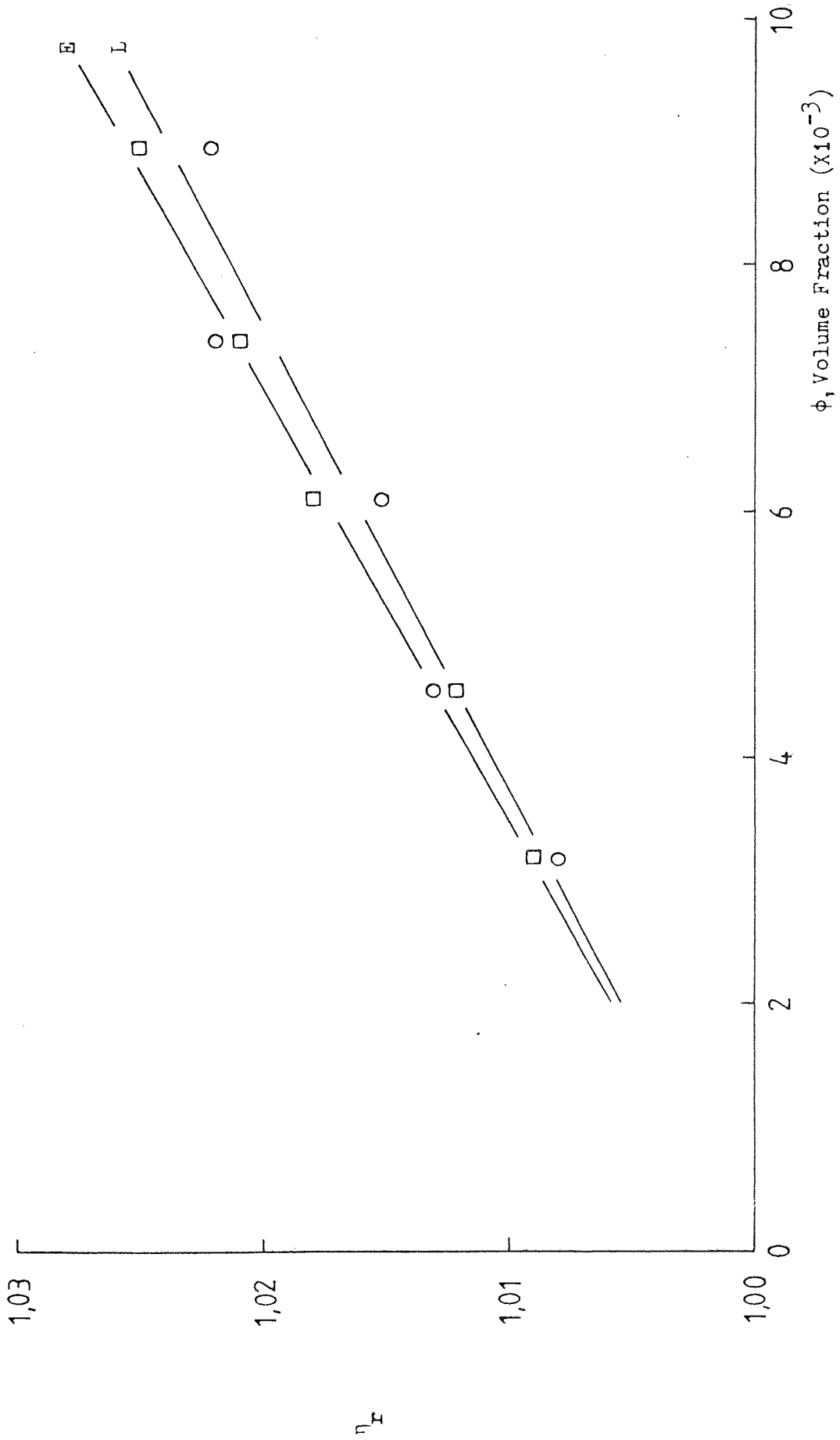


Fig. 40 η_r against ϕ plots of HFC on polystyrene latex 4A.

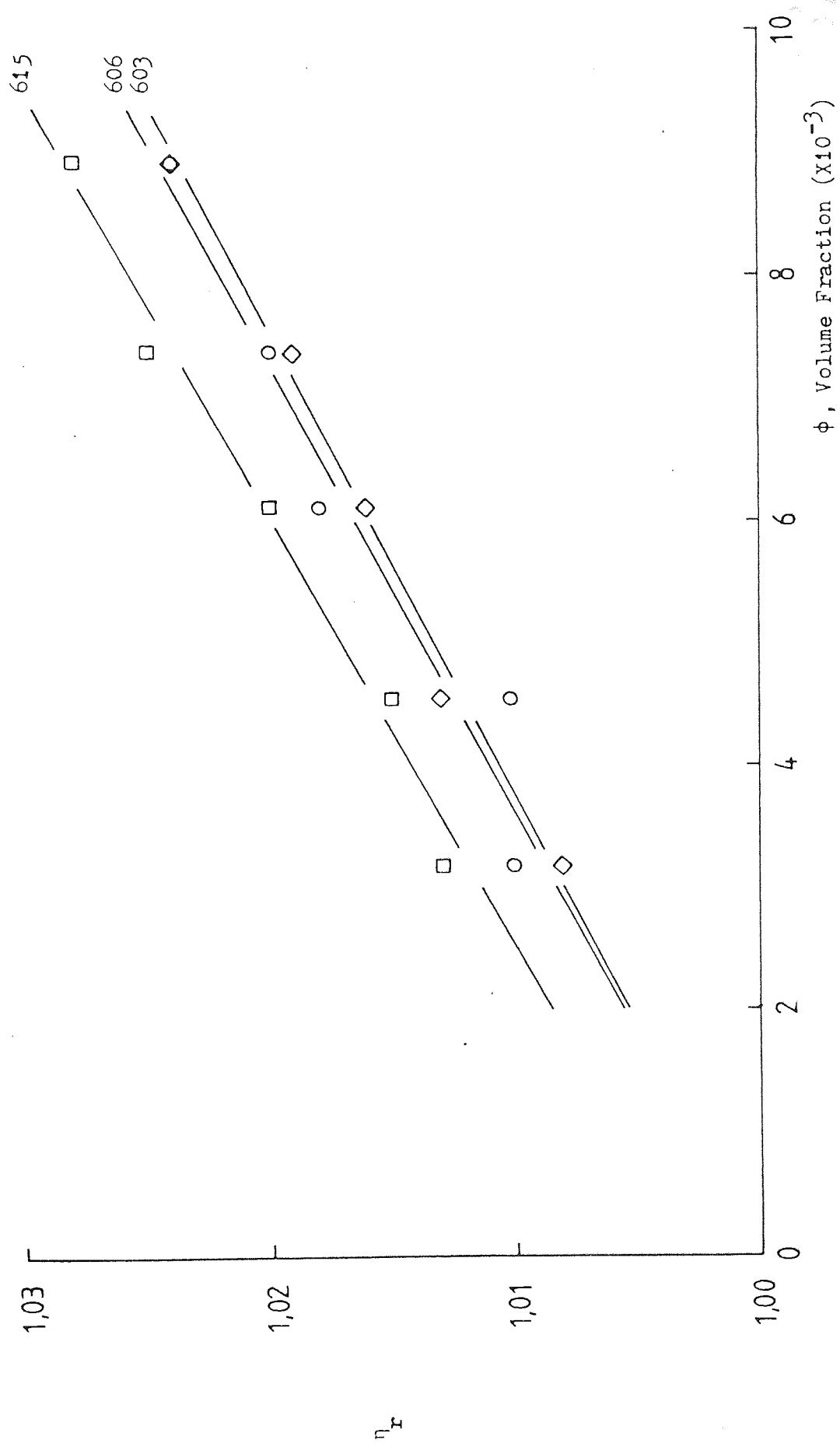


Fig. 41 η_r against ϕ plots of HPMC on polystyrene latex 4A.

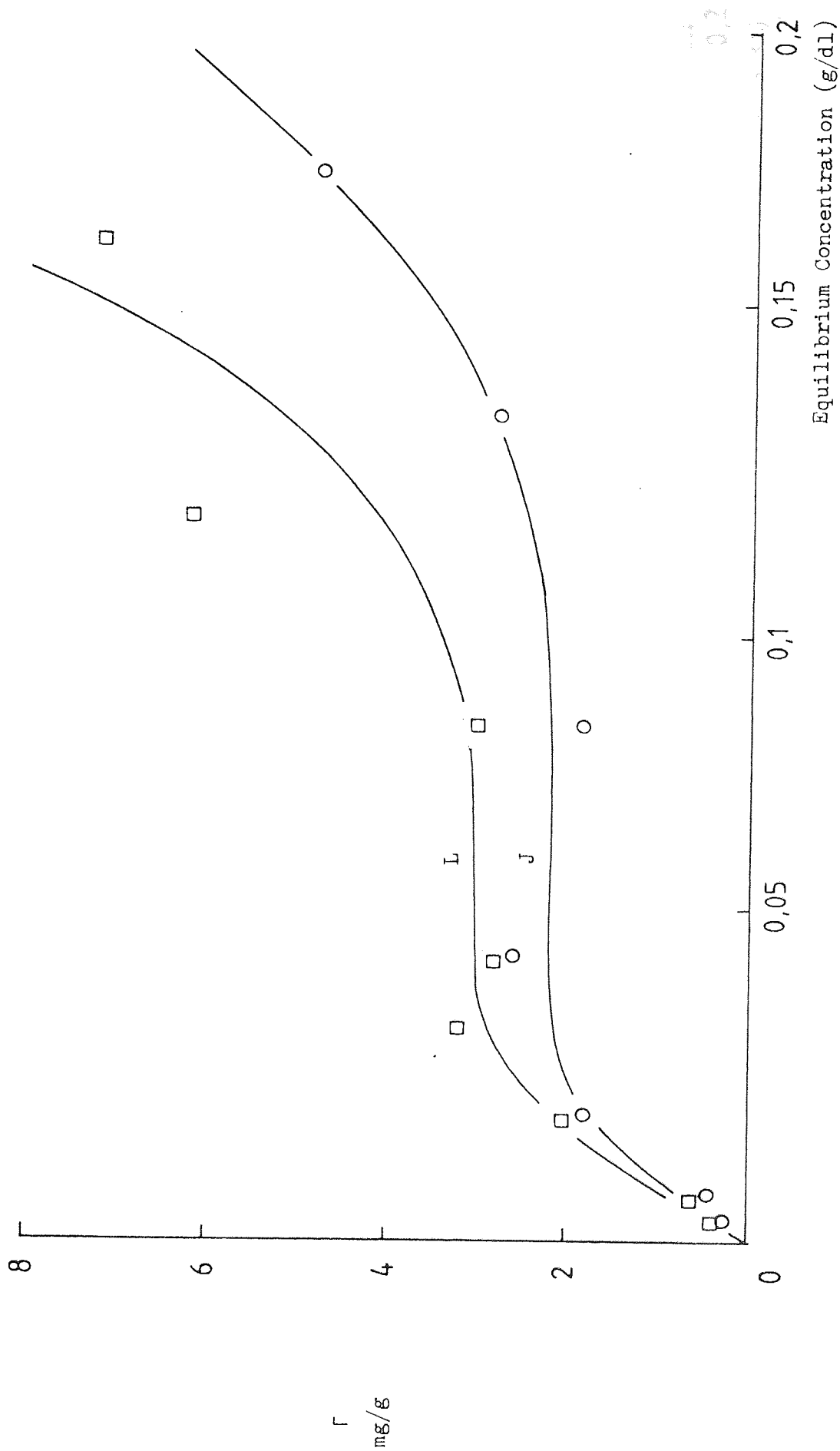


Fig. 42 Isotherms for HEC adsorbed on ibuprofen.

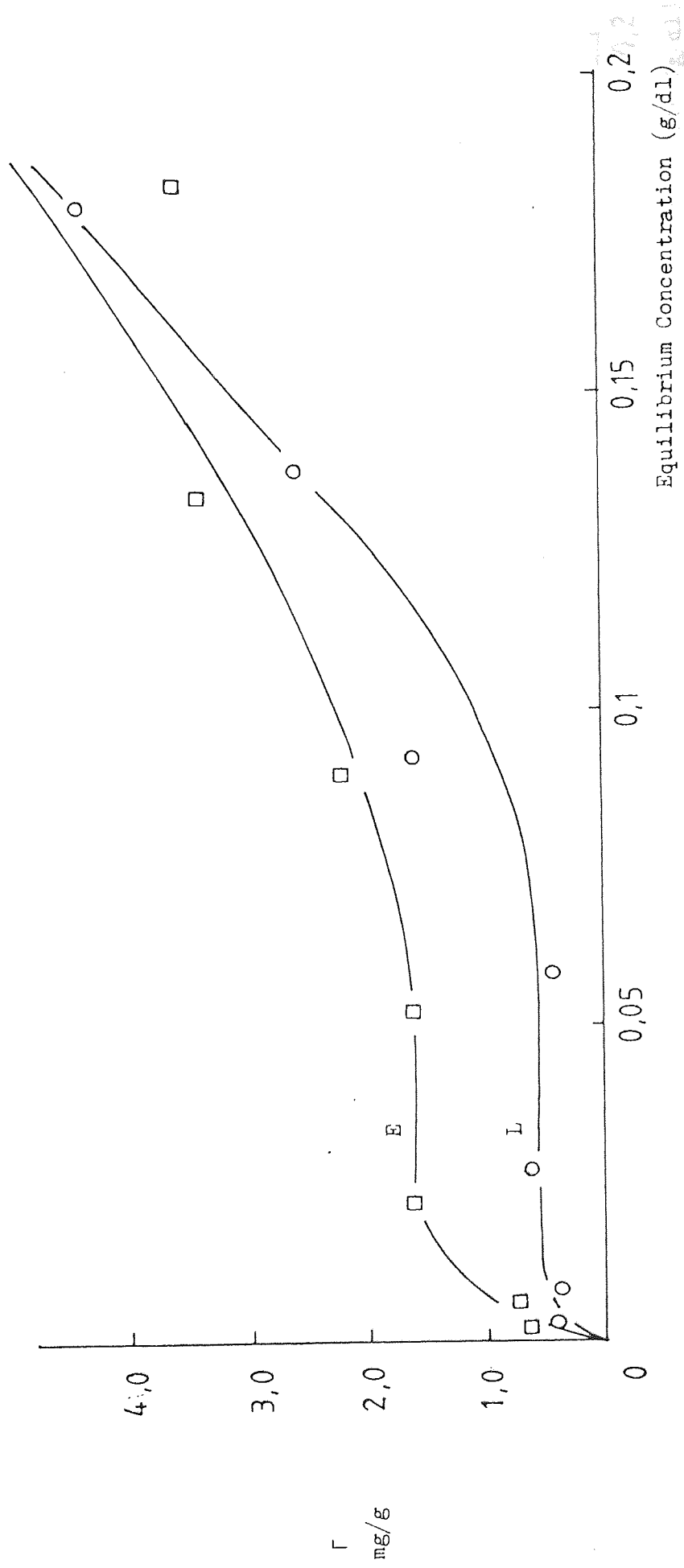


Fig. 43 Isotherms for HPC adsorbed on ibuprofen.

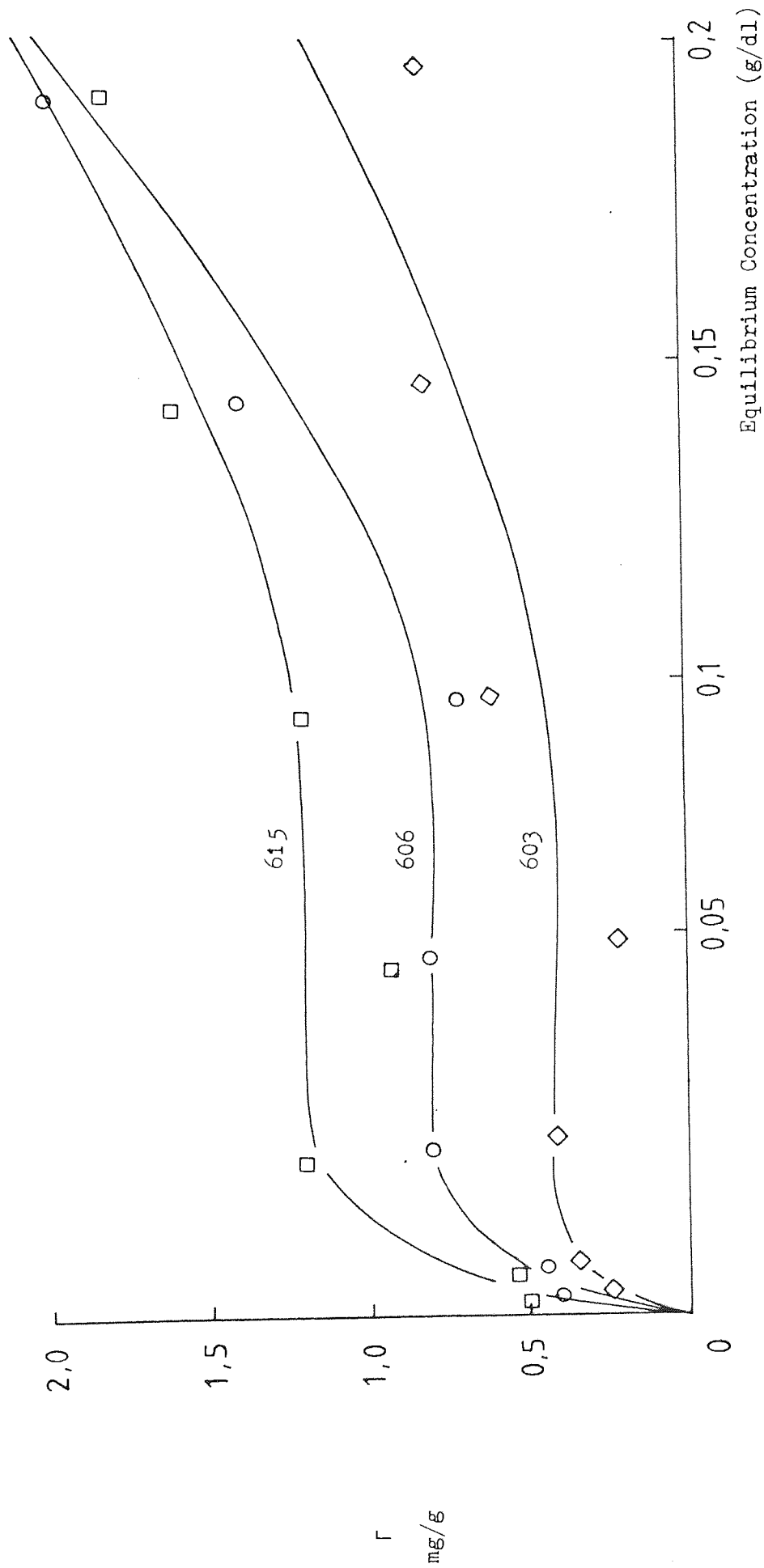


Fig. 44 Isotherms for HPMC adsorbed on ibuprofen.

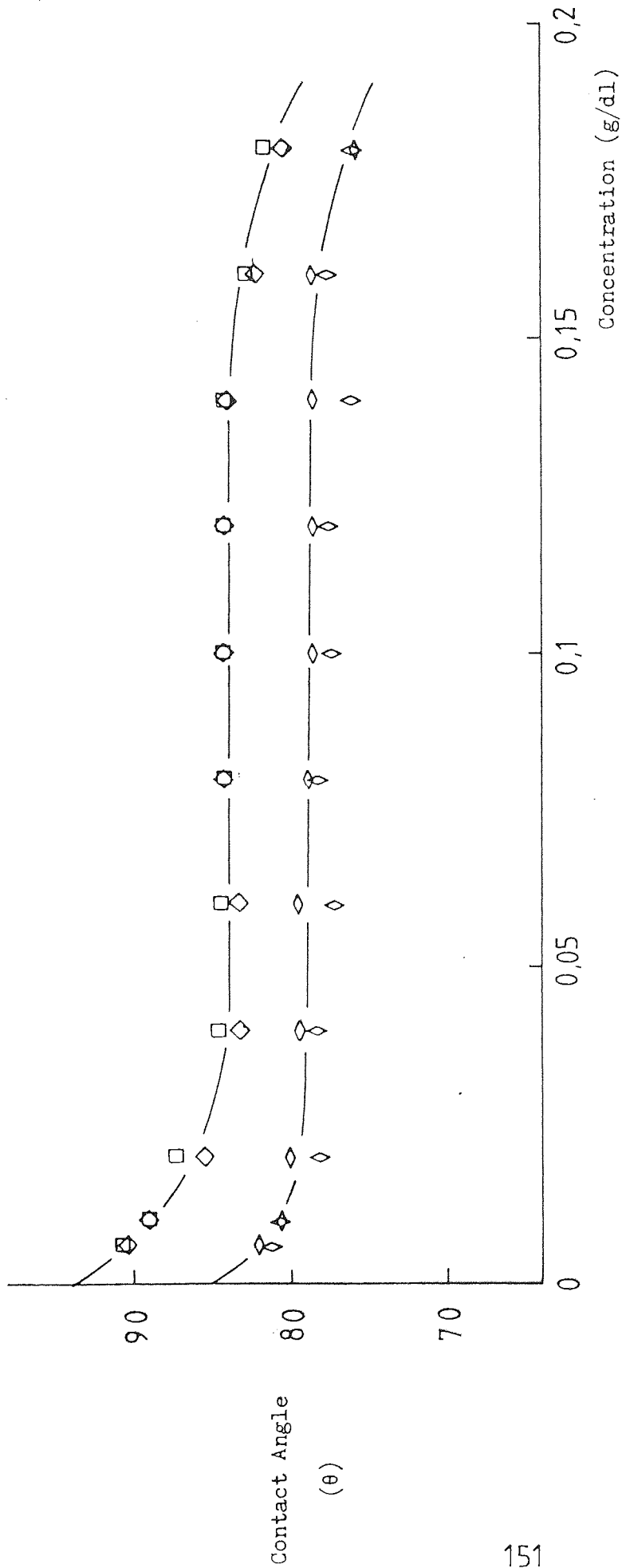


Fig. 46 Contact angle measurements of HEC on ibuprofen and polystyrene surfaces.

◇ HEC L, □ HEC J on polystyrene surface; ◇ HEC L, ◇ HEC J on ibuprofen surface.

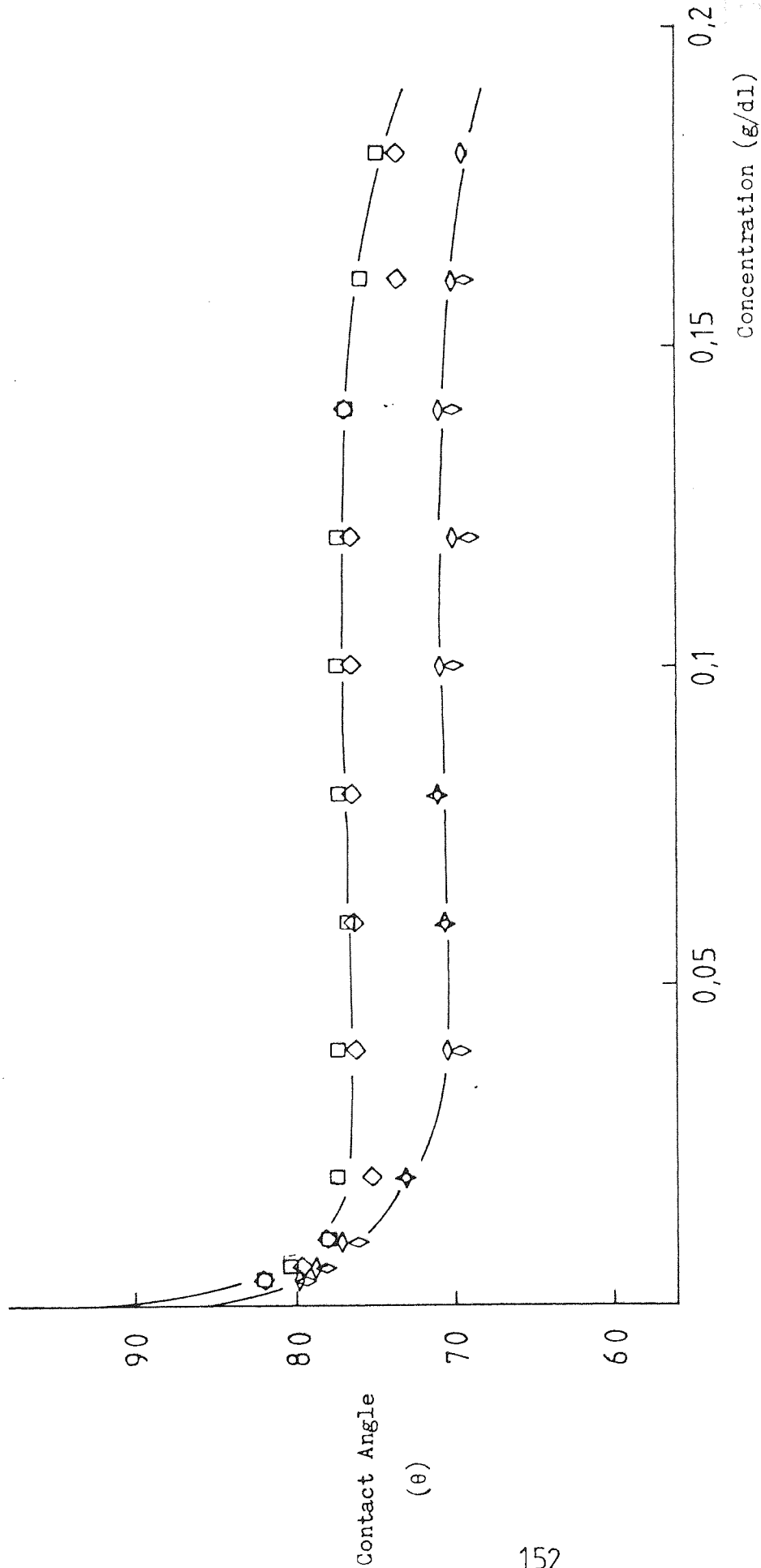


Fig. 47 Contact angle measurements of HPC on ibuprofen and polystyrene surfaces.
 ◇ HPC E, ◊ HPC L on polystyrene surface; □ HPC E, ◊ HPC L on ibuprofen surface.

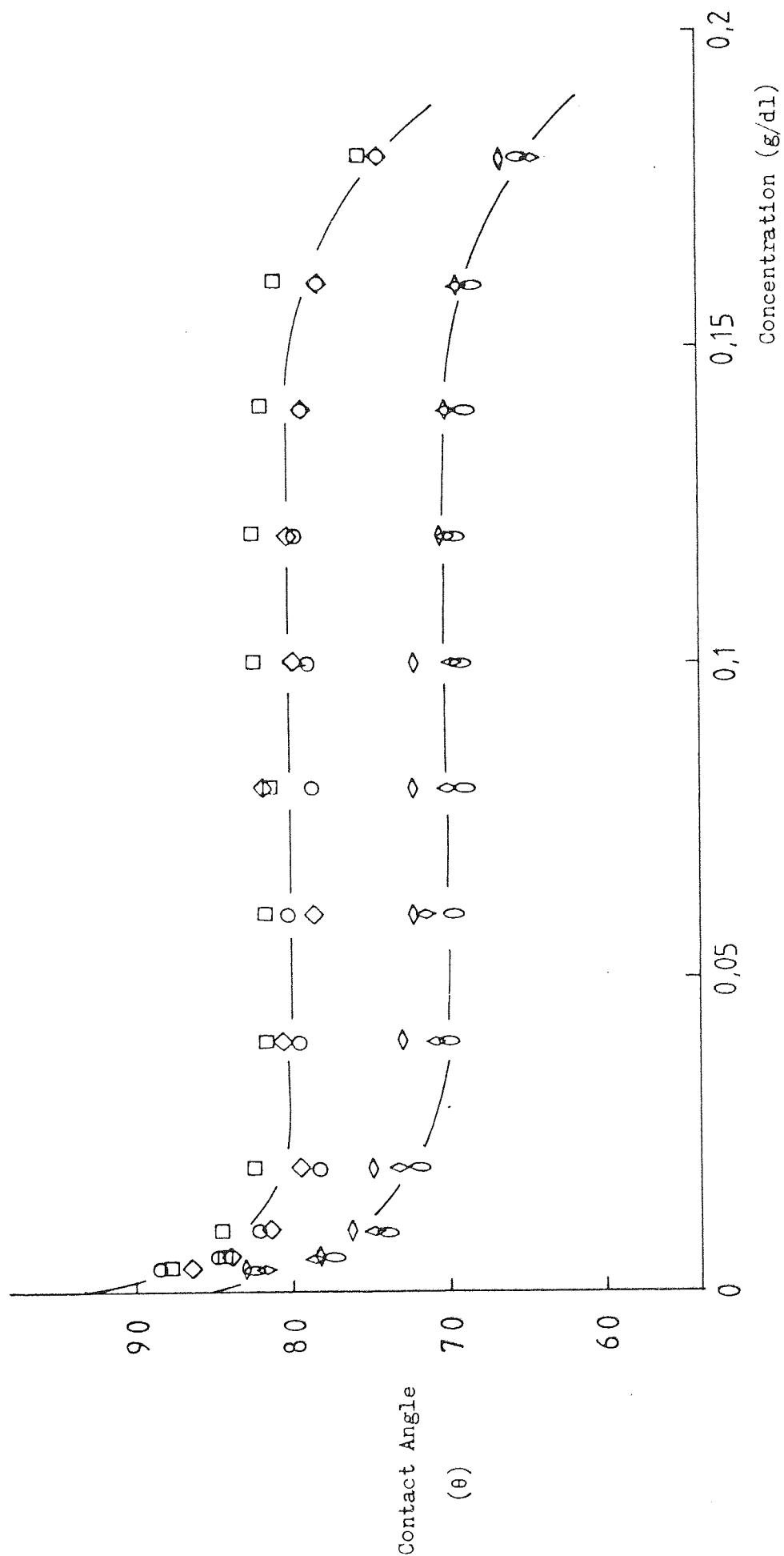


Fig. 48 Contact angle measurements of HPMC on ibuprofen and polystyrene surfaces.

□ HPMC 603, ◇ HPMC 606, ○ HPMC 615 on polystyrene surface;

◇ HPMC 603, ◇ HPMC 606, ○ HPMC 615 on ibuprofen surface.

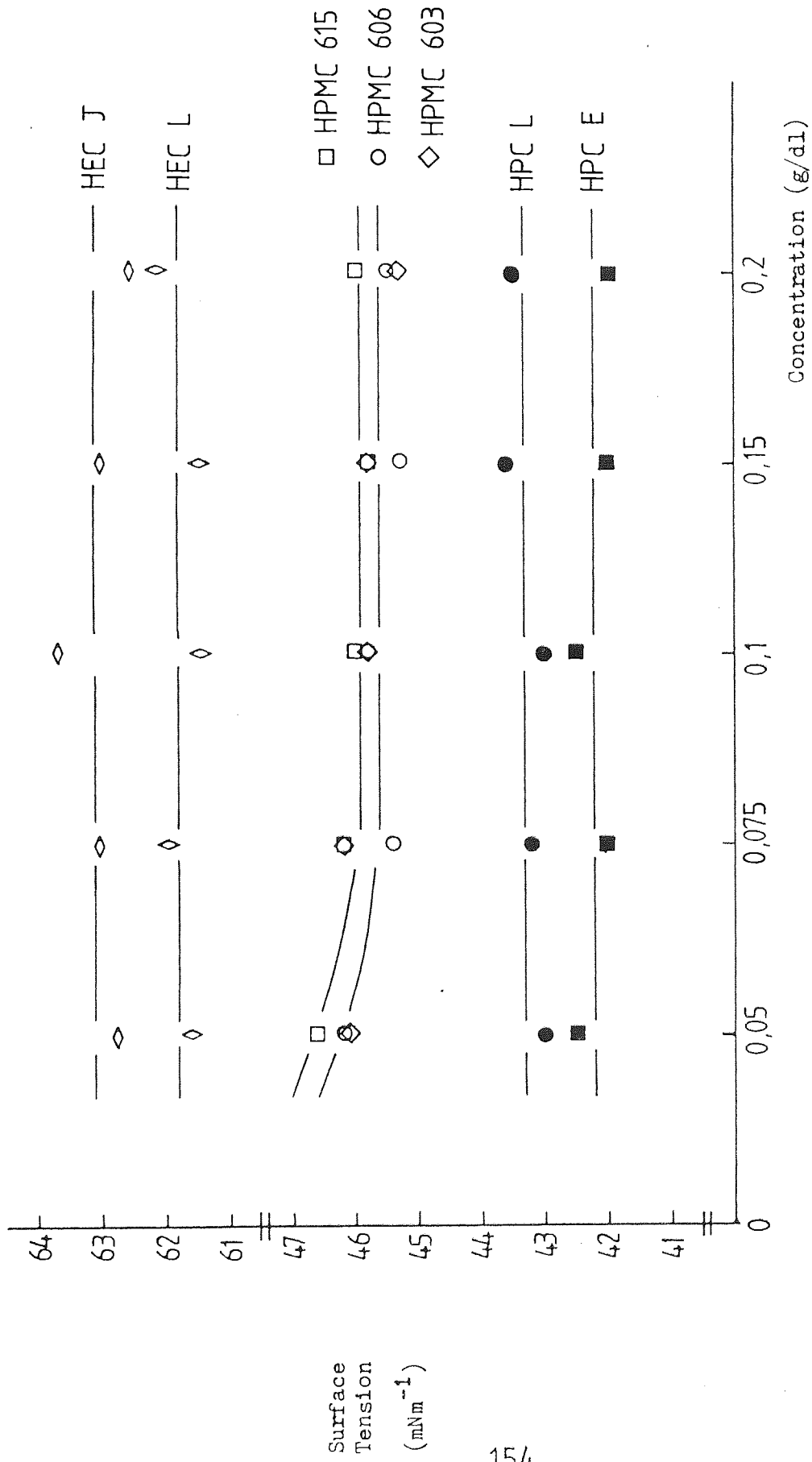


Fig. 49 Surface tension measurements of the Celluloses.

5:1 Methods5:1:1 Preparation of suspensions

(a) The polystyrene latex suspensions in the presence of nonionic surface active agents were prepared in the following manner: 2.35% W/V polystyrene latex 3B suspensions were formulated by addition of water, Texofor stock solutions and electrolyte stock solutions so as to give the desired concentrations when the total volume was 10 cm³. All suspensions were made in 10⁻³M NaCl in order to give a suspending medium of suitable conductivity. The pH of the suspensions was adjusted to that required by means of hydrochloric acid or sodium hydroxide solutions. The suspensions were stoppered in a 15 cm³ flat bottom sample glass tube and equilibrated in a constant shaking water bath (120 throws/min) at 25⁰ ± 0.1⁰C for 24 hours.

(b) Cellulose-polystyrene latex suspensions were prepared as described above but the solid content of polystyrene latex (4A) was 3.25% W/V. The Celluloses used were HEC, HPC and HPMC. All suspensions were made in 10⁻³M NaCl. The pH of the suspensions was 4.0. The equilibration time used was 4 days.

(c) Cellulose-ibuprofen suspensions: 2.5 g of ibuprofen powder was dispersed in water and stock solutions of Celluloses in 40 cm³ glass vials by means of a Whirlimixer and sonicated for 25 minutes. The final volume of the suspensions were made to 25 cm³. The suspensions then were allowed to equilibrate in a constant shaking water bath at

$25^0 \pm 0.1^0\text{C}$ for 4 days. The Celluloses used were HEC, HPC and HPMC. All suspensions were made in 10^{-3}M NaCl. The pH of the suspensions was 4.0.

As mixing procedures may affect the suspension stability (249), the above mixing method was adopted for all experiments.

5:1:2 Microelectrophoresis

It is known that a charged particle or charged material will move along the lines of force through a liquid medium when subjected to an electric field - the phenomenon of electrophoresis which is one of four related electrokinetic phenomena (the others being sedimentation potential, electroosmosis and streaming potential). The electrophoretic velocity can be interpreted to yield a quantity known as the zeta potential, ζ , which is the potential at the plane of shear between the phases in relative motion. When related to the electrical double layer of the particle, the zeta potential can be regarded as the potential difference over the mobile part of the double layer. The exact location of the shear plane is an unknown feature of the electrical double layer; however, in practice it is usually assumed that the zeta potential is identical with the Stern potential ψ_s . The difference between ζ and ψ_s will be most pronounced at high potentials and high electrolyte concentrations (246).

(a) Apparatus: The Rank Particle Microelectrophoresis Apparatus Mark 11 (Rank Bros., Bottisham, Cambridge) was used for microelectrophoretic measurements. It consists of a glass cell which is thin walled and may be cylindrical or rectangular in cross section, an electrode is fitted at either end. The cell is immersed in a thermostatted water

bath. The applied potential is controlled by a rheostat switch connected to a voltmeter and an amperemeter by which the applied voltage and current strength can be read. Illumination is by a quartz iodine 100 watt lamp and the timing system is an electrical timer accurate to 0.02 sec. The particles are observed by a microscope device with an eyepiece which contains a graticule from which the distance the particles move can be measured. The eyepiece graticule was calibrated with a stage micrometer in water, each of the squares in the graticule of the eyepiece was found to be $60 \mu\text{m}^2$ for the X20 microscope objective. The instrument was modified by the addition of a Pye Super Lynx LDM 0001 Television Camera and a Philips television monitor. The graticules in the camera extension tube are projected onto the screen, each square on the television screen was calibrated with the stage micrometer in water. It was found to be $70 \mu\text{m}^2$ for X20 microscope objective.

(b) Electrodes: Platinum black electrodes were used as these are adequate for most salt concentrations commonly in use. For accurate mobility measurements, it is necessary to avoid gas evolution at the electrodes, contamination of the observation chamber with electrode materials and undue electrode polarization. Platinum black electrodes behave reversibly at low current densities. For example, if the channel of an electrophoresis cell has a cross-sectional area of 0.1 cm^2 , platinum black electrodes of area of 1 cm^2 will generally prove to be satisfactory for electrolyte concentrations up to ca. 10^{-2} M (220). In this study, all observations were made in solutions of less than 10^{-2} M electrolyte and the above problems were not noticed during the course of measurement.

(c) Electrophoresis cell: The glass flat cell was used in this

study. The dimensions of the cell were found to be 10.05 mm for height, 1.023 mm for depth and 81.76 mm for the interelectrode distance. The height of the cell was measured using a travelling microscope. The depth of the cell was measured by means of camera focusing using the micrometer on the instrument. The interelectrode distance of the cell was obtained by measuring the conductivity (Wayne Kerr conductivity meter, Type B642) of standard solutions of potassium chloride. The distance between the electrodes l is given by

$$l = KAR$$

where A is the area of the cross section of the cell, R is the resistance of the liquid and K is the known specific conductivity of the solutions of the potassium chloride used.

(d) Stationary levels: The microelectrophoretic measurements are complicated by the simultaneous occurrence of electroosmosis. As the inner surface of the cell wall is generally charged the applied electric field causes not only electrophoresis migration but also an electroosmotic flow of the liquid near to the inner surface of the cell wall together with a compensating return flow of liquid with maximum velocity at the centre of the cell. This results in a parabolic distribution of liquid speed with depth and the true electrophoretic velocity is only observed at the stationary levels in the cell where the electroosmotic flow and return flow of the liquid cancel.

The stationary level of a flat cell can be determined by the equation given by Komagata (223)

$$\frac{s}{d} = 0.5 - \left(0.0833 + \frac{32}{\pi^5} \frac{d}{l} \right)^{\frac{1}{2}} \quad (98)$$

where d is the depth, l is the height and s is the position of the stationary level from the cell wall.

For the flat cell used here, s was calculated to be 0.198 mm. The stationary level was checked by human red blood cells. A mobility of $1.32 \pm 0.05 \times 10^{-8} \text{ m}^2 \text{ s}^{-1} \text{ v}^{-1}$ (in 0.067 molar concentration phosphate buffer with ionic strength 0.173 g ions per dm^3 at pH 7.4 and 25°C) was found. This is in good agreement with the literature value of $1.31 \times 10^{-8} \text{ m}^2 \text{ s}^{-1} \text{ v}^{-1}$ (239).

(e) Operation: The chromic acid cleaned flat cell was mounted vertically against the objective of the microscope in the thermostatted water bath at $25^\circ \pm 0.1^\circ\text{C}$. The point of viewing was midway between the top and bottom of the cell. The stationary level can be brought into focus by adjusting the micrometer.

The cell was washed with distilled water and rinsed with the test dispersion before filling completely. The test dispersion was filled in the cell by means of vacuum suction and care was taken to ensure no trapping of air bubbles. After fitting with electrodes measurements were made at the equilibrium temperature.

Electrophoretic velocities were determined by timing individual particles over a suitable number of the squares on the television screen. The focused particles were timed successively in opposite directions to minimize polarization. At least 10 particles in each direction were timed at a transit times of about 5 to 10 secs and the mean velocity was taken from 20 observations. Timings of this magnitude are optimum with respect to Brownian motion error and operator timing error.

Quite apart from contamination it is necessary for the cell walls to be clean in order that the electroosmotic flow shall be uniform

and lead to an accurate stationary level. The cell was clean regularly with chromic acid and rinsed with distilled water thoroughly.

(f) Calculation of electrophoretic mobility: The electrophoretic mobility u of the particle was calculated using the following expression

$$u = \frac{\text{interelectrode distance}}{\text{applied voltage}} \times \frac{\text{distance moved}}{\text{average time}} \quad (99)$$

where units of the mobility is micron cm/sec volt or $m^2 s^{-1} v^{-1}$.

For polystyrene latex, the standard deviations were normally within 5% but in the case of low mobility deviations reaching about 10% were always found. For drug particles, due to the low mobility in character, 40 observations were taken. The deviations some times reached about 20%.

(g) Calculation of zeta potential: The electrophoretic mobility may be interpreted in terms of zeta potential.

For spheres the shape of the electric double layer can be described by means of a dimensionless term ka where k is the Debye-Huckel reciprocal of the thickness of Gouy-Chapman diffuse double layer and a is the radius of the sphere. Electrophoretic mobility is not always directly proportional to zeta potential, it varies with the shape of the double layer i.e. ka .

(i) The Huckel equation (240)

Assuming ka to be small enough for a spherical particle to be

located as a point charge but large enough for applying Stokes' equation, Huckel proposed the following relation between electrophoretic mobility and zeta potential

$$u = \frac{\epsilon \zeta}{1.5 \eta} \quad (100)$$

where ϵ is the permittivity and η is the viscosity of the medium. The Huckel equation is not likely to be applicable in aqueous medium (220) and is for ka less than 1.0.

(ii) The Smoluchowski equation (241)

For spherical particle with large ka , the double layer can be treated as a flat surface. Smoluchowski proposed an expression

$$u = \frac{\epsilon \zeta}{\eta} \quad (101)$$

which is valid for ka greater than 300. As most suspensions and emulsions fall in this domain the Smoluchowski equation is important in the pharmaceutical field.

(iii) The Henry equation (242)

As the charged particle and its ion atmosphere move in opposite directions (retardation) the applied field and the field of the double layer will be distorted. This mutual distortion could affect the electrophoretic mobility through an abnormal conductivity in the vicinity of the charged surface (surface conductivity) and through the loss of double layer symmetry (relaxation effect). By assuming that the applied field and the field of the double layer are superimposed, Henry derived a general electrophoretic equation for

conducting and non-conducting spheres.

$$u = \frac{\epsilon \zeta}{6\pi\eta} [1 + CF(ka)] \quad (102)$$

where $F(ka)$ varies between zero for small values of ka and 1.0 for large values of ka , and

$$C = \frac{C_0 - C_1}{2C_0 + C_1}$$

where C_0 is the specific conductance of the bulk electrolyte solution and C_1 is the specific conductance of the particle.

For small ka the effect of particle conductance is negligible. For large ka the Henry equation predicts that C should approach -1 and the u approach zero as particle conductance increases.

However, in most cases, because of the rapid polarization of the conducting particles by the applied field the particles behave as non-conductors. For non-conducting spheres, the Henry equation is

$$u = \frac{\epsilon \zeta}{1.5\eta} f(ka) \quad (103)$$

where $f(ka)$ is the function of ka . It varies between 1.0 for small ka and 1.5 for large ka i.e. between the gap of Huckel and Smoluchowski equation.

The Henry equation takes into account the effect of electrophoretic retardation but does not include the relaxation effect. Overbeek (243) and Booth (244) derived equations for spherical particles allowing for the effect of retardation, relaxation and surface conductivity, but their equations are applicable for low zeta potentials (less than 25 mV at 25°C) only. Later, the equations of Overbeek

and Booth have been superseded both in range of validity and convenience of use by the work of Wiersema et al (245). Ottewill and Shaw (253) have tabulated the results of Wiersema et al in a more readily usable form. Mobilities are presented as a function of zeta potential and ka . For the present work, mobilities of polystyrene latex were converted to zeta potentials with the aid of these tables. Whereas, the mobility-zeta potential conversions of drug particles were obtained by using Smoluchowski equation.

In all of the treatments discussed above it has been assumed that permittivity and viscosity are constants throughout the mobile part of the double layer. However, just outside the surface of shear, the electric field strength may be high enough to increase viscosity and/or decrease permittivity significantly, both effects reduce the particle mobility for a given zeta potential. Lyklema and Overbeek (246) examined this problem and concluded that the effect of field strength on permittivity could probably be neglected but the effect on viscosity may be significant, especially at high potential and high electrolyte concentration. However, Hunter (247) has suggested that the variations of permittivity and viscosity are of similar significance and that their combined effect is probably small in most practical situations.

Dealing with the shape effect in the mobility-zeta potential calculation, Overbeek et al (248) have demonstrated that when the particle is insulating and the thickness of the double layer is small compared with the radius of curvature of any point of the particle surface, the Smoluchowski equation is valid irrespective of the form of the particle. Therefore, in the drug suspension systems studied

here, the applicability of the Smoluchowski equation is not affected by the shape of the particles.

5:1:3 Sedimentation volume

The sedimentation volumes were recorded in terms of the ultimate settled height H_u to the original height H_0 and expressed a percentage of the total volume of the suspension.

$$\frac{H_u}{H_0} \times 100\% = \text{Sedimentation Volume (SV)}$$

In some cases, the aggregates formed were found to float on the top of the suspension due to the addition of the aggregating agent or due to the nature of the particles when one would expect all particles to settle at the bottom of the container, and where this occurred the combined volumes were taken.

5:1:4 Redispersibility

The redispersibility of the suspensions were determined by a machine which was constructed by a variable speed motor (Palmer Ltd, E.P. Recording Drum) to revolve the tube through 360^0 to redisperse the sediment. The number of revolutions necessary to redisperse the suspension was recorded and termed the redispersibility value (RV).

5:1:5 Flocculation studies

The polystyrene latex 4 was used in this study. 1 cm^3 of a diluted polystyrene latex (number concentration of $5.4 \times 10^8 / \text{cm}^3$) was transferred

to a polymer preconditioned stoppered glass vial. Water and stock Cellulose solutions were added to a volume of 10 cm³. The suspensions were shaken by a Whirlimixer for about one minute then equilibrated in a constant shaking water bath at 25⁰ ± 0.1⁰C for 4 days. As the mixing procedures may have a significant effect on the extent of flocculation (249), the above method of mixing was followed in all experiments. A portion of the dispersions was carefully transferred to a 10 mm spectrophotometer cell and the absorbance measured at 600 nm (Pye Unicam SP600, Series 2).

5:1:6 Determination of Hamaker constants

The method from Fowkes (250) was used here to determine the Hamaker constants of the substances.

The effect of interfacial tension, γ_{SL} , in the interface can be predicted by the geometric mean of the dispersion force components, γ^d , of the surface tension, γ , of the liquid, L, and the solid, S, such as water and paraffin wax. Therefore,

$$\gamma_{SL} = \gamma_S + \gamma_L - 2(\gamma_S^d \gamma_L^d)^{\frac{1}{2}} \quad (104)$$

$$\gamma^d = \frac{-\pi N^2 P^2 I}{8d^2} \quad (105)$$

where P is the polarizability, I is the ionization potential, d is the intermolecular distance and N is the number of interacting volume elements per unit volume.

The Hamaker constant (147) is given by

$$A = \pi^2 N^2 P^2 I \frac{3}{4} \quad (106)$$

Substitution of Eq. (105) into Eq. (106) gives

$$A = 6\pi d^2 \gamma^d \quad (107)$$

For water and systems with volume elements such as oxide ions, CH_2 or CH groups which have nearly the same size, $6\pi d^2$ equals 1.44×10^{-14} . Combining the Young equation (Eq. (97)) and Eq. (104), γ^d can be obtained. That is

$$\gamma_L \cos \theta = -\gamma_L + 2 \left(\gamma_S^d \gamma_L^d \right)^{\frac{1}{2}} - \pi \quad (108)$$

If $\gamma_L > \gamma_S$, π is zero. Therefore,

$$\cos \theta = -1 + 2 \left(\gamma_S^d \gamma_L^d \right)^{\frac{1}{2}} / \gamma_L \quad (109)$$

Thus, from the contact angle between the liquid and solid and the surface tension values, the Hamaker constant may be determined using the above equations.

The surface tension and contact angles were measured as described in Section 4:1:4 and 4:1:5 respectively. For contact angle measurements the solid surfaces used were hard paraffin and soft paraffin. The contact liquids were the polymer solutions with such strength as to give complete adsorbed layer coverage. For ibuprofen, saturated solution were used as contact liquid.

An attempt was made to use polymer films and flat drug plates as contact surfaces and liquid hydrocarbons as contact liquids for the contact angle measurements. However, due to the fact that the hydrocarbons dissolved the contact surfaces and spreading of contact liquids on the surfaces occurred irreproducible results were obtained. Therefore, it was decided to use solid hydrocarbons as contact solids.

Some comment should be made on the reasons for using paraffin wax and soft paraffin as the reference solid and for predicting that π is zero. Paraffins (hydrocarbons) are low energy solids which have only dispersion force interactions because of their simple hydrocarbon structure. However, for substances of complex structure such as ibuprofen, which contains a carboxyl group and a benzene ring, the structure and functional groups contribute energy to the interface due, not only to the dispersion forces but also to hydrogen bonds (carboxyl group) and π electron interactions (benzene ring) which make the system more complicated than that expressed by Eq. (104). From theoretical and experimental evidence (250), the adsorption of high energy material can not reduce the surface energy of a low energy material. For example, the surface tension of a liquid hydrocarbon is never reduced by adsorbing water. The fact that a given liquid has a contact angle greater than zero degrees on a given low energy solid is evidence that the liquid is a higher energy liquid and therefore π should be zero.

5:1:7 Determination of polymer-solvent interaction parameters

From the osmotic pressure measurement, the polymer-solvent interaction parameter, χ , can be determined

$$\frac{\pi}{cRT} = \frac{1}{M} + \frac{v^2}{V_0} (0.5 - \chi) c + \dots \quad (110)$$

where π is the osmotic pressure, c is the percentage concentration, M is the molecular weight, v is the partial specific volume and V_0 is the molar volume of the solvent. According to the relation derived by Debye (251)

$$\frac{Kc}{R_{90}} = \frac{\delta}{\delta c} \left(\frac{\pi}{RT} \right) \quad (111)$$

$\frac{Kc}{R_{90}}$ is the value obtained from light scattering measurement. Then, Eq. (110) can be written in the following form,

$$\frac{Kc}{R_{90}} = \frac{1}{M} + 2 \left(\frac{v^2}{V_0} \right) (0.5 - \chi) c + \dots \quad (112)$$

Therefore, χ can be determined by this equation using the technique of light scattering (see Section 3:5:2:1).

5:2 Results and discussion

5:2:1 Electrophoretic characterization

5:2:1:1 Polystyrene latex

As shown in the conductometric titration measurements (Section 3:5:3), there are anionic carboxyl and sulphate groups on the surface of the polystyrene latex. Since the electrophoretic mobility of the particle is the response of the charge on the surface, the nature of the particle surface may be determined by the electrophoretic behaviour of the particle.

The polystyrene latex mobility measurements were made in $10^{-3}M$ NaCl as a function of pH at $25^{\circ}C$. The mobility against pH plots for the polystyrene latex 3B and 4A are given in Fig. 50. The curves flatten out in the pH region 2 to 2.5 and do not tend to

zero mobility which is consistent with the presence of strong acidic groups on the surface (211) i.e. the sulphate groups. Over the pH range 2.5 to 5, an increase in mobility of the particles is an indication of the ionization of the carboxyl groups. Above pH 5 the curves show a constant mobility indicating complete ionization of the acidic surface groupings. However, above pH 9 the mobilities rise again. This may be due to the presence of hydroxyl groups. As shown by van der Hul and Van der hof (209), the hydroxyl groups may be combined on the latex at low pH condition during the polymerization. These hydroxyl end groups are likely to be ionized at higher pH range, thus it causes the mobility increase. These results confirm those found from conductometric titration measurements that the latex surfaces contain both the sulphate and carboxyl groups.

Ottewill and Shaw (211) have examined the problem of determining surface dissociation constants from electrokinetic data. From an electrokinetic point of view the dissociation of acidic groupings can be written in the form



where $[H_s^+]$ is the concentration of hydrogen ions and $[HA_s]$ and $[A_s^-]$ are the concentrations of unionized and ionized acidic groupings in the electrokinetic surface of shear respectively. Hence, the dissociation constant can be defined by

$$K_s = \frac{[H_s^+][A_s^-]}{[HA_s]} \quad (114)$$

if activity coefficients are neglected.

The hydrogen ion concentration in the shear plane $[H_s^+]$ can be

related to the bulk hydrogen ion concentration $[H_b^+]$ by the Boltzmann equation,

$$[H_s^+] = [H_b^+] \exp(-e\zeta/KT) \quad (115)$$

Combining Eq. (114) with Eq. (115) gives

$$pK_s = pH_b - \log[A_s^-]/[HA_s] + e\zeta/2.303KT \quad (116)$$

The electrokinetic surface charge density, σ , can be defined by

$$\sigma = n_{As^-} \cdot e \quad (117)$$

where n_{As^-} is the number of ionized groupings per unit area. If σ_0 is the surface charge density under conditions of complete ionization

$$[A_s^-]/[HA_s] = \sigma/(\sigma_0 - \sigma) \quad (118)$$

At small potential σ and ζ are proportional, therefore,

$$[A_s^-]/[HA_s] = \zeta/(\zeta_0 - \zeta) \quad (119)$$

where ζ_0 is the maximum value of zeta potential reached on the curve of zeta potential against pH_b .

At the pH_b where $2\zeta = \zeta_0$, $\log[A_s^-]/[HA_s]$ becomes zero and hence,

$$pK_s = pH_b + e\zeta/2.303KT \quad (120)$$

Thus, a pK_s value can be obtained from the experimental data using Eq. (120).

The maximum mobilities of the latex 3B and 4A when ionization is complete are 5.25 and $6.65 \times 10^{-8} \text{ m}^2 \text{ s}^{-1} \text{ v}^{-1}$ corresponding to a zeta

potential of -70 and -90 mV (253) respectively. The mobilities due to the sulphate groups are 0.85 and $1.65 \times 10^{-8} \text{ m}^2 \text{ s}^{-1} \text{ v}^{-1}$ which give a zeta potential of -11 and -21.6 mV for latex 3B and 4A respectively. In the following calculations the zeta potentials caused by the sulphate groups are subtracted. Thus, $\zeta_0/2$ is 29.5 mV for latex 3B and 34.2 mV for latex 4A. The bulk pH is 3.35 and 3.60 for latex 3B and 4A respectively. Substitution of the relevant values into Eq. (120) gives a pK_s of 3.86 and 4.19 for latex 3B and 4A respectively. This agrees reasonably with that of found by Ottewill and Shaw (211) on carboxylated polystyrene latex dispersions. These authors found that the pK_s values of a number of latices all lie on the same curve of pK_s against $\zeta_0/2$ and lead to a common extrapolated value of 4.64 which agrees well with the calculated value of 4.31 for phenylacetic acid and acidic groupings with a similar structure which can be regarded as the parent compound of the polystyrene carboxyl grouping.

5:2:1:2 Ibuprofen

The effect of pH on the electrophoretic mobility of ibuprofen was examined in 10^{-3} M NaCl and at 25°C . Results are given in Fig. 51. The curve shows an increase in mobility as pH increases. As given in Section 3:4, the ibuprofen structure contains a carboxyl acid group which will ionize with increasing pH causing an increase in mobility. Above pH 7 ibuprofen was dissolved. Divergence of mobilities between batch CMG 09839T and 9692 occurs in higher pH region. This may be due to the presence of impurities in different batches, such as the amide substances (213) which ionize little in high pH conditions. However, the profile of the curves are similar.

From Fig. 51, the dissociation constant can be calculated using

Eq. (120). For batch 9692, the pK_s is 4.31 and for batch CMG 09839T, the pK_s is 4.56. These results agree well with the literature value of 4.45 (213) and the pK_s of phenylacetic acid of 4.31.

5:2:2 Effect of nonionic surface active agents on the stability of polystyrene latex

5:2:2:1 Polystyrene latex in the presence of nonionic surface active agents

The nonionic surface active agents used were Texofor A10, A18, A30, A45 and A60. Measurements were made at pH 7.0 at 25⁰C.

(a) Electrophoresis

Results for the mobility of polystyrene latex in the presence of different Texofors concentrations are shown in Fig. 52. All curves show a decrease in mobility until a plateau region is attained, these being a further fall in mobility at high concentrations. This indicates that the Texofor molecules are adsorbed onto the surface of the polystyrene latex eventually forming a monolayer. The decrease in mobility at high concentrations is due to the increase in viscosity of the surface active agent solution (255). The results found here confirm those observed by Kayes (221). It appears that the cmc of the nonionic surface active agents bears no relation to the mobility. It is because the adsorbed molecules are looped on the particle surface. As the cmc is reached the looped form of the adsorbed molecules shows little change, therefore the mobility does not alter.

In Fig. 52, it is shown that the molecules adsorbed on the

particle surface cause a decrease in mobility. To interpret this it is necessary to consider the effect that the adsorption of nonionic surface active agents have on the structure of the double layer at the charged solid-liquid interface. This situation may be represented schematically as in Fig. 53 (97).

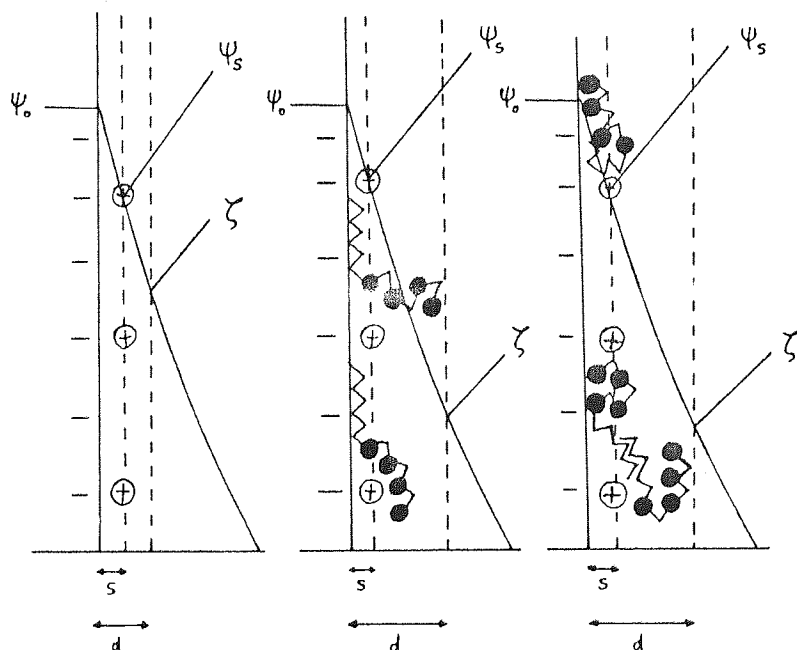


Fig. 53 Schematic representation of the situation at a charged interface in the presence and absence of adsorbed polymers.

In these diagrams, two possible modes of adsorption at low surface coverages are considered. Assuming the adsorbed molecules are the alkyl polyoxyethylene type surface active agents, in Fig. 53 (b) adsorption has occurred via the hydrocarbon chain leaving the ethylene oxide chain in the solution. In Fig. 53 (c) adsorption has occurred mainly through the ethylene oxide chain, but in addition there is also

attachment by the alkyl chain. On both the above modes if the adsorption energy of the adsorbed molecules is greater than that of ions in the Stern layer, some of the ions will be displaced, causing a change of the Stern potential. In both cases, the adsorbed molecules project some way beyond the original plane of shear, and apart from changes in the zeta potential occasioned by changes in Stern potential there will also be a change as a result of the mechanical displacement of the plane of shear into the solution.

(b) Sedimentation volume and redispersibility

The characteristics of the polystyrene latex suspensions were examined after standing undisturbed for 7 days which was found to be the time necessary for the formation of a distinct sediment. The results are given in Table 16.

The sedimentation volumes show no significant difference throughout the concentration range studied. All suspensions were deflocculated and supernatants of the suspensions were turbid. The degree of turbidity of the supernatants were higher at high surface active agent concentrations (above 10^{-4} M) than at low surface active agent concentrations. The redispersibility values show that at high concentrations of Texofors easily redispersed suspensions were produced. In contrast, at low concentrations the sediments were difficult to resuspend and hard caked sediments were found.

The sedimentation volumes in different concentrations of Texofors show no significant difference. This is probably because in the deflocculated system the particles settle individually in a

Initial Concentration of Texofor M	SV	RV	Appearance of Supernatant	Appearance of Sediment
<u>A10</u>				
10^{-2}	6.4	90	Opalescent	Soft caked
10^{-3}	6.9	98	↓	↓
10^{-4}	6.6	100	↓	↓
10^{-5}	6.9	300 +	↓	Hard caked
10^{-6}	6.4	300 +	↓	↓
10^{-7}	6.3	300 +	↓	↓
<u>A18</u>				
10^{-2}	6.4	92	Opalescent	Soft caked
10^{-3}	6.7	90	↓	↓
10^{-4}	6.8	97	↓	↓
10^{-5}	6.7	300 +	↓	Hard caked
10^{-6}	6.1	300 +	↓	↓
10^{-7}	6.8	300 +	↓	↓
<u>A30</u>				
10^{-2}	6.6	81	Opalescent	Soft caked
10^{-3}	6.5	89	↓	↓
10^{-4}	6.6	96	↓	↓
10^{-5}	6.7	300 +	↓	Hard caked
10^{-6}	6.5	300 +	↓	↓
10^{-7}	6.3	300 +	↓	↓

Table 16 (continued)

(continued)

Initial Concentration of Texofor M	SV	RV	Appearance of Supernatant	Appearance of Sediment
<u>A45</u>				
10^{-2}	7.0	82	Opalescent	Soft caked
10^{-3}	6.3	74	↓	↓
10^{-4}	6.4	80		Hard caked
10^{-5}	6.7	300 +		↓
10^{-6}	6.8	300 +		↓
10^{-7}	6.9	300 +		↓
<u>A60</u>				
10^{-2}	6.5	69	Opalescent	Soft caked
10^{-3}	6.5	71	↓	↓
10^{-4}	6.3	71		Hard caked
10^{-5}	6.5	300 +		↓
10^{-6}	7.0	300 +		↓
10^{-7}	6.9	300 +		↓

Table 16 Characteristics of suspensions of polystyrene latex in the presence of Texofors.

slow process resulting in a dense and arranged sediment. At high concentrations due to the existence of an adsorbed layer there should be a volume difference from those at low concentrations where no adsorbed layer formed but this is so small that the sedimentation volume method can not measure the difference. However, at high concentrations the numbers of revolutions to resuspend the suspensions are lower than those values obtained at low concentrations. This may be due to the fact that at high concentrations the particles are in a sterically stabilized state; as particles settle down the adsorbed layers of surface active agents prevent the particles from close contact. Therefore, less revolutions are needed to redispersethe sediment. The redispersibility values at low concentrations are very high; even after 300 revolutions the sediment was little disturbed. To interpret this redispersibility behaviour two mechanisms are proposed. As shown in the adsorption isotherms (Fig. 36), in the concentration range from 10^{-7} to 10^{-5} M the surface active agents adsorbed on the polystyrene latex surface with low surface coverage. Therefore, only parts of the surface are covered by the adsorbed molecules leaving patches of bare latex surface. In this deflocculated system, the particles will settle down and form a small sedimentation volume. Due to the close contact of particles in the sediment, van der Waals attraction may occur especially between the bare surface patches. This effect may give rise to a high redispersibility value and may be regarded as the result of the partial steric stabilization (15). Secondly, The following mechanism is also likely to occur. As the pure polystyrene latex dispersions are deflocculated system in the natural state (pH ca. 6.5), the addition of nonionic polymers into the dispersion, if the nonionic polymers is not a flocculating agent, will not affect its deflocculated behaviour. This can be seen from the appearance of the

suspensions i.e. opalescent supernatant and slow settling process. Therefore, in this deflocculated system, the low surface coverage particles will settle individually on the sediment bed. Due to the close contact of the particles the uncoated area of one particle may contact the coated area of the other particle leading to a mutual adsorption of the adsorbed molecules on bare surface patches as shown in Fig. 54.

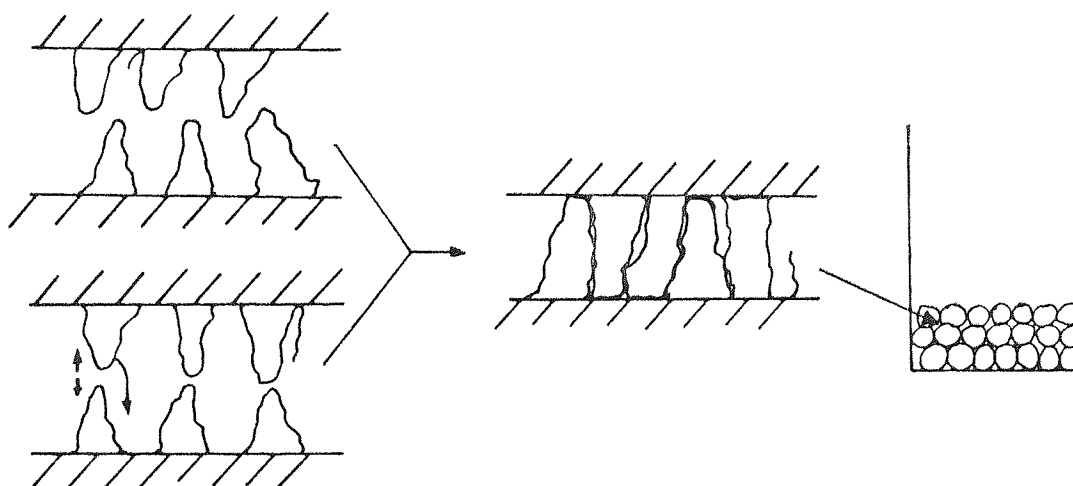


Fig. 54 Schematic representation of the mutual adsorption of adsorbed molecules on close contact particles.

This may cause a sediment of dense and arranged aggregates in which particles are held by the adsorbed molecules and this therefore require more energy to disperse the sediment. It is likely that the above mechanisms can be applied to the hard caked conditions for polystyrene latex in low concentrations of Texofors.

It should be noted that the above second mechanism is easy to mix up with the bridging effect which was proposed by La Mer et al (256). These authors described that at low surface coverage a single polymer molecule would be adsorbed on two adjacent particles forming a

bridge. As a result, particles would be flocculated producing a porous sediment. They also judged flocculated dispersions by means of a filtration technique where maximum filtration rates were obtained in this flocculated state.

The system studied here, however, is not the case which La Mer et al described. From the opalescent supernatants and slow subsidence rates of the suspensions, although the sedimentation volumes are not significant, it indicates that the system is not a flocculated system. Also, the polymer studied in the case of La Mer et al has been shown to protrude from surface with the extended segments of several or hundred nm in length, hence these segments could be in a position to form bridges. The Texofors used here are comparatively short chain polymers. From the adsorbed layer thickness measurements it seems that these looped adsorbed molecules are too short to produce bridging flocculation. It also appears that the flocculation due to the bridging effect is a fast interaction which occurs almost instantly. The mutual adsorption shown here is a slow interaction brought about by the assistance of the gravitational force.

From Table 16 it can be seen that the redispersibility values at high concentrations decrease as the chain length of the stabilizing adsorbed molecules increases. Similar results were obtained for diloxanide furoate-nonylphenylethoxylate suspensions (15). From the adsorbed layer thickness values (Table 10) it is shown that redispersibility values decrease with increasing adsorbed layer thickness. Therefore, in this deflocculated system, within the range of the molecular chain length studied the presence of the larger adsorbed layer thickness gives an easier redispersion of the suspension.

5:2:2:2 Polystyrene latex in the presence of nonionic surface active agents and electrolyte

The nonionic surface active agents used were Texofor A10, A18, A30, A45 and A60. Measurements were made at 25⁰C. The electrolyte used was aluminium chloride which has previously been used in the study of pharmaceutical suspensions (21,31,32). The pH was 3.5. At this pH the electrolyte is completely ionized (256,257). A visual test of the Texofors mixed with aluminium chloride solution showed no precipitation. Wiese and Healy (257) have shown that using titanium dioxide, at pH 3.5 aluminium ions do not adsorb onto the surface. Here, it can be assumed that aluminium ions are not adsorbed on the surface of the polystyrene latex; they only function as a double layer compressing agent. The aluminium chloride stock solution was added after adsorption had taken place. The final concentration of the aluminium chloride in the suspension was 5×10^{-3} M.

(a) Electrophoresis

Electrophoretic measurements in the presence of aluminium chloride are shown in Fig. 55. In all cases, the mobility drops to a plateau value at about 1×10^{-4} M of Texofors concentration, then remains steady until about 1×10^{-3} M and then falls off at higher concentrations due to viscosity increase.

An investigation was made by comparing the electrophoretic mobility results in the presence of aluminium chloride with the adsorption isotherms. As shown in Figs. 56 - 60, the adsorption of the surface active agent molecules onto latex are reflected in the form

of the mobility curves. The plateau regions of the adsorption isotherms and of the mobility curves are parallel. The formation of the complete adsorbed layer is found at about 1×10^{-4} M concentration of Texofors. Therefore, it appears that at low concentrations of Texofors adsorption results in a low surface coverage of surface active agents on the particle surface and the adsorbed molecules in this state would take a flatter conformation on the surface. As concentration increases the adsorbed molecules would rearrange to form a dense layer in which surface active agent molecules occupy less surface area and the segments project more into the solution, at saturated coverage a complete adsorbed layer is formed. Thus, at low concentrations the mobility shows a gradually decrease from 1×10^{-7} to 1×10^{-4} M due to the gradual extruding of the plane of shear by projected molecules then remains steady as complete adsorbed layer formation occurs.

For the mobility results of polystyrene latex in the presence of Texofors without the aluminium chloride (Fig. 52), the starting of the plateau region (complete adsorbed layer formation region) is quite ambiguous. When mobility curves are compared with the adsorption, if the plateau values start at about 1×10^{-6} M concentration of Texofors as shown in Fig. 52, there is no reason why the plateau values of the mobility curves do not correlate with those of the adsorption isotherms. Kayes and Rawlins (255) studied the adsorbed layer thickness of nonionic surface active agents of polyoxyethylene polyoxypropylene block co-polymers on polystyrene latex by intensity fluctuation spectroscopy and microelectrophoresis. They found that the results from IFS agreed with the electrophoretic results. It is likely that the assumptions made using the double layer equations are correct. Therefore, the adsorbed polymer molecules in this case only displace

the plane of shear but do not affect the double layer conditions. Also, the mobility results they found are similar to those found here (Fig. 52). In the case here, if the adsorbed nonionic surface active agents only displace the plane of shear, the mobility results should mirror the form of the adsorption isotherms. Hence, aluminium chloride, the double^{layer}/compressing agent, which leads to a decrease in mobility will provide a relative background such that a more sensitive result can be obtained.

(b) Sedimentation volume and redispersibility

The sedimentation volume and redispersibility results in the presence of Al^{3+} are given in Table 17. In this system, there is a sudden increase in sedimentation volume at the concentrations below complete adsorbed layer concentration of about 1×10^{-4} M of Texofors. At high concentrations, due to the presence of the adsorbed layer, the system should be sterically stabilized. However, at high ionic strength the electrostatic repulsive force is suppressed. This leaves the steric force and the van der Waals force in action. Under this condition, there would be a steric minimum resulting in a coagulation of the particles if the adsorbed layer is not thick enough to provide a full range steric stabilization.

As pointed out by Schenkel and Kitchener (18), the height of the sedimentation volume is dependent on the aggregation rate. Slow aggregation produces small sedimentation volumes while rapid aggregation results in high sedimentation volumes. Here, the rate of aggregation of the particles was observed by changing the degree of turbidity of the supernatant of the suspension. In this system, at high concentrations

Initial Concentration of Texofor M	SV	RV	Appearance of Supernatant	Appearance of Sediment
<u>A10</u>				
10^{-2}	7.2	40	Very slight haze	Soft aggregated
10^{-3}	6.8	39	↓	↓
10^{-4}	6.9	39	↓	↓
10^{-5}	33.0	2	Clear	Fluffy
10^{-6}	33.0	1	↓	↓
10^{-7}	38.1	1	↓	↓
<u>A18</u>				
10^{-2}	7.0	41	Very slight haze	Soft aggregated
10^{-3}	6.9	45	↓	↓
10^{-4}	7.0	51	↓	↓
10^{-5}	47.6	1	Clear	Fluffy
10^{-6}	50.0	1	↓	↓
10^{-7}	52.0	1	↓	↓
<u>A30</u>				
10^{-2}	6.7	55	Very slight haze	Soft aggregated
10^{-3}	6.9	52	↓	↓
10^{-4}	6.8	57	↓	↓
10^{-5}	42.9	1	Clear	Fluffy
10^{-6}	45.0	1	↓	↓
10^{-7}	57.4	1	↓	↓

Table 17 (continued)

(continued)

Initial Concentration of Texofor M	SV	RV	Appearance of Supernatant	Appearance of Sediment
<u>A45</u>				
10^{-2}	7.0	64	Very slight haze	Soft aggregated
10^{-3}	6.8	67	↓	↓
10^{-4}	6.9	62	↓	↓
10^{-5}	30.2	1	Clear	Fluffy
10^{-6}	36.5	1	↓	↓
10^{-7}	40.0	1	↓	↓
<u>A60</u>				
10^{-2}	6.6	67	Very slight haze	Soft aggregated
10^{-3}	6.8	64	↓	↓
10^{-4}	6.8	69	↓	↓
10^{-5}	30.0	1	Clear	Fluffy
10^{-6}	44.3	1	↓	↓
10^{-7}	57.6	1	↓	↓

Table 17 Characteristics of suspensions of polystyrene latex in the presence of Texofors with aluminium chloride.

the rate of aggregation was very slow, as shown in Table 17, after 7 days observation the supernatants of the suspensions still showed a slight haze. Also, at these concentrations the viscosity of the medium may reduce the motion of the particles. Therefore, it is not surprising that a low sedimentation volume is formed. Moreover, if the sedimentation rate of the particles is greater than or comparable to the aggregation rate, a low sedimentation volume would also occur. This might be fit the case which was suggested by Hiestand (10) that after enough surface has been protected with adsorbed polymeric material so that a large coordination number is not probable, electrolyte coagulation/flocculation may be advantageous. This might produce a low sedimentation volume. Although the sedimentation volume was low, because these particles were not strongly held in the shallow energy minimum, the particles could be redispersed again.

At low surface active agent concentrations and in the presence of aluminium chloride, the steric and electrostatic repulsive force contributions would be small and the attractive force dominant. Turbidity observation of this system showed a clear supernatant after 4 minutes mixing with aluminium chloride solution i.e. a rapid aggregation. As a result, the particles in these suspensions came rapidly together and seized on contact. A voluminous sediment was quickly formed. The particles in the sediments aggregated in a random packing form with small coordination number ~~of the particles~~ and therefore a large void volume was produced between the aggregates or particles. These sediments were loose structured and could be resuspended easily.

Photomicrographs for this system after redispersion were taken and are shown in Fig. 61 (only the Texofor A18 system is shown here).

At high concentrations the particles were redispersed and separated individually whereas at low concentrations aggregated particles were separated in the floc forms. Redispersion of these flocs from aggregates were easier than those particles in small sediments. To explain this phenomenon one may use Overbeek's comments (5). He states that if the large particles (aggregates) in the sediment resting on the top of a surface is exposed to the shearing action of a liquid in laminar flow, the average velocity of the vehicle flowing past the particles is directly proportional to its diameter; also the force acting on the particle due to liquid flow is given by Stokes' law and is directly proportional to the square of the particle diameter. Therefore, the force acting to dislodge a particle is proportional to the square of the particle diameter. However, for small and compact sediment the particles can only be attacked by hydrodynamic motions layer by layer which evidently is a slow process.

The redispersibility values at high concentrations without electrolyte (Table 16) are higher than those with electrolyte (Table 17) although the sedimentation volume heights are similar. The former, a colloidally stable system, the particles settled resulting in a dense and arranged sediment and the latter because of a steric energy minimum caused the particles to aggregate. As mentioned above, due to a slow aggregation rate small sedimentation volumes resulted. It is likely that the coordination number in the former would be higher than those in the latter. Hence, this gives higher redispersibility values in the former than in the latter.

5:2:3 Effect of nonionic celluloses on the stability of polystyrene latex

(a) Electrophoresis

The results of the electrophoretic mobility against concentration plots for polystyrene latex in the presence of HEC, HPC and HPMC are given in Figs 62, 63 and 64 respectively. All curves show a similar trend with mobility decreasing with an increase in Cellulose concentration, until a plateau region is attained. Then, a further decrease in mobility is observed at high concentrations. As mentioned in Section 4:1:2:2, in the initial adsorption stages the Cellulose molecules adopt a flat conformation on the solid surface; as adsorption proceeded, more Cellulose molecules are adsorbed leading to a close packed and extended adsorbed layer. Hence, this would give a shift in the plane of shear further to the solution or displace the ions on the particle surface gradually causing a gradual lowering of the mobility, until saturation adsorption is attained resulting in a steady mobility. Multilayer adsorption is shown in the adsorption isotherms at higher concentrations. Therefore, mobility would further decrease at these concentrations. Another reason for the further decrease of mobility may be attributed to the increase in viscosity. Similar results of the adsorption of nonionic polymers causing the decrease in mobility have also been observed for other system such as polyvinyl alcohol (PVA)-polystyrene latex (15,228) and PVA-silver iodide (261). Brooks and Seaman (259) have shown that the apparent zeta potential of human blood cells was raised when dextrans were adsorbed onto the surfaces. They explained this effect as due to the presence of the adsorbed dextrans expanding the diffuse double layer adjacent to the charged adsorbent. The expansion alters the relationship between the surface charge and surface potential so that if the surface charge density remains constant, the surface potential is increased leading to an increase in zeta potential. This effect will be significant at the high ionic strength

condition in which the double layer thickness is small or the depth of the adsorbed polymer layer is large. However, this effect is not the case observed here where the zeta potential of the particles decreases with the adsorption of Celluloses.

As given in Section 4:1:3, from the electrophoretic adsorbed layer thickness result deviations, it is likely that the double layer condition would be affected by the adsorption of the Cellulose molecules in one or more of the following processes: the displacement of the plane of shear, the desorption of the specifically adsorbed ions from the Stern plane, the alteration of the surface charge density and the charge distribution in the double layer.

(b) Sedimentation volume and redispersibility

Results for polystyrene latex-Celluloses systems after 7 days storage are given in Table 18. In all cases, the sedimentation volumes are of the same magnitude in the concentration range studied. Whereas, the redispersibility values show an increase with increasing concentration. The supernatants of the suspensions (except HEC systems at concentrations of 0.004 and 0.008 g/dl) were opalescent throughout the concentration range studied. In case of HEC systems at low concentrations of 0.004 and 0.008 g/dl clear supernatants were obtained (slight haze for HEC L at 0.008 g/dl); therefore, it is likely that aggregation by the polymers might occur at these concentrations (see(c) in this section).

The redispersibility values at high polymer concentrations are greater than those at low concentrations. This may be due to (a) network formation of the sediment, and/or (b) flocculation of the

Initial Concentration of Cellulose g/dl	SV	RV	Appearance of Supernatant	Appearance of Sediment
<u>HEC L</u>				
0.16	14	27	Opalescent	Soft caked
0.08	14	23	↓	↓
0.04	14	23	↓	↓
0.016	14	25	↓	↓
0.008	14	16	Slight haze	↓
0.004	15	10	Clear	↓
<u>HEC J</u>				
0.16	14	39	Opalescent	Soft caked
0.08	14	27	↓	↓
0.04	14	21	↓	↓
0.016	14	26	↓	↓
0.008	15	4	Clear	↓
0.004	15	5	Clear	↓
<u>HPC E</u>				
0.16	14	29	Opalescent	Soft caked
0.08	14	28	↓	↓
0.04	14	20	↓	↓
0.016	14	25	↓	↓
0.008	14	4	↓	↓
0.004	14	10	↓	↓

Table 18 (continued)

Initial Concentration of Cellulose g/dl	SV	RV	Appearance of Supernatant	Appearance of Sediment
<u>HPC L</u>				
0.16	14	26	Opalescent	Soft caked
0.08	14	26	↓	↓
0.04	14	19	↓	↓
0.016	14	5	↓	↓
0.008	14	5	↓	↓
0.004	14	10	↓	↓
<u>HPMC 603</u>				
0.16	14	42	Opalescent	Soft caked
0.08	14	32	↓	↓
0.04	14	33	↓	↓
0.016	14	24	↓	↓
0.008	14	17	↓	↓
0.004	14	9	↓	↓
<u>HPMC 606</u>				
0.16	14	34	Opalescent	Soft caked
0.08	14	27	↓	↓
0.04	14	26	↓	↓
0.016	14	26	↓	↓
0.008	14	11	↓	↓
0.004	14	11	↓	↓

Table 18 (continued)

Initial Concentration of Cellulose g/dl	SV	RV	Appearance of Supernatant	Appearance of Sediment
<u>HPMC 615</u>				
0.16	14	30	Opalescent	Soft caked
0.08	14	29	↓	↓
0.04	14	27		
0.016	14	16		
0.008	14	5		
0.004	14	6		

Table 18 Characteristics of suspensions of polystyrene latex in the presence of Celluloses.

particles by the polymers at low concentrations and network formation at high concentrations.

After storage, the gravitational forces cause the particles to settle down and therefore a sediment is formed. If the surfaces of the particles are coated with a polymer layer, overlapped volumes of the adsorbed layers or intimate contact of the adsorbed layer sheaths will occur between the particles in the sediment. As a result, the solubility of the polymer in the overlapped volume or the junction point will decrease under this condition i.e. the concentration will increase. If the solubility limit is surpassed, the polymers tend to cohere to each other. The molecules in the adsorbed layers may form cohesive junction points with other molecules at several places simultaneously and it is clear that this will give rise to the formation of a molecular network structure throughout the sediment in which the particles participate in the formation of the links between the network molecules. Here, the polymer molecules should be sufficiently long to form a molecular network. The concentration of the polymer in the overlapped volume or junction point is important. As the main force causing cohesion of the nonionic polymer is the attractive force the strength of this is dependent upon the concentration of the polymer in the adsorbed layer. The concentrations of the Celluloses in the adsorbed layer at plateau adsorption are given in Table 19. The concentrations of the Celluloses in the adsorbed layer are much higher than those in the bulk solution. As shown in the adsorption isotherms multilayer adsorption occurs at high concentrations. The Cellulose concentrations in the adsorbed multilayer will be much higher. Therefore, it is not surprising that under these conditions network structure formation would occur.

Whereas, in the initial stages of adsorption low adsorbed polymer concentration will be obtained; if no flocculation by the polymer or no mutual adsorption of the adsorbed polymers or attraction on the patches of the bare surface occur, it will form a weak molecular network or no such network will form but the particles stay in the high repulsive energy state. Hence, this will give redispersibility values which will increase with increasing concentration of the polymers.

Cellulose	HEC L	HEC J	HPC E	HPC L	HPMC 603	HPMC 606	HPMC 615
Conc. g/dl	6.0	3.4	4.5	4.2	3.0	4.2	4.5

Table 19 Concentrations of the Celluloses in the adsorbed layer for polystyrene latex.

Details of the redispersibility values of the sediment and the adsorption of the polymer of the polystyrene latex-HPMC 603 system is given in Fig. 65. It is clearly shown that the increase of adsorption increases redispersibility. This supports the above molecular network formation possibility.

Secondly, if the polymers play the role as a flocculating agent, at low concentrations polymers will flocculate the polystyrene latex particles giving an easily redispersed suspension. However, this is not the cases for HPC and HPMC. This will be shown in (c) of this section; HPC and HPMC show no flocculating effect in this concentration range

studied, but for HEC flocculation of the particles occurred. Therefore, one can not rule out the possibility of flocculation of the particles by HEC polymers at low concentrations resulting in low redispersibility values, although small sedimentation volumes are shown. Nevertheless, the network formation mechanism can also be applied at high concentration conditions where high redispersibility values were found.

(c) Flocculation studies

La Mer and Healy (256) and Ruehrwein and Ward (261) demonstrated that for high molecular weight polymers at low concentrations polymer flocculation will occur by forming bridges between particles. Saunders and Sanders (275) showed the effect of methyl cellulose on the electrolyte stability of dilute latices (styrene and saran). They found that the methyl cellulose function is similar to the sensitizing and protecting action observed when certain hydrophilic colloids are added to hydrophobic colloids. When a small amount of methyl cellulose was added to a dilute latex, the methyl cellulose adsorbed at the polymer water interface. As a result, the zeta potential was reduced, aggregates formed, and the electrolyte stability decreased. When sufficient methyl cellulose was present to cover the surface of the particles, a protective action was produced which stabilized the particles due to the steric effect of the methyl cellulose layer. The flocculation of particles by hydroxyethyl cellulose was demonstrated by Miyata et al (262). In the concentration range studied from 0.002 to 0.01 g/dl with HEC of molecular weight of about 100,000, bridging effect of the polymers flocculated the kaolin particles.

In this study, the diluted polystyrene latex 4 dispersion was used

and the degree of the turbidity was investigated. Absorbance against concentration plots for HEC, HPC and HPMC are given in Figs 66, 67 and 68 respectively. The low absorbance is equivalent to a clear supernatant which represents effective flocculation.

For HEC systems, in the concentration range of 0.0001 - 0.008 g/dl, particles were flocculated. At higher concentrations the flocculation effect decreased. For HPC and HPMC systems, flocculation occurred at concentrations about 0.00015 g/dl and 0.00004 g/dl respectively. At higher concentrations the curves remain steady showing a stable dispersion.

The extent of flocculation for HEC J is greater than that of for HEC L. This may be due to the higher molecular weight substance providing a longer molecular chain for more effective bridging. As pointed out by La Mer et al (256) and Kitchener (264) the efficiency of flocculation is greatly dependent on the molecular weight of the polymer whose segments can stretch out long enough to allow bridging to occur. This has been demonstrated by Ash and Clayfield (265) using polyethers to flocculate polystyrene latex. For the systems of HPC and HPMC, the effect of molecular weight on flocculation does not show so significantly due to the poor reproducibility which was about 10%.

5:2:4 Effect of nonionic Celluloses on the stability of ibuprofen

(a) Electrophoresis

For all drug suspensions, the results (Figs 69, 70 and 71) of electrophoretic mobility are similar to those obtained from polystyrene latex systems (Section 5:2:3) i.e. mobility decreases with

increasing Cellulose concentration, then levels off, and decreases again at higher concentrations. Therefore, the concept used in Section 5:2:3 for latex systems can be applied here for ibuprofen suspensions.

Comparing the mobilities of the HEC-latex systems with the HEC-ibuprofen systems, it shows that the mobility decreases in the plateau region due to the adsorbed HEC is more significant for the former than for the latter. One would envisage that the HEC molecules would adopt a flatter conformation on the surface of the ibuprofen than on the latex, if the polymer molecules have the same effect on the double layer of both systems. Whereas, for HPC and HPMC systems, the decrease in mobility for latex and for ibuprofen at plateau adsorption are in the same proportion within experimental error. Therefore, it is likely that the adsorption of HPC and HPMC molecules on polystyrene latex and ibuprofen would have the same apparent conformation.

(b) Sedimentation volume and redispersibility

Sedimentation volume and redispersibility values were obtained after 24 hours storage. The short storage time is due to the quick settlement of the drug particles. Two and three days storage were tried. This resulted in caked suspensions which were difficult to resuspend.

Results are given in Table 20. In all cases, the sedimentation volumes increase with increasing concentration of the polymer. However, for the redispersibility a lower value is shown at intermediate concentrations.

For HPC and HPMC and ibuprofen suspensions, at low polymer

Initial Concentration of Cellulose g/dl	SV	RV	Appearance of Supernatant	Appearance of Sediment
<u>HEC L</u>				
0.2	50	3220	Clear	Loose aggregated
0.16	54	2360	↓	↓
0.08	55	280		
0.04	59	3400		
0.016	51	850		
0.008	55	300		
0.004	60	500	↓	↓
<u>HEC J</u>				
0.2	45	980	Clear	Loose aggregated
0.16	48	760	↓	↓
0.08	50	600		
0.04	48	260		
0.016	49	920		
0.008	51	530		
0.004	53	520	↓	↓
<u>HPC E</u>				
0.2	15	200	Hazy	Caked
0.16	15	147	↓	↓
0.08	21	111		Aggregated
0.04	20	110	↓	↓
0.016	25	120	Clear	
0.008	30	95	↓	Loose aggregated
0.004	35	100	↓	↓

Table 20 (continued)

Initial Concentration of Cellulose g/dl	SV	RV	Appearance of Supernatant	Appearance of Sediment
<u>HPC L</u>				
0.2	14	94	Hazy	Caked
0.16	14	90	↓	↓
0.08	19	76	↓	Aggregated
0.04	19	74	Clear	↓
0.016	23	84	↓	↓
0.008	30	80	↓	↓
0.004	49	60	↓	Loose aggregated
<u>HPMC 603</u>				
0.2	15	300	Hazy	Caked
0.16	15	130	↓	↓
0.08	16	100	↓	↓
0.04	25	74	↓	Aggregated
0.016	27	80	Clear	↓
0.008	36	89	↓	↓
0.004	53	86	↓	Loose aggregated
<u>HPMC 606</u>				
0.2	15	200	Hazy	Caked
0.16	15	120	↓	↓
0.08	18	90	↓	↓
0.04	25	73	↓	Aggregated
0.016	25	82	Clear	↓
0.008	25	79	↓	↓
0.004	49	38	↓	Loose aggregated

Table 20 (continued)

Initial Concentration of Cellulose g/dl	SV	RV	Appearance of Supernatant	Appearance of Sediment
<u>HPMC 615</u>				
0.2	14	100	Hazy	Caked
0.16	14	89	↓	↓
0.08	15	73	↓	↓
0.04	15	67	↓	↓
0.016	22	57	Clear	Aggregated
0.008	25	52	↓	↓
0.004	49	23	↓	Loose aggregated

Table 20 Characteristics of suspensions of ibuprofen in the presence of Celluloses.

concentrations the drug surface was not wet completely. Due to the hydrophobic nature of the drug particles some of the particles floated on the top of the suspension and some of them settled down formed a loose structured sediment. A degasing technique was used to remove entrapped air and it was shown that the sedimentation volume before and after degasing changed little. This loose structure of flocs showed an inelegant appearance and some particles adhered to the wall of the glass tube. As concentration increased the particles on the surface decreased and the volume of sediment increased but the total height of the sedimentation volume decreased. In this low concentration range the redispersibility values show an increase as concentration increases due to the dense sediment formed gradually. At intermediate concentrations, the sedimentation volume values show not very clearly but lower redispersibility values were obtained. This may be due to formation of the complete adsorbed layer creating a steric energy minimum leading to an aggregation of the particles (see Section 5:2:7:4). Therefore, easy redispersions of the suspensions were obtained. It is noted that this minimum aggregation is different from the aggregation at low polymer concentrations. As concentration increased, multilayer formation occurred. This would give a very shallow steric energy minimum or no such minimum would exist. Therefore, particles were in a deflocculated state which resulted in a low sedimentation volume and high redispersibility value. Also, at these concentrations the molecular network structure of the Cellulose molecules could possibly form. As given in Table 21, high adsorbed Cellulose concentrations were found in the adsorbed phase.

Cellulose	HEC L	HEC J	HPC E	HPC L	HPMC 603	HPMC 606	HPMC 615
Conc. g/dl	23.8	15.8	15.2	6.8	9.4	11.4	13.2

Table 21 Concentrations of Celluloses in the adsorbed layer for ibuprofen.

For the HEC-ibuprofen systems, the values of the sedimentation volumes (including the floating flocs) decrease as concentration increases. In all cases, the supernatants were clear. This indicates a flocculated suspension system. However, at concentration of 0.04 g/dl for HEC J and 0.08 g/dl for HEC L lower redispersibility values were obtained. From the adsorption isotherms, these concentrations fall in the plateau adsorption region. Also, a high concentration of the adsorbed polymers in the adsorbed phase was obtained (Table 21). Therefore, it seems likely that the aggregation mechanism at low concentrations and at high concentrations is different. The former is probably due to the deep attractive energy minimum and HEC bridging effect flocculating the particles. The latter may be due to the steric energy minimum and the polymer aggregation between the particles (see Section 5:2:7:4). The appearance of the suspensions were lumpy and frothy. Smears of particles adhered on the wall of the glass tube were found after redispersion.

5:2:5 Hamaker constants

The results of the Hamaker constants of the materials used are given in Table 22.

The values of the Hamaker constants obtained for surface active agents show an increase as the ethylene oxide chain length increases. This confirms the trend of the results found by Elworthy and Florence (266). However, the quantitative values of A obtained are not in line with the published data (266). For example, the A for $C_{16}E_{10}$ of $1.19 \times 10^{-19} \text{ J}$ compared with $C_{16}E_9$ of $6.71 \times 10^{-20} \text{ J}$ (266) is about 1.8 times greater and for $C_{16}E_{30}$ of $1.43 \times 10^{-19} \text{ J}$ compared with $C_{16}E_{25}$ of

Material	γ_L^d mNm ⁻¹	A_{sm} X10 ⁻²⁰ J	A_s X10 ⁻¹⁹ J
HEC L	34.9	5.03	1.61
HEC J	38.8	5.59	1.71
HPC E	21.6	3.11	1.25
HPC L	24.6	3.55	1.34
HPMC 603	22.1	2.90	1.21
HPMC 606	23.4	3.38	1.30
HPMC 615	24.7	3.56	1.34
Texofor A10	20.0	2.81	1.19
A18	24.3	3.49	1.33
A30	28.0	4.03	1.43
A45	28.7	4.13	1.45
A60	30.8	4.43	1.50
Ibuprofen	14.5	2.09	1.03

Table 22 Hamaker constants of materials.

7.46×10^{-20} J (266) is about 1.9 times greater. As suggested by Schenkel and Kitchener (18), the limits of error of the A value is probably correct within a factor of 2. For most of the organic substances the calculated A values are within the range of 10^{-20} J (267). The A values from literatures are inconsistent and vary quite widely (267). For example, the A value for polystyrene-water found by Watillon and Joseph-Petit (268) is 4.22×10^{-21} J, by Ottewill and Shaw (269) is 1.11×10^{-21} J and by Schenkel and Kitchener (18) is 9.0×10^{-20} J. Fowkes

(250) found that the A value for polystyrene-water is 5×10^{-21} J using the interfacial tension method. This is in good agreement with the calculated value of 5.5×10^{-21} J from dispersion data (267). As pointed out by Gregory (267) the interactions of the molecules operated at the interface are short range interactions and have no additive effects which would not contribute to longer range forces such as those between colloidal particles. Therefore, it is likely that the good agreement of the results obtained by the Fowkes method compared with that calculated from the dispersion data is coincident. Therefore, the results obtained here, due to the above reasons and also the complicity arising from the structure of the polymer and solvent at the interface, is difficult to justify. However, it does provide some semiquantitative information of the values of the materials used.

In the present work the above values for A_S are used in the attractive energy calculations together with the assumed value of 1×10^{-20} J.

5:2:6 Polymer-solvent interaction parameter, χ_1

The results of the polymer-solvent interaction parameters for Celluloses in water are given in Table 23.

To choose the value of χ_1 is a difficult problem. As V_S is greatly dependent on χ_1 , this is shown by Eq. (23) in which V_S is proportional to $(0.5 - \chi_1)$. For example, a change of the χ_1 value from 0.497 to 0.3 causes a sixty-seven fold increase in V_S . Ottewill and Walker (19) have calculated the free energy of mixing for polystyrene latex coated with $C_{16}E_6$ using the value of χ_1 from 0 to 0.4. It was

Cellulose	Second Virial Coefficient $\text{cm}^3 \text{mole/g}^2 \times 10^{-4}$	χ_1
HEC L	9.11	0.471
HEC J	8.28	0.473
HPC E	0.43	0.499
HPC L	9.54	0.478
HPMC 603	19.4	0.446
HPMC 606	6.65	0.482
HPMC 615	6.83	0.481

Table 23 Polymer-solvent interaction parameters for Celluloses in water.

shown that free energy before overlap occurs is zero, but as overlap begins free energy increases steeply with decreasing distance between the particles. The smaller the value of χ_1 the steeper the increase in free energy. Therefore, small experimental errors in the evaluation of χ_1 may introduce large errors in calculation of V_S .

The values for Texofors in water such as $C_{16}E_9$ is 0.494 and $C_{16}E_{21}$ is 0.497 (271). Here, the χ_1 value used in the calculations is assumed to be 0.497 for Texofors in all cases.

As χ_1 is a function of phase volume it is reasonable to expect that χ_1 will vary with the amount adsorbed or with the concentration in the adsorbed phase. This was observed in the system of $C_{16}E_x$ (x is from 3 to 25) in the oil phase of anisole and chlorobenzene (266).

For the systems studied here, the X_1 values for HEC and HPMC do not follow the pattern described in the previous paragraph in which it gives the X_1 values increase with increase of the amount adsorbed.

5:2:7 Potential energy of interaction between particles

5:2:7:1 Polystyrene latex and nonionic surface active agent systems

An attempt is made to relate the stability phenomena of the suspensions to the DLVO theory and steric stabilization.

The total energy of interactions was calculated by using Eq. (2). In calculation of V_A , the allowance of the attraction of the adsorbed layer on the particle interactions and the retardation effect between particles were made by using Vincent equations (153) i.e. Eqs (63), (65) and (66). The Hamaker constant for polystyrene latex, A_p , was taken as 7.8×10^{-20} J (15); A_m for water was taken as 3.7×10^{-20} J (272). The critical separation for the retardation effect calculated from Eq. (67) is 3.94 nm for radius of 1,042 nm polystyrene latex (3B).

Values of V_R were obtained using Eq. (49), where the radius used in calculations was taken as $a + \delta$ due to the presence of the adsorbed layer.

The steric free energies for polystyrene latex-Texofor systems were calculated by using Ottewill and Walker equation (Eq. (23)). As this equation has been used by a number of workers for adsorbed surface active agent systems (15,22,32,266), reasonable results were obtained. The concentrations of Texofors in the adsorbed layer, c , taken

from adsorption studies are 1.26, 1.11, 0.70, 0.64 and 0.41 g/cm³ for Texofor A10, A18, A30, A45 and A60 respectively. The molecular volume of the water molecules is 18.02 cm³/mol. The values of the adsorbed layer thickness in Table 10 obtained from the electrophoretic method were used in the calculations. The adsorbed layer thickness obtained from electrophoretic technique has been criticized by Garvey et al (228). They found that for PVA on polystyrene latex the electrophoretic results were invariably higher than those obtained by the other methods and were dependent on the electrolyte concentration employed. They attributed this as being due to the uncorrected assumptions which were made in the calculation. However, for nonionic surface active agents of polyoxyethylene-polyoxypropylene block copolymers adsorbed on polystyrene latex, the electrophoretic results agree closely with IFS results (255). Hence, it seems that the using of the double layer equations to obtain the adsorbed layer thickness is dependent on the type of polymer-substrate system. In the case here, therefore it is reasonable to use the electrophoretic results of adsorbed layer thickness in the calculations of V_S .

Computer programmes were written to evaluate the potential energy of interactions between particles using an ICL 1904S computer. Results of total potential energy diagrams are shown in Figs 72, 73, 74, 75 and 76 for Texofor A10, A18, A30, A45 and A60 respectively.

From the potential energy curves, at concentrations above the complete adsorbed layer concentration, the curves increase steeply nearly vertically at close distances due to the presence of the adsorbed layer generating steric free energy as particles approach each other. This system is a deflocculated system. Particles are in the dispersed

state. However, due to the gravitational effect particles did settle down and formed a small sediment. At low concentrations, the curves are similar to that obtained from bare polystyrene latex but the potential energy obtained in this case is lower than that of obtained in the case of bare latex. This is due to the adsorption of small amount of surface active agents which slightly lower the zeta potential of the particles as shown in the mobility curves. However, the potential energy is still strong enough to maintain the particles in the deflocculated state. As a result, small sedimentation volumes were found.

Napper (273) has considered that the value of V_m necessary to stabilize the system is about 10 - 20 KT. Whereas, a value of 25 KT was given by Schenkel and Kitchener (18). Here, the V_m for polystyrene latex is about 210 KT; a highly stable dispersion is shown.

The effect of the Hamaker constant of the adsorbed surface active agents on V_A such as Texofor A45 is demonstrated in Table 24.

A_s $\times 10^{-20} \text{ J}$	Interaction distance nm	V_A -KT
14.5	8.5	17.70
1.0	8.5	0.875
14.5	1.0	567.3
1.0	1.0	103.6

Table 24 Effect of the Hamaker constant of the adsorbed Texofor A45 on V_A .

When the interaction distance between two particles is 8.5 nm

i.e. the adsorbed layers of two particles just in contact, the Hamaker constant of the adsorbed surface active agent changes from 1×10^{-20} J to 1.45×10^{-19} J leading to a V_A change from -0.875 KT to -17.70 KT which is about 20 fold increase in the values of V_A . At 1 nm interaction distance, the increase of the values of V_A is 5.5 fold when A_s changes from 1×10^{-20} J to 1.45×10^{-19} J. Therefore, it can be seen that the effect of A_s on V_A varies with the interaction distance of the adsorbed layer between the particles and it is important at the beginning distances of the interaction of the adsorbed layers.

5:2:7:2 Polystyrene latex and nonionic surface active agents in the presence of electrolyte

Results of total energy curves are shown in Fig. 77. At complete adsorbed layer concentrations due to the presence of the adsorbed layer providing the steric energy, a sharp cut-off occurs in the curves creating a steric energy minimum. The depth of the minimum is heavily dependent on the A_s value. For example, for the Texofor A10-polystyrene latex system, the depth of the minimum is -42.5 KT when the experimental value of A_s of 1.19×10^{-19} J is used. Whereas, the depth of the minimum is -4.0 KT when the assumed value of A_s of 1×10^{-20} J is used. The difference between the results obtained using the assumed value and the experimental value is about 11 times.

Verwey and Overbeek (4) demonstrated that for one micron particles in the presence of 10^{-3} M 1:1 electrolyte, a secondary minimum of 6 KT could cause loose aggregation of particles. While, Schenkel and Kitchener (18) showed that for ten micron polystyrene latex in various concentration of KNO_3 the onset of slow aggregation is 4 KT depth of

the minimum at 100 nm separation and in the stable region the minimum is less than 1 KT deep. In this study, the particles of the suspensions were not in loose structure aggregates and small sedimentation volumes were obtained due to the slow aggregation of the particles. However, easy redispersions of the suspensions were obtained. This shows that particles were aggregated in the minimum. The redispersibility values varied with the depth of the minimum as shown in Table 25.

Texofor	Depth of Minimum -KT	RV
A10	42.5	39
A18	34.0	45
A30	23.5	52
A45	18.5	67
A60	16.5	64

Table 25 The relation of depth of the minimum and the redispersibility.

It can be seen that the deeper the energy minimum the easier the redispersion of the suspension. This is in agreement with the systems of diloxanide furoate-nonionic surface active agents (15). It is also shown that as the adsorbed layer thickness increases (Table 10) the depth of the minimum decreases. That is to say, suspension will cake if the adsorbed polymer layer on the particle is too thick.

At low concentrations of surface active agents, the steric effect is not significant and the electrostatic force is suppressed, hence the attractive force is predominant as shown in Fig. 77(a). Coagulation

of particles in loose structure and a voluminous sediment were shown. This floc structure is irreversible in the colloid sense but easy to redisperse in practice.

5:2:7:3 Polystyrene latex and nonionic Cellulose systems

In this study, for the calculation of the steric energy Napper's equations (Eqs (32), (34) and (36)) were used. Since Napper's equations give allowance for the interpenetration and the compression effects for adsorbed layer interactions. The most important feature is to take into account the density distribution of the adsorbed segments. In Ottewill and Walker equation (Eq. (23)), it is assumed that the density in the adsorbed layer is uniform; the polymer concentration in the overlapped volume is the sum of the concentrations in the separated volume. These assumptions may be fit for short chain length molecules or low molecular weight polymers and for small degrees of interaction.

For high molecular weight polymers or thick adsorbed layers the assumption of uniform density in the adsorbed layer and the additive polymer concentration in the interaction volume is obviously incorrect.

Here, Eqs (32), (34) and (36) for polymer loops on spherical particles were used and also the elastic energy due to the interpenetration and compression interaction was included in the calculations.

The values of the adsorbed layer thickness used in this calculation are assumed to be equal to those used in the polystyrene latex systems. As pointed out in Section 4:2:3:2, the electrophoretic adsorbed layer thickness results obtained from polystyrene latex and from ibuprofen

are of the same magnitude. Therefore, this assumption seems quite reasonable.

The total potential energy diagrams for HEC, HPC and HPMC systems are given in Figs 78, 79, and 80 respectively. A very sharp increase in energy is shown at concentrations above the complete adsorbed layer concentrations and a maximum peak is given at low concentrations. For HPC and HPMC systems, opalescent supernatants were observed and soft caked sediments were obtained. It is expected that these systems are deflocculated systems. For HEC systems, opalescent supernatants were obtained only at high concentrations whereas at low concentrations of 0.004 and 0.008 g/dl clear supernatants were found (for HEC L suspensions at 0.008 g/dl the supernatant was slightly hazy). Therefore, it seems that at these concentrations particles were flocculated although sedimentation volumes showed no open structure which may be due to the slow flocculation effect by the polymers. As given in Section 5:2:3 of flocculation experiments in which HEC polymers play a role as a flocculating agent at low concentrations. Hence, for HEC systems, total energy curves show a stable system at low concentrations which is not in accord with the experimental data. It is suggested that the total energy of the system should be $V_T = V_A + V_R + V_S + V_F$ where V_F is the flocculation energy of the polymer as described in Section 6. However, it is difficult to obtain the value of V_F .

5:2:7:4 Ibuprofen and nonionic Cellulose systems

The results of the total energy curves for HEC, HPC and HPMC systems are shown in Figs 81, 82 and 83 respectively. At low concentrations of polymers attraction between particles completely overwhelms

electrostatic repulsion and no steric effect is involved in the interaction leading to a rapid aggregation of the particles. As given in Table 20, loose aggregated sediments and clear supernatants were obtained.

At complete adsorbed layer concentration, particles were restricted in the steric energy minimum. In all cases, aggregated sediments were found. The depths of the minima and the characteristics of the suspensions are shown in Table 26.

Cellulose	Depth of Minimum -KT	δ nm	RV	SV
HEC L	44	53.6	280	55
HEC J	48	52.8	600	50
HPC E	51	42.8	111	21
HPC L	69	32.1	76	19
HPMC 603	122	17.0	100	16
HPMC 606	76	27.9	90	18
HPMC 615	57	36.4	73	15

Table 26 Depths of the steric minima and characteristics of suspensions.

On examining the effect of the adsorbed layer of HPC and HPMC on the depth of the minimum it is found that increasing the adsorbed layer thickness decreases the depth of the minimum. One would envisage that caked suspension would occur with the thicker adsorbed layer especially when multilayers are present (Table 19). However, for the

HEC systems, loose aggregated particles were found although the adsorbed layer thickness are large. Also, in Table 26, voluminous sediments are shown but the smallest minima were found. This is difficult to explain. It is probably due to aggregation between the adsorbed polymers on the particles occurred.

An attempt has been made to relate the redispersibility values to the depths of the minima. Unfortunately, the redispersibility values do not correlate with the depths of the minima. This is due to the fact that some of the particles adhered on the wall of the container. In these systems the wall effect hindered the accuracy of the redispersion.

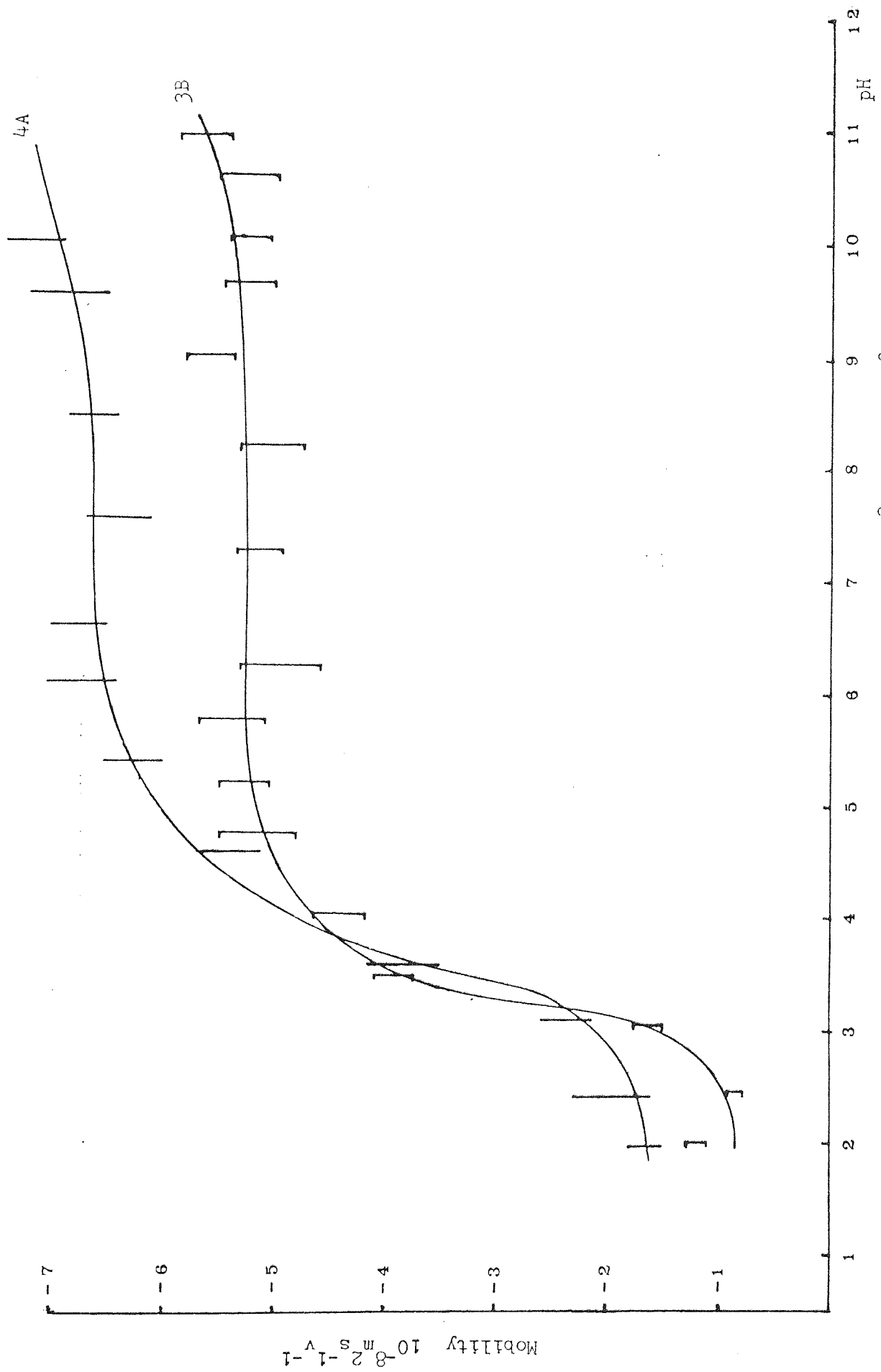


Fig. 50 Mobility - pH plots for polystyrene latex 3B and 4A in 10^{-3} M NaCl at 25°C .

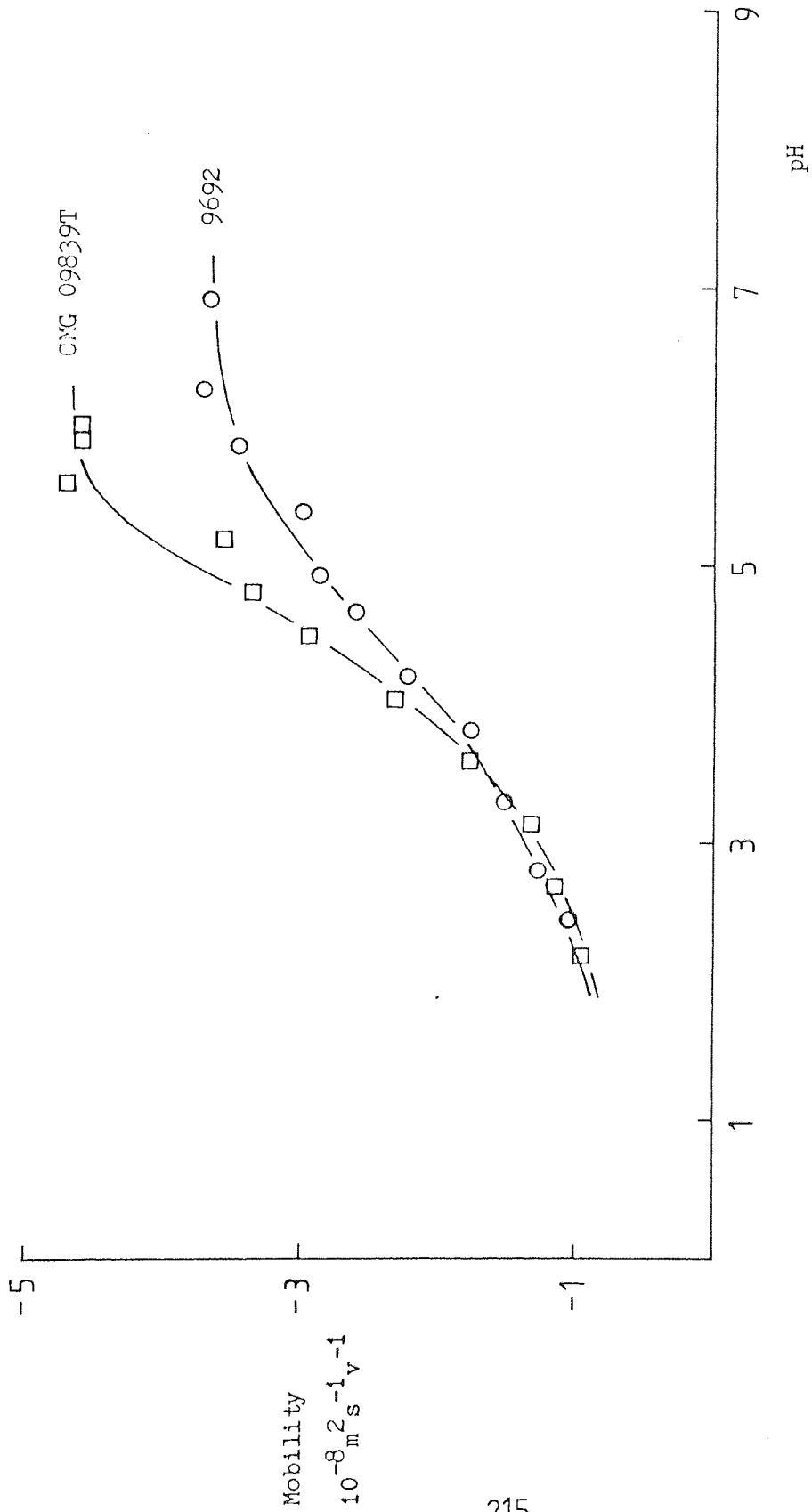


Fig. 51 Mobility - pH plots for ibuprofens in 10^{-3} M NaCl at 25°C .

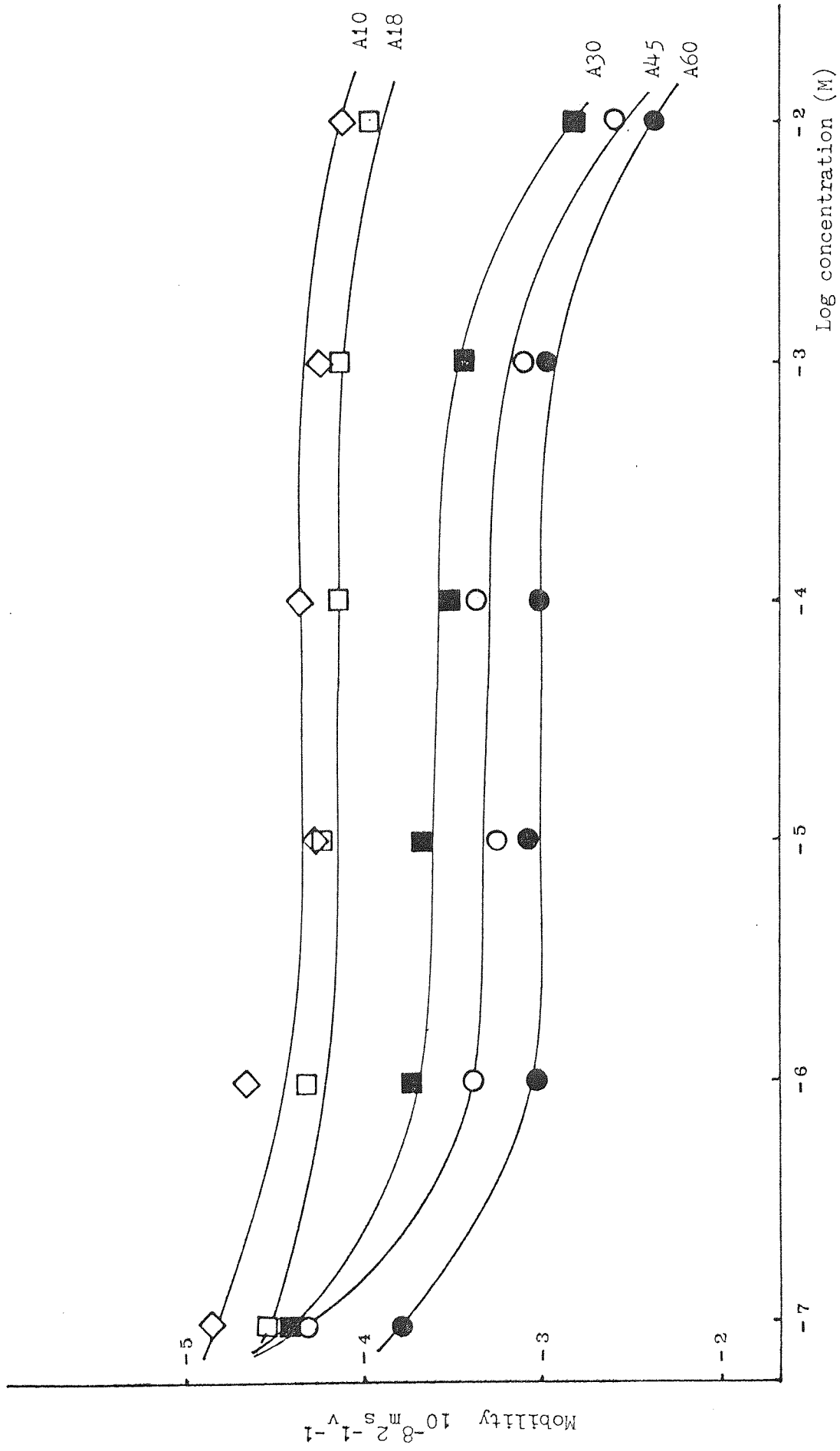


Fig. 52 Mobility - concentration plots for polystyrene latex in the presence Texofors.

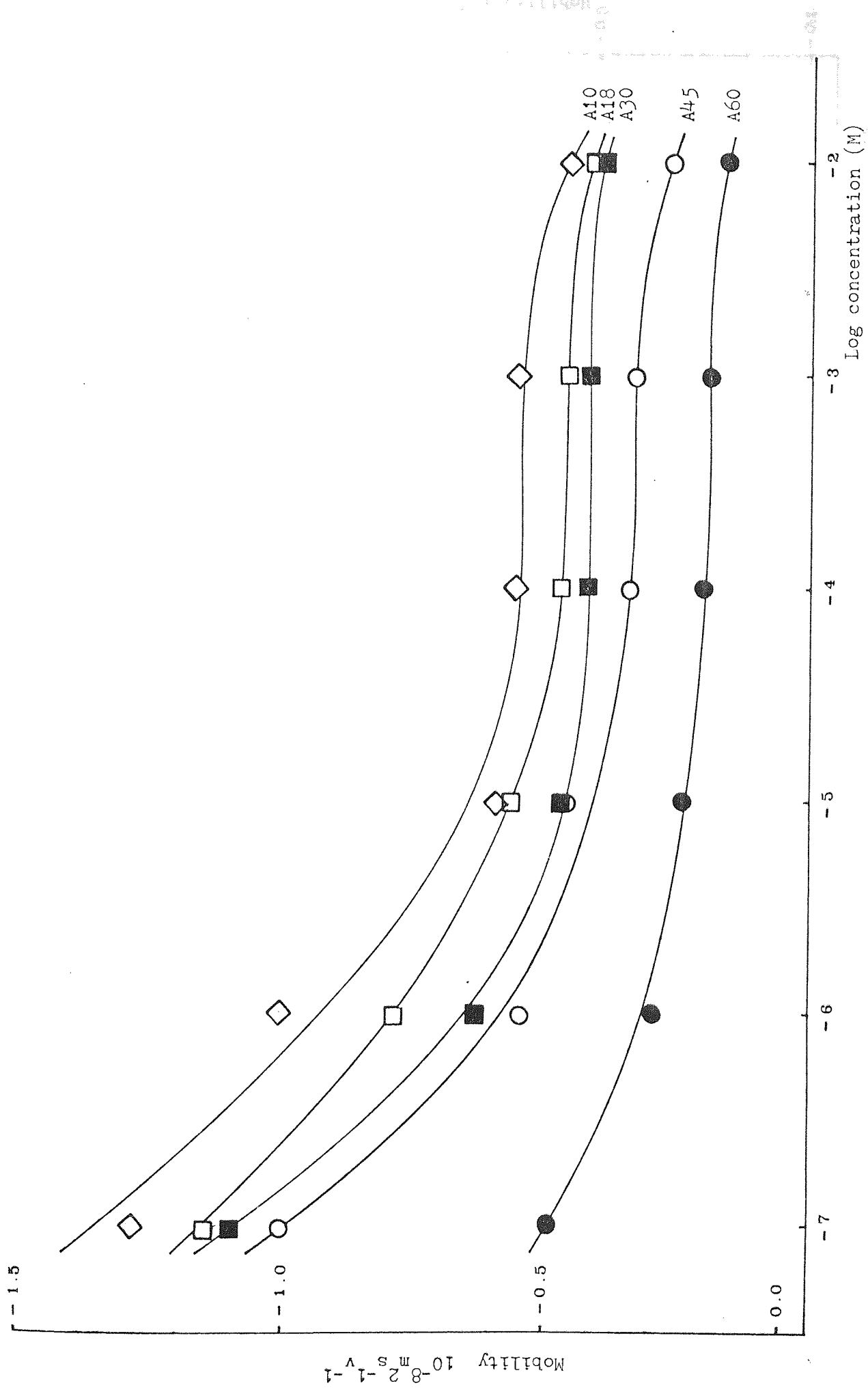


Fig. 55 Mobility - concentration plots for polystyrene latex in the presence of Texofors with Al^{3+} .

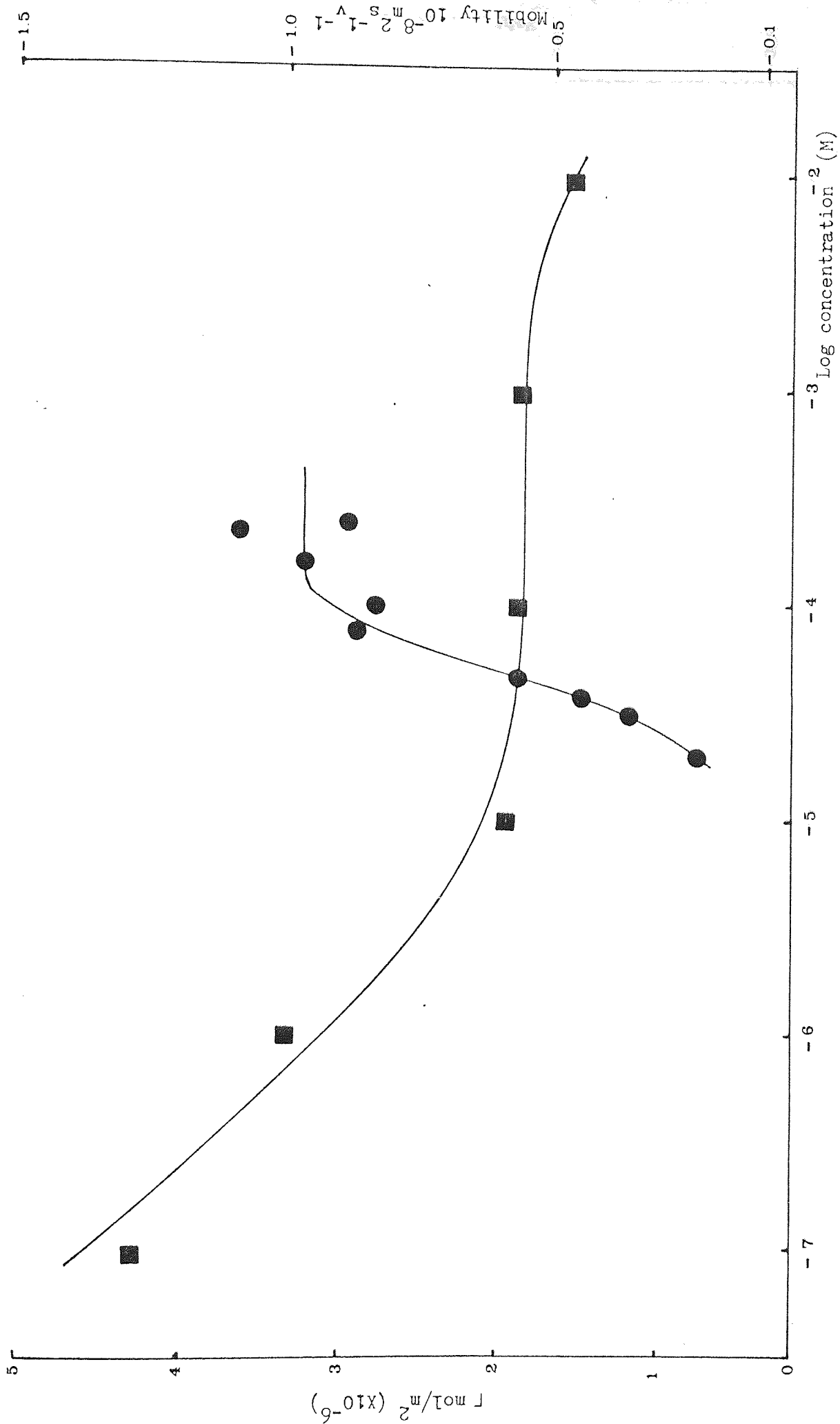


Fig. 56 Adsorption isotherm of Texofor A10 and mobility curve in the presence of Al^{3+} for polystyrene latex.

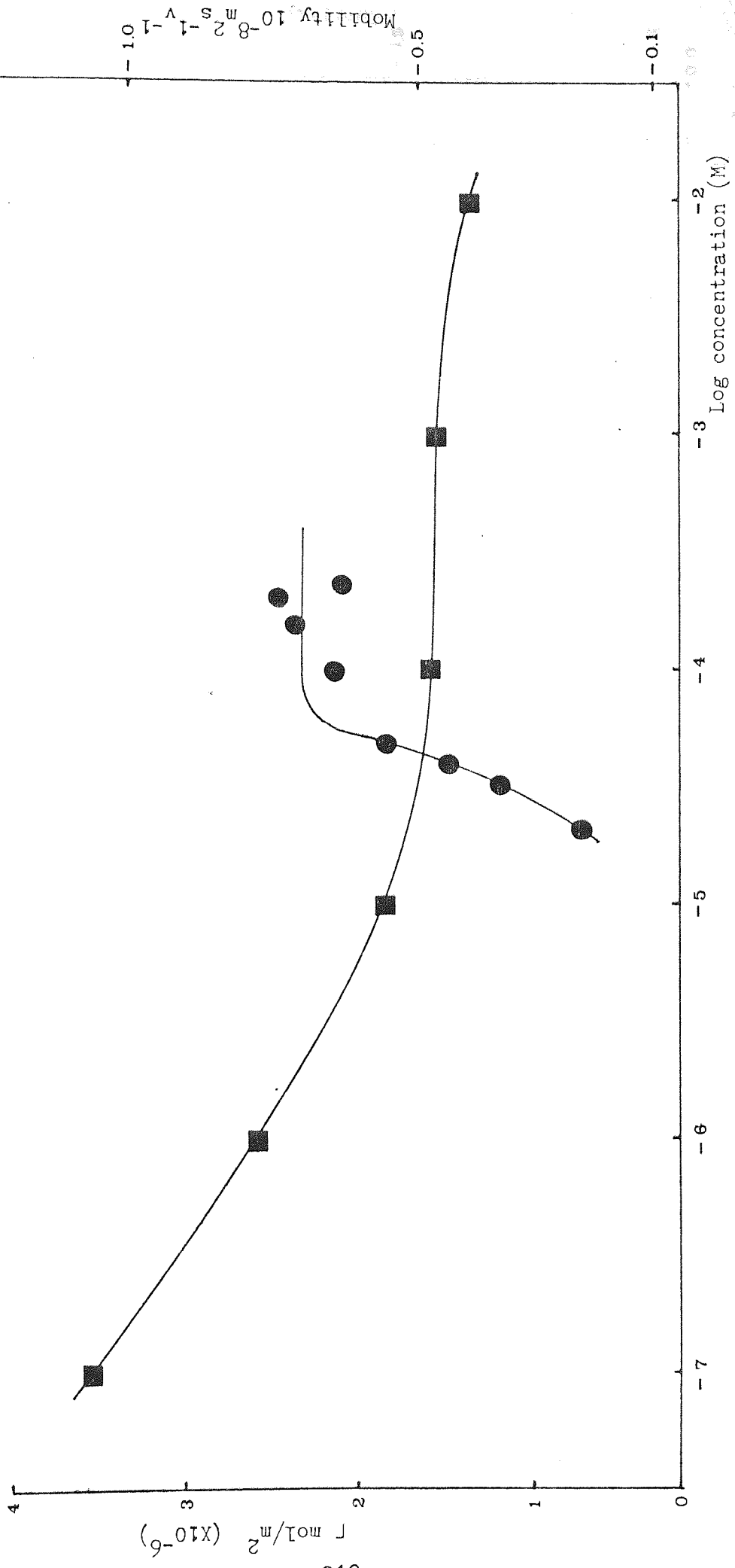


Fig. 57 Adsorption isotherm of Texofor A18 and mobility curve in the presence of Al^{3+} for polystyrene latex.

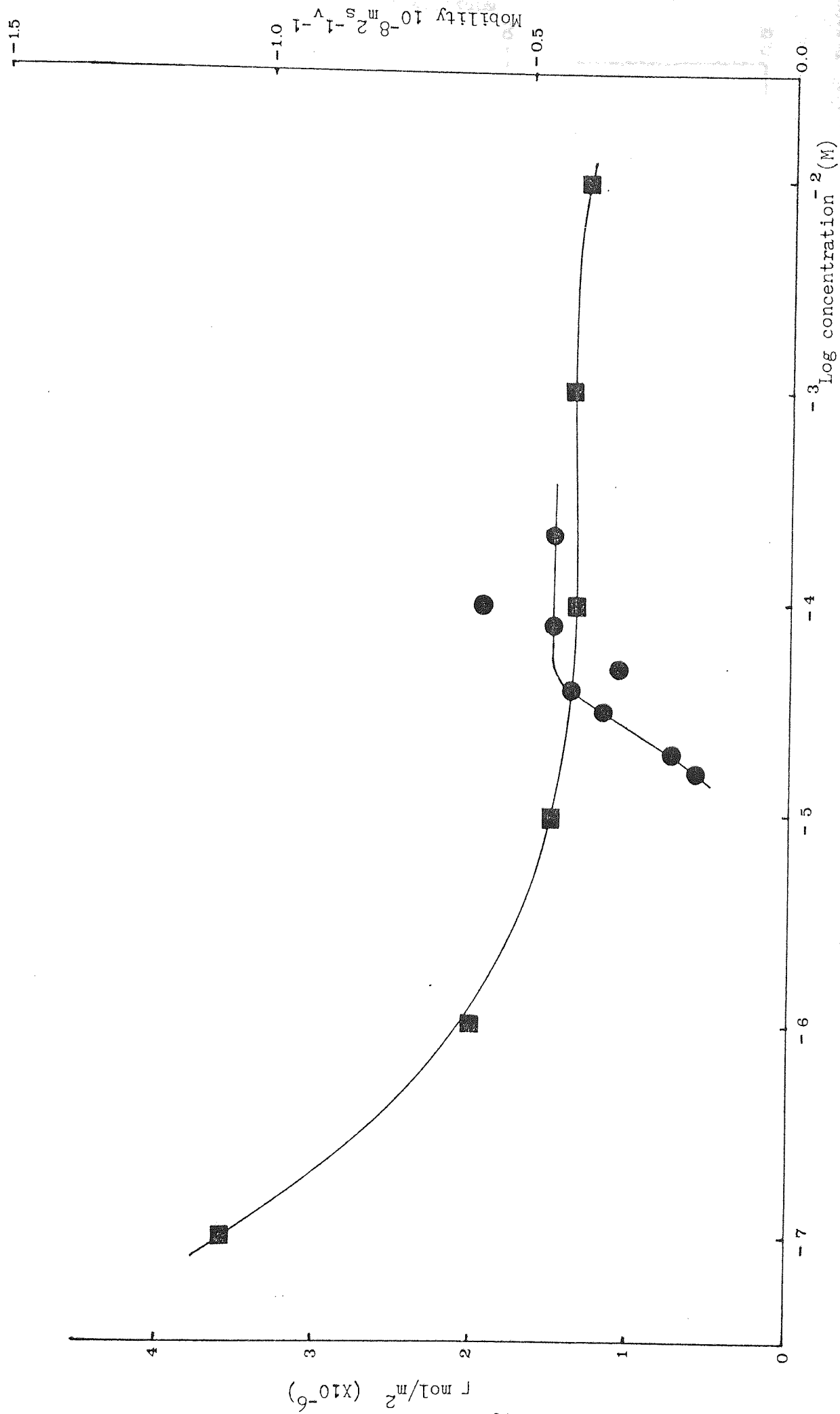


Fig. 58 Adsorption isotherm of Texofor A30 and mobility curve in the presence of Texofor A30 with Al^{3+} for polystyrene latex.

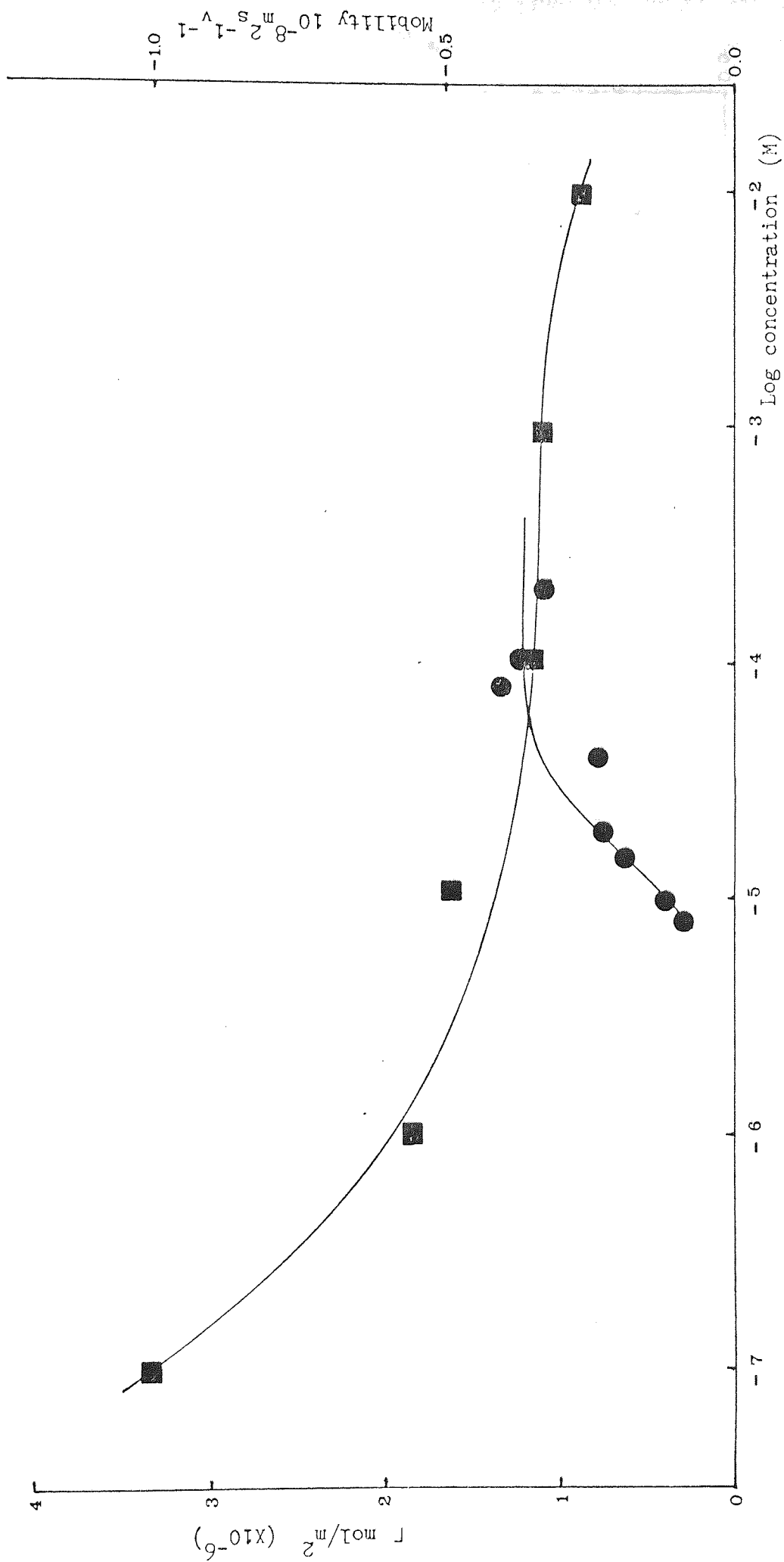


Fig. 59 Adsorption isotherm of Texofor A45 and mobility curve in the presence of Texofor A45 with Al^{3+} for polystyrene latex.

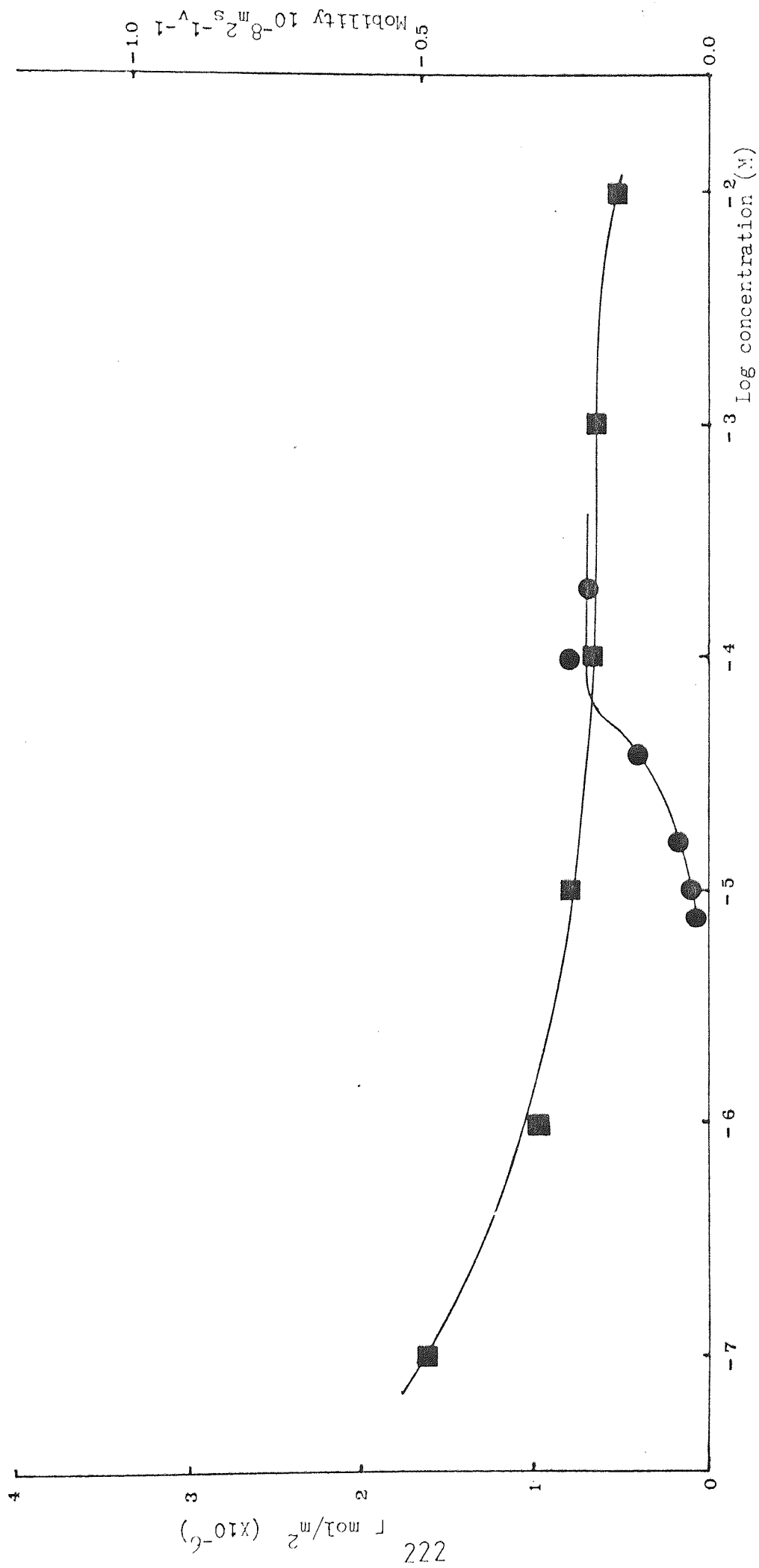


Fig. 60 Adsorption isotherm of Texofor A60 and mobility curve in the presence of Al^{3+} for polystyrene latex.

Fig. 61(a) Photomicrograph of polystyrene latex in the presence of 10^{-2} M of Texofor A18 with Al^{3+} .

Fig. 61(b) Photomicrograph of polystyrene latex in the presence of 10^{-3} M of Texofor A18 with Al^{3+} .

Fig. 61(c) Photomicrograph of polystyrene latex in the presence of 10^{-4} M of Texofor A18 with Al^{3+} .

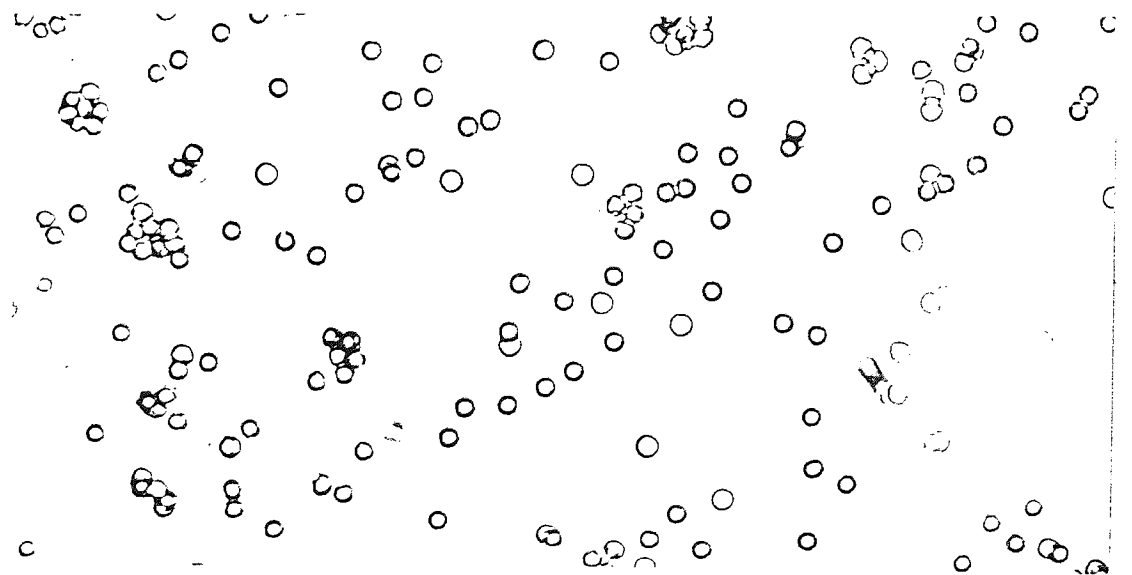
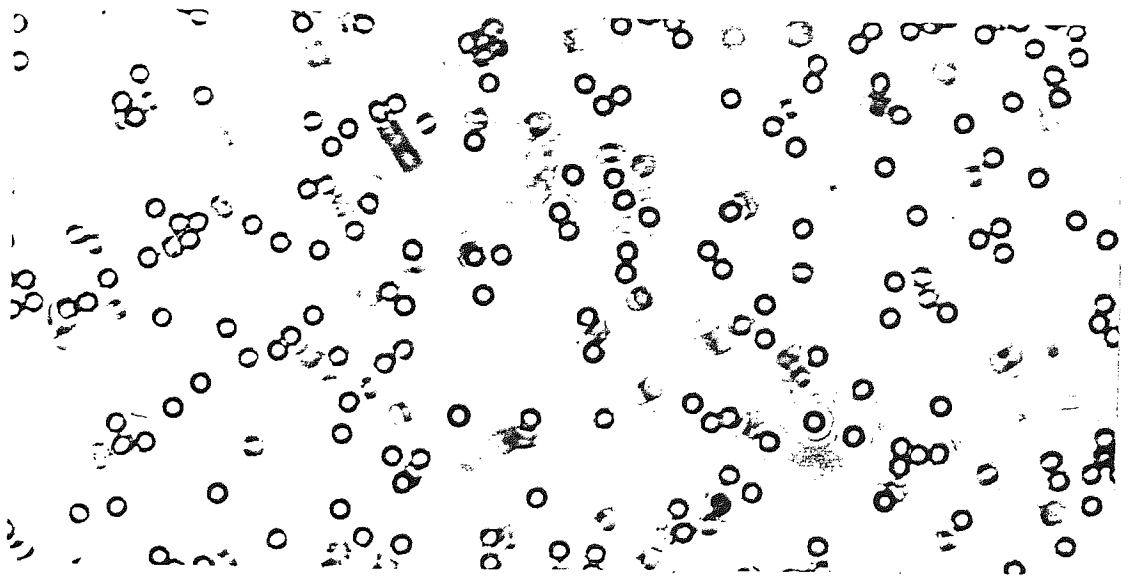
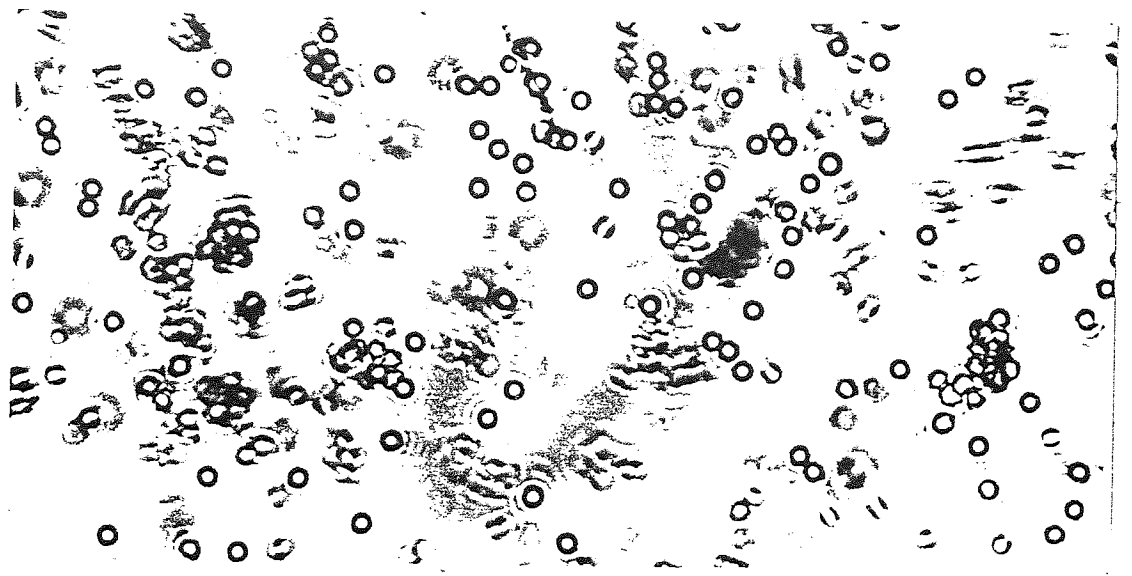
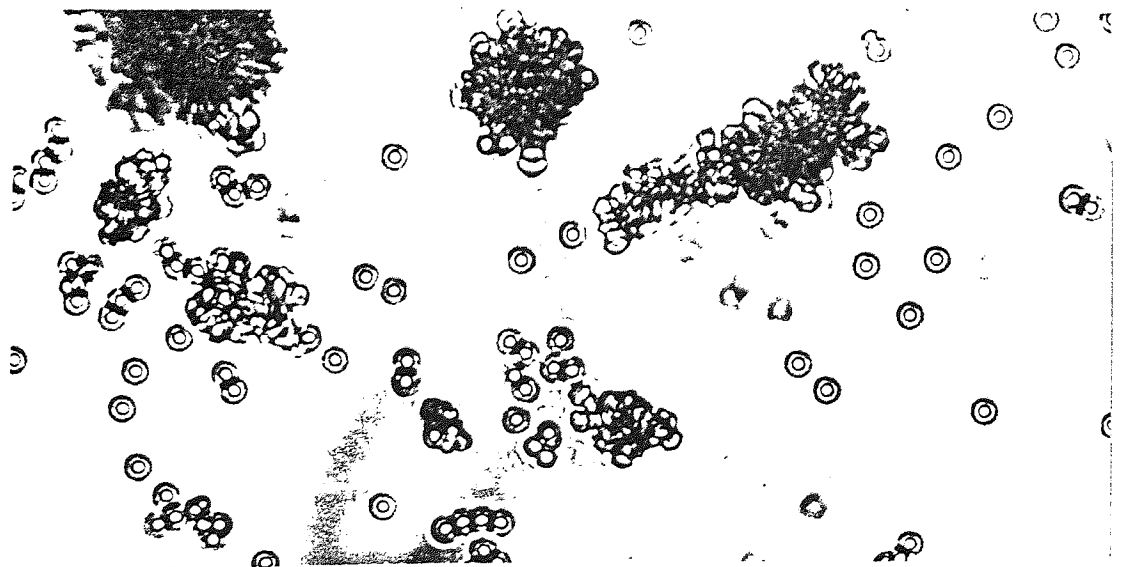
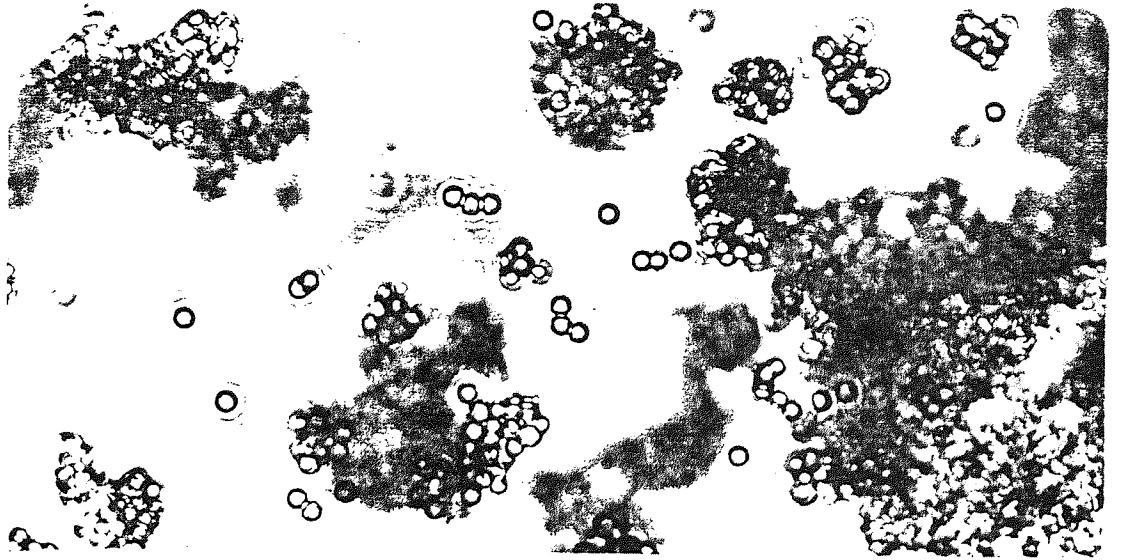
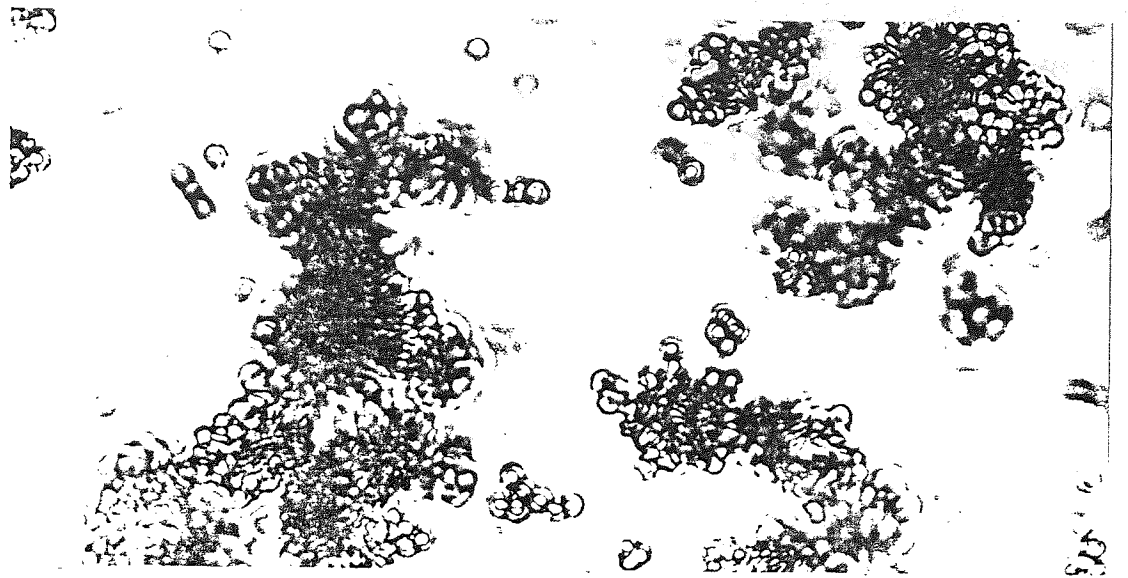


Fig. 61(d) Photomicrograph of polystyrene latex in the presence of 10^{-5} M of Texofor A18 with Al^{3+} .

Fig. 61(e) Photomicrograph of polystyrene latex in the presence of 10^{-6} M of Texofor A18 with Al^{3+} .

Fig. 61(f) Photomicrograph of polystyrene latex in the presence of 10^{-7} M of Texofor A18 with Al^{3+} .



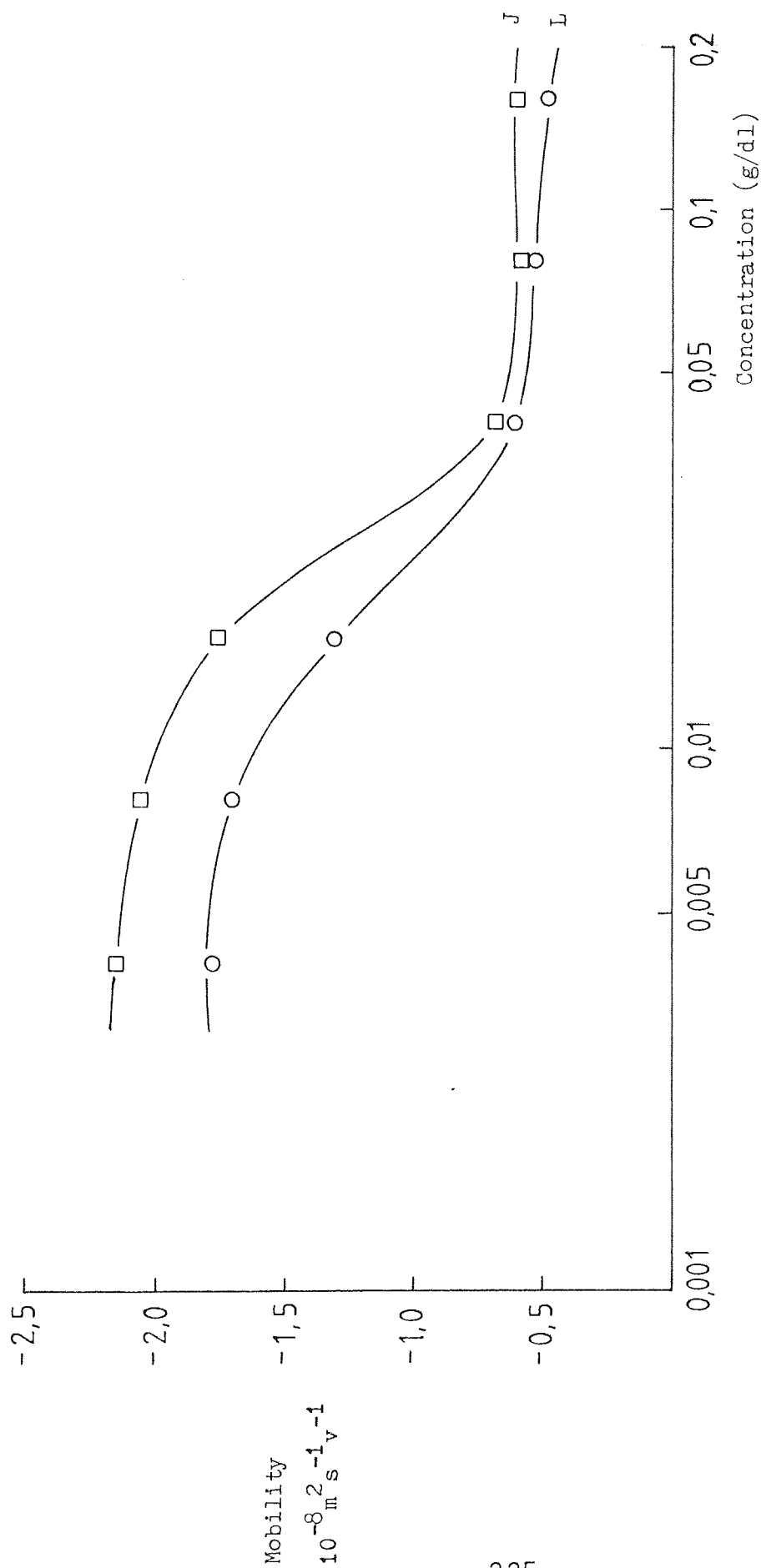


Fig. 62 Mobility - concentration plots for polystyrene latex in the presence of HEC.

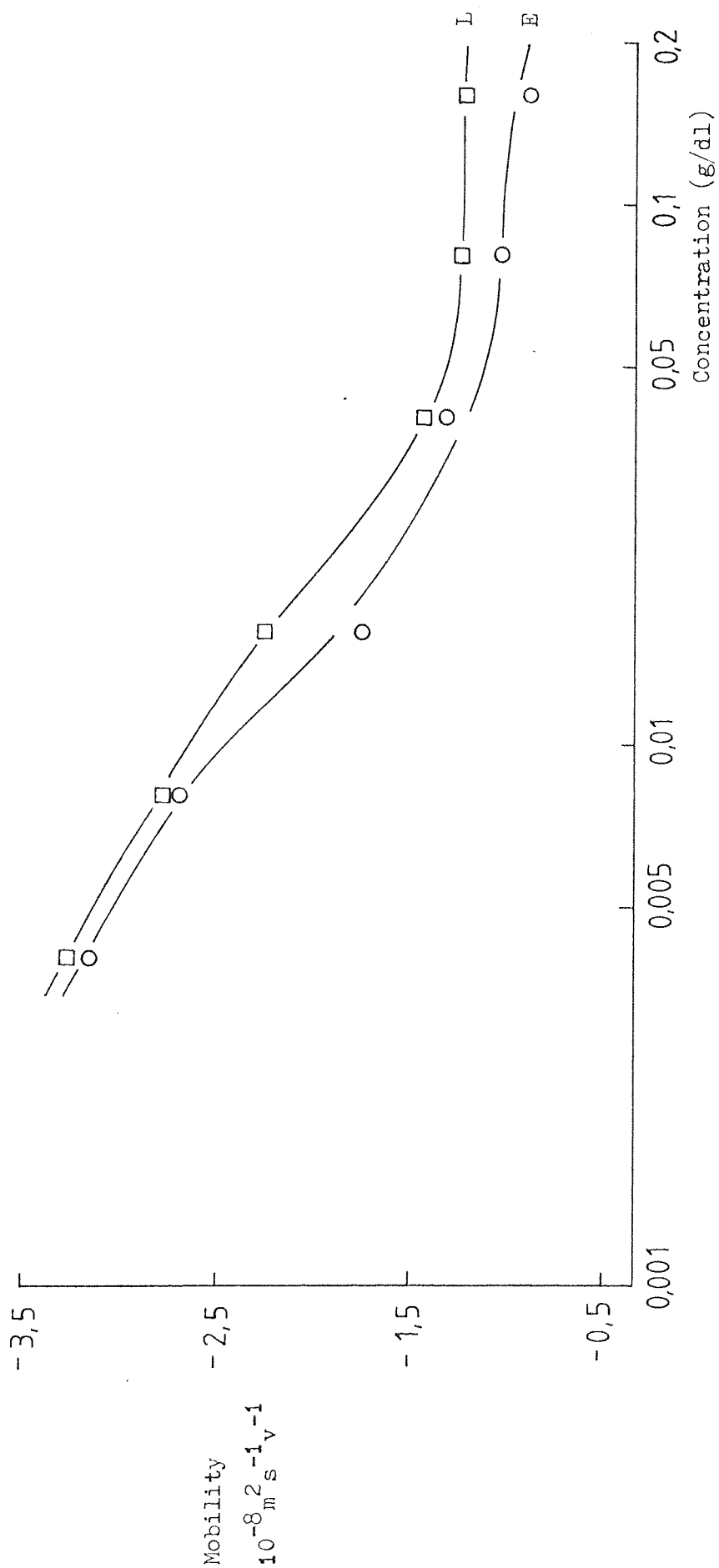


Fig. 63 Mobility - concentration plots for polystyrene latex in the presence of HPC.

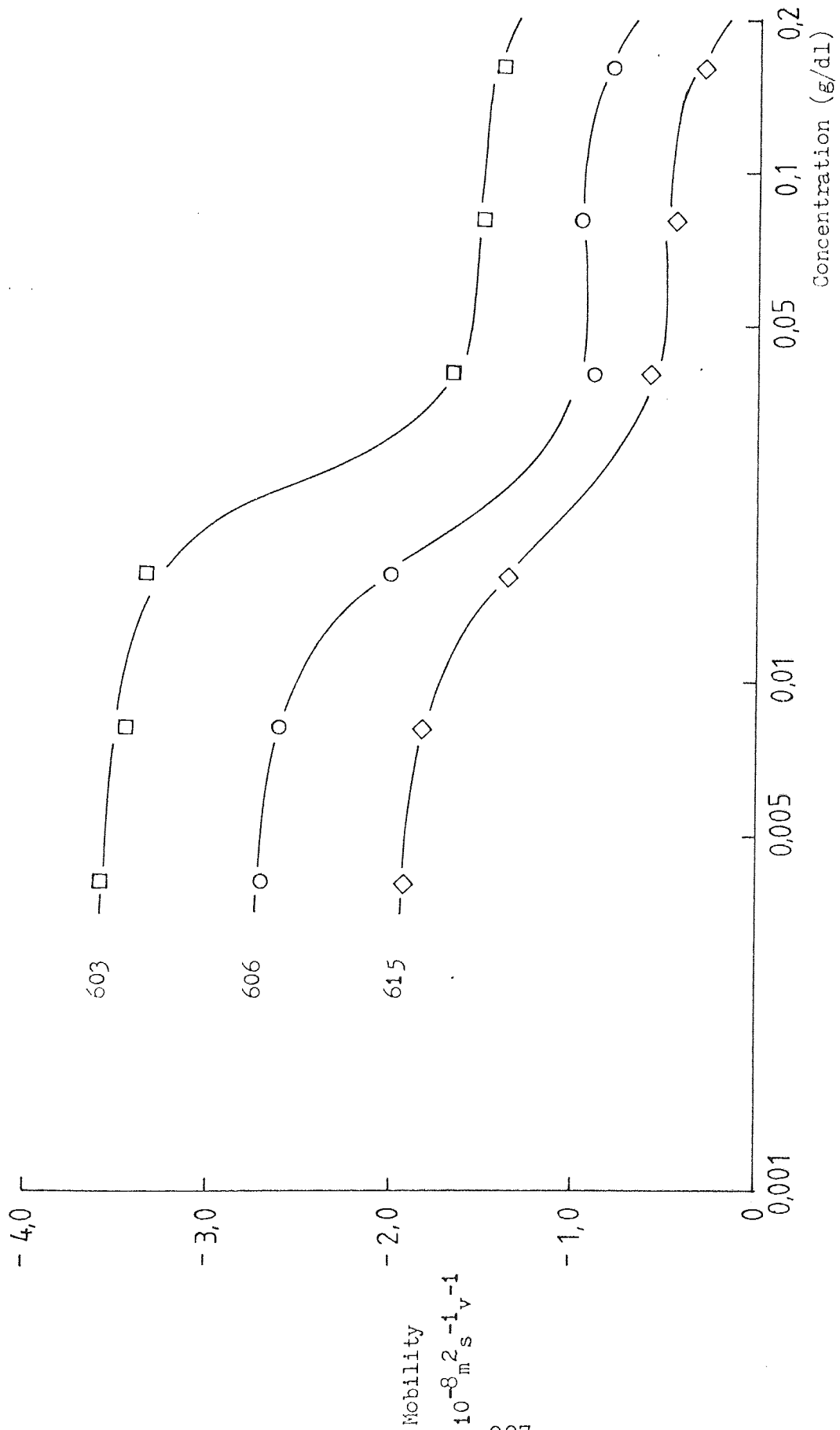


Fig. 64 Mobility - concentration plots for polystyrene latex in the presence of HPMC.

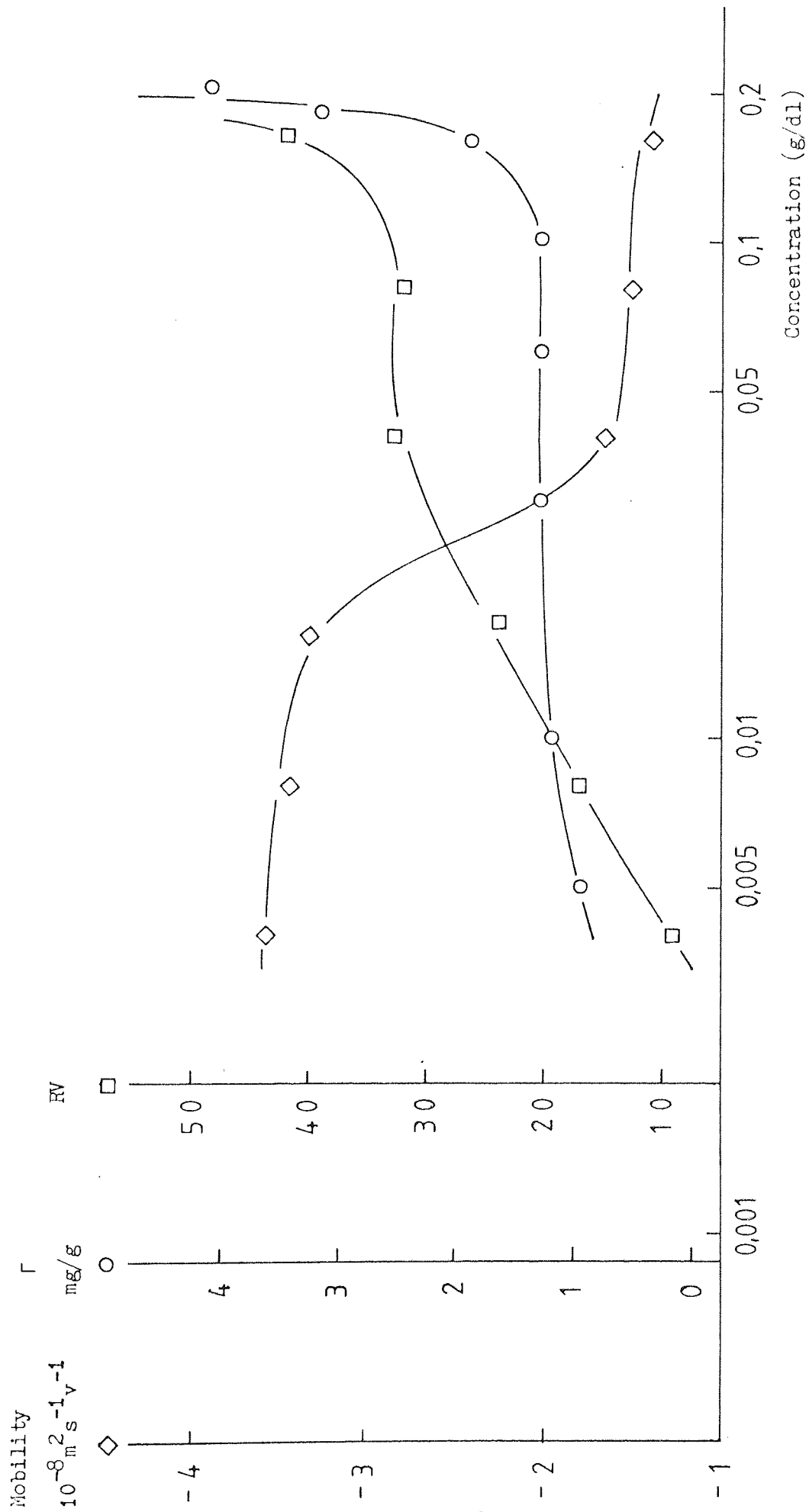


Fig. 65 Characteristics of polystyrene latex - HPMC 603 suspensions.

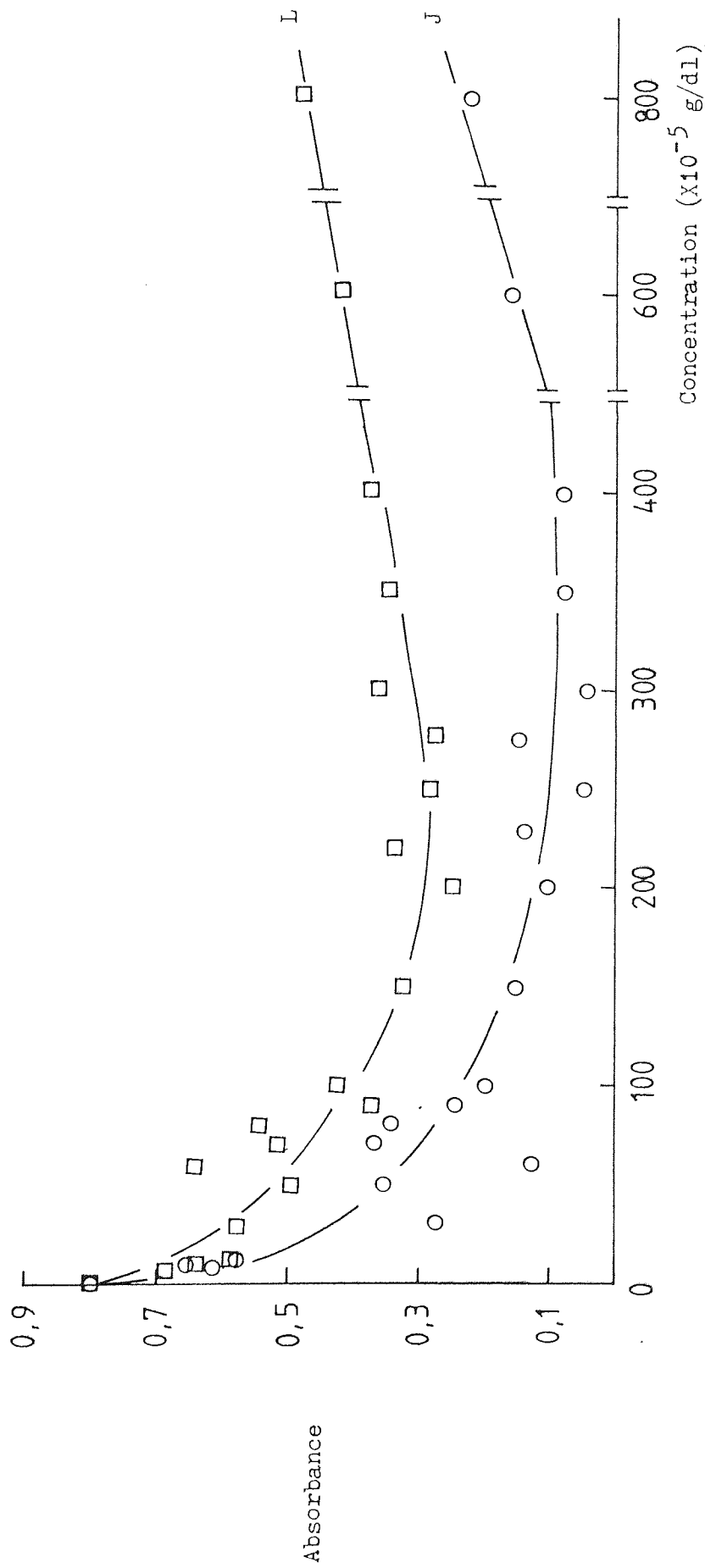


Fig. 66 Absorbance - concentration plots of polystyrene latex in the presence of HEC.

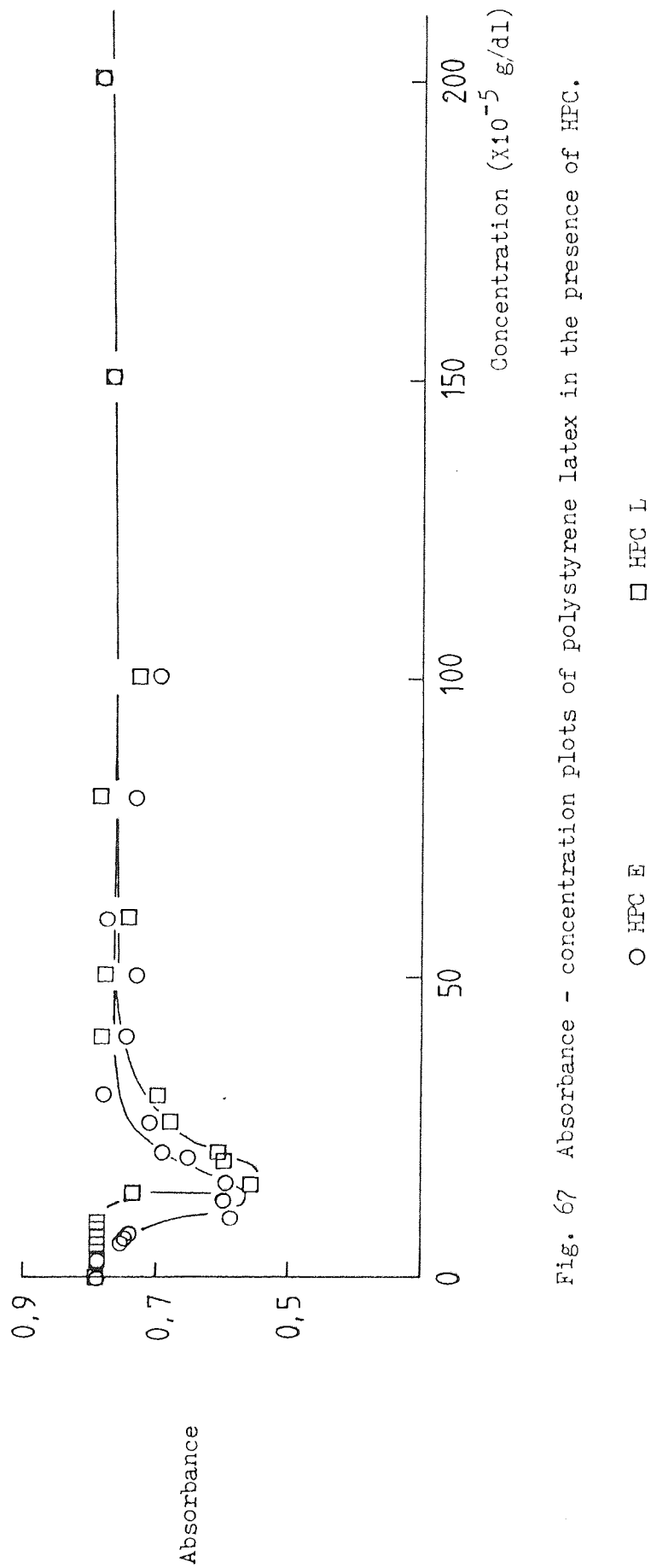


Fig. 67 Absorbance - concentration plots of polystyrene latex in the presence of HFC.

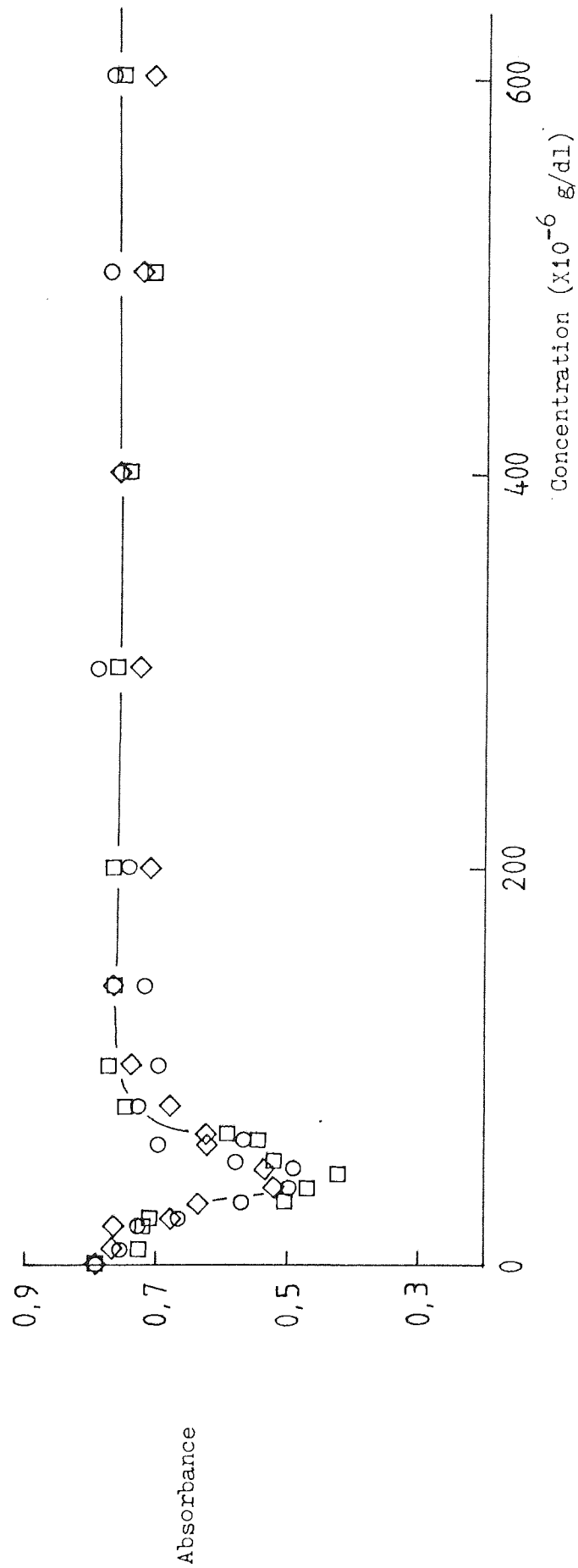


Fig. 68 Absorbance - concentration plots of polystyrene latex in the presence of HPMC.

◇ HPMC 603 ○ HPMC 606 □ HPMC 615

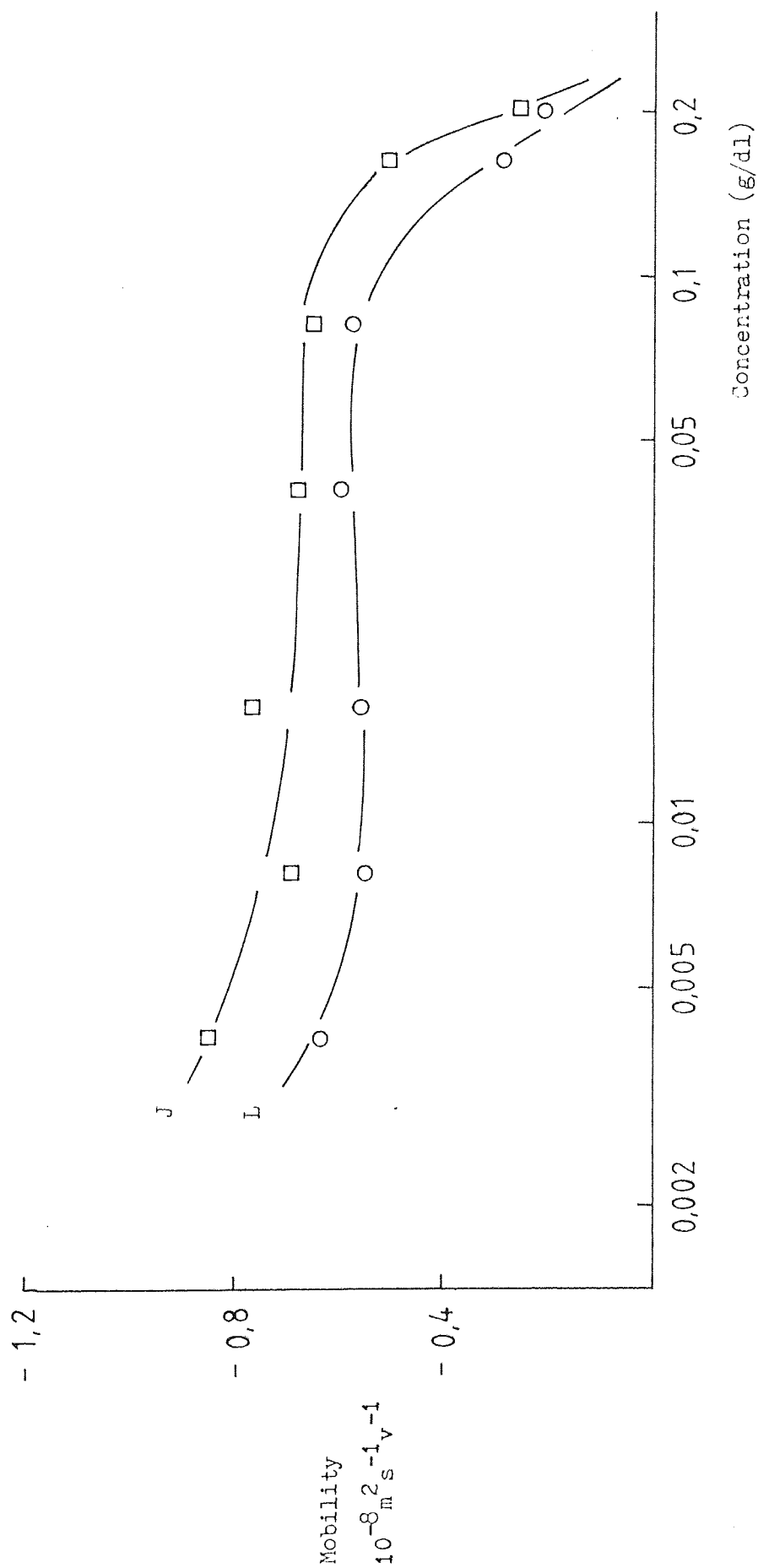


Fig. 69 Mobility - concentration plots for ibuprofen in the presence of HEC.

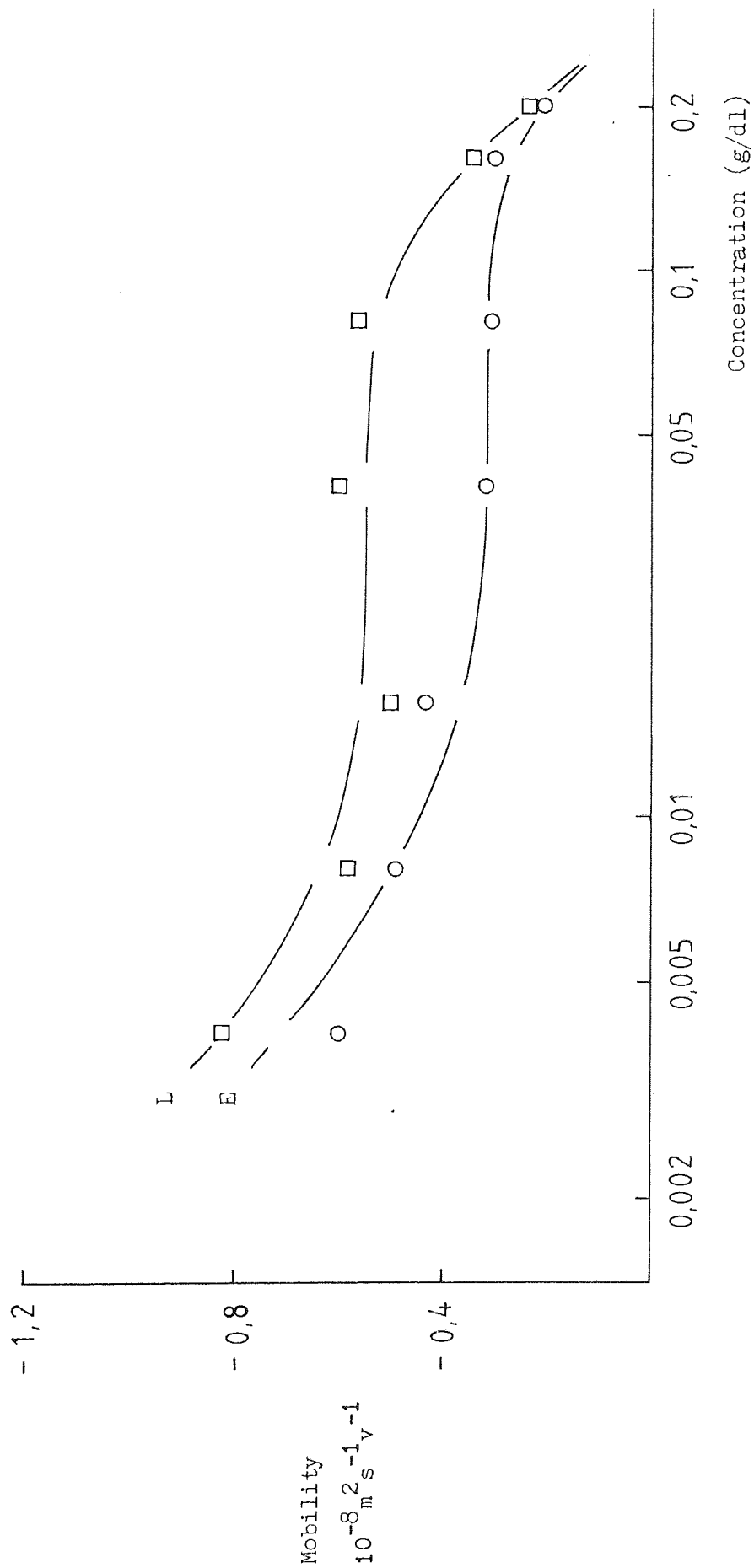


Fig. 70 Mobility - concentration plots for ibuprofen in the presence of HPC.

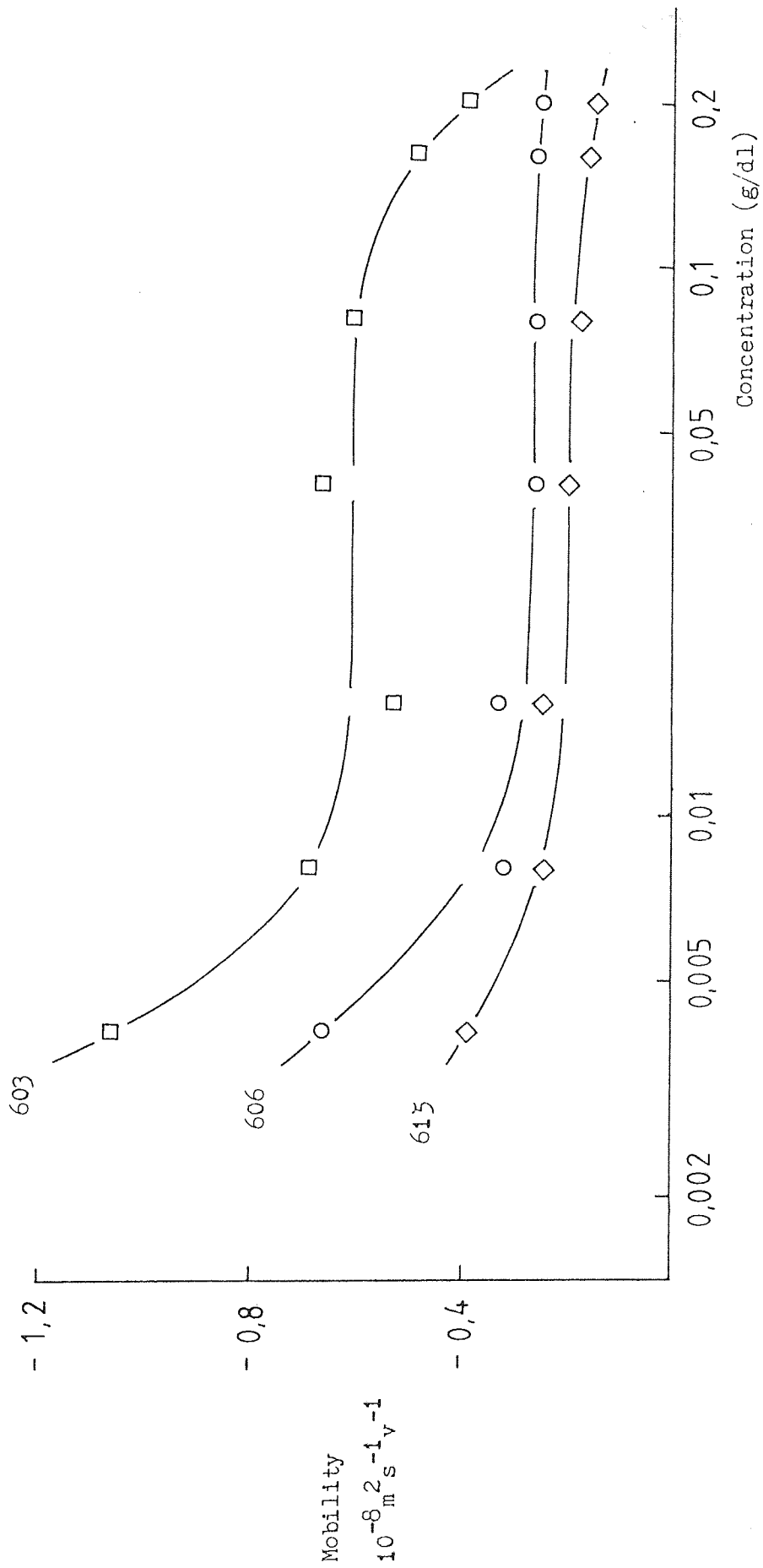


Fig. 71 Mobility - concentration plots of polystyrene latex in the presence of HPMC.

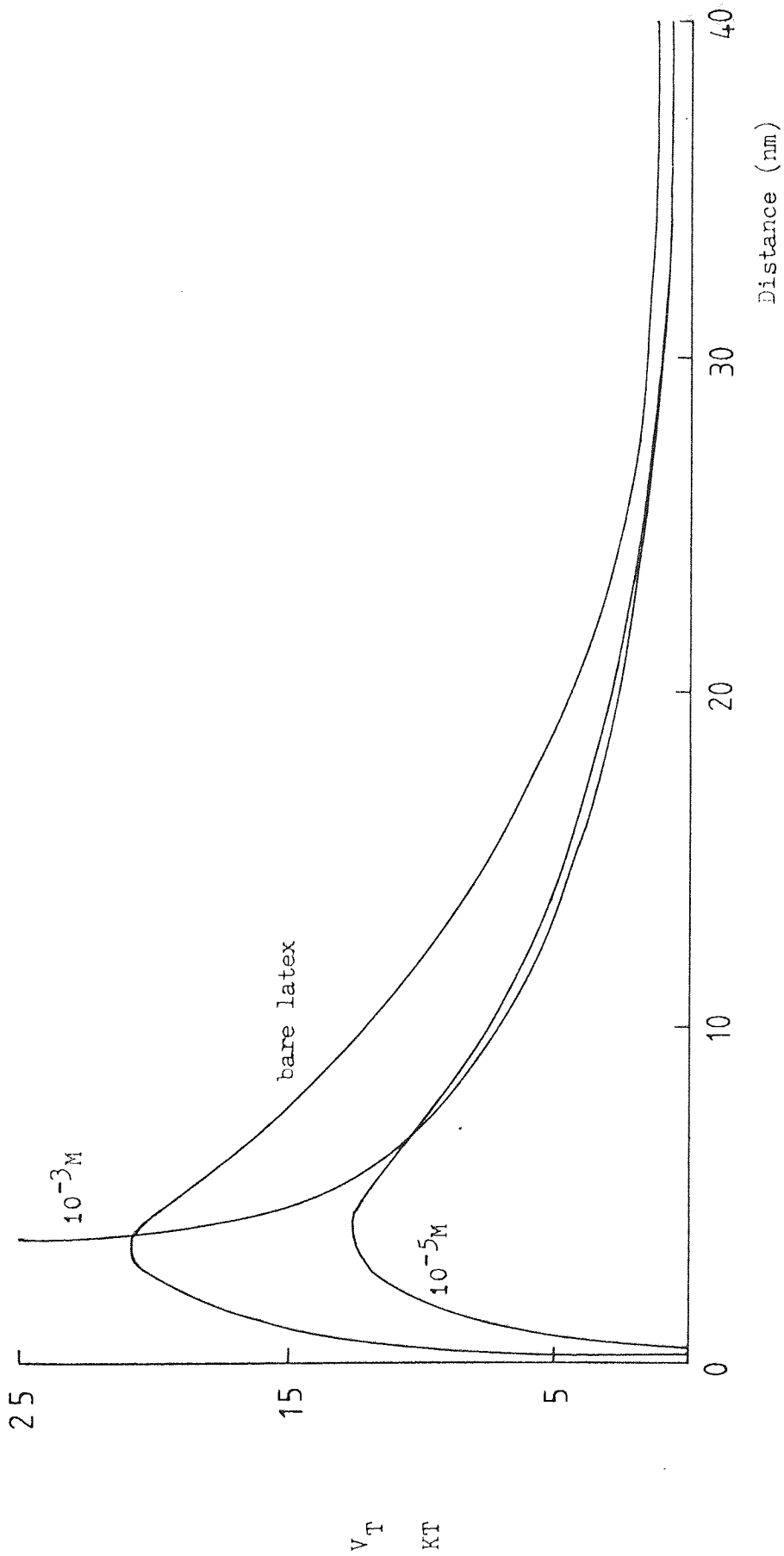


Fig. 72 Total potential energy curves for polystyrene latex in the presence of Texofor A10.

V_T
 $\times 10^3$ KJ

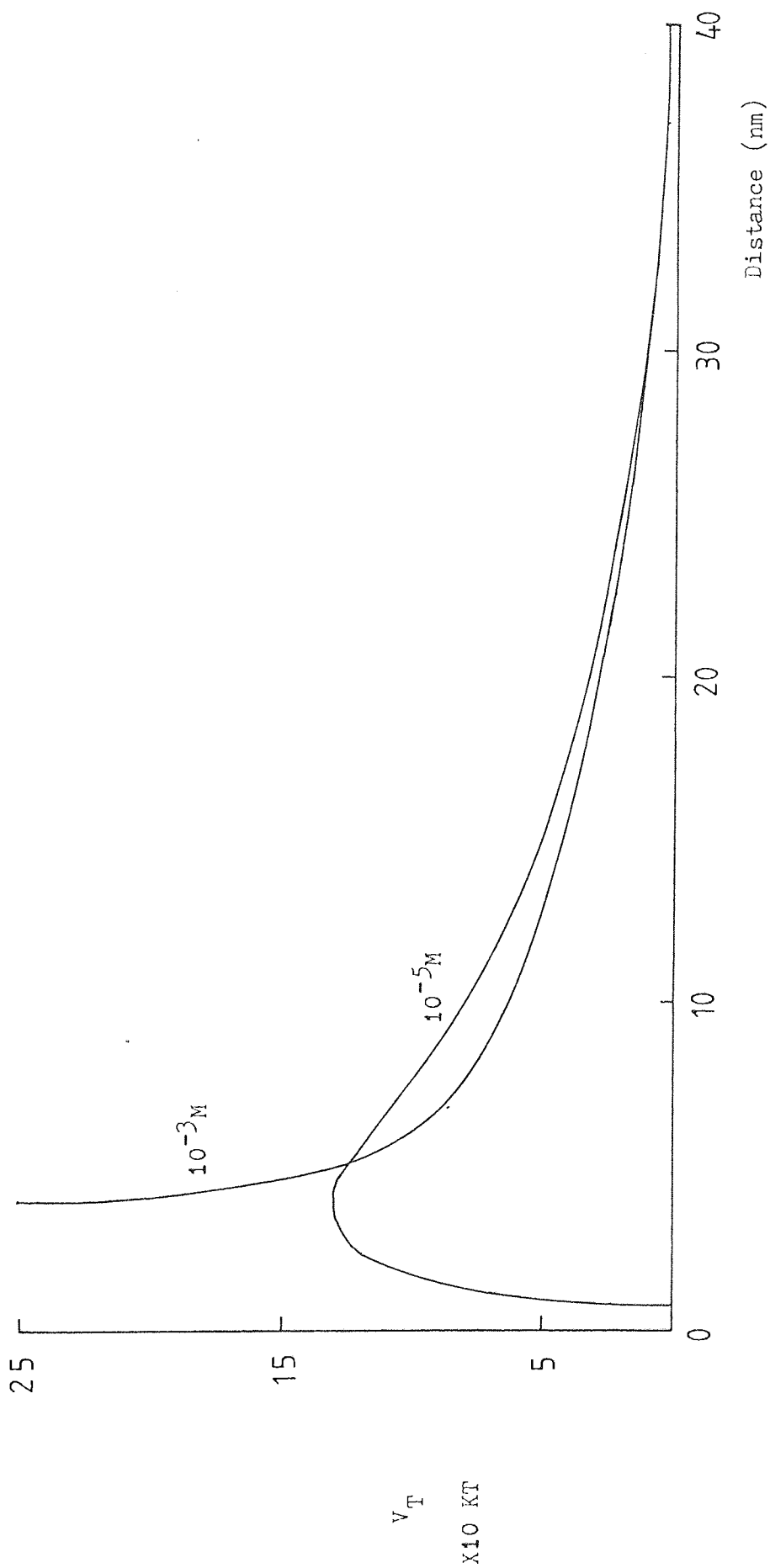


Fig. 73 Total potential energy curves for polystyrene latex in the presence of Texofor A18.

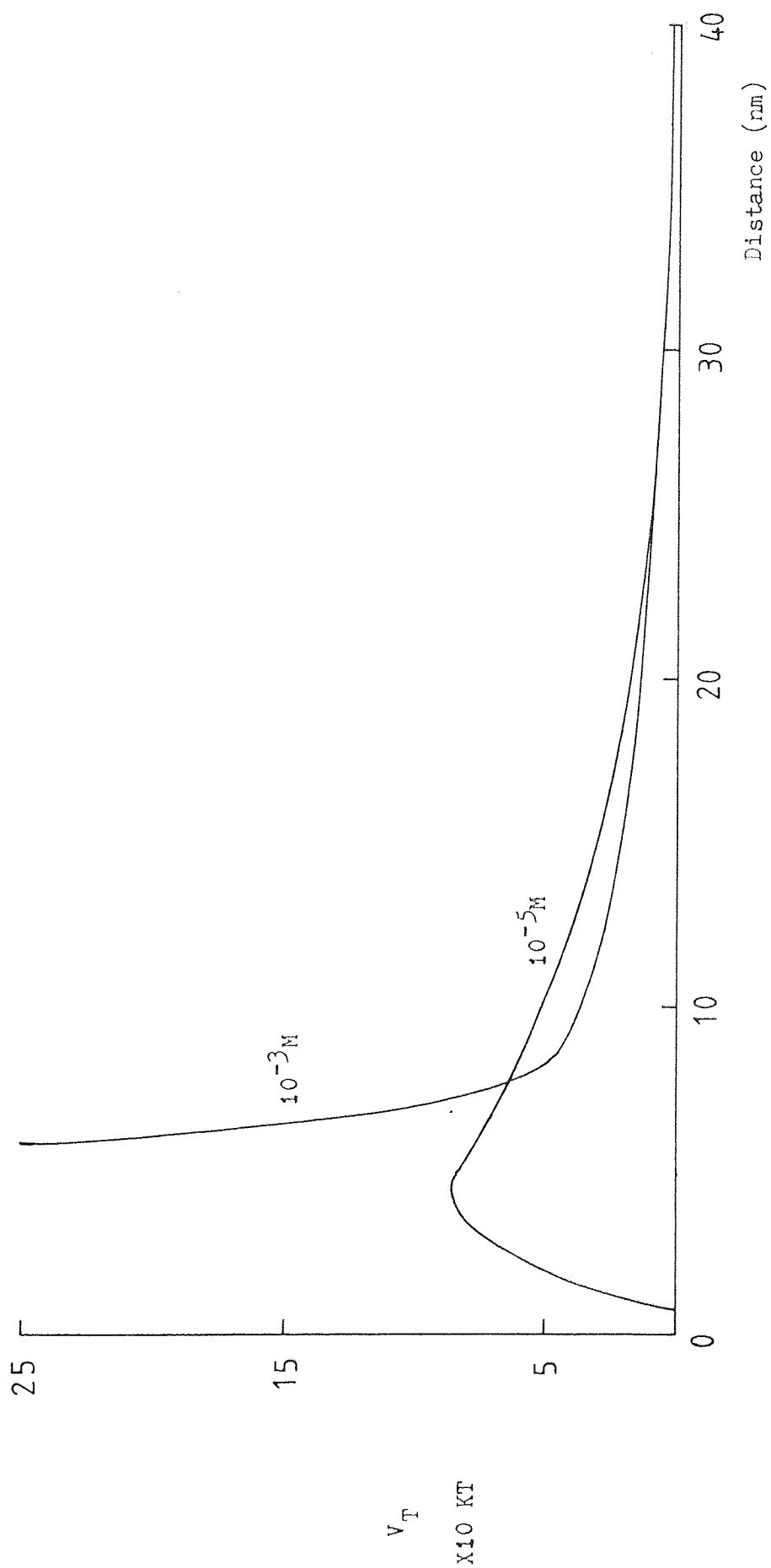


Fig. 74 Total potential energy curves for polystyrene latex in the presence of Texofor A30.

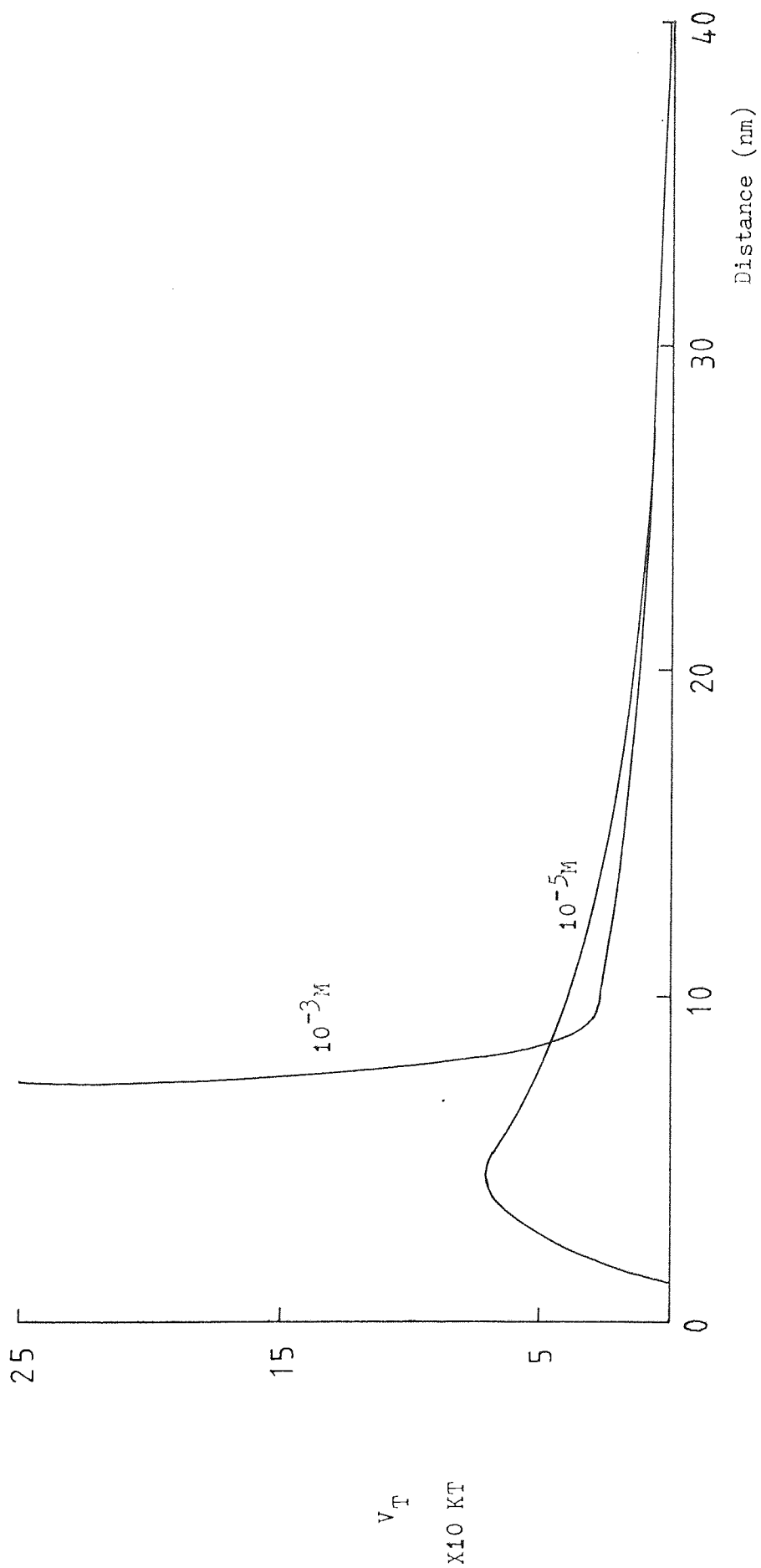


Fig. 75 Total potential energy curves for polystyrene latex in the presence of Texofor A45.

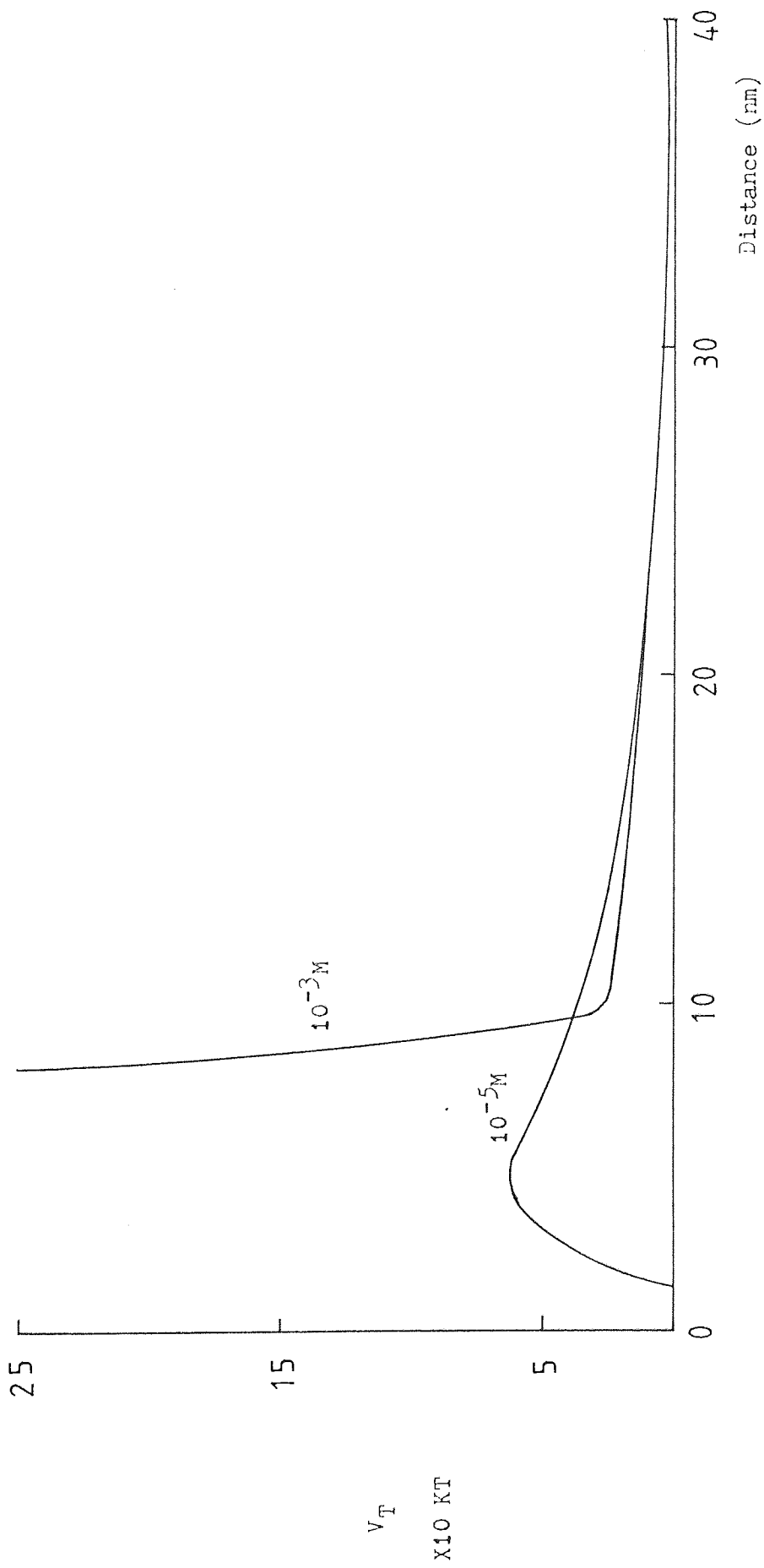


Fig. 76 Total potential energy curves for polystyrene latex in the presence of Texofor A60.

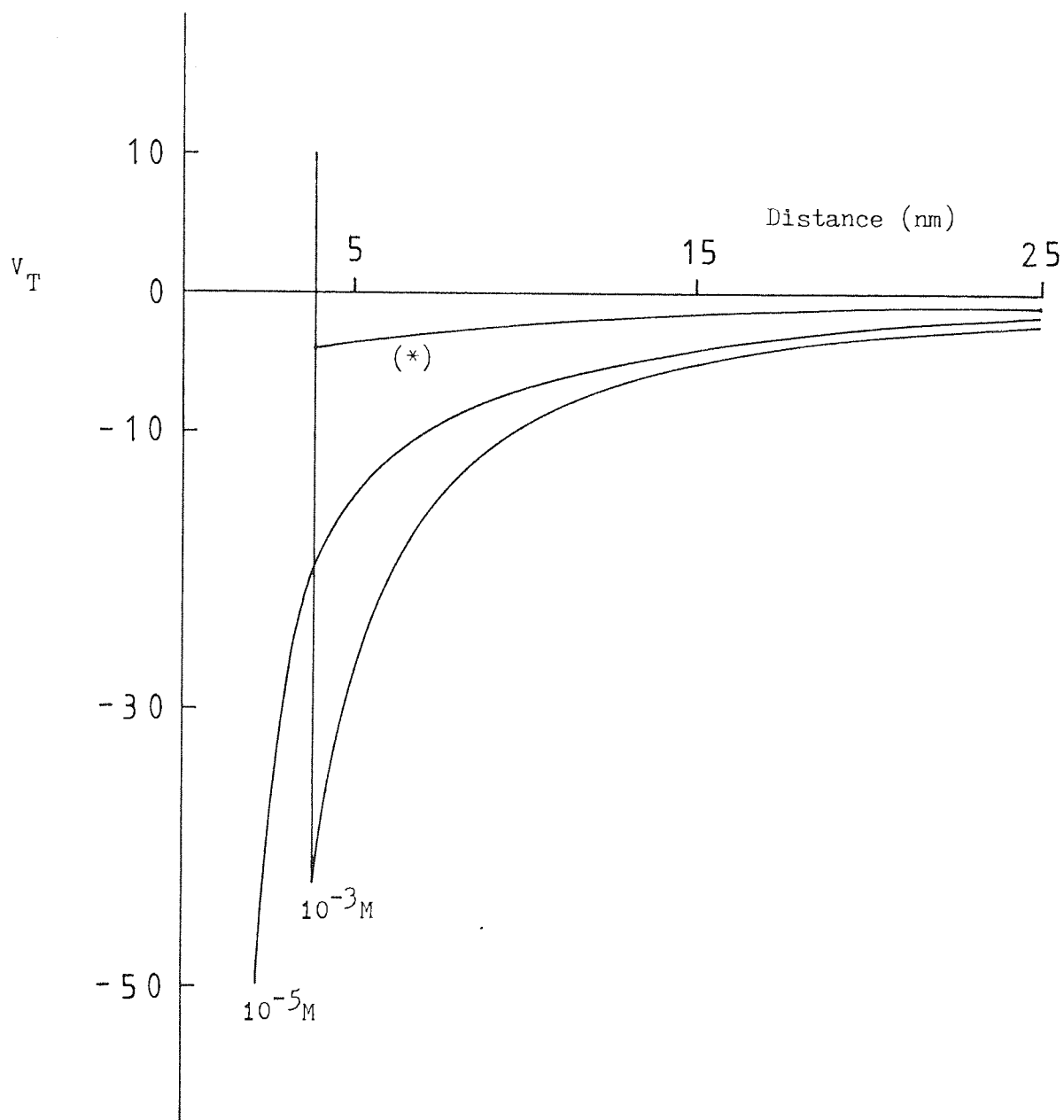


Fig. 77(a) Total potential energy curves for polystyrene latex in the presence of Texofor A10 with electrolyte; (*) for $A_s = 1 \times 10^{-20} J$.

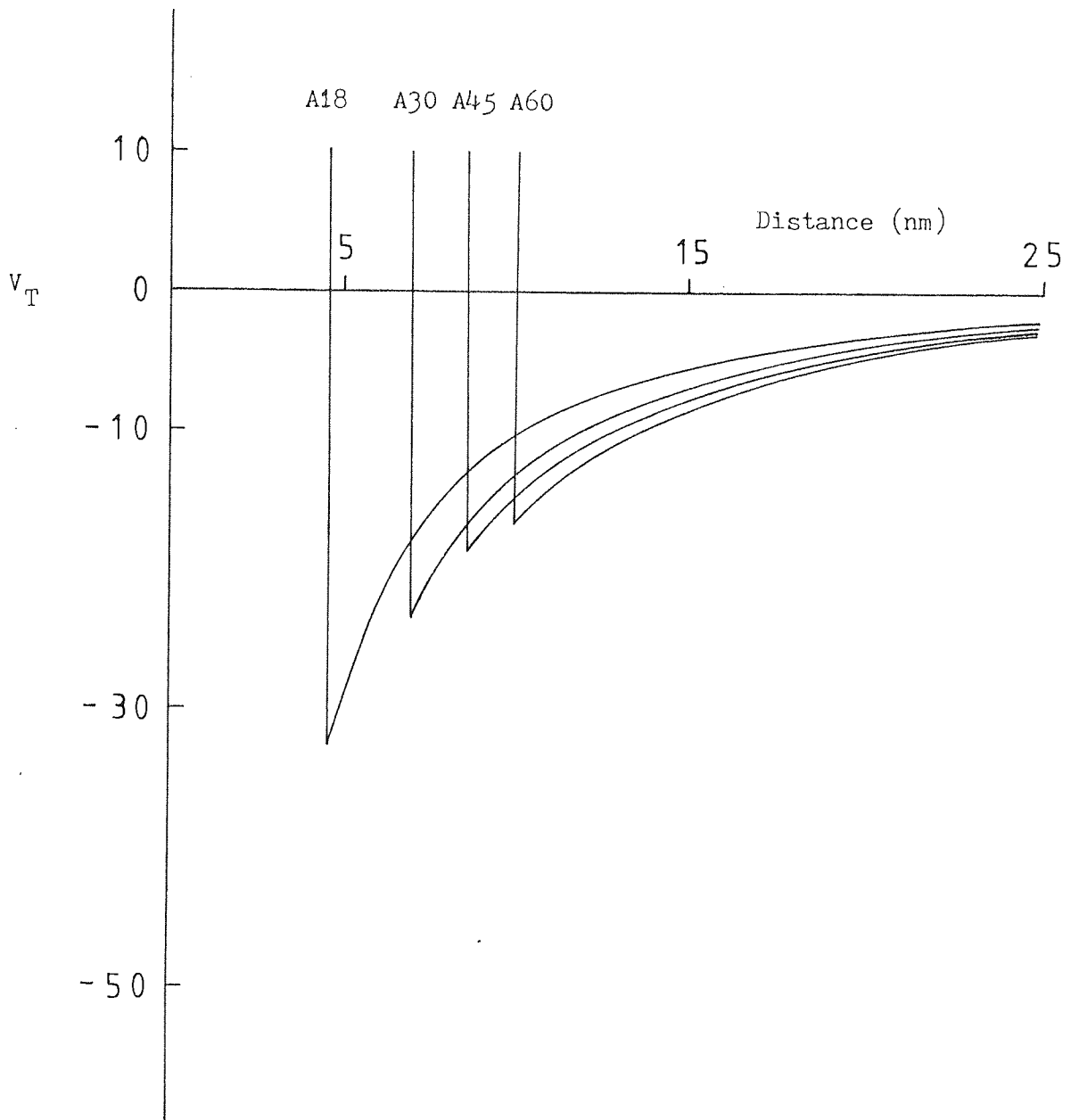


Fig. 77(b) Total potential energy curves for polystyrene latex in the presence of Texofors at concentration of $10^{-3} M$ with electrolyte.

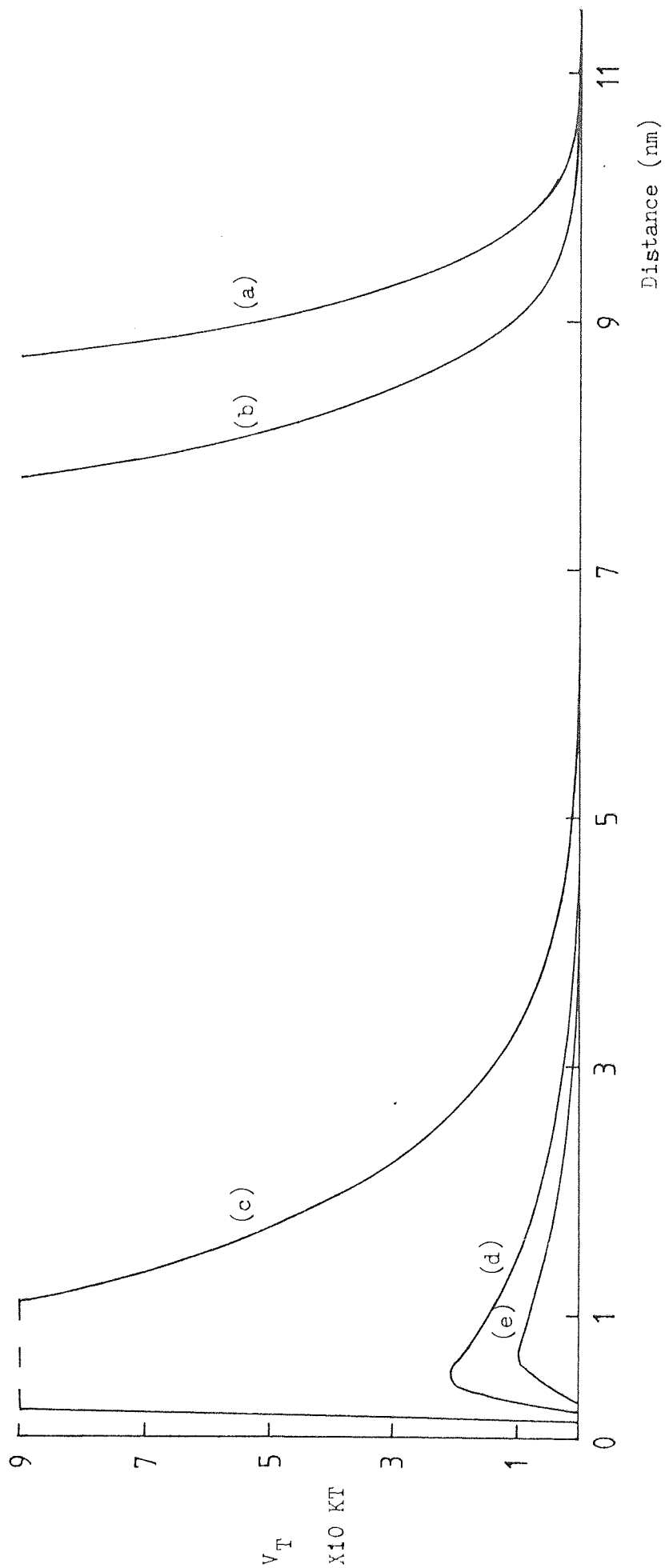


Fig. 78 Total potential energy curves for polystyrene latex in the presence of HEC.

(a) at 0.1 g/dl HEC L (b) at 0.1 g/dl HEC J (c) bare latex (d) at 0.004 g/dl HEC J

(e) at 0.004 g/dl HEC L

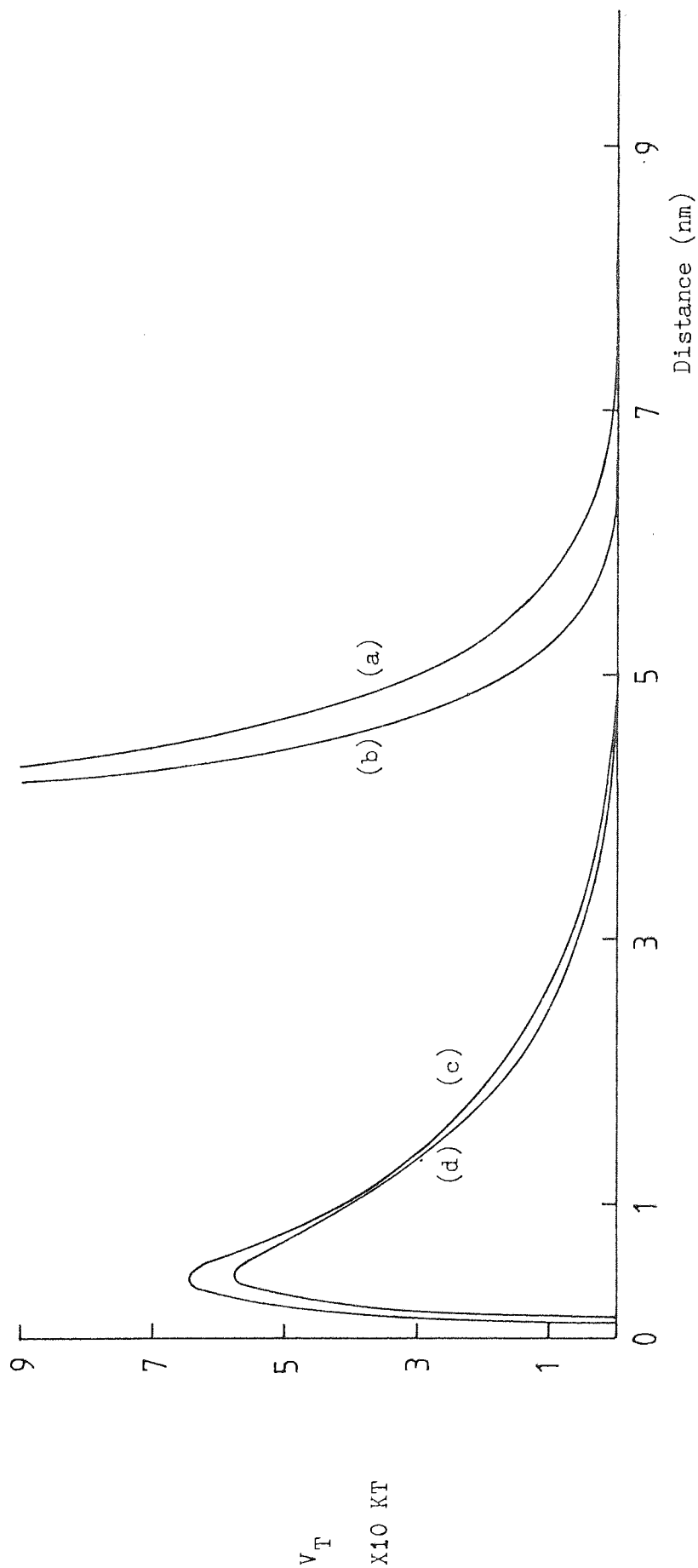


Fig. 79 Total potential energy curves for polystyrene latex in the presence of HPC.

(a) at 0.1 g/dl HPC E (b) at 0.1 g/dl HPC L (c) at 0.004 g/dl HPC L

(d) at 0.004 g/dl HPC E

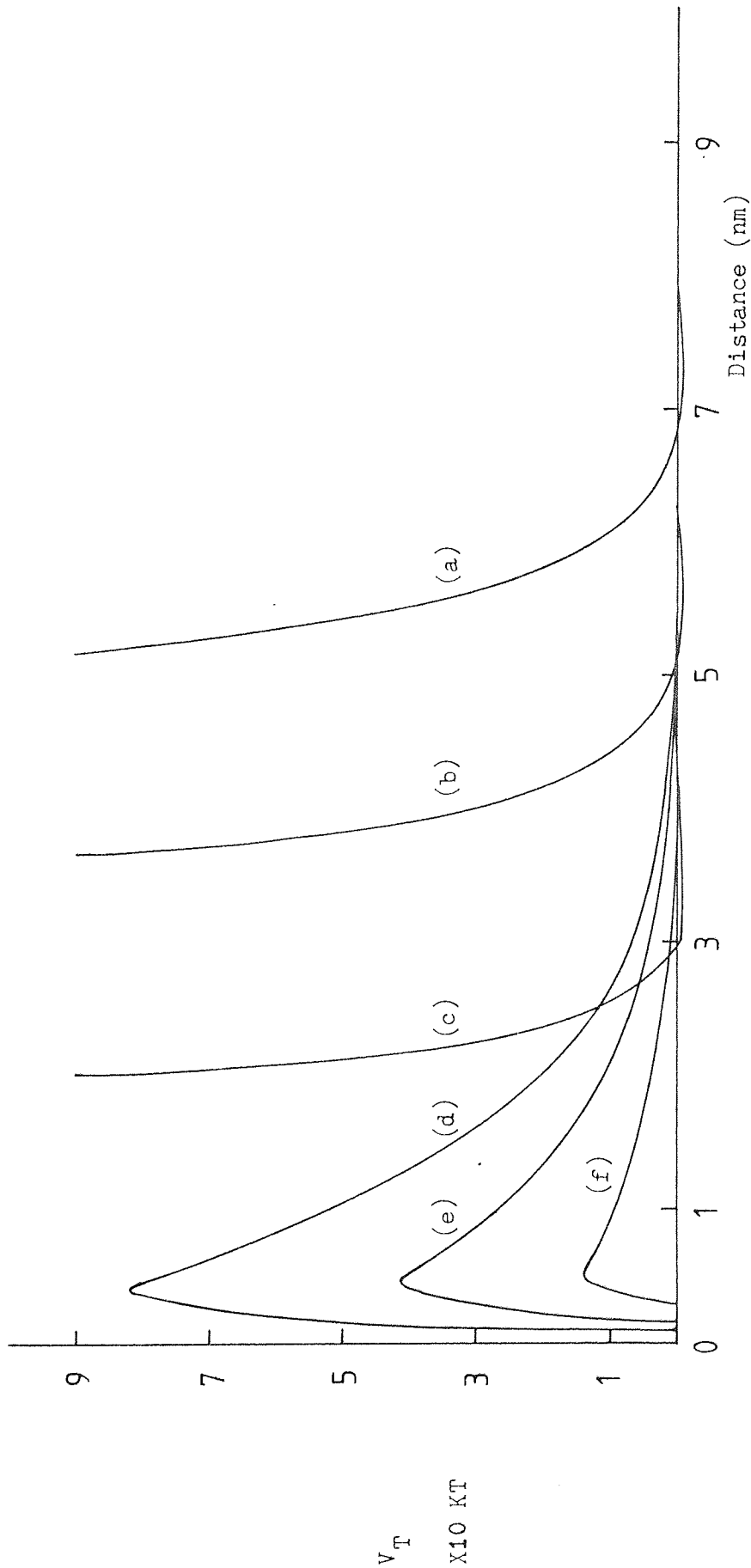


Fig. 80 Total potential energy curves for polystyrene latex in the presence of HPMC.

(a) at 0.08 g/dl HPMC 615 (b) at 0.08 g/dl HPMC 606 (c) at 0.08 g/dl HPMC 603

(d) at 0.004 g/dl HPMC 603 (e) at 0.004 g/dl HPMC 606 (f) at 0.004 g/dl HPMC 615

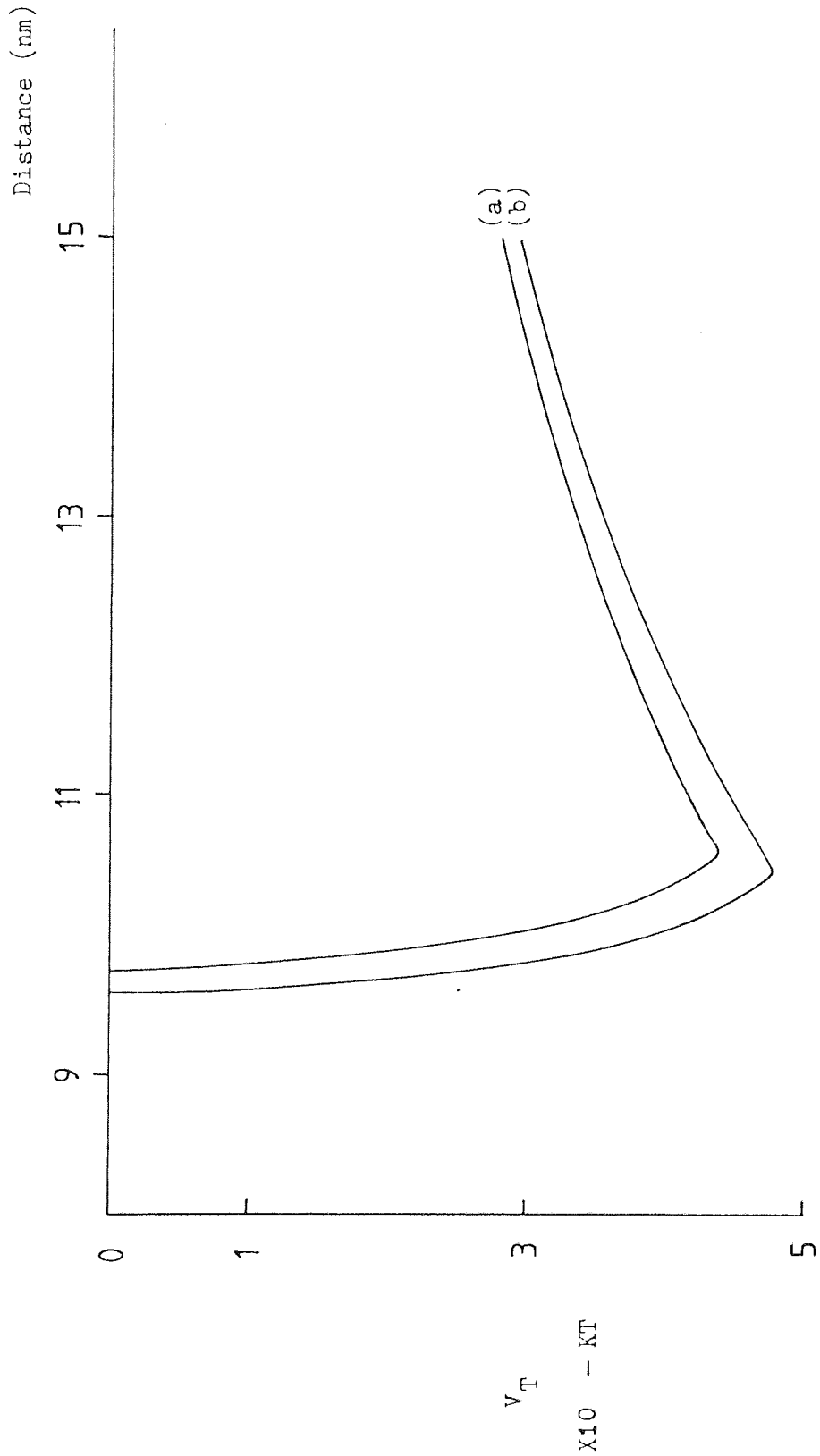


Fig. 81 Total potential energy curves for ibuprofen in the presence of HEC.

(a) at 0.1 g/dl HEC L (b) at 0.1 g/dl HEC J

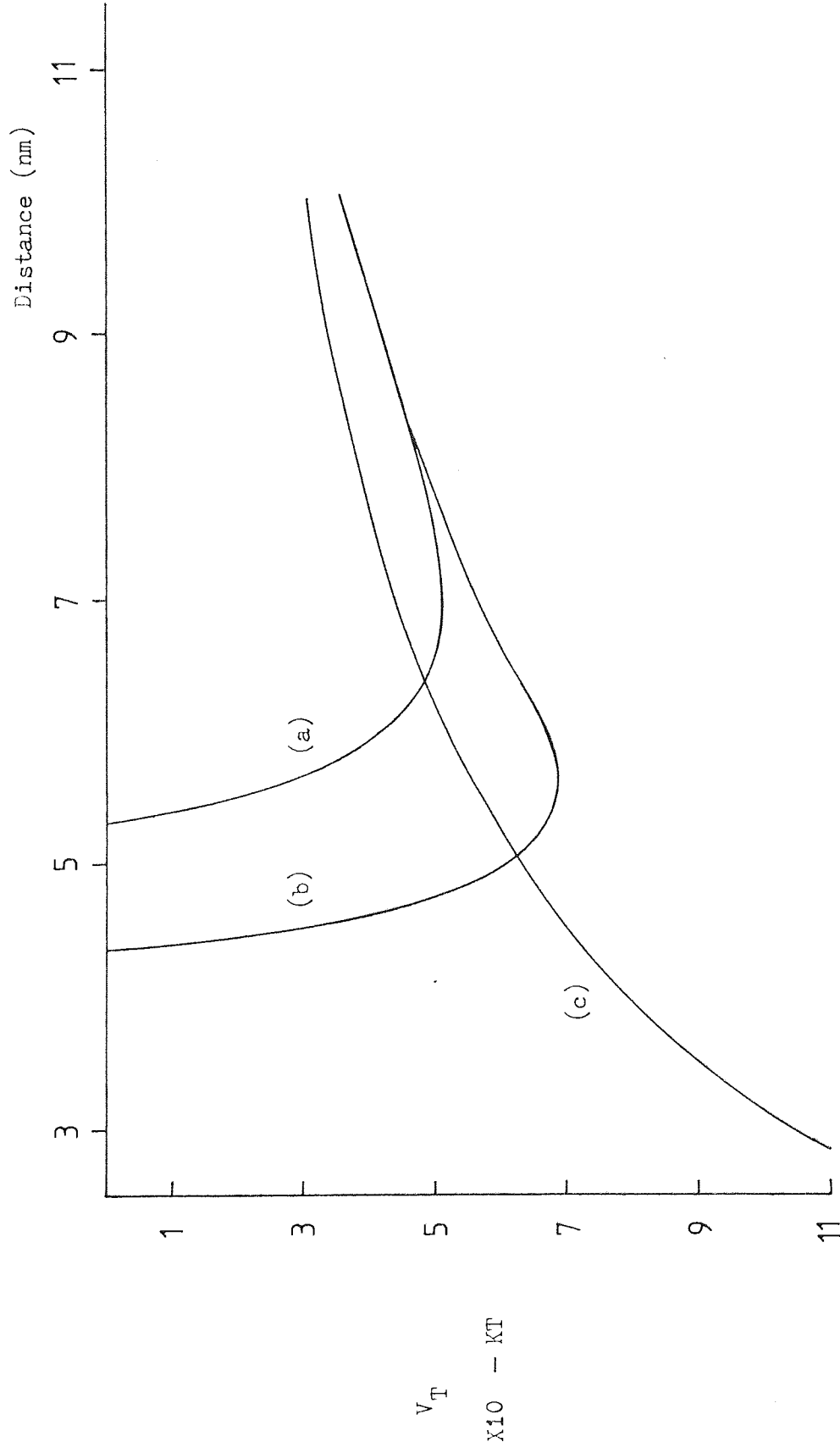


Fig. 82 Total potential energy curves for ibuprofen in the presence of HPC.

(a) at 0.08 g/dl HPC E (b) at 0.08 g/dl HPC L (c) at 0.004 g/dl HPC L

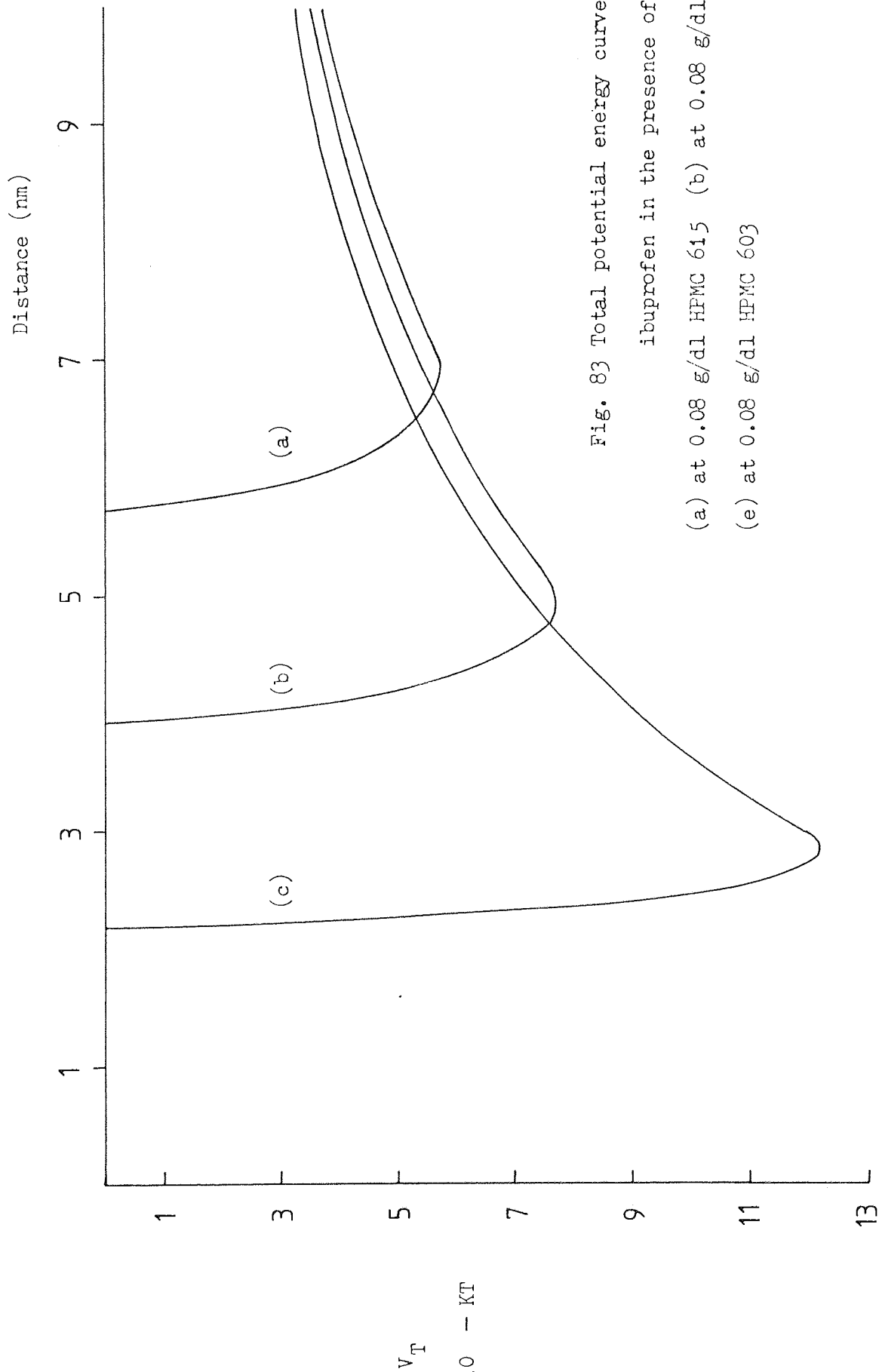


Fig. 83 Total potential energy curves for
ibuprofen in the presence of HPMC.

(a) at 0.08 g/dl HPMC 615 (b) at 0.08 g/dl HPMC 606

(c) at 0.08 g/dl HPMC 603

6:1 Methods6:1:1 Instrument

The equipment used for rheological examination was the Weissenberg Rheogoniometer (Sangamo Controls Ltd, Bognor). The basis of this instrument is the simple cone and plate viscometer, developed from the original ideas of Weissenberg, which was intended to measure not only shear stress in steady rotation but also normal stresses and oscillatory stresses.

A three phase synchronous motor of 1 hp drives a 60 speed gearbox covering nearly six decades of angular velocity in approximately logarithmic steps so that the period of rotation of the platen can be varied from 0.16 to 1.27×10^5 sec/rev. It is necessary to stop the motor to change gear. The output shaft of the gearbox is connected to a drive box containing an electromagnetic brake/drive unit which is provided so that extremely rapid starts and stops can be made during measurement, the motor gearbox unit being left running. The horizontal output shaft of the drive box carries a worm engaging with a worm wheel on the main vertical drive shaft of the instrument. The fluid under test is held between a platen attached to the top of this shaft and a platen attached to the bottom of the air bearing rotor in the torsion head. Normally the upper platen is flat and the lower platen is conical.

The torsion head consists of a torque bar which is available in a wide range of standard rigidity calibrated by the manufacturer.

The top of the torsion bar is clamped firmly at the top of the air bearing casting and the bottom is held on the top of the air bearing rotor which in turn carries the upper platen. The twist of the torsion bar due to the rotation of the bottom platen and the presence of the test substance can be measured with a variable inductance displacement transducer, the armature being attached to a radius arm of 100 mm long clamped to the bottom of the torsion bar. Direct reading can be made from the transducer meter and the range of measurable torques is enormous, ranging from about 2×10^{-8} to 20 Nm. The entire torsion head assembly can be moved vertically along a precision slide, its movement being monitored by a second transducer so that the platens may be separated for cleaning or changing platens and return precisely to the correct spacing. The setting of gap between the cone and plate can also be made by using the above transducer.

The entire instrument is made with high precision and gives accurate measurements. The sensitivity in the simple role of a cone and plate viscometer is such that viscosity of fluids from $10^7 \text{ Nm}^{-2} \text{ s}$ down to that of materials as low as $10^{-7} \text{ Nm}^{-2} \text{ s}$ can be measured. The overall sensitivity range of more than 10^{12} is available. The range of shear rates available is from 7×10^{-4} to $9 \times 10^3 \text{ s}^{-1}$ ($18 \times 10^3 \text{ s}^{-1}$ with the high speed motor). A diagram of the instrument is shown in Fig. 84 (280).

6:1:2 Settling studies

The cellulose polymers used were HEC L, J and HPMC 603, 606, 615. The concentration range studied for HEC was from 0.1 to 3.0 g/dl and for HPMC was from 0.5 to 3.5 g/dl. The mixing procedures were followed as described in Section 5:1:1. The measurements were made at 25⁰C.

For coarse suspensions, particle settling will occur if no appropriate measures are taken to prevent it. With regard to sedimentation, the particles settling in diluted suspensions of noninteracting spheres can be described by the well known Stokes' law

$$v = \frac{2r^2(d - d_0)g}{9\eta} \quad (121)$$

where v is the velocity of the sedimentation of the particle, r is the particle radius, d is the density of the particle, d_0 is the density of the medium, g is the acceleration due to gravity and η is the viscosity of the medium. Therefore, as the equation indicates, it can predict the sedimentation velocity of the particles from the density difference between the particle and medium, particle diameter and the viscosity of the medium.

For concentrated suspensions, the settling process becomes more complex. As the concentration of the particle increases, interaction between the particles will take place and hindering between the particles will occur during settling. Moreover, due to the concentrated solid phase the density and the viscosity of the whole suspension is more important than that of the medium of the suspension (276). Also, for pharmaceutical suspensions, heterodispersed and irregularly shaped particles are involved. All these factors make the situation more difficult to handle.

Higuchi (277) has considered the settling problem for concentrated suspensions. He obtained an equation by assuming that the settling of particles in a concentrated suspension as analogous to a liquid moving through a porous bed by using the Kozeny equation, that is,

$$v = \frac{r^2 (d - d_o) g}{9\eta K} \cdot \frac{\epsilon^3}{1 - \epsilon} \quad (122)$$

where K is the Kozeny constant and ϵ is the porosity of the bed. Stienour (278) and Richardson and Zaki (279) have shown the dependence particle concentration on the velocity of settling in concentrated suspensions by a modified Stokes' equation. In all the above treatments, the interactions between particles which do occur in concentrated suspensions was not taken into account.

In the preparation of pharmaceutical suspensions, Stokes' law is mostly used by the formulators as a 'trial and error' procedure to control particle settling. These methods are summarized as follows: (a) As equation (121) indicates, the effect of particle size on the settling velocity is in a squared term. Reducing the particle size will probably increase the stability of the suspension. However, the reduction of the particle size for example by milling only breaks down the large particles into certain limited small units. This can only improve the settling conditions of the suspension. (b) By increasing the density of the medium, as given by Stokes' law, if $d = d_o$, the particle settling velocity is zero and may lead to a stable suspension. However, care should be taken to prevent creaming of the particles which would give an inelegant appearance to the suspension. The substances used in pharmacy to increase the density of the medium usually are syrup and glycerol. (c) By increasing the viscosity of the medium, the velocity of the particle settling can be reduced. Therefore, suspending agents or thickener are used. Suspending agents are substances such as natural gums, celluloses, clays and surface active agents (2,281) which can effectively increase the viscosity of the

vehicle. Cellulose polymers among others are the most common use suspending agents (59,281,282,283). Cellulose polymers have a wide molecular weight range and only small quantities of the higher molecular weight fractions can provide good suspending effect.

6:1:3 Rheometric studies of particle aggregation

As the above observations (Table 20) given, ibuprofen particles in the presence of the HEC polymers showed aggregation behaviour throughout a rather wide concentration range. The aggregation mechanisms due to the presence of polymers are probably bridging between particles when the polymer concentration is low and attraction between the adsorbed polymer layers when the polymer concentration is high. It is interesting to look at these interactions of the aggregated particles and the energy contributions from the polymer needed to form flocculation, since there is little published work dealing with the determination of the flocculation energy for the polymer in the flocculated suspensions. An attempt is made here to obtain the flocculation energy by using a rheometric method.

Higuchi and Stehle (284) have studied particle-particle binding energies in suspensions and interpreted the rheological data obtained in terms of the magnitude of the interaction between the particles. Their method used was according to Gillespie (285) who deduced a relationship for the pseudoplastic behaviour of concentrated suspensions and applied it to a number of different situations such that particle binding energy can be determined from these situations. The treatment is as follows: A concentrated suspension of monodispersed spherical particles with pseudoplastic flow behaviour, at high shear rates,

can be described by the following equation of summation of the

$$S = \eta G + C \quad (123)$$

where S and G are the shear stress and shear rate respectively, η is the Newtonian viscosity and C is the ultimate dynamic yield value. According to the model,

$$C = \frac{E_a KN^2}{2} \quad (124)$$

where E_a is the particle-particle interaction energy i.e. the energy required to separated a doublet, N is the number concentration of the suspension and K is the shear induced rate constant for collision.

The K value can be obtained from (286)

$$K = \frac{32 a^3}{2} \quad (125)$$

where a is the particle radius. In the situations studied here E_a in Eq. (124) can be regarded as the total separation energy between particles. Thus,

$$E_a = V_A + V_F - V_R - V_S \quad (126)$$

where V_A is the energy of attraction between polymer coated particles, V_F is the energy of attraction of the polymers, V_R is the electrostatic repulsive energy and V_S is the steric energy (if the steric effect is present). Therefore, for a system, if the values of V_A , V_R and V_S are known, the V_F value can be evaluated from the rheological yield value which is by extrapolation of the linear portions of the shear stress - shear rate plot to zero shear rate.

The above equations for calculating the separation energy are based on crude approximations and also when they are applied to drug suspension systems deviations may be large. However, this may

give a qualitative prediction of the energy of attraction of the polymers and the effect on particle aggregation.

6:2 Results and discussion

6:2:1 The effect of viscosity on the settling of particles and the sediment conditions after settling

The settling curves are shown in Figs 85, 86 and 87 for HPMC 603, 606 and 615 systems respectively. The curves show that the higher the viscosity of the medium the slower the particle settling velocity which is as predicted by Stokes' law. Therefore, for practical use of HPMC as suspending agent, the higher viscosity grade fractions will give a good effect in preventing particle settling.

In the settling of the ibuprofen particles in the HEC solutions studied, it was difficult to justify the measurements due to most of the aggregated particles floating on the upper part of the suspensions. However, from the sedimentation volumes, it showed a voluminous structure of aggregates in the polymer concentration range of from 0.1 to 1.5 g/dl; whereas, from 2 to 3 g/dl concentration, in the majority cases, the particles were suspended in small structured flocs and a small portion of the particles settled down forming a hard caked sediment.

The redispersibility of the HPMC-ibuprofen suspensions after 36,000 revolutions of redispersion the sediments were resuspended little. The sediments were heavily caked. The appearance of the supernatants after redispersion showed that a greater degree of turbidity was found at low concentrations than at high concentrations. This may be explained

as follows: as polymer concentration increases, more polymer is adsorbed onto the surface of the particles; when the particles are settled, the adsorbed polymers form a large structure of molecular network in which the interwoven chains in the network hold the particles strongly. This is somewhat like the approach of gel formation of the cellulose polymers in the sediment. This supports the mechanism of network formation in the sediment given in Section 5:2.

6:2:2 Particle-particle interactions of aggregated suspension in the presence of Hydroxyethyl Cellulose polymers

The plots of shear stress against shear rate for HEC L and HEC J ibuprofen suspensions are shown in Figs 88 and 89 respectively. The yield values of the suspensions together with the yield values of the suspension medium at different concentrations are given in Table 27. With all the yield values, the reproducibility was about 7% except that at concentration of 3 g/dl of HEC J the reproducibility was 9%. For the medium at low concentrations the curves are Newtonian within experimental error. The estimations of the V_F were made at concentration of 0.1 g/dl where, from the adsorption isotherms, plateau adsorption was found and at particles separation where the deepest energy minimum occurred. For HEC L system at a distance of separation of 106 nm between two particles the V_A , V_R and V_S values are 44.1 KT, 0.0008 KT and 0.38 KT respectively. The E_a value is 7,000 KT calculated by using Eq. (124). Therefore, by using Eq. (126), the V_F value can be found out. In this case, because the values of V_A , V_R and V_S are so small, when compared with the value of E_a , they can be neglected and the V_F value can be taken as 7,000 KT. For HEC J system at the separation of 104.5 nm between two particles, $V_A = 47.5$ KT,

Yield Value 10^{-1} Nm^{-2}

Initial Concentration g/dl	Yield Value 10^{-1} Nm^{-2}	
	HEC L	HEC J
	Ibuprofen Suspension	
0.1	2.0	15
0.5	4.0	30
1.0	6.0	45
1.5	8.5	75
2.0	15	90
2.5	20	195
3.0	35	295
	Suspension Medium	
0.1	-	-
0.5	-	-
1.0	-	5
1.5	2	20
2.0	4	40
2.5	8	75
3.0	15	125

Table 27 Yield values of the suspensions and suspension medium of HEC-ibuprofen systems.

$V_R = 0.0011 \text{ KT}$, $V_S = 0.39 \text{ KT}$ and $E_a = 5.25 \times 10^4 \text{ KT}$ therefore V_F is about $5.25 \times 10^4 \text{ KT}$.

Higuchi and Stehle (284) found that for system of silica particles in the presence of surface active agents, the stronger binding energies resulted in larger sedimentation volumes. The values of the sedimentation volumes found here are rather uncertain as shown in Table 20. This may be because of the voluminous and fluffy structure leaving an unclear boundary between the supernatant and the aggregates and may also be due to the wall effect. Therefore, it is difficult to compare the results of V_F with the sedimentation volume values. However, a voluminous sediment was found in both HEC L and HEC J systems.

If one relates the V_F values to the molecular weight or molecular chain length, one will find that the larger the molecular weight or the longer the molecular chain length the higher the V_F value i.e. the stronger the aggregation effect. It seems that this is contradictory to the adsorbed layer thickness values of HEC on ibuprofen. As given in Table 15, it shows that the value of the adsorbed layer thickness of HEC L is greater than that of HEC J. Thus, it should give a higher V_F value for the HEC L system. Again, looking at the adsorbed layer thicknesses used here for the particle interaction energies, these were taken from those values obtained by viscometric measurements on polystyrene latex. The conformations of the polymers on the ibuprofen particle were determined by an electrophoretic method. The assumption was made that the adsorbed layer thicknesses obtained by the electrophoretic method on both polystyrene latex and ibuprofen are comparable (Section 4:2:3:2). For these electrophoretic measurements readings were taken only on the suspended individual particles and not

on the particle aggregates which were difficult to determine. This is due to such as the fast settling of the large aggregates and the fluid trapped in the aggregates which will hinder the electrophoretic migration of the aggregated particles. Therefore, the electrophoretic results of the individual particles can not represent those of the aggregates. The conformations of the polymers in the aggregate are still uncertain. It is possible that the adsorbed polymers could exhibit a draining effect which would affect the adsorbed layer thickness on the surface. Hence, due to the above problems, it is difficult to relate the V_F results to the adsorbed layer thickness results of the polymers.

The dependence of the yield value on the polymer concentration as given in Table 27 shows that as the concentration of HEC increases the yield value of the system increases i.e. the particles bind more effectively. At high concentrations, due to the increase of viscosity of the suspension medium it is difficult to decide whether the yield value due to the particles interaction will increase or not. In this case, under the shear field not only the aggregated particles but also the viscous medium will participate in the energy dissipation process. The continuous network structure of the suspension at high concentration will be more rigid (287,288). This gives a finite yield which must be exceeded before any flow behaviour occurs; thus, a term due to the network energy should be considered. These factors make the system more complicated than by simply using Eq. (124) to evaluate the binding energies. However, it is obvious that at concentrations of 0.1, 0.5 and 1.0 g/dl for HEC L and 0.1 and 0.5 g/dl for HEC J where Newtonian flow of the medium occurred, the binding energies between particles increase with increasing polymer concentration. Also, a loose structure of aggregates was observed at these concentrations.

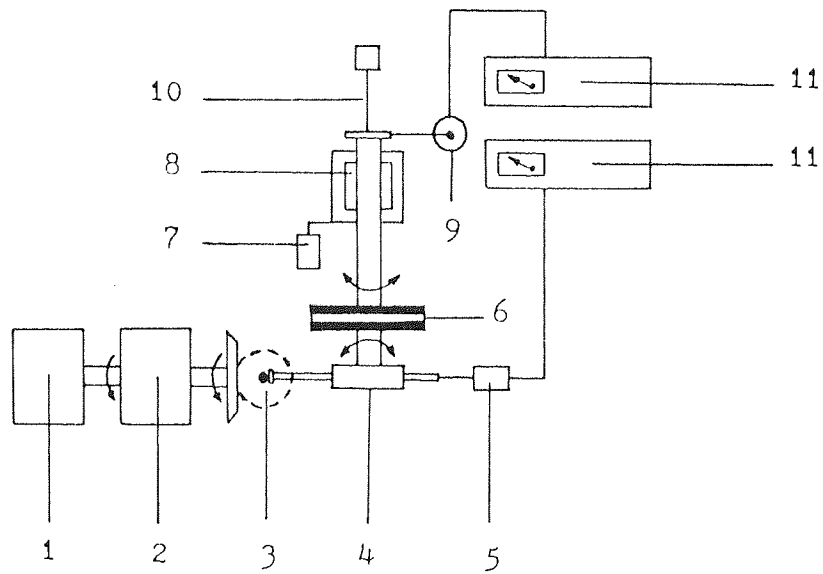


Fig. 84 Diagram of the Weissenberg Rheogoniometer (280).

- 1, motor; 2, gear box; 3, variable sine wave generator;
- 4, worm screw; 5, input oscillation transducer;
- 6, platens containing sample; 7, gap setting transducer;
- 8, air bearing; 9, output oscillation transducer;
- 10, torsion bar; 11, transducer meter.

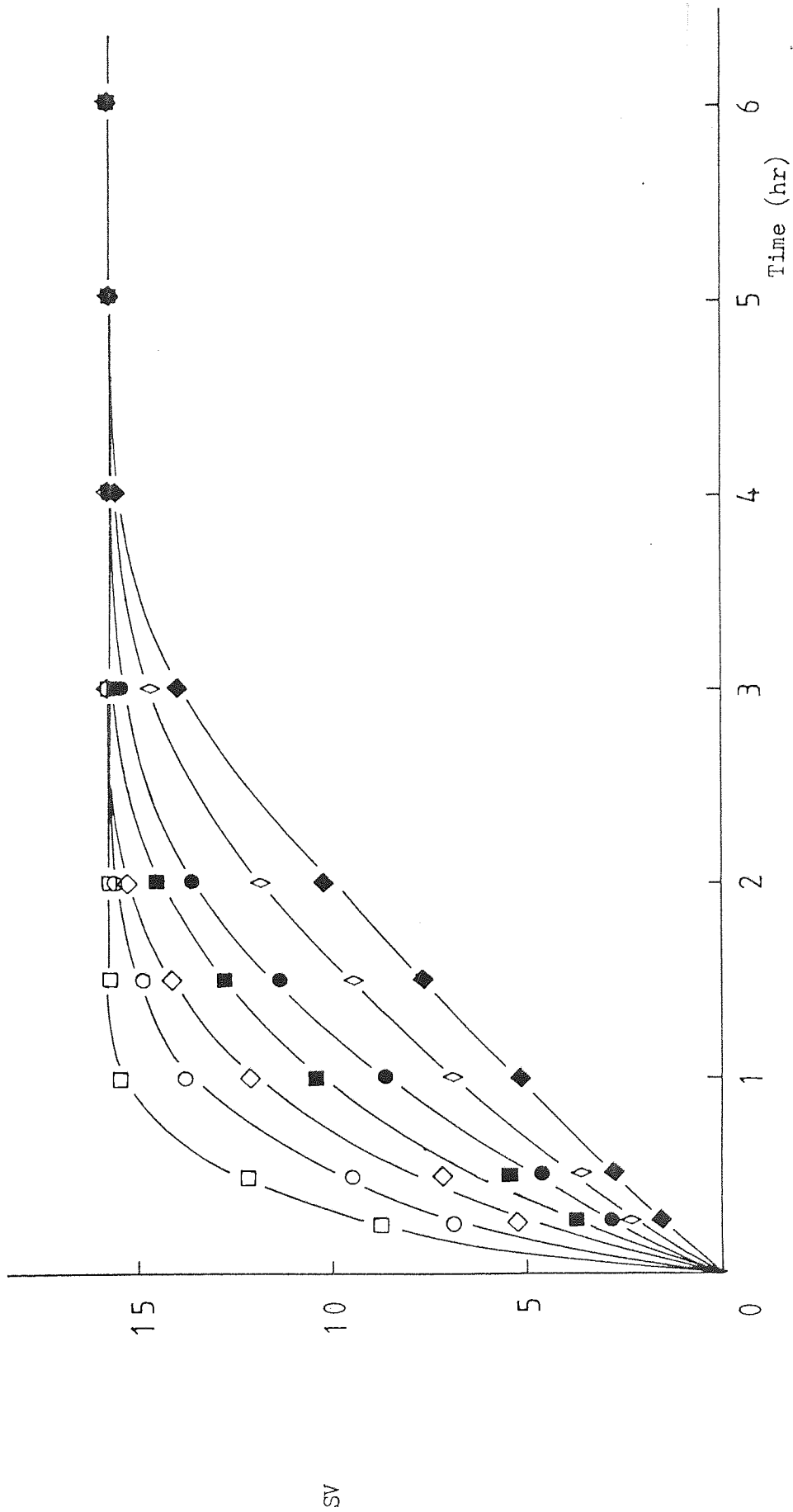


Fig. 85 Settling curves for ibuprofen in the presence of HPMC 603.

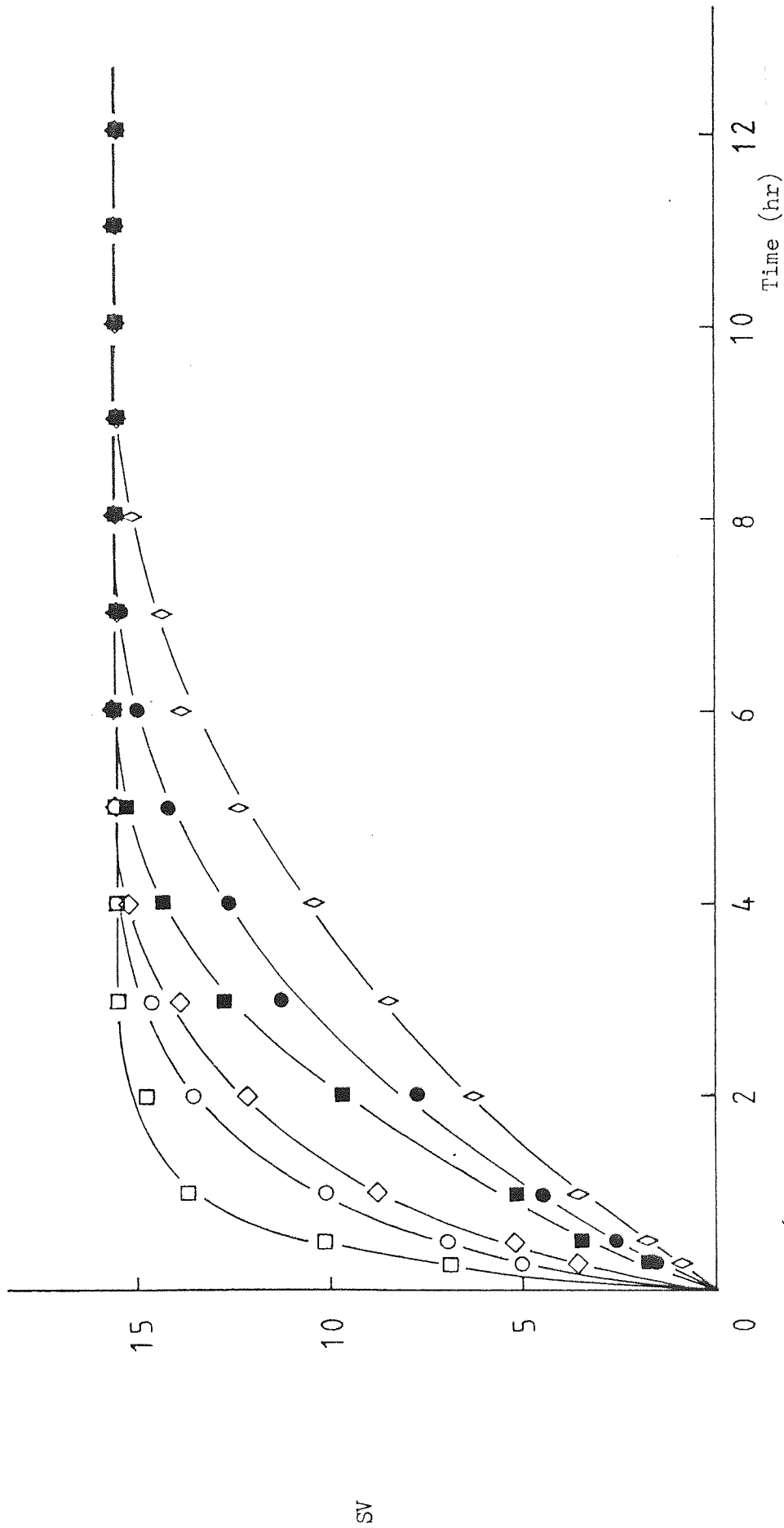


Fig. 86 Settling curves for ibuprofen in the presence of HPMC 606.

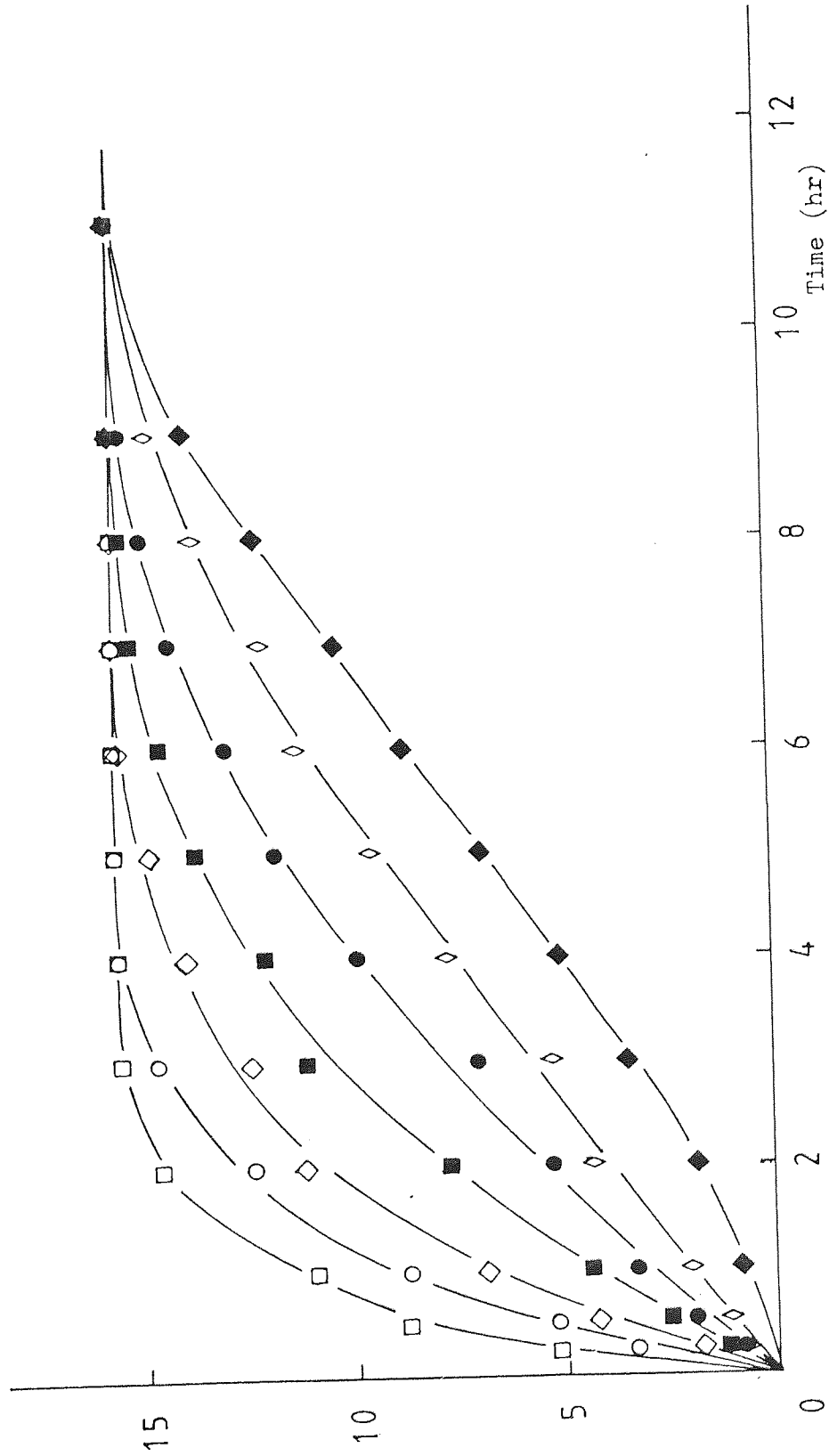


Fig. 87 Settling curves for ibuprofen in the presence of HPMC 615.

Concentration (g/dl): 0.5 1.0 1.5 2.0 2.5 3.0 3.5
 Viscosity ($10^{-3} \text{Nm}^{-2}\text{s}$): 2.5 3.7 7.0 12.5 19.5 32.0 51.1

SV

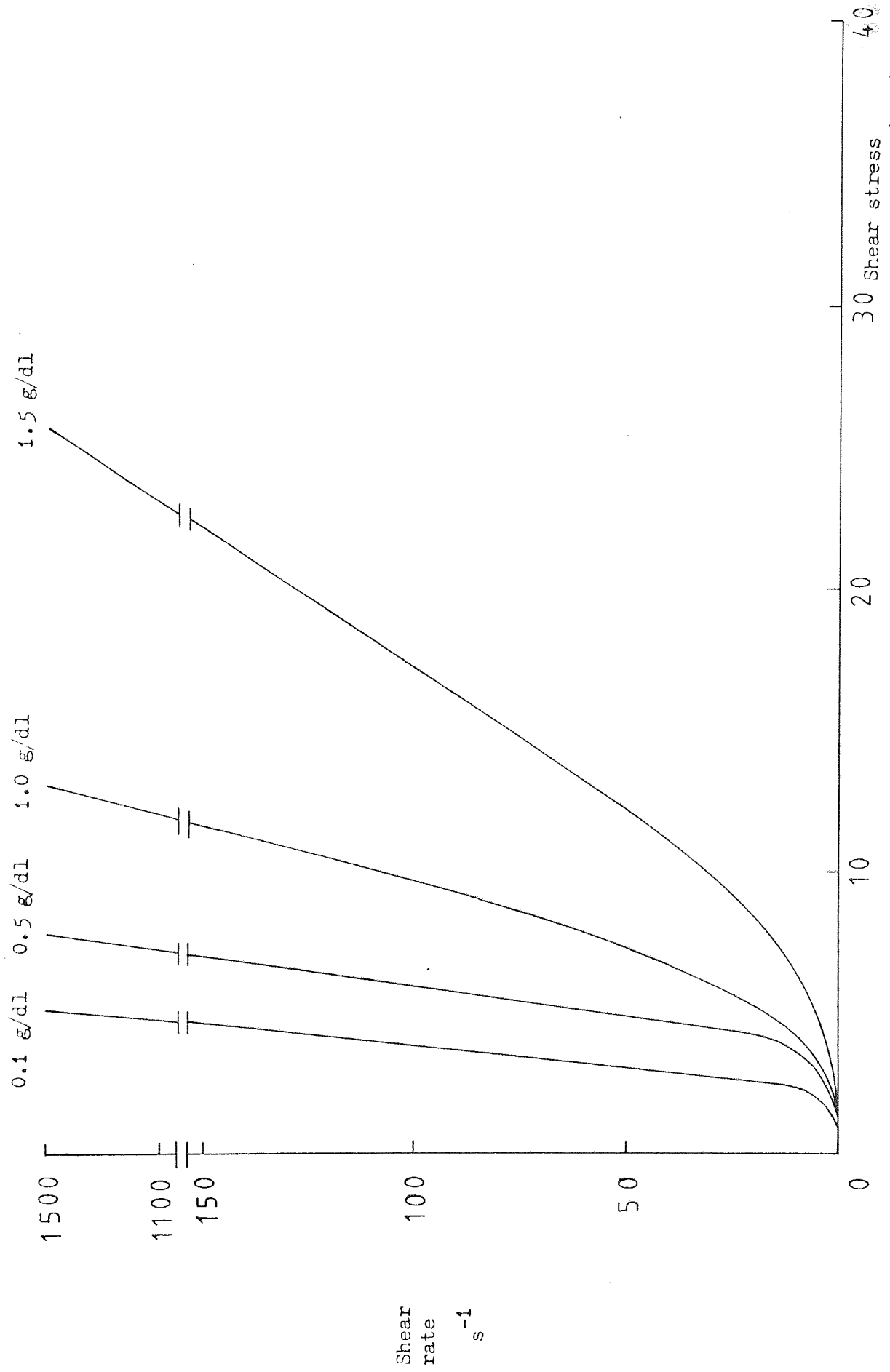


Fig. 88(a) Shear stress - shear rate curves for ibuprofen - HEC I suspensions. (10⁻¹ Nm⁻²)

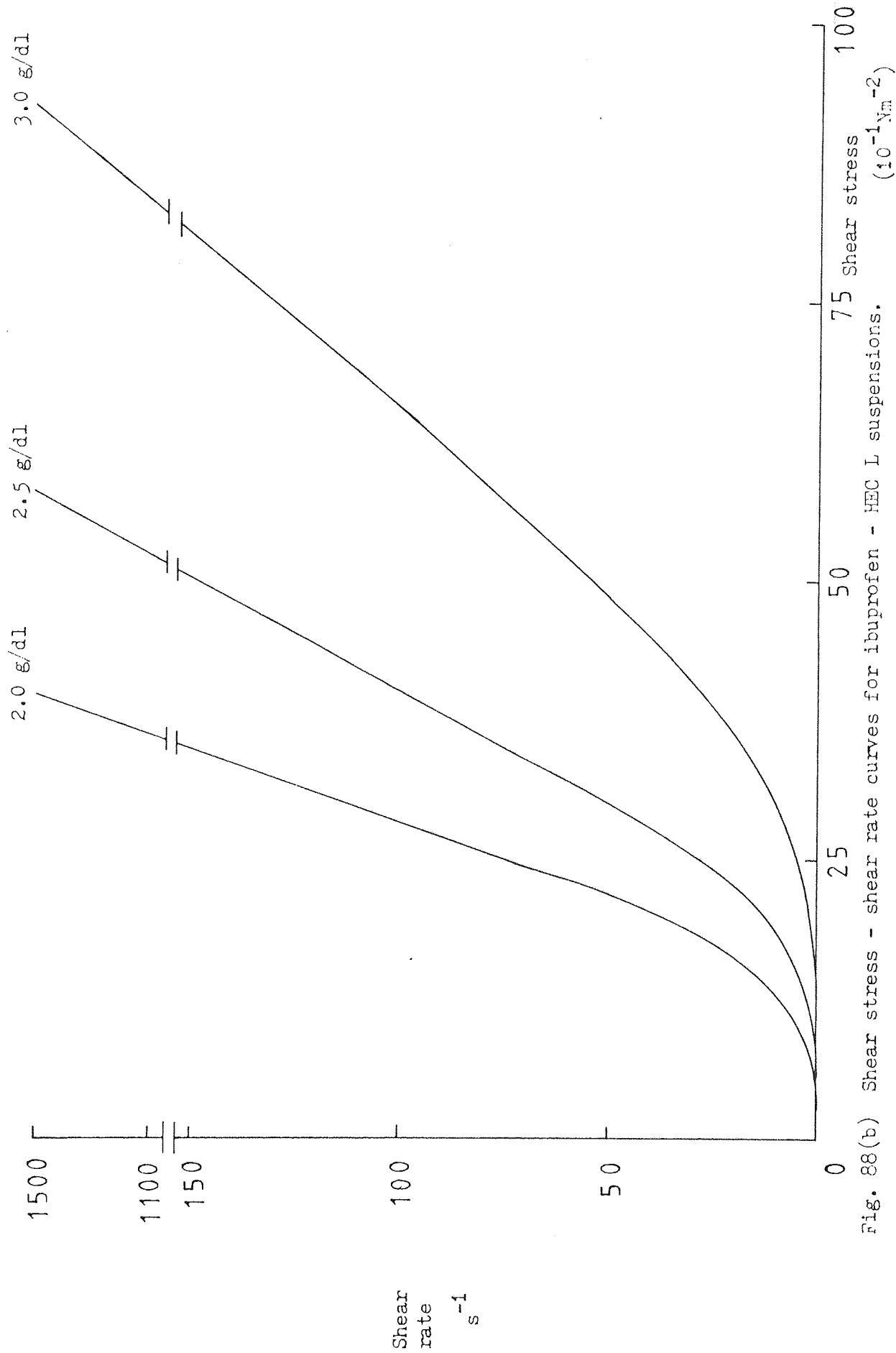


Fig. 88(b) Shear stress - shear rate curves for ibuprofen - HEC L suspensions.

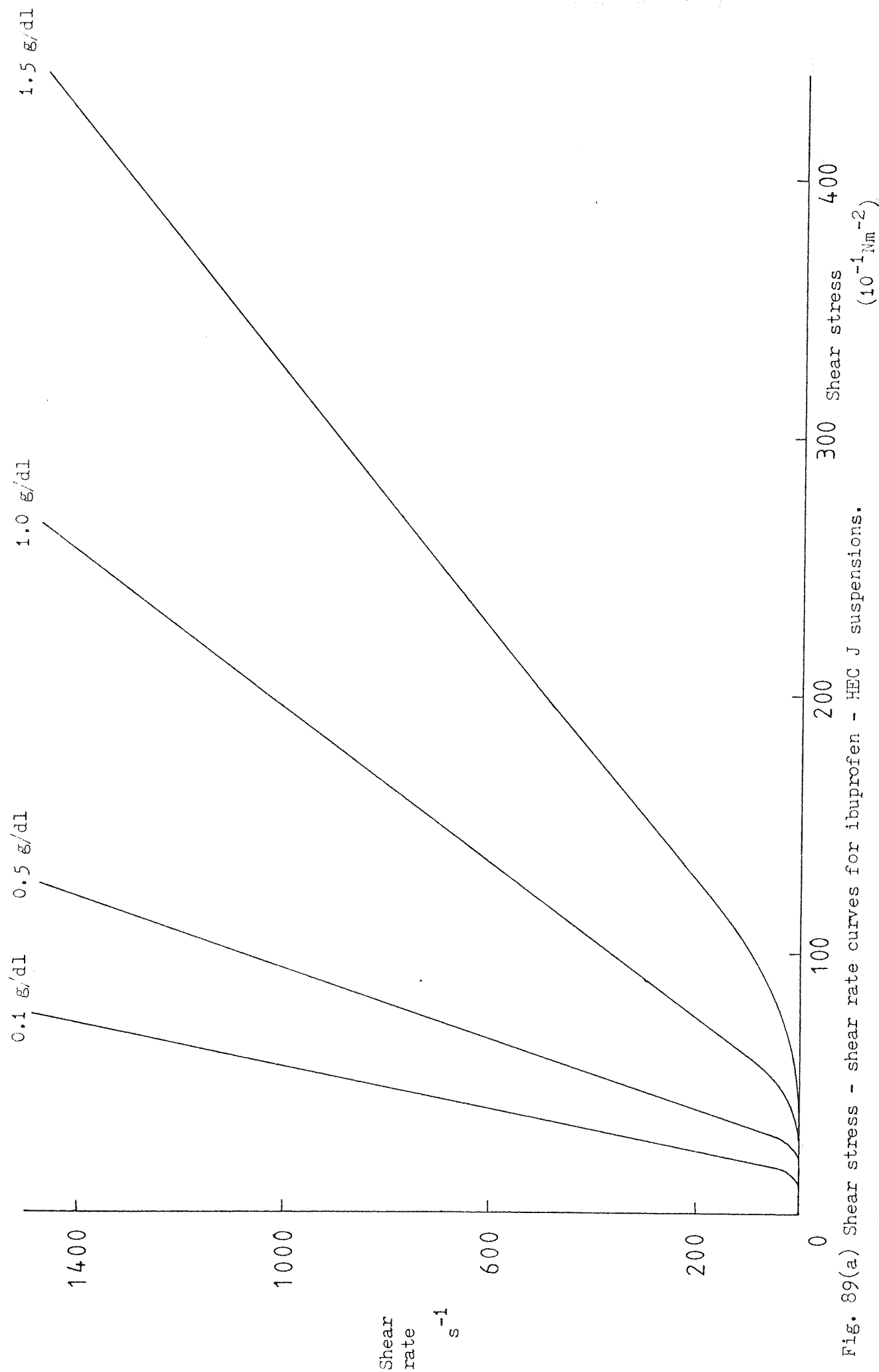


Fig. 89(a) Shear stress - shear rate curves for ibuprofen - HEC J suspensions.

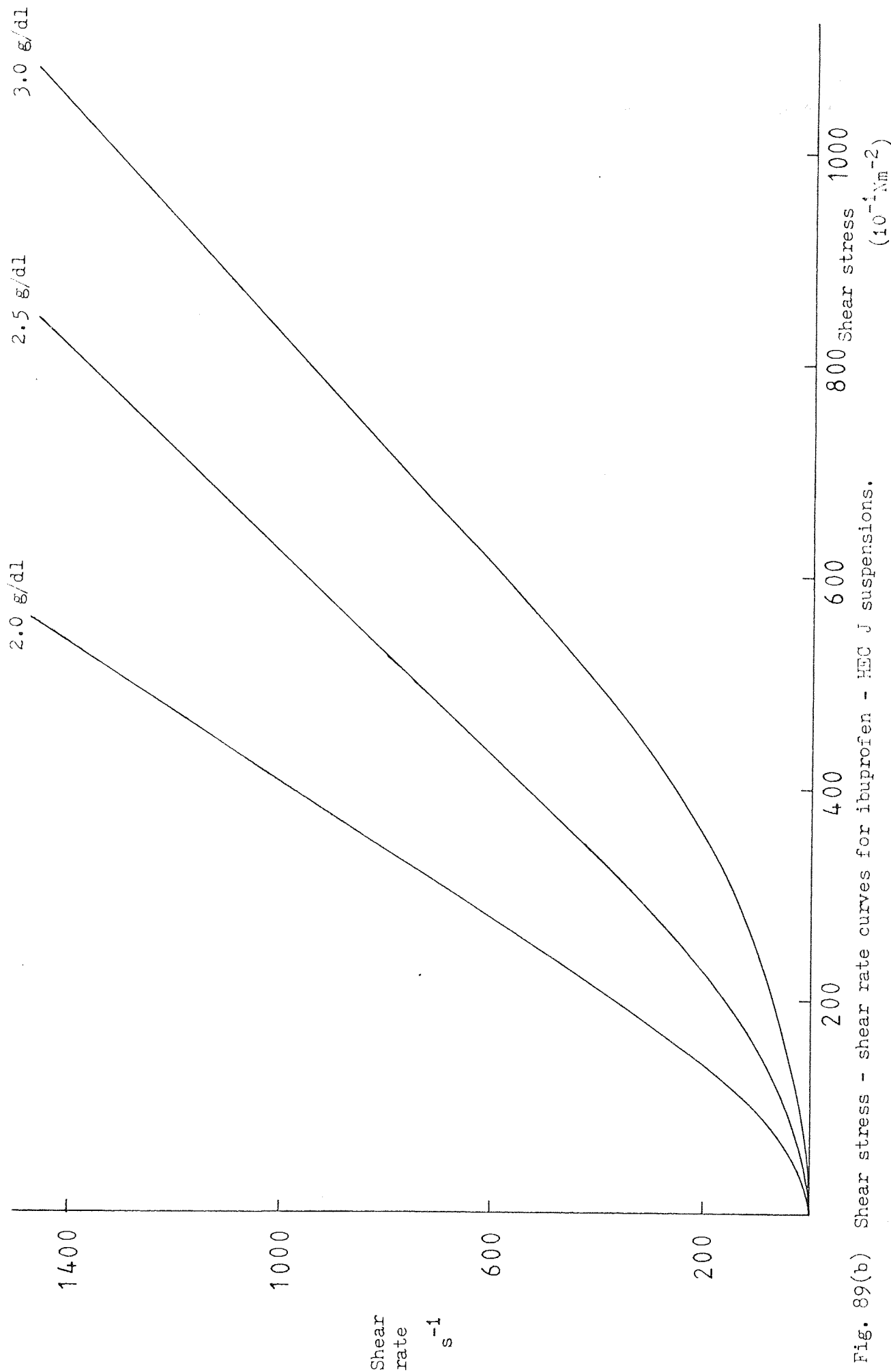


Fig. 89(b) Shear stress - shear rate curves for ibuprofen - HEC J suspensions.

The adsorption of nonionic surface active agents, polyethylene glycol monoethers of n hexadecanols (the Texofor series) on polystyrene latex has been studied. Langmuir type isotherms were obtained. In the plateau region, deductions from the results of the molecular adsorption area and adsorbed layer thickness indicated that the nonionic surface active agent molecules were probably adsorbed in a loop form with both the polyoxyethylene and hydrocarbon chain attached to the surface. The adsorption of the polyoxyethylene and the hydrocarbon chain interacted on the surface of the particle by means of hydrogen bonds and the hydrophobic effect respectively.

The adsorption of nonionic cellulose polymers of HEC, HPC and HPMC were carried out on polystyrene latex and ibuprofen drug particles. Examination of adsorption isotherms showed in all cases plateau adsorption at intermediate concentrations. At high concentrations multilayer adsorptions were found. For HEC and HPC adsorption, the amount adsorbed increased with decreasing molecular weight whereas for adsorption of HPMC an increase of the amount adsorbed was found with increasing molecular weight. Similar adsorption profiles were found in both polystyrene latex and ibuprofen systems, but larger amounts adsorbed were found with polystyrene latex than with ibuprofen and the adsorption area occupied per molecule for polystyrene latex was smaller than those for ibuprofen. This was probably due to the difference in hydrophobicity of the surfaces.

The conformation of the adsorbed molecules on the surfaces obtained from the adsorption isotherms and adsorbed layer thickness

data suggests that the polymer molecules formed 'wrinkles' and loops on the surface. The adsorbed layer thicknesses of the Celluloses on the surface were obtained by viscometric with large and small latex. It was found that the adsorbed layer thickness of the Celluloses was not dependent on particle size. Microelectrophoretic technique were also used to determine the adsorbed layer thicknesses on both polystyrene latex and ibuprofen particles. With polystyrene latex, the results obtained by using the electrophoretic method were lower than those found using viscometry. This may be due to the assumptions made in the calculation of the electrophoretic measurements. Comparison of the values of the electrophoretic results of the adsorbed layer thickness on ibuprofen with those obtained on polystyrene latex showed that for HPC and HPMC, the adsorbed layer thicknesses on both ibuprofen and polystyrene latex were of the same magnitude; for HEC, the values with ibuprofen were lower than those with polystyrene latex. This was probably due to the internal conformations for the adsorbed molecules of HPC and HPMC being different on latex and ibuprofen i.e. the number of the anchor sites on ibuprofen for adsorption was reduced and therefore the molecules occupied larger adsorbed areas. For HEC adsorption on ibuprofen the molecules would take a flatter conformation on the surface.

The binding forces for nonionic polymer adsorption were attributed to van der Waals forces, hydrogen bonds and hydrophobic bonds. Contact angle measurements were studied to assess the hydrophobic effect. It was found that the contact angles were independent on the molecular weight of the polymers used on both ibuprofen and polystyrene surfaces. However, a higher value for the contact angle was observed on polystyrene surface than on ibuprofen surface indicating that the former was more hydrophobic.

The effect of the adsorption of nonionic surface active agent molecules resulted in a decrease in mobility of the particles. This was attributed to the plane of shear around the particle being displaced by the adsorbed molecules. The results of the mobility curves in the presence of the electrolyte mirrored the adsorption isotherms confirming the formation of the complete adsorbed layer.

The stability of the suspensions were investigated by means of sedimentation volume and redispersibility. The sedimentation volumes of the surface active agent and latex systems in the absence of electrolyte showed no significant variations. However, the redispersibility measurements showed low values at high concentrations, in contrast, at low concentrations hard caked suspensions were found. This was probably due at low concentration conditions, to the strong attraction between the bare patches of the surface of the incompletely covered particles or the mutual adsorption of the adsorbed molecules on the bare patches of the surface when particles were in close contact. The sedimentation volumes in the presence of the electrolyte showed that a voluminous sediment occurred at low concentrations resulting in a very low redispersibility. This was extended by potential energy diagrams showing that attraction was dominant in this situation. At high surface active agent concentrations due to the presence of the adsorbed layer a steric energy minimum was created. The particles were restricted in this minimum by a slow aggregation rate; therefore, small sedimentation volumes were found. The relation of the depths of the minimum and the values of the redispersibility showed that a decrease in the depth of the minimum occurs with increasing redispersibility.

The effect of the Hamaker constant of the adsorbed nonionic

surface active agents on the attractive energy was found that the increase of the value of the Hamaker constant within the range studied is more important for V_A at the beginning distances of the adsorbed layer interaction than at the close interaction distances.

Sedimentation volumes of the Cellulose-polystyrene latex systems showed no significant difference in all cases. The redispersibility values at high polymer concentrations were greater than those at low concentrations. It was assumed that continuous network of the adsorbed molecules formed in the sediment, or slow aggregation occurred at low concentrations and network formation occurred at high concentrations. For HEC systems, flocculation of the polystyrene latex by the polymers was observed at low polymer concentrations. Therefore, for HEC-polystyrene latex systems, the above two possibilities may have occurred. For HPC and HPMC systems probably the first possibility has taken place.

The energy diagrams for HEC-polystyrene latex systems showed a stable system at low concentrations which was not the case found experimentally. To explain this it is suggested that the total energy of the system should be $V_T = V_A + V_R + V_S + V_F$ where V_F is the flocculation energy of the polymer.

For the systems of HPC-ibuprofen and HPMC-ibuprofen, at the plateau adsorption concentrations, sedimentation volumes showed an aggregated suspension. This correlated with the total energy curves where a steric energy minimum was shown. The redispersibility at these concentrations showed an intermediate value when compared those at low and high concentrations. While, for HEC-ibuprofen systems,

voluminous aggregates were found in all cases. An easily redispersed suspension was found at complete adsorbed layer concentration. The energy minima found did not correlate with the suspension characteristics; the voluminous sedimentation volume occurred with a smallest energy minimum. This was probably due to the V_F factor operating in these systems.

Study of the settling of the particles with the HPMC polymers used demonstrated that the higher the viscosity of the medium the lower the particle settling velocity. Therefore, in practice the higher viscosity grade fractions will give good suspending effect in preventing particle settling.

For studying the V_F energy of the HEC polymers, a rheometric method was employed. The V_F values obtained for the higher molecular weight or longer molecular chain length polymer were large. Thus, a stronger binding effect of the polymer would be expected. It was also shown that at low polymer concentrations, the binding energy between the particles increased with increasing polymer concentration.

The results of this work show the role that the nonionic surface active agents and nonionic cellulose polymers play in the stability of suspensions. In different concentration ranges they function in different ways. For example, nonionic surface active agents of the polyoxyethylene glycol n hexadecanols series, when present in concentrations sufficient to form a complete adsorbed layer protected the particles from aggregation due to steric stabilization; at low concentrations of HEC polymer caused bridging flocculation while at high concentrations of HPC and HPMC the particles settled and formed

a very hard caked sediment, due to network formation by the polymer molecules.

REFERENCES

1. Rainsford, K.D. J.Pharm. Sci. 30, 129, 1978.
2. Martin, A.N., Swarbrick, J. and Cammarata, A. 'Physical Pharmacy'
2nd Ed., Lea and Febiger, Philadelphia 1969.
3. Derjaguin, B. and Landau, L. Acta Physiochem. 14, 633, 1941.
4. Verwey, E.J.W. and Overbeek, J.T.G. 'Theory of the Stability
of Lyophobic Colloids', Elsevier 1948.
5. Kruyt, H.R. 'Colloid Science' Vol.1, Elsevier 1949.
6. Ottewill, R.H. 'Colloid Science' Vol.1, Chemical Society, London
1973, p.173.
7. Lachman, L., Lieberman, H.A. and Kanig, J.L. 'Theory and Practice
of Industrial Pharmacy' 2nd Ed., Lea and Febiger, Philadelphia 1976.
8. Osol, A. Ed. 'Remington's Pharmaceutical Sciences' 16th Ed.,
Mack Pennsylvania 1980.
9. Shotton, E. and Ridgway, K. 'Physical Pharmaceutics' Clarendon
Oxford 1974.
10. Hiestand, E.N. J.Pharm. Sci. 61, 268, 1972.
11. Ecanow, B., Grandman, R. and Wilson, R. Am. J. Hosp. Pharm.
23, 404, 1966.
12. La Mer, V. K. J. Colloid Sci. 19, 291, 1964.
13. Hiestand, E.N. J. Pharm. Sci. 53, 1, 1964.
14. Bondi, J.V., Schnaare, R.L., Niebergall, P.J. and Sugita, E.T.
J. Pharm. Sci. 62,1731, 1973.
15. Rawlins, D.A. Ph.D. thesis, University of Aston 1979.
16. Matthews, B.A. and Rhodes, C.T. J. Pharm. Pharmc. 20, 204s, 1968.
17. Zsigmondy, R. Z. Anal. Chem. 40, 697, 1901.
18. Schenkel, J.H. and Kitchener, J.A. Trans. Faraday Soc. 56, 161, 1960.
19. Ottewill, R.H. and Walker, T. Kolloid z. 227, 108, 1968.

20. Martin, A.N. J. Pharm. Sci. 50, 513, 1961.
21. Haines, B.A. and Martin, A.N. J. Pharm. Sci. 50, 228, 753, 756, 1961.
22. Kayes, J.B. J. Pharm. Pharmac. 29, 199, 1977.
23. Schott, H. J. Pharm. Sci. 65, 855, 1976.
24. Wilson, R.G. and Ecanow, B. J. Pharm. Sci. 52, 757, 1963.
25. Ecanow, B. and Wilson, R.G. J. Pharm. Sci. 52, 1031, 1963.
26. Wilson, R.G. and Ecanow, B. J. Pharm. Sci. 53, 782, 1964.
27. Flory, P.J. 'Principles of Polymer Chemistry' Cornell University Press, Ithaca N.Y. 1953.
28. Tabor, D. and Winterton, R.H.S. Nature 219, 1120, 1968.
29. Tabor, D. and Winterton, R.H.S. Proc. Roy. Soc. A312, 435, 1969.
30. Tabor, D. J. Colloid. Interface Sci. 31, 364, 1968.
31. Matthews, B.A. and Rhodes, C.T. J. Pharm. Sci. 57, 569, 1968.
32. Matthews, B.A. and Rhodes, C.T. J. Pharm. Sci. 59, 521, 1970.
33. Jones, R.D.C., Matthews, B.A. and Rhodes, C.T. J. Pharm. Sci. 59, 518, 1970.
34. Short, M.P. and Rhodes, C.T. Can. J. Pharm. Sci. 8, 46, 1973.
35. Matthews, B.A. and Rhodes, C.T. Pharm. Acta. Helv. 45, 52, 1970.
36. Stanko, G.L. and DeKay, H.G. J. Am. Pharm. Sci. Ed. 47, 104, 1958.
37. Nash, R.A. and Haeger, B.E. J. Pharm. Sci. 55, 829, 1966.
38. James, A.M. and Goddard, G.H. Pharm. Acta. Helv. 46, 708, 1971.
39. James, A.M. and Goddard, G.H. Pharm. Acta. Helv. 47, 244, 1972.
40. Otsuka, A., Sunada, H. and Yonezawa, Y. J. Pharm. Sci. 62, 751, 1973.
41. Nakamura, Y., Otsuka, A. and Nakagaki, M. J. Pharm. Sci. 94, 833, 1974.
42. Otsuka, A. and Kakinchi, C. J. Pharm. Sci. Japan 96, 110, 1976.
43. Felmeister, A., Kuchtyak, G.M., Koziol, S. and Felmeister, C. J. Pharm. Sci. 62, 2026, 1973.

44. Caramella, C., Cocchi, G.A., Catellani, P., Conte, U., Colombo, P. and La Manna, A. *Boll. Chim. Farm.* 115, 658, 1976.
45. Takamura, K., Kaneniwa, N. and Imagawa, K. *J. Pharm. Sci. Japan* 94, 1580, 1974.
46. Kaneniwa, N. and Takamura, K. *J. Pharm. Sci. Japan* 94, 1607, 1974.
47. Takamura, K. and Kaneniwa, N. *J. Pharm. Sci. Japan* 94, 1612, 1974.
48. Farley, C.A. and Lund, W. *Pharm. J.* 26, 562, 1976.
49. Liao, W.C. and Zatz, J.L. *J. Soc. Cosmet. Chem.* 31, 107, 123, 1980.
50. Zatz, J.L. *Intern. J. Pharm.* 4, 83, 1979.
51. Zatz, J.L., Schnitzer, L. and Sarpotdar, P. *J. Pharm. Sci.* 68, 1491, 1979.
52. Heyd, A. and Dhabhar, D. *Drug Cosmet. Ind.* 42, 125, 1979.
53. Kayes, J.B. and Rawlins, D.A. *J. Pharm. Pharmc.* 30, 75p, 1978.
54. Rawlins, D.A. and Kayes, J.B. *J. Pharm. Pharmc.* 31, 50p, 1979.
55. Rawlins, D.A. and Kayes, J.B. *Drug Dev. Ind. Pharm.* 6, 427, 1980.
56. Flory, P.J. *J. Chem. Phys.* 10, 51, 1942.
57. Kabre, S.P., DeKay, H.G. and Banker, G.S. *J. Pharm. Sci.* 53, 492, 495, 1964.
58. Storz, G.K., DeKay, H.G. and Banker, G.S. *J. Pharm. Sci.* 54, 85, 1965.
59. Whistler, R.L. Ed. 'Industrial Gums' 2nd Ed., Academic Press, London 1973.
60. Flory, P.J. and Krigbaum, W.R. *J. Chem. Phys.* 18, 1086, 1950.
61. Huggins, M.L. *Ann. N.Y. Acad. Sci.* 43, 1, 1942.
J. Phys. Chem. 46, 151, 1942.
J. Am. Chem. Soc. 64, 1712, 1942.
62. Jenkel, F. and Rumbach, B. *Z. Elektrochem.* 55, 621, 1955.
63. Perkel, R. and Ullman, R. *J. Polym. Sci.* 54, 127, 1961.
64. Ellerstein, S. and Ullman, R. *J. Polym. Sci.* 55, 161, 123, 1961.

65. Silber erg, A. J. Chem. Phys. 48, 1281, 1969.
66. Koral, I., Ullman, R. and Eirich, F. J. Phys. Chem. 62, 541, 1958.
67. Freundlich, H. 'Colloid and Capillary Chemistry'
Methuen, London 1926.
68. Langmuir, I. J. Am. Chem. Soc. 40, 1361, 1918.
69. Hobden, I. and Ellinek, H. J. polym. Sci. 11, 365, 1953.
70. Frisch, H.L., Hellman, M.J. and Lundberg, J.L.
J. polym. Sci. 38, 444, 1959.
71. Bindford, I. and Gessler, E. J. Phys. Chem. 63, 1376, 1959.
72. Frisch, H.L., Simha, R. and Eirich, F. J. Phys. Chem. 58, 507, 1954.
73. Simha, R., Frisch, H.L. and Eirich, F. J. Phys. Chem. 57, 584, 1953.
74. Silberberg, A. J. Phys. Chem. 66, 1872, 1962.
75. Silberberg, A. J. Phys. Chem. 66, 1884, 1962.
76. Lipatov, Yu. S. and Sergeeva, L.M. 'Adsorption of Polymer'
Halsted Press, N.Y. 1974.
77. Hoeve, C.A.J. J. Chem. Phys. 43, 3007, 1965.
78. Hoeve, C.A.J. J. Chem. Phys. 44, 1505, 1966.
79. Roe, R.J. Proc. Nat. Acad. Sci. U.S.A. 53, 50, 1965.
80. Roe, R.J. J. Chem. Phys. 43, 1591, 1965.
81. Rubin, R.J. J. Chem. Phys. 43, 2392, 1965.
82. Rubin, R.J. J. Res. Nat. Bur. Stand. Sect. B. 69, 301, 1965.
83. Silberberg, A. J. Chem. Phys. 46, 1105, 1967.
84. Silberberg, A. J. Chem. Phys. 48, 2835, 1968.
85. Silberberg, A. J. Colloid Interface Sci. 38, 217, 1972.
86. Hesselink, F. Th. J. Electroanal. Chem. Interfacial Electrochem.
37, 317, 1972.
87. DiMarzio, E.A. and Rubin, R.J. J. Chem. Phys. 55, 4318, 1971.
88. Hoeve, C.A.J. J. Polym. Sci. C. 30, 361, 1970.
89. Hoeve, C.A.J. J. Polym. Sci. C. 34, 1, 1971.

90. Hoeve, C.A.J., Dimarzio, E.A. and Peyser, P.
J. Chem. Phys. 42, 2558, 1965.
91. Hoffmann, R.F. and Forsman, W.C.
J. Polym. Sci., A-2, Polym. Phys. 8, 1847, 1970.
92. Forsman, W.C. and Hughes, R.J. J.Chem. Phys. 38, 2130, 1963.
93. Hesselink, F.Th. J. Phys. Chem. 73, 3488, 1969.
94. Hesselink, F.Th. J. Phys. Chem. 75, 65, 1971.
95. Elworthy, P.H. and Guthrie, W.G. J. Pharm. Pharmac. 22, 114s, 1970.
96. Corkill, J.M., Goodman, J.F. and Tate, J.R.
Trans. Faraday Soc. 62, 979, 1966.
97. Ottewill, R.H. in 'Nonionic Surfactant' Shick, M.J. Ed.,
Arnold, London 1967.
98. (Ref. 17)
99. Heller, W. and Pugh, T.L. J. Chem. Phys. 22, 1778, 1954.
J. Polym. Sci. 47, 203, 219, 1960.
100. van der Waardan, M. J. Colloid Sci. 57, 317, 1950.
101. Napper, D.H. and Hunter, R.J. Ind. Eng. Chem. Prod. Res. Dev.
9, 467, 1970.
102. Napper, D.H. and Hunter, R.J. MTP International Review of Science,
Physical Chemistry Series one, 7, 249, 1972.
103. Napper, D.H. J. Colloid Interface Sci. 32, 106, 1970.
104. Napper, D.H. Kolloid z.u.z. Polym. 234, 1149, 1969.
105. Napper, D.H. and Netschey, A.J. Colloid Interface Sci. 37, 528, 1971.
106. Evans, R., Davison, J.B. and Napper, D.H.
J. Polym. Sci. B. Polym. Letters 10, 449, 1972.
107. Mackor, E.L. J. Colloid Sci. 6, 492, 1952.
108. Mackor, E.L. and van der Waals, J.H. J. Colloid Sci. 7, 535, 1952.
109. Bagchi, P. and Vold, R.D. J. Colloid Interface Sci. 33, 405, 1970.
110. Ash, S.G. and Findengg, G.H. Trans. Faraday Soc. 67, 212, 1971.

111. Clayfield, E.J. and Lumb, E.C. Disc. Faraday Soc. 42, 314, 1966.
 J. Colloid Sci. 22, 269, 1966.
 J. Colloid Sci. 22, 285, 1966.
 Macromolecules 1, 133, 1968.
112. Bagchi, P. and Vold, R.D. J. Colloid Interface Sci. 38, 652, 1972.
113. Bagchi, P. J. Colloid Interface Sci. 41, 380, 1972.
114. Weidman, J.J., Kuhn, H. and Kuhn, W.J. J. Chem. Phys. 50, 226, 1953.
115. Bagchi, P. and Vold, R.D. J. Colloid Interface Sci. 41, 392, 1972.
116. Smitham, J.B., Evans, R. and Napper, D.H.
 J. Chem. Soc. Faraday Trans. I 71, 285, 1975.
117. Fischer, E.W. Kolloid. z. 160, 120, 1958.
118. Evans, R. and Napper, D.H. Kolloid z.u.z. Polym. 251, 329, 1973.
119. Meier, D.J. J. Phys. Chem. 71, 1861, 1967.
120. Hesselink, F.Th., Vrij, A. and Overbeek, J.Th.G.
 J. Phys. Chem. 75, 2094, 1971.
121. Evans, R. and Napper, D.H. Kolloid z.u.z. Polym. 251, 409, 1973.
122. Derjaguin, B.V. Kolloid z. 69, 155, 1934.
123. Doroszkowski, A. and Lambourne, R. J. Colloid Interface Sci.
43, 97, 1973.
124. Evans, R., Smitham, J.B. and Napper, D.H.
 Colloid Polym. Sci. 255, 161, 1977.
125. Smitham, J.B. and Napper, D.H. Colloid Polym. Sci. 257, 748, 1979.
126. Hesselink, F.Th. J. Polym. Sci. Polym. Symp. 61, 439, 1977.
127. Napper, D.H. and Hunter, R.J. MTP International Review of Science,
 Physical Chemistry Series Two, 7, 194, 1975.
128. Dolan, A.K. and Edwards S.F. Proc. Roy. Soc. A343, 427, 1975.
129. Jackel, K. Kolloid z. 197, 143, 1964.
130. Smitham, J.B. and Napper, D.H. J. Colloid Interface Sci. 54, 467, 1976.
131. Haydon, D.A. 'Recent Progress in Surface Science' Academic Press,
1, 94, 1964.

132. Gouy, G. J. Phys. 2, 457, 1910.
133. Chapman, D.L. Phil. Mag. 25, 475, 1913.
134. Debye, P. and Huckel, E. Physik. Z. 24, 305, 1923.
135. Stern, O. Z. Elektrochem. 30, 508, 1924.
136. Grahame, D.C. Chem. Revs. 41, 441, 1947.
137. Esin, O.A. and Markov, B.F. Z. Fiz. Khim. 13, 318, 1939.
138. Levine, S. and Bell, G.M. J. Colloid Sci. 17, 838, 1962.
139. Loeb, A.L., Overbeek, J.Th.G. and Wiersema, P.H.
 'The Electrical Double Layer Around a Spherical Particle'
 M.I.T. Press, 1961.
140. Hogg, R., Healy, T.W. and Fuerstenau, D.W. Trans. Faraday Soc.
62, 1638, 1966.
141. Honig, E.P. and Mul, P.M. J. Colloid Interface Sci. 36, 258, 1971.
142. Brenner, S.L. and McQuarrie, D.A. J. Colloid Interface Sci.
44, 298, 1973.
143. van der Waals, J.D. Thesis Leyden 1873.
144. Keesom, W.H. Z. Physik 22, 129, 1921.
145. Debye, P. Z. Physik. 22, 302, 1921.
146. London, F. Z. Physik. 63, 245, 1930.
147. Hamaker, H.C. Physica. 4, 1058, 1937.
148. Casimir, H.B.G. and Polder, D. Phys. Rev. 73, 360, 1948.
 Nature 158, 787, 1946.
149. Hunter, R.J. Austral. J. Chem. 16, 774, 1963.
150. Schludko, A., Platikanov, D. and Manev, E. Disc. Faraday Soc.
40, 253, 1965.
151. Clayfield, E.J., Lumb, E.C. and Miller, W.L.
 Proc. Int. Congr. Surface Active Subst. 5th 2, 25, 1969.
152. Clayfield, E.J., Lumb, E.C. and Mackey, P.H.
 J. Colloid Interface Sci. 37, 382, 1971.

153. Vincent, B. J. Colloid Interface Sci. 42, 270, 1973.
154. Kallman, H. and Willstatter, M. Naturwiss 20, 952, 1932.
155. Vold, M.J. J. Colloid Sci. 16, 1, 1961.
156. Osmond, D.W.J., Vincent, B. and Waite, F.A.
J. Colloid Interface Sci. 42, 262, 1973.
157. Kayes, J.B. Ph.D. thesis University of Aston 1975.
158. Lifshitz, E.M. Zhur. Eksp. Teor. Fiz. 29, 94, 1955.
159. Dzyaloshinskii, I.E., Lifshitz, E.M. and Pitaevskii, L.P.
Advan. Phys. 10, 165, 1961.
160. Parsegian, V.A. and Ninham, B.W. J. Colloid Interface Sci.
37, 332, 1971.
161. Ninham, B.W. and Parsegian, V.A. Biophys. J. 10, 646, 1970.
162. Parsegian, V.A. and Ninham, B.W. Biophys. J. 10, 664, 1970.
163. Ninham, B.W. and Parsegian, V.A. J. Chem. Phys. 52, 4578, 1970.
164. Ninham, B.W., Parsegian, V.A. and Weiss, G.H.
J. Stat. Phys. 2, 323, 1970.
165. Parsegian, V.A. and Weiss, G.H. J. Colloid Interface Sci.
40, 25, 1972.
166. Parsegian, V.A. and Weiss, G.H. J. Adhesion 3, 259, 1972.
167. Ash, s.g., Everett, D.H. and Radke, C.
J. Chem. Soc. Faraday Trans II 69, 1256, 1973.
168. Smith, E.R., Mitchell, D.J. and Ninham, B.W.
J. Colloid Interface Sci. 45, 55, 1973.
169. Evans, R. and Napper, D.H. J. Colloid Interface Sci. 43, 138, 1973.
170. Gingell, D. and Parsegian, V.A. J. Colloid Interface Sci.
44, 456, 1973.
171. Langbein, D. J. Chem. Phys. 58, 4476, 1973.
172. Mitchell, D.J. and Ninham, B.W. J. Chem. Phys. 56, 1117, 1972.
173. Mitchell, D.J., Ninham, B.W. and Richmond, P.
Biophys. J. 13, 370, 1973.

174. Mitchell, D.J., Ninham, B.W. and Richmond, P.
Biophys. J. 13, 359, 1973.
175. Mitchell, D.J., Ninham, B.W. and Richmond, P.
J. Theor. Biol. 37, 251, 1972.
176. Davies, B., Ninham, B.W. and Richmond, P.
J. Chem. Phys. 58, 744, 1973.
177. Imura, H. and Okano, K. J. Chem. Phys. 58, 2763, 1973.
178. Parsegian, V.A. J. Chem. Phys. 56, 4393, 1972.
179. Mitchell, D.J. and Ninham, B.W. J. Chem. Phys. 59, 1246, 1973.
180. Parsegian, V.A. and Ninham, B.W. J. Theor. Biol. 38, 101, 1973.
181. Encyclopedia of Polymer Science and Technology, Vol 3,
Interscience Publishers 1965.
182. 'Natrosol' Hercules Incorporated 1978.
183. 'Klucel' Hercules Incorporated 1976.
184. 'Pharmacoat' Shiu-Etsu Chemical Co Ltd.
185. Chung-Li, Y., Goodwin, J.W. and Ottewill, R.H.
Progr. Colloid Polym. Sci. 60, 163, 1976.
186. Ross, S. and Oliver, J.P. J. Phys. Chem. 63, 1671, 1959.
187. Guveli, D., Davis, S.S. and Kayes, J.B.
J. Pharm. Pharmac. 26s, 127, 1974.
188. Svedberg, T. and Pedersen, K.O. 'The Ultracentrifuge'
Clarendon Press, Oxford 1940.
189. Huggins, M.L. J. Am. Chem. Soc. 64, 2716, 1942.
190. Simha, R. J. Appl. Phys. 23, 1020, 1952.
191. Cheng, P.Y. and Schachman, H.K. J. Polym. Sci. 16, 19, 1955.
192. Brown, W. Arkiv For Kemi 18, 227, 1961.
193. Mark, H. in 'Der Feste Korper' Sanger, R. Ed. Hirzel,
Leipzig 1938.
194. Houwink, R.J. Prakt. Chem. 157, 15, 1940.

195. Van Krevelen, D.W. and Hoftyzer, P.J. 'Property of Polymers'
Elsevier, Amsterdam 1976.
196. Elias, H.G. 'Macromolecules 1' Plenum Press, N.Y. 1977.
197. 'Handbook on Methocel' Dow Chemical Co. 1975.
198. Wieick, M. and Waldman, M. J. Appl. Polym. Sci. 14, 579, 1970.
199. Brown, W., Henley, D. and Ohman, J. Makromol. Chem. 64, 49, 1963.
200. Rayleigh, Lord (Strutt, J.W.) Phil. Mag. (4) 41, 107, 224, 447, 1871.
201. Debye, P. J. Appl. Phys. 15, 338, 1944.
J. Phys. Colloid Chem. 51, 18, 1947.
202. Zimm, B.H. J. Chem. Phys. 16, 1093, 1099, 1948.
203. 'Brice-Phoenix Differential Refractometer Model BP-2000-V'
Philadelphia U.S.A..
204. 'Photo Gonio Diffusometer Model 42000' Societe Franeaise D'instruments
De Controle Et D'analyses, Le Mesnil-Saint-Denis France.
205. Macfarlane, C.B. Ph.D. thesis Glassgow.
206. Goring, D.A.I. and Napier, P.G. J. Chem. Phys. 22, 147, 1954.
207. Guveli, D.E. Ph.D. thesis University of Aston 1976.
208. Hearn, J., Ottewill, R.H. and Shaw, J.N. Br. Polym. J.
2, 116, 1970.
209. Van der Hull, H.J. and Vanderhoff, J.W. Br. Polym. J. 2, 121, 1970.
210. Kolthoff, I.M. and Miller, I.K. J. Am. Chem. Soc. 73, 3055, 1951.
211. Ottewill, R.H. and Shaw, J.N. Kolloid z.u.z. Polym. 218, 314, 1967.
212. 'Handbook of Chemistry and Physics' 61st Ed. 1980-1981 CRC.
213. Formulation Research Group, The Boots Co. Nottingham. (private
communication)
214. 'EEL Photoextinction Sedimentometer Operating Instructions'
Evans Electroselenium Ltd.
215. Shaw, D.J. 'Introduction to Colloid and Surface Chemistry'
2nd Ed., Butterworths, London 1972.

216. Smith, A. Ph.D. thesis University of Aston 1975.
217. Howard, G. and McConnel, P. J. Phys. Chem. 71, 2974, 2981, 2991, 1967.
218. Peterson, C. and Kwei, T.K. J. Phys. Chem. 65, 1330, 1961.
219. Kipling, J.J. 'Adsorption from Solutions of Nonionic Electrolytes'
Academic Press, N.Y. 1965.
220. Shaw, D.J. 'Electrophoresis' Academic Press, London 1969.
221. Kayes, J.B. J. Colloid Interface Sci. 56, 426, 1976.
222. Tanford, C. 'The Hydrophobic Effect' 2nd Ed., Wiley Interscience,
N.Y. 1980.
223. Komagata, S. J. Electrochem. Soc. Japan 1, 97, 1933.
224. Doroszkowski, A. and Lambourne, R. J. Colloid Interface Sci.
26, 214, 1968.
225. Simha, R. J. Chem. Phys. 13, 188, 1945.
226. Kraemer, O. J. Franklin Inst. 231, 1, 1941.
227. Badgley, W.J. and Mark, H. J. Phys. Chem. 51, 58, 1947.
228. Garvey, M.J., Tadros, Th.F. and Vincent, B.
J. Colloid Interface Sci. 55, 440, 1976.
229. Vincent, B. Advan. Colloid Interface Sci. 4, 193, 1974.
230. Lerk, C.F., Schoonen, A.J.M. and Fell, J.T.
J. Pharm. Sci. 65, 843, 1976.
Lerk, C.F., Lagas, M., Boelstra, J.P. and Broersma, P.
J. Pharm. Sci. 66, 1480, 1977.
231. Chang, S.A. and Gray, D.G. J. Colloid Interface Sci. 67, 255, 1978.
232. Mathai, K.G. and Ottewill, R.H. Trans. Faraday Soc. 62, 750, 1966.
233. Milwidsky, B.M. Tenside Detergents 10, 14, 1973.
234. Tadros, Th.F. in 'Colloidal Dispersion and Micellar Behavior'
Mittal, K.L. Ed. ACS. P.173.
235. Einstein, A. Ann. Physik. 19, 289, 1906.
236. Jefferies, G.B. Proc. Roy. Soc. London A102, 161, 1923.

237. Vand, V. J. Phys. Colloid Chem. 52, 277, 330, 1948.
238. Mooney, M. J. Colloid. Sci. 6, 162, 1951.
239. Abramson, H.A., Moyer, L.S. and Gorin, M.H. 'Electrophoresis of Proteins and the Chemistry of Cell Surfaces' Reinhold, N.Y. 1942.
240. Huckel, E. Phys. Z. 25, 204, 1924.
241. von Smoluchowski, M. Bull. Acad. Sci. Gracovie 1903.
242. Henry, D.C. Proc. Roy. Soc. 133A, 106, 1931.
243. Overbeek, J.Th.G. Advan. Colloid Sci. 3, 97, 1950.
244. Booth, F. Nature 161, 83, 1948.
Proc. Roy. Soc. 203A, 514, 1950.
245. Wiersema, P.H., Loeb, A.L. and Overbeek, J.Th.G.
J. Colloid. Interface Sci. 22, 78, 1966.
246. Lyklema, J. and Overbeek, J.Th.G. J. Colloid Sci. 16, 501, 1961.
247. Hunter, R.J. J. Colloid Sci. 22, 231, 1966.
248. Overbeek, J.Th.G. and Wiersema, P.H. 'Electrophoresis' Bier, M. Ed. Vol 2, Chapter 1, Academic Press, N.Y. 1967.
249. Fleer, G.J. thesis Wageningen 1971.
250. Fowkes, F.M. in 'Chemistry and Physics of Interfaces' Gushee, D.E. Ed. ACS 1965.
251. Debye, P. J. Phys. Chem. 51, 18, 1947.
252. Ottewill, R.H. and Shaw, J.N. Kolloid z.u.z. Polym. 218, 34, 1967.
253. Ottewill, R.H. and Shaw, J.N. J. Electro. Chem. 37, 133, 1972.
254. Rawlins, D.A. Private Communication 1980.
255. Kayes, J.B. and Rawlins, D.A. Colloid and Polym. Sci. 257, 622, 1979.
256. La Mer, V.K. and Healy, T.W. Rev. Pure Appl. Chem. 13, 112, 1963.
257. Wiese, G.R. and Healy, T.W. J. Colloid Interface Sci. 51, 434, 1975.
258. Stumm, W. and Morgan, J.J. J. Am. Water Works Assoc. 54, 971, 1962.
259. Brooks, D.E. and Seaman, G.V.F. J. Colloid Interface Sci. 43, 670, 1973.

260. Fleer, G.J., Koopal, L.K. and Lyklema, J.
Kolloid z.u.z. Polym. 250, 689, 1972.
261. Ruehrivein, R.A. and Ward, D.W. Soil Sci. 73, 485, 1952.
262. Miyata, N., Sakata, I. and Senju, R.
Nippon Kagaku Kaishi 9, 1782, 1974.
263. Long, J.A., Osmond, D.W.J. and Vincent, B.
J. Colloid Interface Sci. 42, 545, 1973.
264. Kitchener, J.A. Br. Polym. J. 4, 217, 1972.
265. Ash, S.G. and Clayfield, E.J. J. Colloid Interface Sci.
55, 645, 1976.
266. Elworthy, P.H. and Florence, A.T. J. Pharm. Pharmac. 21, 79s, 1969.
267. Gregory, J. Advan. Colloid Interface Sci. 2, 396, 1969.
268. Watillon, A. and Joseph-Petit, A.M. Disc. Faraday Soc.
42, 143, 1966.
269. Ottewill, R.H. and Shaw, J.N. Disc. Faraday Soc. 42, 154, 1966.
270. Fowkes, F.M. J. Colloid interface Sci. 28, 493, 1968.
271. Florence, A.T. and Rogers, J.A. J. Pharm. Pharmac. 23, 153, 1971.
272. Ottewill, R.H. and Walker, T. J. Chem. Soc. Faraday Trans. I
70, 917, 1974.
273. Napper, D.H. Sci. Progr. 55, 91, 1967.
274. Sonntag, H. and Strenge, K. 'Coagulation and Stability of Disperse
Systems' Halsted Press, N.Y. 1972.
275. Saunders, F.L. and Sanders, J.W. J. Colloid Sci. 11, 260, 1956.
276. Robinson, C.S. Ind. Eng. Chem. 36, 618, 1944.
277. Higuchi, T. J. Am. Pharm. Assoc. Sci. Ed. 47, 657, 1958.
278. Steinour, H.H. Ind. Eng. Chem. 36, 618, 840, 901, 1944.
279. Richardson, J.F. and Zaki, W.W. Inst. Chem. Eng. 32, 35, 1954.
280. Warburton, B. and Davis, S.S. Rheol. Acta. 8, 205, 1969.
281. Gerding, P.W. and Sperandio, G.J. J. Am. Pharm. Ass. Pract. Ed.
15, 356, 1954.

282. Lesshafft, C.T.Jr. and DeKay, H.G.
J. Am. Pharm. Ass. Pract. Ed. 15, 410, 1954.
283. Pienta, J.J.Jr., Marcus, A.D. and Benton, B.E.
J. Am. Pharm. Ass. Pract. Ed. 15, 414, 1954.
284. Higuchi, W. and Stehle, K.G. J. Pharm. Sci. 54, 265, 1965.
285. Gillespie, T. J. Phys. Chem. 66, 1077, 1962.
J. Colloid Sci. 15, 219, 1960.
286. von Smoluchowski, M. Z. Physik. Chem. 92, 129, 1917.
287. Michaels, A.S. and Bolger, J.C. Ind. Eng. Chem. Funda.
1, 153, 1962.
288. Firth, B.A. and Hunter, R.J. J. Colloid Interface Sci.
57, 266, 1976.